

FINAL REPORT
OF
SL-1 RECOVERY OPERATION

SL-1 Project
Idaho Test Station
General Electric Company
July 27, 1962

United States Atomic Energy Commission
Contract No. AT (10-1) 1095

DISCLAIMER

This report was prepared as an account of work sponsored by an agency of the United States Government. Neither the United States Government nor any agency Thereof, nor any of their employees, makes any warranty, express or implied, or assumes any legal liability or responsibility for the accuracy, completeness, or usefulness of any information, apparatus, product, or process disclosed, or represents that its use would not infringe privately owned rights. Reference herein to any specific commercial product, process, or service by trade name, trademark, manufacturer, or otherwise does not necessarily constitute or imply its endorsement, recommendation, or favoring by the United States Government or any agency thereof. The views and opinions of authors expressed herein do not necessarily state or reflect those of the United States Government or any agency thereof.

DISCLAIMER

Portions of this document may be illegible in electronic image products. Images are produced from the best available original document.

ABSTRACT

In May, 1961, it was determined no renewed nuclear reaction in the SL-1 pressure vessel was possible as long as water was excluded. It was therefore possible to proceed with the final phase of the SL-1 recovery, known as phase 3. This work consisted of moving the pressure vessel and core to the Hot Shop at the north end of the National Reactor Testing Station, dissecting and analyzing the reactor and its components, cutting up and burying the reactor building, and decontaminating the rest of the SL-1 area. These things were accomplished by the General Electric Company between May 1961 and July 1962.

It was determined that the central control rod was bound in its shroud at a position corresponding to 20 inch withdrawal. Analysis of the pertinent data shows that the amount of reactivity associated with this rod position, inserted at a rate compatible with manual withdrawal of the rod, can explain all the significant evidence which has been collected. No other means of withdrawing the rod has been found to be in accordance with the evidence. The most striking and unexpected phenomenon discovered was that the relatively low yield (130 Mw-sec) nuclear excursion produced a water hammer with pressures up to 10,000 psi, which, in turn, caused the pressure vessel to rise some 9 feet in the air.

TABLE OF CONTENTS

	<u>Page</u>
Abstract	ii
Table of Contents	iii
List of Figures	vi
List of Tables	xii
I. Introduction and Summary	I-1 thru I-7
1. History of Project	I-1
2. Highlights of the Recovery Operation	I-2
3. Evidence for Evaluation	I-4
4. Analysis and Conclusions	I-5
II. Recovery Operations	II-1 thru II-119
1. Site Cleanup	II-1
1.1 Method of Operation	II-1
1.2 Equipment	II-7
1.3 Cleanup Operations	II-15
1.3.5 Reactor Removal and Transfer Operations	II-37
2. SL-1 Hot Shop Operations	II-55
2.1 Preliminary Operations	II-55
2.2 Head Removal	II-59
2.3 Initial Parts Removal and Inspection	II-61
2.4 Pressure Vessel and Core Measurements	II-63
2.5 Lower End Inspection	II-63
2.6 Post-Incident Critical Experiment	II-70
2.7 Final Disassembly and Disposal	II-82
3. Health Physics	II-88
3.1 Radiological Conditions	II-88
3.2 Control Procedures	II-108
3.3 Protective Clothing and Equipment	II-109
3.4 Dosimetry	II-111
3.5 Bioassay	II-114
3.6 Material Transportation and Waste Disposal	II-114
3.7 Exposure Statistics	II-116
III. Evidence and Related Investigations	III-1 thru III-119
1. Mechanical Evidence	III-1
1.1 Shield Plug Assembly #9	III-1
1.2 Shield Plug - Identification, Etc.	III-19
1.3 Reconstruction of Fan Room Floor, Etc.	III-29
1.4 Steam Baffle, Etc.	III-36
1.5 Pressure Vessel Deformation, Etc.	III-39
1.6 Aberdeen Tests	III-42
1.7 Core and Thermal Shield Deformation	III-47
1.8 Cadmium Blades and Shrouds	III-51

TABLE OF CONTENTS (Cont'd)

	<u>Page</u>
2. Chemical and Related Evidence	III-64
2.1 Identification of Deposits	III-64
2.2 Burnable Poison Strips	III-64
2.3 Boric Acid Deposit Analysis	III-73
2.4 Chemical Explosives	III-74
2.5 Aluminum-Water Reaction	III-75
3. Fuel Elements	III-77
3.1 Extent of Melting	III-77
3.2 Temperature Ranges	III-81
3.3 Uranium Inventory	III-84
3.4 Fuel Element Thermal Effects	III-87
3.5 Flux Wire Thermal Effects	III-91
3.6 Aluminum-Uranium Ratio	III-91
4. Nuclear Evidence	III-95
4.1 Flux Wires	III-95
4.2 Other Activation Data	III-101
4.3 Fission Product Release	III-104
4.4 Excess Reactivity	III-105
4.5 Central Control Rod Withdrawal	III-109
4.6 Reactivity Insertion Rate	III-111
4.7 Critical Experiment Results	III-117
IV. Analysis and Conclusions	IV-1 thru IV-27
1. Nuclear Excursion	IV-1
1.1 Initiating Mechanism	IV-1
1.2 Power Behavior	IV-2
1.3 Shutdown Mechanisms	IV-5
1.4 Temperature Distribution, Etc.	IV-7
2. Effects Following Excursion	IV-14
2.1 Acceleration of Water Slug	IV-14
2.2 Effects of Water Slug	IV-15
2.3 Subsequent Excursions	IV-17
3. Core Damage	IV-19
3.1 Temperatures, Destruction, Melt and Vaporization	IV-19
3.2 Energy Distribution and Metal Water Reaction	IV-20
3.3 Activation	IV-22
4. Summary of Excursion	IV-25

TABLE OF CONTENTS (Cont'd)

	<u>Page</u>
Appendix A	A-1 thru A-5
Description of SL-1	
Appendix B	B-1 thru B-6
List of SL-1 Photographs by Series Number	
Appendix C	C-1 thru C-4
Stanford Research Institute Report	
Appendix D	D-1 thru D-7
Fuel Element Areas Destroyed and Unmelted	
Appendix E	E-1 thru E-7
Flux Wire Results	
Appendix F	F-1 thru F-5
Analog Computer Study of Reactor Incident	

List of Figures

<u>Figure No.</u>	<u>Title</u>	<u>Page No.</u>
II-1	Reactor Vessel Head After Placement of Shield Bags	II-2
II-2	Steel Punchings Near Head of Reactor Vessel	II-2
II-3	Steel Plate and Cooling Lines Displaced by Accident	II-3
II-4	Insulation on Floor Between Shield Blocks	II-3
II-5	Equipment and Debris on Operating Room Floor	II-4
II-6	South Side of Operating Room	II-4
II-7	Shielded Crane Used for Remote Operation	II-8
II-8	Camera Shielding Box	II-10
II-9	Operating Room Floor	II-18
II-10	Exposure Rate - Operating Room	II-20
II-11	Isodose Map - Operating Room Floor	II-24
II-12	Isodose Map - Operating Room Floor	II-26
II-13	Isodose Map - Fan Floor	II-28
II-14	Isodose Map - Operating Room Floor	II-29
II-15	Isodose Map - Fan Floor	II-30
II-16	Stairway to Fan Floor	II-32
II-17	Hole in Fan Room Floor	II-34
II-18	Shield Plug on Fan Room Floor	II-34
II-19	Remaining Fan Room	II-35
II-20	Operating Room Ceiling	II-35
II-21	Bottom View of Reactor	II-38
II-22	Bottom View of Reactor	II-38
II-23	Upper End of Pressure Vessel	II-40
II-24	SL-1 Reactor Removal	II-44
II-25	Inside of Support Cylinder	II-46
II-26	Bottom of Support Cylinder	II-46
II-27	SL-1 Reactor Transfer Operation	II-48
II-28	ANP Hot Shop	II-54
II-29	Shielding Material	II-54
II-30	SL-1 Pressure Vessel	II-56
II-31	Pressure Vessel Dished Head	II-58
II-32	Pressure Vessel Head	II-58

List of Figures (Continued)

<u>Figure No.</u>	<u>Title</u>	<u>Page No.</u>
II-33	SL-1 Core	II-60
II-34	Deposits on Core Parts	II-60
II-35	Pressure Vessel Measurements	II-62
II-36	SL-1 Core	II-64
II-37	Core Support Bracket	II-66
II-38	Bottom of Core	II-66
II-39	Equipment for Hole Cutting	II-69
II-40	Inside Bottom of Pressure Vessel	II-69
II-41	Test Assembly	II-72
II-42	Core in Critical Equipment Tank	II-73
II-43	Critical Experiment Rod Position	II-73
II-44	Location and Travel Distances of Control Rods	II-76
II-45	Nuclear Instrumentation Schematic	II-77
II-46	Nuclear Sensor Locations	II-78
II-47	Nuclear Instrument Panel	II-79
II-48	Control Console for Critical Experiment	II-80
II-49	Cutting off Pressure Vessel	II-83
II-50	Upper Control Rod Shrouds	II-83
II-51	Remaining Core	II-84
II-52	#1 Control Rod and Shroud	II-85
II-53	Thermal Shield	II-85
II-54	SL-1 Site Isodose Survey	II-89
II-55	Dose Rate to Whole Body	II-92
II-56	Dose Rate to Skin	II-92
II-57	Accumulated Radiation Dose	II-93
II-58	Weekly Whole Body Dose	II-93
II-59	Radiation Hot Spots (Operating Floor)	II-98
II-60	Gamma Radiation Levels (Operating Floor)	II-99
II-61	Radiation Levels (Operating Floor)	II-100
II-62	Radiation Survey (Fan Floor)	II-101
II-63	Radiation Survey (Fan Floor)	II-102
II-64	Radiation Survey - SL-1 Area	II-104

List of Figures (Continued)

<u>Figure No.</u>	<u>Title</u>	<u>Page No.</u>
II-65	SL-1 Area Radiation Levels	II-105
II-66	Soil Samples Taken at SL-1	II-106
II-67	Whole Body Doses	II-118
II-68	Total Skin Doses	II-118
II-69	Whole Body Dose	II-119
II-70	Skin Dose	II-119
III-1	Shield Plug #9, Lying Across Reactor Head	III-2
III-2	Shield Plug #9, Lying Across Reactor Head	III-3
III-3	General Assembly of a Typical Shield Plug	III-4
III-4	Shield Plug #9, Guide Tube Collapse	III-6
III-5	Shield Plug #9, Cross Section of Seized Control Rod	III-6
III-6	Shield Plug #9, Upper Section Showing Flange Deformation	III-7
III-7	Shield Plug #9, Imprint on bolt hole from impact	III-7
III-8	Shield Plug #9 Assembly	III-9
III-9	Shield Plug #9, Extension rod, showing fracture	III-11
III-10	Shield Plug #9, Stress cracks in rack section	III-11
III-11	Shield Plug #9, Top of rack, nut and washer	III-12
III-12	Handling Tool with broken end of #9 rack	III-13
III-13	Matching of broken stud of central control rod rack	III-13
III-14	Shield Plug #9, Connector rod showing sheared roll pins	III-15
III-15	Shield Plug #9, Relative position of extension rod and guide tube	III-15
III-16	Shield Plug #9, Seized region of guide tube	III-16
III-17	Shield Plug #9, Plaster cast of guide tube impression	III-16
III-18	Broken "C" Clamp Recovered from Fan Room Floor	III-17
III-19	Shield Plug #1, Showing Damage to Spring Housing	III-21
III-20	Shield Plug #1, Matching Imprint of Shield Plug #7	III-21
III-21	Upper Section Retained in Shield Plug #3	III-23
III-22	Shield Plug #3, Showing Flange Deformation	III-23
III-23	Shield Plug #3, Mating of Fractured Nut	III-24
III-24	Shield Plug #4, Showing Flange Deformation	III-25
III-25	Number 5 Guide Tube and Rack	III-25

List of Figures (Continued)

<u>Figure No.</u>	<u>Title</u>	<u>Page No.</u>
III-26	Showing Spring Housing and Flange Deformation	III-31
III-27	Nut from Instrument Flange #8	III-31
III-28	Superimposing Fan Room Floor with Pressure Vessel Head	III-32
III-29	Reconstruction of Reactor Head and Plug Assemblies	III-33
III-30	Section of Fan Room Floor Showing Areas of Damage	III-33
III-31	View of Vessel Head	III-34
III-32	Baffle Plate Showing Areas of Impact	III-38
III-33	Collapsed Still Well Pipe	III-38
III-34	Cross-Section of Still Well Pipe	III-40
III-35	Fractured Weld, Auxiliary Still Well Bracket	III-40
III-36	Deformation of Flange and Vessel	III-41
III-37	Deformation of Pressure Vessel Head Nozzles	III-43
III-38	Deformation of Pressure Vessel Head Nozzles	III-43
III-39	1/4 Scale Model of Pressure Vessel Head Assembly	III-44
III-40	1/4 Scale Model of Pressure Vessel Head	III-44
III-41	Pressure-Time History	III-48
III-42	Bottom View of Core	III-50
III-43	Core Tee Stanchions	III-50
III-44	Shroud and Blade Assembly #1	III-52
III-45	Shroud and Blade Assembly #1	III-52
III-46	Blade #1	III-53
III-47	Shroud and Blade Assembly #2	III-53
III-48	Cadmium Blade from Assembly #2	III-54
III-49	Shroud #3 and #4 Assemblies	III-54
III-50	Shroud Assembly #5	III-55
III-51	Shroud Assembly #5	III-55
III-52	Shroud Assembly #5	III-56
III-53	Shroud Assembly #6	III-56
III-54	Cadmium Blade, Assembly #6	III-58
III-55	Shroud Assemblies #7 and #8	III-58
III-56	Control Blade #7	III-59
III-57	Sample Section from Control Blade #9	III-59

List of Figures (Continued)

<u>Figure No.</u>	<u>Title</u>	<u>Page No.</u>
III-58	Control Blade #9, Bound in its Shroud	III-60
III-59	Shroud Relief Hole Imprint on Control Blade #9	III-61
III-60	Shroud and Control Blade #9	III-61
III-61	Cadmium Blade Showing Weld Separation	III-63
III-62	Lower End of #9 Control Blade	III-63
III-63	Vaporized Deposits on Shield Plug #5	III-65
III-64	Deposits on Rod Assembly #4	III-65
III-65	Boron Strip Loading	III-68
III-66	Corrosion and Deterioration of Boron Strip	III-69
III-67	Portions of Corroded Boron Strips	III-69
III-68	Cutter Loaded with Debris from Pressure Vessel	III-70
III-69	Deposit Underneath Reactor Head Surface	III-70
III-70	Schematic View of Core	III-78
III-71	Sections of Fuel Plate Recovered from Fan Room	III-79
III-72	Section of Fuel Plate from Element #7	III-79
III-73	Fuel Material Spatter from Element #3	III-80
III-74	Extraneous Material in Fuel Element #52	III-80
III-75	Molten Metal on Boron Strip	III-82
III-76	Fuel Plate from Fuel Element #4	III-82
III-77	Cross-Section Through Fuel Plate	III-83
III-78	Screened Debris from Pressure Vessel	III-83
III-79	Fuel Elements #60 and #18	III-88
III-80	Fuel Element Side Plate	III-88
III-81	Upper Section of Fuel Element #4	III-89
III-82	Fuel Element #3	III-89
III-83	Fuel Element #3	III-90
III-84	Fuel Element #52	III-90
III-85	Sample Locations on Fuel Element #5	III-93
III-86	Sample Locations on Fuel Element #6	III-93
III-87	Cross-Sectional View of Fuel Plate	III-94
III-88	Sample Locations on Fuel Element #39	III-94
III-89	Flux Wire Locations in Core	III-96

List of Figures (Continued)

<u>Figure No.</u>	<u>Title</u>	<u>Page No.</u>
III-90	Energy Released per Element	III-98
III-91	Longitudinal Flux Distributions	III-99
III-92	Longitudinal Flux Distributions	III-99
III-93	Energy Distribution During Excursion	III-100
III-94	Co-60 Activation Data	III-103
III-95	Differential Worth Curve for Central Rod	III-108
III-96	Two Experimental Rod-Withdrawal Situations	III-110
III-97	Analog Computer Traces	III-113
III-98	Analog Computer Traces	III-114
III-99	Analog Computer Traces	III-115
III-100	Comparison of Rod Withdrawal Rates	III-116
III-101	Multiplication Curves	III-118
IV-1	Temperature Distribution 4 m-sec before Peak	IV-9
IV-2	Temperature Distribution at Peak	IV-10
IV-3	Temperature Distribution at End of Excursion	IV-11
IV-4	Summary of Excursion	IV-27
A-1	SL-1 Plant Area	A-2
A-2	SL-1 Plant Perspective	A-3
A-3	SL-1 Reactor Perspective	A-4
A-4	SL-1 Core Plan	A-5
F-1	Analog Circuit Used for Excursion	F-4
F-2	Typical Transient Power Run	F-5

List of Tables

<u>Table No.</u>	<u>Title</u>	<u>Page</u>
II-1	Tabulations of Core Measurements	II-65
II-2	Radiation Levels at SL-1 Site	II-94
II-3	Final Contamination Levels in Support Facilities	II-97
II-4	Exposures During Phase 3 of SL-1 Recovery	II-117
III-1	Condition of Control Rod Components	III-30
III-2	Analysis of Samples from Vessel and Core	III-66
III-3	Boron Strip Recovery Data	III-71
III-4	Insoluble Residue Data	III-76
III-5	SL-1 Fuel Inventory	III-85
III-6 (a)	Aluminum-Uranium Ratios	III-91
III-6 (b)	Aluminum-Uranium Ratios	III-92
III-7	Activation Samples from Victims	III-101
III-8	Pre-Incident Critical Rod Positions	III-106
III-9	Period-Reactivity Relationship for SL-1	III-107
III-10	Manual Rod-Withdrawals with Maximum Effort	III-109
IV-1	Excursion Values Using Two-Term Burst Approximation	IV-5
IV-2	Temperatures at Surface and Center of Plate for Excursions of Different Periods	IV-13
IV-3	Energy Rapidly Deposited in Water	IV-20
IV-4	Aluminum-Water Reaction in SL-1	IV-22

I. INTRODUCTION AND SUMMARY

1. History of Project

1.1 Phase 1

On January 3, 1961, a nuclear accident occurred at the SL-1 reactor facility, operated by Combustion Engineering for the Atomic Energy Commission, at the National Reactor Testing Station in Idaho. This accident resulted in fatal injuries to the three reactor operators, all military personnel, who were on duty at the time. During the period from January 3 to January 10, 1961, an NRTS disaster plan was in effect for the recovery of the three casualties from the reactor building and for the assessment of the reactor shutdown condition. This portion of the recovery operation was designated as Phase 1. During this phase, the reactor was determined to be in a non-critical condition. However, the physical condition of the reactor core, the location of control rods, and the presence or absence of water in the pressure vessel were unknown. Therefore, no conclusion could be drawn as to whether or not the reactor might at anytime sustain a renewed nuclear excursion.

1.2 Phase 2

This phase of the recovery operations was undertaken by Combustion Engineering with the objectives of establishing the nuclear status of the reactor core and of assuring that a renewed nuclear excursion would not occur. This work included radiation surveys, the installation of neutron and gamma monitoring instruments, viewing the top of the pressure vessel head, viewing the vessel interior to determine the condition of the core, and determining the water level in the pressure vessel. Because of the concern over the possibility of renewed nuclear excursions, all of these operations were performed by means remote to the reactor building interior. Phase 2 of the recovery operation was concluded in May 1961, with the determination that the pressure vessel contained no water and that subsequent nuclear excursions could be prevented by keeping the vessel dry.

1.3 Phase 3

This phase of the recovery operation began on May 23, 1961, when the Idaho Operations Office of the Atomic Energy Commission and the General Electric Company signed a letter contract under the terms of which General Electric undertook the remaining recovery efforts. The objectives of this phase of the operation were as follows:

- a. To gather and evaluate data concerning the accident.
- b. To remove the SL-1 core for examination, evaluation and disposal.
- c. To raze the reactor building completely.
- d. To decontaminate the SL-1 area and ready it for potential beneficial occupancy.

These objectives were successfully completed on July 27, 1962.

2. Highlights of the Recovery Operations

2.1 Site Cleanup

The job of cleaning up the SL-1 site was started on May 23, 1961, and was completed on June 22, 1962. During this period, General Electric personnel and volunteers representing many organizations and professions contributed toward the successful fulfillment of a very difficult task.

Several overall plans for the recovery operation were considered. The decision was made to remove the pressure vessel and transport it, for purposes of core examination, to the Hot Shop used for the former Aircraft Nuclear Propulsion program. Pursuant to this end, plans were made to overcome the many problems associated with such an undertaking. These problems included: (1) radiation levels up to 200 R/hr, (2) widely scattered contamination within the reactor building, (3) a severe congestion of equipment and material in the operating room, (4) an operating room floor which was 21 feet above ground level, and (5) the need to preserve and record the condition and orientation of all evidence pertinent to the incident.

General plans for the site recovery were to reduce the general radiation levels and recover major evidence, to dismantle the upper part of the reactor building, to remove the pressure vessel and take it to the ANP Hot Shop, to raze the reactor building, and finally, to decontaminate the remaining area.

Recovery operations were initiated by establishing an entry control point in a building located near the SL-1 perimeter fence. This building was subsequently used for briefing and debriefing entry teams, for health physics monitoring and control, for assembly and maintenance of equipment, and for decontamination. Radiation and photographic surveys were made of the reactor building and a special roadway was constructed between the control point and the reactor building.

General radiation levels in the reactor building were greatly reduced by removing large pieces of highly contaminated equipment, by sweeping or vacuuming up the smaller debris, and by placing shielding over the pressure vessel head. Although as much of this work was accomplished by remote means as was consistent with cost and schedule objectives, the bulk of it was performed manually, using carefully controlled personnel exposures. Special TV monitoring systems, vacuuming systems and handling equipment were designed as required to fit the occasion. Extensive health physics monitoring and control were exercised at all times and wide photographic coverage was given to the various operations using both still and movie cameras. Material removed from the reactor building was either sent to the ANP facilities for inventory and subsequent laboratory analysis, if deemed necessary for incident evaluation, or placed in a specially prepared burial area near the SL-1 site, if it was deemed to be scrap.

After the reactor building had been sufficiently cleaned, the upper sections were removed and the equipment on the fan floor above the operating room was dismantled. Again, special equipment was designed and fabricated as necessary for specific applications. To provide a drain for any water that otherwise might accidentally accumulate in the core as a result of removing the roof of the building, and to permit inspection of the core before moving the vessel, a hole was drilled through the shielding, gravel, support cylinder, and pressure vessel below the core. Through this hole, with the aid of a boroscope, the under side of the core was examined and photographed.

With the area above the pressure vessel clear, the vessel itself was removed with a 60-ton construction crane, placed in a large cask, and transported by a lowboy trailer to the ANP Hot Shop.

Subsequent site operations consisted of razing the reactor building and decontaminating the remaining service buildings and work areas. Thus, on June 22, 1962, 18 months after the incident and 13 months after Phase 3 recovery operations were started, the SL-1 facility area was available to the AEC for future projects.

2.2 Hot Shop Work

The Hot Shop work consisted of receiving and inspecting the the reactor pressure vessel, recording and preserving all evidence, conducting a critical experiment, and dismantling the vessel and the core. This work was started immediately after receipt of the pressure vessel on November 30, 1961.

The ANP Hot Shop is ideally suited for work on highly radioactive materials as it is heavily shielded and contains an abundance of remotely operated equipment for handling and viewing. Upon receipt of the pressure vessel in this area, the highly contaminated shielding material on the vessel head was cleaned off and the core was examined with a boroscope through the severed steam line. It was determined that no significant dislocation of parts had occurred during the removal of the vessel from the SL-1 site and its transfer to the Hot Shop. After removing or severing parts connecting it to the core, the head of the vessel was removed, an unexpectedly difficult operation because of the flange and stud deformation.

With extensive photographic coverage to document parts location, loose components lying above the active core region were removed with remote manipulators. These parts included the central control blade, tightly bound in its shroud in a position corresponding to 20-inch withdrawal.

With the vessel in its shielding cask, holes were drilled through cask and vessel to permit a boroscope examination of the under side of the core. This examination not only confirmed that all the control blades except the central one were fully inserted, but showed that the core possessed enough mechanical integrity to permit the performance of a critical experiment. In further preparation for the critical experiment, an 8-3/4 inch hole was cut in the bottom of the vessel, and all loose debris scraped and washed from that region.

The critical experiment, performed in a specially constructed tank, revealed that the core was highly sub-critical, even when filled with water.

Following the critical experiment, the pressure vessel was cut apart and the core completely dismantled. All core components, samples of deposits, and samples of the pressure vessel were subjected to laboratory analysis.

2.3 Health Physics

Because of the high radiation levels and the wide spread of radioactive contamination, health physics monitoring and control played a predominant part in the recovery operations. As previously stated, an entry control point was established in a building near the SL-1 perimeter fence. Through this control point passed all personnel and equipment, both entering and leaving the contaminated area. Health physics personnel were responsible for supervising the dressing and undressing of all entry teams in suitable protective clothing, for briefing entry personnel on the required safety precautions, for monitoring the entry working times and for maintaining adequate records on individual radiation dosages.

Throughout the recovery operation, radiation exposures were controlled to be in accordance with the radiation protection guides recommended by the Federal Radiation Council for exposure to external sources of radiation during normal operations. In spite of the fact that dose rates were extremely high and variable, less than six percent of the approximately 475 individuals involved received doses in excess of the guide values, the highest of these technical overexposures amounting to 16 percent.

The control of waste disposal was also a health physics responsibility. Approximately 80,000 cubic feet of contaminated equipment and material were buried at the SL-1 site. For all material, a log was kept of items buried, location, radiation level, volume, curie content and burial date.

3. Evidence for Evaluation

3.1 Control Rod Positions

Determining the position of all control rods in the reactor at the time of the incident was of primary importance. Consequently, great emphasis was placed upon the examination of any evidence pertinent to this determination. The recovered parts of all control rod mechanisms were carefully inspected and matched. Reconstruction of the severed parts of these mechanisms revealed that all rods except the central control rod were in the normal or shutdown position at the time of the incident. The central control rod, however, was determined beyond all reasonable doubt to be in a 20-inch withdrawn position.

3.2 Vessel Condition

The detailed inspection of the pressure vessel in the Hot Shop revealed that it had been subjected to extremely high pressures. It was bulged radially in several places and the top flange was severely distorted. The nozzles on the top head were also bulged to varying degrees. Subsequent tests made at the Army Aberdeen Proving Ground on a scale model of the pressure vessel produced many of the same distortions.

Inspection of the core revealed that melting or vaporization of the central fuel elements had occurred. The entire core was in a state of severe disruption with many of the core components badly distorted and displaced both laterally and vertically. The entire core was measured to be displaced upward by almost half a foot.

3.3 Flux Wires

Fortunately, new flux wires had been placed in the reactor core prior to the accident. Most of these flux wires were recovered and analysis of them provided a direct measurement of the flux and energy densities for the incident.

3.4 Laboratory Analysis

Chemical analysis was performed in the laboratories on many samples taken during the recovery operations and on the debris recovered from the pressure vessel. Metallurgical analysis was also performed on many samples of fuel elements and other reactor components. These analyses were especially valuable in establishing the range of temperatures and pressures reached during the incident.

4. Analysis and Conclusions

4.1 Initiation of the Excursion

The recovery of the central control rod, locked in its shroud at the 20-inch withdrawn position and with evidence of no relative motion after seizure, definitely established the condition which made the reactor supercritical. The reactor was not normally operated with only the central control rod withdrawn, but from the limited critical experiment data available for this rod configuration, it is estimated that the reactor would have been critical with the central rod withdrawn to 16.7 inches. At the 20-inch position, the reactivity would have been $(2.4 \pm 0.3)\% \Delta k/k$.

Tests on a mockup of the rate at which the central control rod could be withdrawn have shown that manual withdrawal to the 20-inch position could occur in less time than is actually necessary to create the excursion. Other explanations for the 20-inch rod withdrawal have been sought, without success. Chemical tests and examinations of vessel and core components have ruled out the possibility that a chemical explosive lifted the central control rod. Likewise, an explosion of hydrogen, accumulated from the decomposition of water in a radiation field, cannot account for the initiation of the incident. Though positive proof is lacking, all information indicates that the excursion was caused by the manual withdrawal, with less than maximum effort, of the central control rod during the assembly of the rod-drive mechanism.

4.2 The Power Excursion

Following the insertion of approximately 2.4% of excess reactivity, the power rose on approximately a four millisecond period until sufficient steam was formed to end the power increase at $(1.9 \pm 0.4) \times 10^{10}$ watts. At this time,

the plates in the highest flux regions of the core were just reaching the vaporization temperature of 2060°C (at 1 atmosphere) in the center of the meat. However, because of the thick plate cladding, none of the outer cladding surface had yet reached the melting temperature.

During the interval from the start of power decrease to the end of the excursion, 5% of the plate area in the center 16 elements attained vaporization temperature, resulting in the violent destruction of these areas and a very rapid production of additional steam. Throughout 20% of the entire core, melting proceeded to the cladding surface and destroyed these regions of the core.

The total nuclear energy generated was 130 ± 10 megawatts-seconds. The chemical reaction of the hot molten and vaporized plates with water released additional energy which probably was no more than 25% of the nuclear energy release.

4.3 The Effects of the Excursion

The rapid formation of steam in the core accelerated the seven foot column of water above the core and slammed it into the lid of the pressure vessel with an approximate velocity of 160 feet per second. This impact compressed the water to a peak pressure about 10,000 psi, and transferred momentum to the shield plugs and the underside of the pressure vessel head. The shield plugs were ejected from the top head at velocities up to 50 feet per second along with much of the top head shielding. The momentum transferred to the pressure vessel itself sheared the connecting piping and lifted the vessel approximately nine feet in the air. The vessel then fell back into its support cylinder, ripping off some of its insulation which was scattered and eventually found on the operating floor. The time involved in the incident from the beginning of control rod withdrawal to the time that the vessel fell back into its support cylinder was between two and four seconds.

The neutron activation subsequently observed on the operating floor was produced by delayed neutrons, both from the fuel in the vessel during the time the vessel was in the air, and from fuel ejected from the vessel. The activation from the prompt neutrons would have been several orders of magnitude less. On the basis of the best data available, approximately 5% of the gross fission products were ejected from the pressure vessel.

4.4 Analysis of the evidence obtained during the recovery operations combined with the results of other relevant tests and calculations are sufficient to render a reasonable and internally consistent reconstruction of the incident. The data obtained adequately explain the position of all the various objects and the extent of the damage observed. The discovery that 10,000 psi impact pressures had been produced from 500 psi steam identified a new and hitherto unexpected effect, and one that produced an impressive amount of damage from a relatively low yield (130 MW-sec) excursion. The partially filled vessel with its heavy, tightly-bolted lid

made conditions ideal for the production of high impact pressures. In an open top vessel, for example, the most destructive effects would not have occurred at all. The importance of the mode of reactor core containment may be emphasized by pointing out that the kinetic energy which produced all the mechanical displacements observed was less than 1% of the total energy released.

Once the mechanism by which destruction occurred had been identified, existing engineering knowledge was sufficient to account for the observed phenomena. In particular, the underlying assumptions and conclusions as to the quantitative behavior of the reactor are consistent with our current knowledge of reactor safety, and no new theories need be postulated to account for any of the events that occurred.

II. RECOVERY OPERATIONS

1. Site Cleanup
- 1.1 Method of Operation
- 1.1.1 Conditions at Start

The initial radiation measurements were made in the operating room at the start of the Phase 3 recovery operations on May 29, 1961. These measurements indicated that the gamma radiation ranged from 20 R/hr four feet inside the freight door to 100 R/hr over the reactor core. Subsequent measurements revealed that the source of this radiation was widely distributed throughout both the operating room and the fan room above it. A high ratio of beta to gamma radiation existed so that the beta exposure was operationally limiting to personnel working in the building.

Photographs, both those existing at the start of this phase of operations and those taken during subsequent entries, revealed that the operating room was congested with shield blocks and equipment. The shield blocks had been moved back from the head of the reactor prior to the accident and limited access to the operating room to the point where the use of large personnel shields or mobile equipment was severely restricted. A clearance of only three feet of free space existed between the tops of the shield blocks and the bottom of the building bridge crane. Early photographs showed that in addition to the large items of equipment such as bell housings, stretchers, etc., a great deal of debris existed on the floor in the form of blotting paper, insulating material, steel punchings and gravel. The conditions described above are illustrated in Figures II-1 through II-6.

Further complications in the possible use of remote manipulating equipment or personnel shields were imposed by the facts that the operating room floor was some 21 feet above grade and that it was accessible only by two narrow personnel stairways and a cargo door normally serviced by a monorail crane which had been previously dismantled. In addition, the outer portions of the operating room floor would not support large concentrated loads.

Subsequent radiation measurements, described in Section II, 1.3.2, revealed that a significant amount of contamination existed in the fan room above the operating floor. This room was normally accessible only through a vertical ladder and air lock. The virtual impossibility of staging rescue operations through this narrow passage in the event of an emergency precluded its use at any time. The creation of a new entry way to this floor

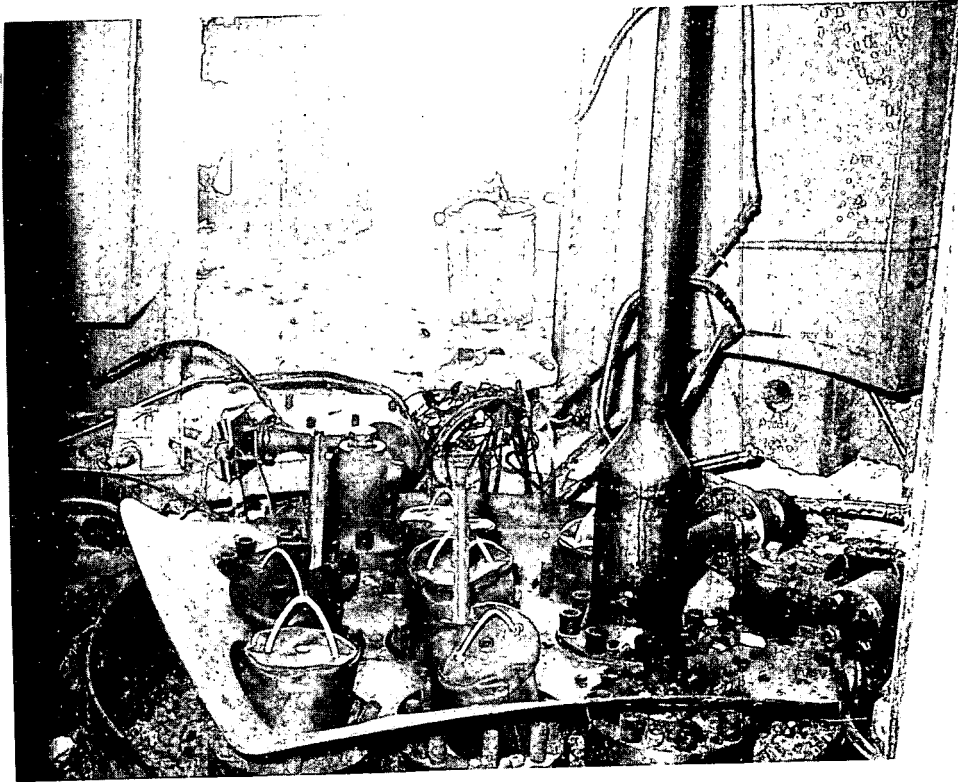


Figure II-1 Reactor vessel head after placement of shield bags



Figure II-2 Steel punchings near head of reactor vessel



Figure II-3 Steel plate and cooling lines displaced by accident



Figure II-4 Insulation on floor between shield blocks

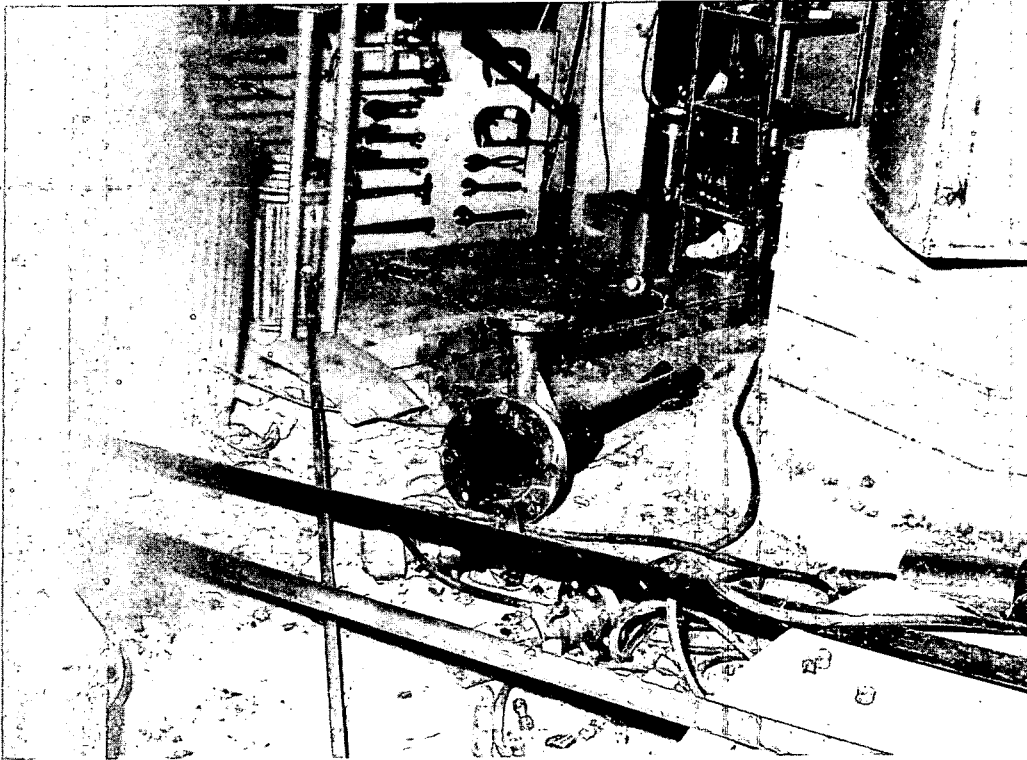


Figure II-5 Equipment and debris on floor of operating room

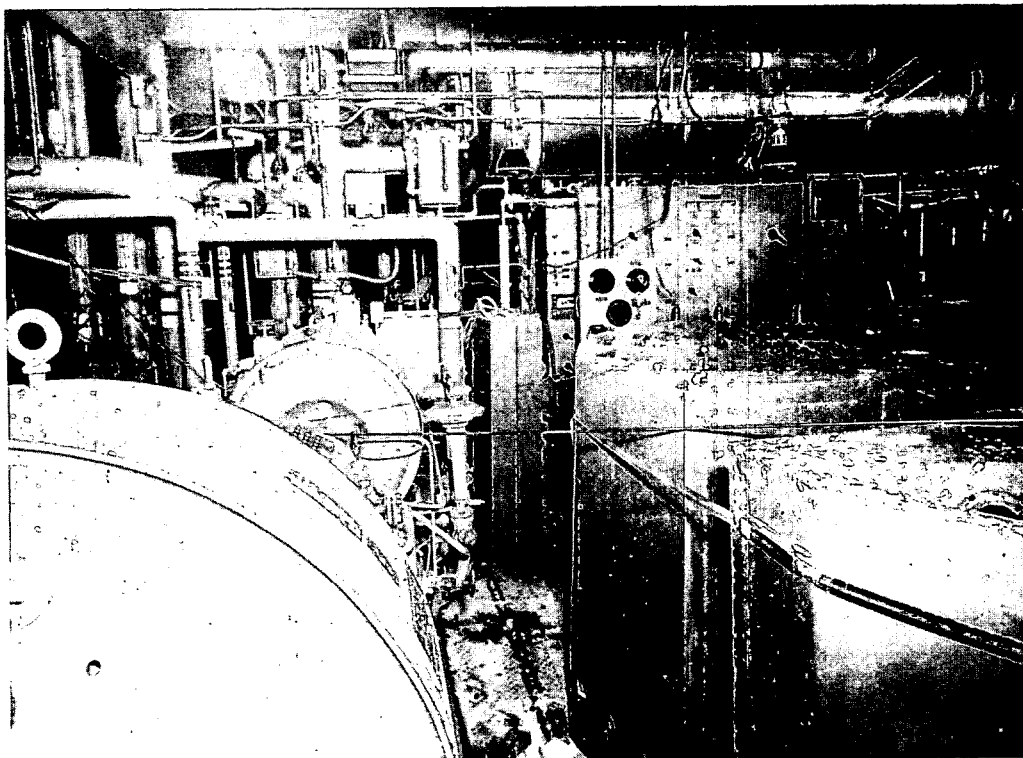


Figure II-6 South side of operating room

required the solution to the problems of erecting a working platform 35 feet above the ground in a radiation field of 1 to 5 R/hr and of cutting through the steel wall of the fan room and the inflammable insulation inside it. The successful accomplishment of this access is described in Section II, 1.3.3.

Two additional complications existed which rendered the recovery operation more difficult than might otherwise have been the case. The first of these was the necessity of avoiding any possibility of renewed criticality of the reactor. The nuclear safety of the reactor was predicated upon the absence of water in the pressure vessel. All recovery operations were undertaken with the requirement of keeping any water from entering the vessel, severely limiting the choice of clean-up procedures. The second complication was the requirement to collect and preserve all possible evidence of the cause and effect of the excursion. This requirement was met by extensive photographic recording of the positions of objects in the reactor building and the subsequent detailed examination and inventory of the items after their removal.

1.1.2 Overall Plans

At the start of the Phase 3 recovery operations, various overall plans to dismantle the core were considered in some detail. The basic choice was between attempting this operation in place at the SL-1 site vs. transporting the vessel and its contents to the ANP Hot Shop at the north end of the National Reactor Testing Station. This latter alternative was greatly preferred, studies having shown it to be the quickest and cheapest method, to permit the earliest restoration of the SL-1 area to useful service, and to provide, by a large margin, the most information relative to the accident. A second series of alternatives involved the addition of shielding material to the pressure vessel in the hopes of reducing radiation levels. Materials such as borated water and sand were considered at some length. It was decided, as a first step, to place bags of lead shot over the open nozzles in the pressure vessel head in order to reduce the presumed streaming of radiation from these openings. This operation, described in Section II, 1.3.1, resulted in negligible reduction in radiation levels. This fact, together with estimates made of the radiation levels from the pressure vessel during transit showed it would be unprofitable to add any material to the pressure vessel for shielding purposes. It was also known that the addition of any material to the vessel ran considerable risk of obscuring or destroying evidence by abrasion, by shifting the relative position of core components, or by inducing additional core damage through impairment of natural afterheat removal. It was decided, therefore, to proceed as rapidly as possible with the cleanup of the building and the reduction of radiation levels so as to permit the removal of the pressure vessel containing the core, and its transportation to the ANP Hot Shop.

1.1.3 Remote vs. Manual Operation

Some of the problems with using remote manipulating equipment to accomplish the SL-1 recovery operations have been described above. In addition, no suitable manipulating equipment was on hand at the start of this operation. Its use would have required skilled personnel and, in general, the operation would have proceeded at a much slower pace. On the other hand, with proper planning and adequate health physics controls, the measured radiation levels permitted useful working times in the reactor building within the quarterly guide values for personnel exposure. It was, therefore, decided to proceed with a manual cleanup and recovery operation, supplemented, where possible, by such remote means as could be devised in a timely manner, and by use of personnel shielding whenever possible.

1.1.4 Personnel

Since quarterly exposures were to be used up in a matter of a very few minutes, it was evident that a large number of personnel would be required for the operation. It eventually developed that approximately 475 people were used including volunteers from the Atomic Energy Commission and the U.S. Army in addition to General Electric personnel.

1.1.5 Control Point

By the time that the Phase 3 recovery operations started, general area radiation levels had decreased so that a new control point for access to the SL-1 area could be established. The temporary control point was a group of trailers on Filmore Boulevard, which had been set up a half mile from the site immediately after the accident. The new control point was in the maintenance building SF-627, approximately 500 feet from the SL-1, which had ample space and utilities. A temporary road was constructed from this building to the back side of the SL-1 security fence. Use of this road made it possible to keep contaminated vehicles off Filmore Boulevard. The new control point was used for assembling and briefing crews, for putting on and removing protective health physics clothing, for the construction, maintenance, and assembly of equipment, and for decontamination. Radio contact was maintained between this control point and the personnel at the SL-1 site itself, but, in general, no attempt was made to control the detailed operations from this 500 foot distance.

1.1.6 Briefing

Because of the large number of volunteers used in the manual recovery operations, it was inevitable that most of them had little or no familiarity with the SL-1 reactor building, nor frequently with the specific type of

work they were asked to do. Furthermore, in many cases they had never worked in a high radiation field nor used protective health physics clothing. In addition, normal supervisory methods could not be used. For these reasons, rather extensive briefing sessions were conducted.

The first step in the briefing was to assemble all of the individuals scheduled to make an entry during the day. A discussion was held which covered the general layout of the building, pointed out specific items of equipment that could be used as landmarks, outlined the general operations which were planned, gave specific instructions on operating the appropriate equipment, described the health physics procedures to be used, and answered any questions that might arise. It was the purpose of these group briefings to familiarize the volunteers with the general procedures and with the conditions in the reactor building so that they could recognize familiar objects and orient themselves readily on entry. A model of the reactor building, drawings, and pictures were used as aids to the briefings.

Following the group briefing, the men were assigned an order of entry. The first man was then given more specific and detailed instructions for the particular job he was to perform. More work was assigned to him than he could be expected to finish so as to minimize the radiation exposure due to time spent getting into and out of the work area. A health physics specialist kept track of the time the man was in the radiation field, and called him out to read his dosimeters after an appropriate interval, as described in more detail in Section II, 3.2. A rescue team (never required) stood by to assist the worker if an emergency arose. Men familiar with the SL-1 were used for the more exacting assignments, if available. Up to date photographs proved to be of considerable value in achieving maximum utilization of radiation exposures expended.

When a man returned to the control point, he was debriefed to find out what he had accomplished. The next man was then briefed on the basis of the previous man's information. During the debriefings a good initial briefing paid additional dividends. If the man had been well briefed he could recall things about the work and area in which he worked that were not in the condition that had been anticipated from previous information. This saved considerable time and radiation exposure.

1.2 Equipment

1.2.1 Remote Operations

All of the remote operations that were undertaken during the Phase 3 SL-1 cleanup made use of an Austin-Western model 580 crane. This crane had been modified by the addition of an electrically driven horizontal auxiliary

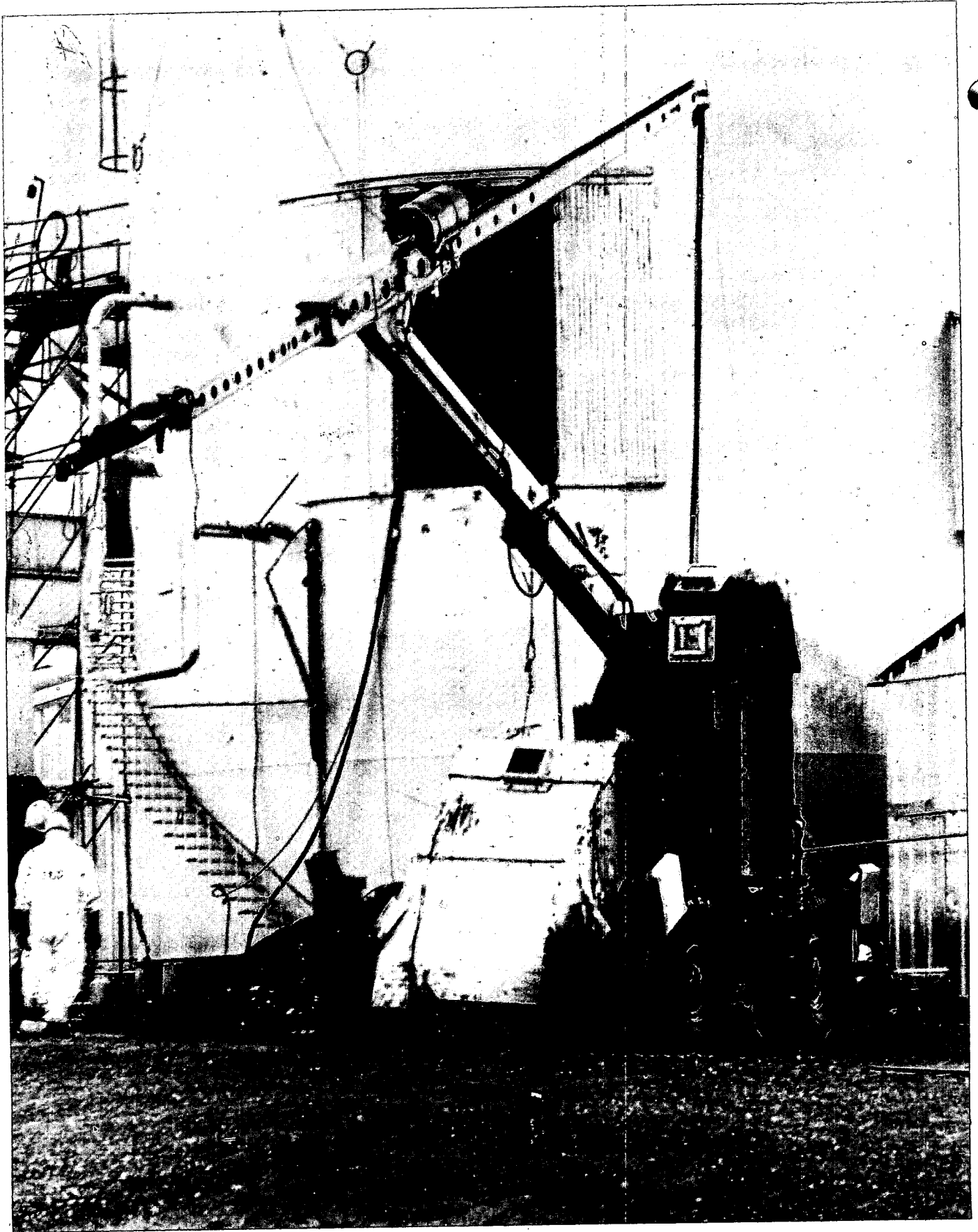


Figure II-7 Shielded crane used for remote operations

boom, which could be raised in a horizontal position to a height of about 35 feet above the ground, a requirement made necessary by the elevation of the operating room. The boom with an extension could reach about 29 feet in front of the crane. This equipment could cover the area over the pressure vessel completely, but could reach less than 20% of the entire operating room, and none of the fan room. A shielded cab with a lead glass viewing window was provided for the crane operator and another shield, similarly equipped with lead glass windows, was provided for the boom operator. A television monitor was also provided for the boom operator. A variety of attachments was fabricated for the end of the horizontal boom. These attachments permitted use of the crane for such jobs as removing buckets of contaminated material from the operating room, placing shielding components over and around the reactor vessel head, removing magnetic material with an electromagnet, and making photographic and radiation surveys. Figure II-7 is a photograph of the equipment with the television camera and boom extension mounted.

The electromagnet used for the remote removal of steel punchings was a "Portamag" plate clamp and lifting magnet manufactured by Lupear Tool Products. The magnet was designed to be used on flat surfaces as a clamp or lifting device and as such as not ideally suited for picking up irregularly shaped objects. The effective surface area of the magnet was about 4" x 16". The magnet was raised and lowered by cable which passed along the bottom of the horizontal boom, then down to a manually operated winch at the auxiliary operator's position.

The equipment used for making the radiation and photographic surveys is shown in Figure II-8. As depicted in this figure, two Bell and Howell 16 mm movie cameras and two collimated ion chambers were mounted in a lead-shielded box. This box provided 1/2 inch of lead shielding for the cameras. The collimators used in conjunction with the ion chambers provided a minimum of 2" of lead shielding for each ion chamber. The beam hole in each collimator was 2 inches long and 0.4 inches in diameter. The box was mounted so that one camera and one ion chamber were pointed directly up and the others directly down. Four Sylvania "Sun Gun" lights were chosen because of their intensity and relatively constant light output over their life span. An aluminum feeler plate, not shown in the drawing, was mounted on the front of the instrument box. This spring loaded plate was mounted so that it would ring a warning bell in the event that the box contacted an obstacle. The radiation detection system used was a Jordan remote area monitor. This system was chosen because of its simplicity, the small size of the ion chamber, and the response time of less than one second.

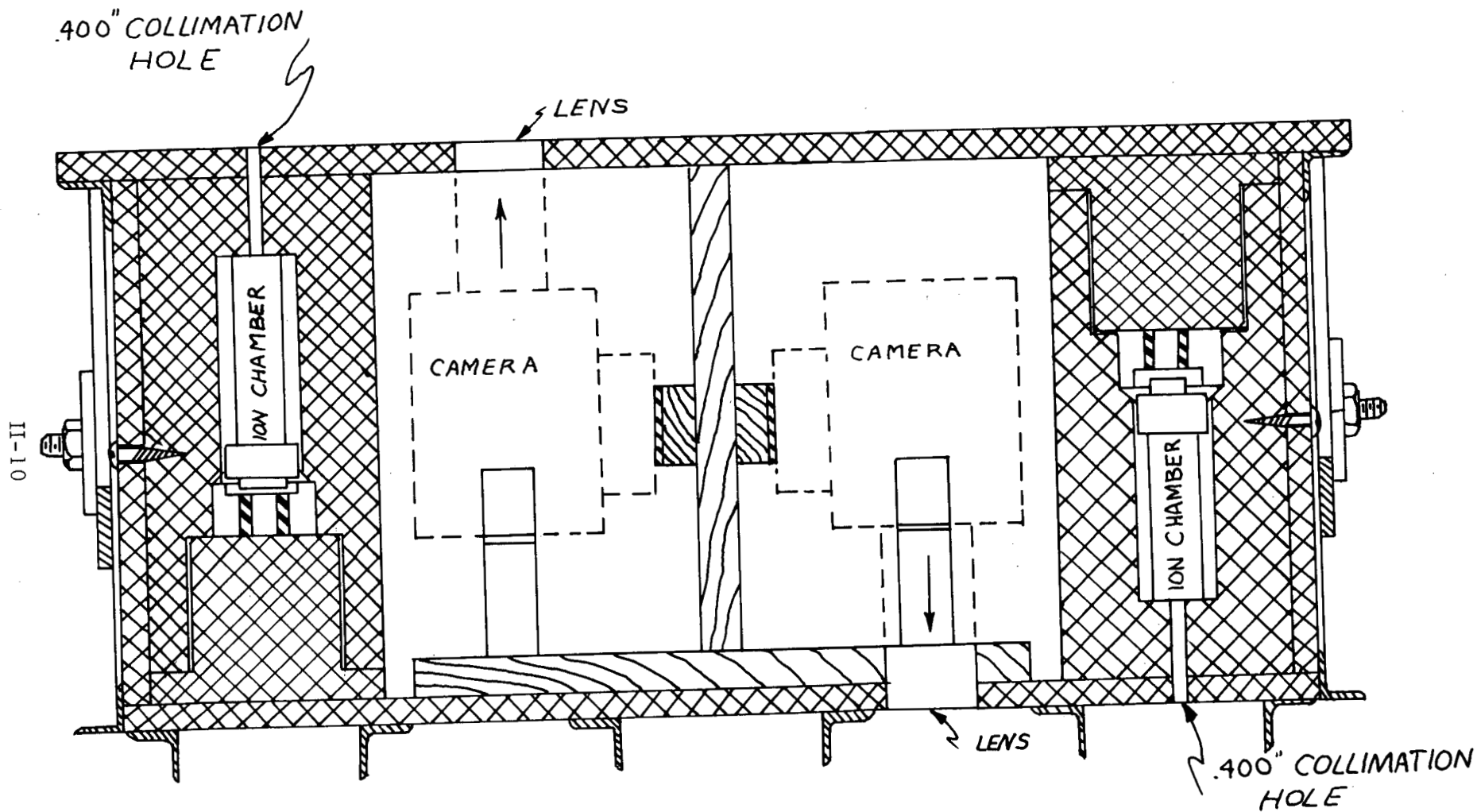


Figure II-8 Camera Shielding Box

1.2.2 Equipment for Observations

Closed circuit television was used extensively as an aid to operations. One camera was mounted on a tripod in the operating room to provide surveillance during manual entries and to assist the Austin-Western boom operator to avoid obstacles. This unit had remote control lens selection and was mounted on a pan and tilt base which allowed complete coverage of the operating floor. Despite the absence of artificial illumination, this camera provided valuable assistance to the operation.

A second television camera with a single lens and a tilt mechanism was mounted on the Austin-Western crane boom. The boom operator was provided with a monitor, and could control the tilt function. This system provided the only direct guide to the boom operator, since he could not see onto the operating floor directly. Without this system, the utility of the Austin-Western crane would have been greatly reduced.

The control circuits and master monitors for both television systems were located in a trailer which was placed behind the SL-1 area water tank for radiation shielding.

During the pressure vessel removal both cameras were used to monitor the operation, and again in the Hot Shop operations (Section II, 2.5) television was vital.

The equipment used for these operations was as follows:

Cameras (with non-browning lenses)	General Electric	4PX33A1
Pan and Tilt	General Electric	PT-10002
Control Console	General Electric	4TH5A3
Monitor	Conrac	CL14A

As has already been mentioned, a great deal of reliance was placed on photography, both to record the position and condition of the equipment in the reactor building, and to serve as a guide during briefing of personnel and cleanup of the building. Several hundred photographs were taken using a hand held 35 mm camera and electronic flash attachment. All pictures were obtained with an F 16 setting on Plus X film. Since the volunteer taking the pictures may have had a scanty knowledge of the SL-1 beyond that obtained in the general briefing just prior to his entry, it was found most effective to specify in considerable detail the location and direction of each picture rather than to permit the photographer latitude in shooting items of interest. By this technique it was possible to obtain 20 pictures in less than three minutes.

Photographs inside the pressure vessel were taken through the plug nozzles during the later stages of recovery at the SL-1 site. For some of these pictures, the 35 mm camera and flash attachment was lowered through the nozzles. For other pictures, a 16 mm motion picture camera and a 30 inch long boroscope were used, both looking straight down, and with a mirror looking up at the under side of the pressure vessel head. The 16 mm movie photographs looking straight down, with an exposure rate of 8 frames per second and using the illumination from three "Sun Guns", resulted in pictures which were under exposed on Kodak Plus X film. By hand cranking of the camera, longer exposure times were obtained providing quite satisfactory pictures. For the 35 mm pictures, the camera was equipped with a wide angle lens focused at 2.7 feet and exposures were made at 1/50 of a second, F22, using one electronic flash light and Kodak Panatomic X film. The camera was manually withdrawn and the film advanced between each shot. It was possible to take about 9 exposures in this manner before radiation darkening of the film became a serious problem.

During the later stages of the recovery operation in the Hot Shop, a 35 mm camera with an automatic film advance was obtained. This camera, held by a remote manipulator, was able to take approximately 12 frames in a period of 2 minutes in the core region itself without losing significant detail from radiation fogging of the film. In the Hot Shop a press camera held by a manipulator over the open pressure vessel was also used extensively to record the location of components in the vessel. Stereo pictures were also taken using this technique.

Photographs were taken underneath the core at the SL-1 site and later in the Hot Shop. At the SL-1 site these photographs were taken through a 26 foot long boroscope 1-3/4 inches in diameter. The photographs were made with a 35 mm camera using a half second exposure on Kodak Plus X film with light from a single 1000 watt light bulb mounted on the end of the boroscope. A total of 46 photographs were taken in this manner.

The equipment used for photographic operations included the following:

35 mm cameras:

Praktina Fx
Exakta VX
Nikon F

Strobe light:

Meteor II Ultrablitz Strobe

Movie Cameras:

16 mm Bell and Howell Model 70

1.2.2 Pinhole Camera

A pinhole camera, furnished by the U.S. Naval Radiological Defense Laboratory, San Francisco, was used to locate sources of high radiation. The camera held a 4 x 5 film holder, in which was placed a piece of light sensitive film, a sheet of black paper and a piece of gamma sensitive film. These films were stapled together to provide line up marks for superimposing the two negatives during later comparisons. A conventional picture and a gamma picture were thus obtained with a single exposure. By comparing the two pictures, the radiation sources could be located.

Exposures were made for 24 hours on X-ray film for the gamma photographs. The light sensitive exposures depended on the level of illumination, but were nominally one hour in most cases.

Pictures taken outside the building were useful mainly in confirming the fact that there were high intensity sources on the fan room floor above the operating room. Photographs taken later inside the fan room showed areas of high contamination on the floor, the condenser, and the fan drive, thus assisting the cleanup and equipment removal operation. No attempt was made to determine source strength from the photos since there were many variables involved and an extensive experimental calibration would be required.

In order to get pictures inside the building, it was necessary to make three entries: first to position the camera, second, to terminate the light sensitive picture and third, to remove the camera. Because of the high radiation fields, these operations frequently resulted in an exposure to one man of between 1/2 and 2 R for each picture. This points up the desirability of equipment for remotely positioning the camera, and of a remotely operable shutter, for extensive use in an application such as this. The field of view of the camera was quite narrow so that a single picture taken inside the building covered only a relatively small area. For a general area survey a large number of pictures would have been required. Since an exposure time of approximately 24 hours was required for each gamma picture, any extensive survey would have become quite costly, both in terms of personnel exposure and of delay to subsequent operations.

The lead shielding on the back and sides of the camera was adequate as long as the source was in front of the camera. However, if there was a strong source behind the camera, the film would be fogged from this source to an extent that obscured the picture. It was impractical to consider a greater thickness of shielding if the camera were to be positioned manually since its weight was all one man could handle.

1.2.3 Cleaning Equipment

Considerable manual cleaning was required in the SL-1 building. The equipment used included brushes, dust pans, brooms, square-nose shovels, 5 gallon buckets with lids and locking bails, 55 gallon open barrels with bails, and 4' x 8' x 4' deep box with bails for crane handling.

Two vacuum cleaning systems were extensively used and proved to be an important method of reducing radiation and achieving cleanliness.

The first system used two 1-1/2 horsepower "Tornado" centrifugal blowers mounted in a cast aluminum head which was secured to the open end of a 55 gallon drum. The inlet to the drum was arranged to give a centrifuging effect to increase the amount of material which would be dropped out in the barrel. The blowers drew suction from the barrel and exhausted into bag filters, the flow from which passed through an absolute filter and then to the atmosphere. All this equipment was outside the building with a long 2" ID vacuum hose running to the work area.

The second system used a positive displacement Roots-Connersville Model AF60 blower driven with a 15 HP electric motor. This blower drew from an absolute filter, bag filters, and a centrifuging barrel in series. This system was also mounted outside the building with a long hose to the work area. This second system proved to be more effective because of its ability to operate at a higher pressure ratio, especially at low air flow conditions. This system also incorporated an improvised 5 gallon collection bucket in the work area near the end of the hose to alleviate any plugging problems.

In both systems the radiation from the centrifuge barrel built up sufficiently (as high as 500 R γ at the surface of the barrel) to make shielding of this barrel advisable. This was accomplished by building a barrel shaped shielding cask, with 3 inch thick lead walls, into which the vacuum barrel was placed. The bag filter radiation level was approximately 10% of the barrel level and the absolute filter radiation level was approximately 10% of the bag filter level. Thus these two components constituted much less of a radiation problem.

The most commonly used vacuum tools were an 18" wide floor brush, a straight piece of 2 inch tubing, and a crevice tool consisting of 1-1/2 inch tubing flattened to a 1/4 inch gap and cut off at an angle.

A portable steam generator was used for equipment decontamination at the control point and later for building decontamination. Detergents used with

the steam ranged from green soap to caustic solutions for the more difficult decontamination problems. Extremely cold winter weather led to problems of water line freezing and fuel line freezing (in the case of LP gas fuel).

1.2.4 Cranes and Truck

Besides the Austin-Western crane, described previously, considerable use was made of a 25 ton, self-propelled, rubber tired Link-Belt crane. The boom was standard type with 5 foot, 10 foot and 20 foot sections for boom length changes. No boom jib was used although the use of a 10 foot jib is recommended for similar jobs. The operator's compartment was shielded with 1/2 inch of lead on the front incorporating an equivalent lead glass shielding window.

For the heavier lifts, particularly the pressure vessel, a 60 ton Manitowac Model 3900 crane was used. A shield of 5-1/4" of steel topped by a 9" thick lead glass window protected the operator.

For material transfer inside the SL-1 contaminated area, a large double axle dump truck was used. Material transfer outside of the SL-1 area was accomplished with a smaller flatbed truck of 3-ton capacity. This truck had the bed clad with steel, a 2-3/8" steel shield for the driver, was painted to facilitate decontamination, and carried a containment cask which would accept various liners or other receptacles. In practice, the crane would pick up a liner full of contaminated material which had been delivered to the control point and place it in this containment cask. The containment cask would then be closed, sealed, and the truck and cask decontaminated as necessary. The truck could then transport the material to the ANP Hot Shop without risk of contaminating the roadway. A similar technique was used for unloading.

1.3 Cleanup Operations

1.3.1 Operating Room

The first entry was for the purpose of shielding the control rod actuator nozzles in the top of the reactor head. This was done remotely, using the Austin-Western crane to position specially shaped bags of lead shot in each of the nozzles. A television camera was mounted on the boom of the crane, with a monitor at the operators position to allow the bags to be accurately placed. A remote reading radiation instrument was also mounted on the crane boom. Its readings demonstrated that, while the narrow beams from the nozzles were eliminated, the general radiation field, even in the area of the reactor head, was not decreased noticeably.

The second entry was performed by personnel to drain the demineralized water tank (which was full) and the hot well tank (which was empty) through hoses to the outside of the building. This removed the possibility of this water draining into the reactor. In addition, one man made a radiation survey around the outside of the shield blocks. The results of this survey are reported with the Health Physics section of this report (Section II, 3.0).

The next entries were for photographic recording of conditions. A 35 mm camera with electronic flash gun was used. The lens aperture, shutter speed and focusing were fixed and the entire camera, except for the front of the lens and the winding knob covered with plastic and taped to prevent contamination.

With the photographic information in hand, the cleaning of the operating room was started. The cleaning operations were divided into several major steps. The first step was to remove manually all of the large items such as step ladders, bell housings, lifting fixtures, etc. Smaller loose items such as tools were also picked up.

Next the area around the outside of the shield blocks was cleaned by scooping or throwing the larger debris into garbage pails and vacuuming up the fine debris. This cleaning operation started in front of the covered entrance of the operating room and progressed around the outside of the shield blocks. An effort was made to keep from recontaminating the cleaned areas, but in some cases this was impossible. If a man noticed that a previously cleaned area had some more debris scattered on it, he vacuumed that area again.

In addition to cleaning, some of the sources were shielded and left until the general field had been lowered or, in the case of the top of the reactor, until cleanup could be accomplished remotely in the Hot Shop.

The next area cleaned was between the shield blocks and between the shield blocks and the reactor. There were large amounts of steel punchings in this area. These punchings were stuck together with a mixture of rust and boric acid, consequently they had to be broken loose from the floor. The best implement for this job was a square-nosed shovel. The lifting-lug wells on the tops of the shield blocks were also cleaned during this operation.

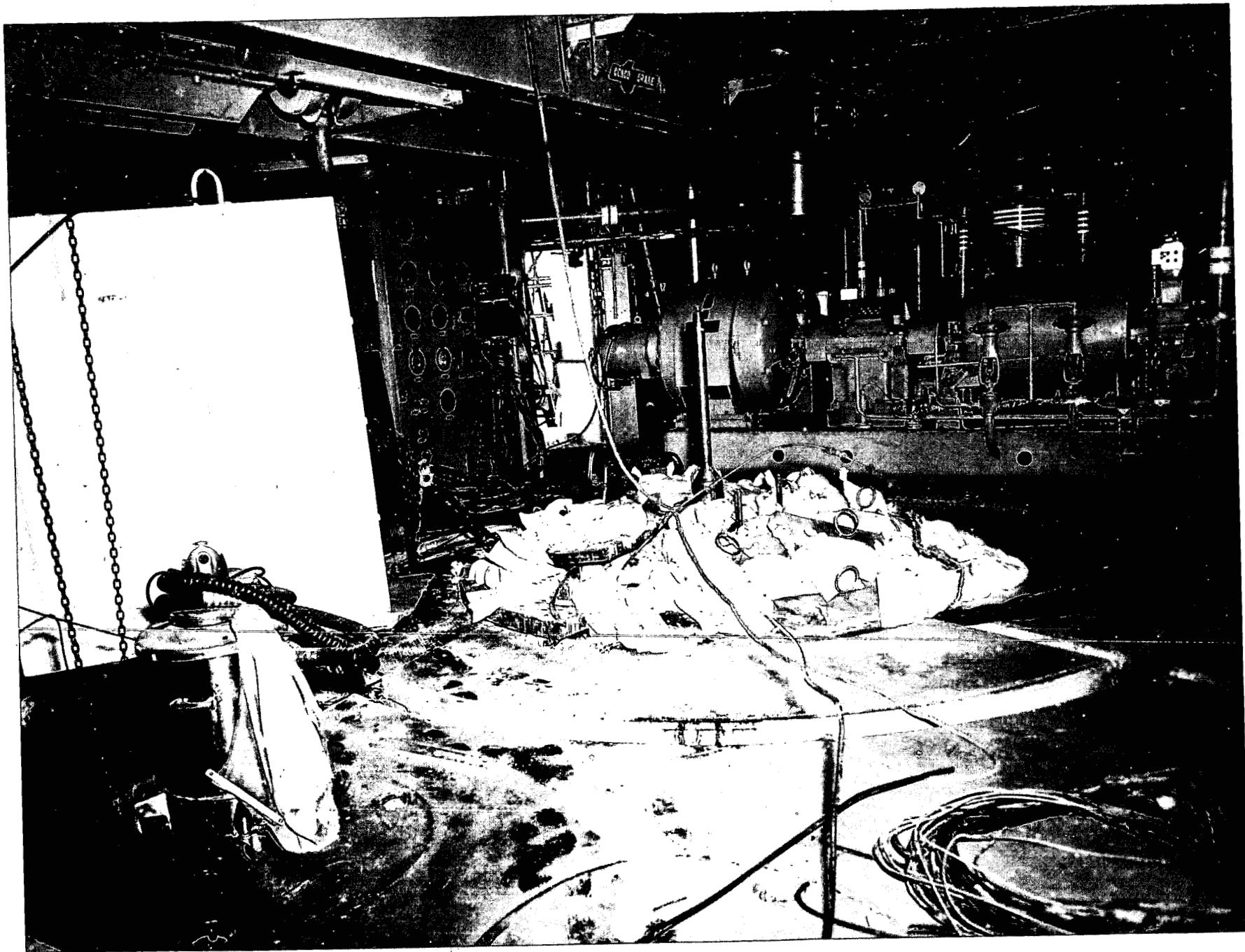
Since the general field was still too high to carry out the involved cleaning operation required for the top of the reactor, it was covered with bags of shot. This had a rather marked effect on the radiation field within the area enclosed by the shield blocks.

During the cleaning around the shield blocks, it became evident from the exposure of the individuals that the area behind and at each end of the turbine-generator was a high radiation zone. This was cleaned next and one 400 R/hr hot spot was removed. At this point, it was decided that the cleanup of the operating room had proceeded as far as it could without removing the shield blocks. For this reason the building bridge crane was repaired and the remaining shield plug that had been lodged in the ceiling was removed to allow full travel of the bridge. After the repairs on the bridge crane were completed, the shield block removal was started. This operation was complicated by the fact that the cargo doors could not be reached with the bridge crane and the monorail crane running to the cargo doors had been dismantled shortly after the incident. The blocks, which weighed up to 19,600 lbs., could not be skidded on the rough floor, and exceed the safe floor loading between beams. To resolve these problems, a heavily greased steel plate 1/4" thick was inserted through the cargo doors. A piece of plywood or skid was laid on the plate and the bridge crane used to set a shield block on the plywood or skid. A cable connected to a tractor on the ground was then attached to the shield block and it was slid out through the cargo doors and allowed to drop onto a pile of sand at the base of the building. This method of removing the shield blocks worked very well.

Removing the shield blocks uncovered more debris thus causing the general field in the operating room to increase. The floor was swept and vacuumed again, the wire trenches surrounding the reactor were uncovered, the wires cut loose with bolt cutters and removed, and the trenches vacuumed.

At this point a thorough manual radiation survey was taken. This survey revealed that there was a source under some of the steel floor plates where the contaminated water had leaked through the cracks between the plates. The center section of the fan room floor was also contributing materially to the radiation levels in the operating room. The vertical surfaces of the operating room were a third general source. From these surveys it was apparent that any further significant reduction of the radiation field in the operating room would involve a large amount of effort. After some consideration it was concluded that the general field in the operating room was low enough that the dose received by the majority of the persons working on subsequent operations preparatory to removing the pressure vessel would be governed by the sources they were required to uncover and how they conducted themselves around these sources. Experience proved this to be so.

II-18



U-5043-1

Figure II-9 Operating Room Floor

Figure II-9 is a general view of the operating room floor. The wire from the wire trenches had not been removed from the operating room when the photograph was taken. The large white object at the left is a personnel shield consisting of 1" thick slabs of steel welded together to form the top, front, and right side of a 5' x 5' x 6' cube.

The first operation undertaken following the decision to dispense with further general cleaning of the operating room was the cleaning and re-shielding of the top of the pressure vessel. Initially it was planned to remove the shield can cover and vacuum out all of the steel punchings remaining in the shielding can on the top of the pressure vessel. An attempt at vacuuming was made and revealed that the punchings were stuck together and that it was impractical to try to vacuum all of them out; therefore, only the loose punchings were vacuumed up. Since the remaining punchings were highly contaminated, the larger cavities in the punchings were filled with bags of shot. Finally the shield can was filled to within a half an inch of the top of the control rod nozzles with loose shot.

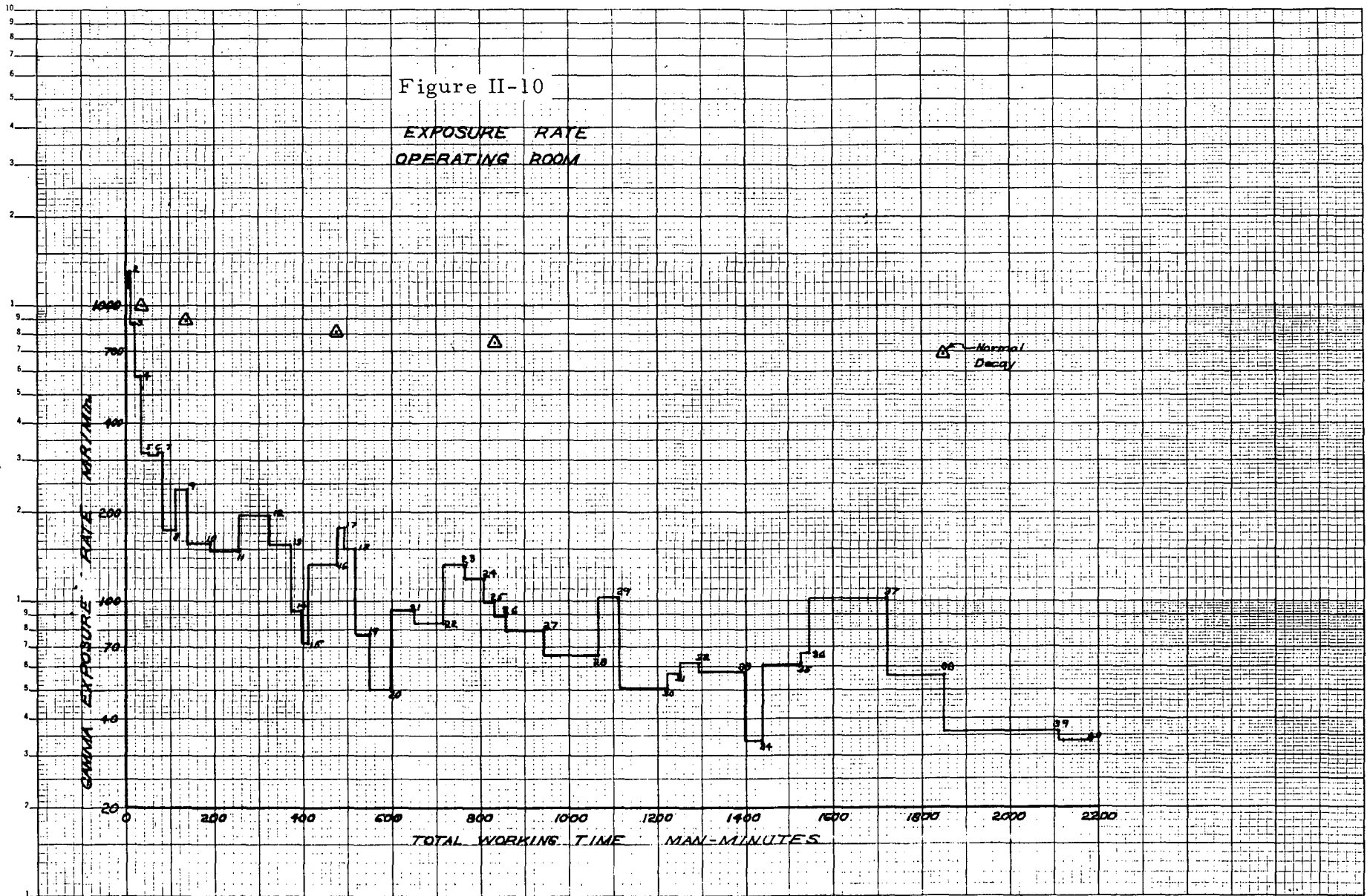
The final cleaning operation prior to lifting the pressure vessel was the cleaning of the air gap between the operating room floor and the head of the pressure vessel and its shielding can. As a result of the incident this air gap was filled with a mixture of insulation, punchings, and water. As the insulation dried out the whole mass solidified, so that cleaning was not easy. The vacuum system with a separator bucket near the cleaning tool was used and worked quite well for this operation.

The exposure rate in the operating room versus accumulated man-minutes is shown in Figure II-10. It should be pointed out that the dose rate shown on the curve was obtained by dividing the total film badge exposure for all of the people entering the operating room on a particular entry by the total time on the floor accumulated by those particular people. Also the man-minutes shown are for all people that entered the operating room regardless of whether they cleaned, took pictures, or made radiation surveys.

The most noteworthy feature about the curve is the large reduction in exposure rate obtained by the first few cleaning entries when compared to the normal decay curve above. The big items were thrown out of the building and the smaller pieces of equipment picked up during the first three entries, which resulted in a reduction of a factor of about three in the dose rate. Entries 4 through 11 were of the same general nature except that some vacuuming was done. These first 11 rough cleanings resulted in a total reduction of a factor of about 8.5. This large reduction points up the extreme value of the initial rough overall cleanup of the operating room. Also, it becomes evident that it would have been very helpful had the operating room been kept free of extraneous tools, fixtures, and equipment during normal operation and maintenance.

Figure II-10

EXPOSURE RATE
OPERATING ROOM



During work periods 12 and 13, the floor between the shield blocks and between the shield blocks and the top of the reactor was cleaned. Work period 12 is a good sample of how the exposure rate increased when a new area was cleaned. Work period 13 then shows a decrease in the field as that particular area was cleaned thoroughly.

Entries 14 and 15 are good examples of how the exposure rate varied according to the local area in which the men worked. The individuals involved in these two entries were carrying bags of shot from the cargo doors, a relatively cool area, to and placing them over the reactor, a relatively hot area. Again the dose rate decreased as the job progressed.

The exposure rate increased again for work periods 16 and 17 because the cleaning was carried out in the previously uncleaned area behind the turbine-generator.

The dose rate stayed fairly high for work period 18 because the individuals were working near the operating room ceiling which was never cleaned and was therefore fairly hot.

Entries 19 and 20 were low again because the people who were preparing to remove the shield blocks were working in the vicinity of the cargo doors.

During the operation of removing the shield blocks, the dose rate increased as is shown on entries number 21, 22 and 23. This was due to the fact that the shield blocks had voids under them that had become filled with debris at the time of the incident.

Recovery operations 24, 25 and 26 represent the floor cleanup after the shield blocks had been removed. It is interesting to note that the people worked in the same general areas for recovery operations 21, 24 and 26; and the dose rate for recovery operation 26 was almost the same again as for 21.

The wire trenches were cleaned out on recovery operations 27, 28 and 30. As mentioned previously, at the end of operation 30 it was decided to discontinue any further cleaning in the operating room until a new vacuum cleaner could be secured and then to uncover the top of the reactor and clean it. This decision was based on the feeling that the general background was low enough that the exposure rate for subsequent operations up through the removal of the pressure vessel would be determined by what was uncovered. Photo entries numbers 29, 31, 34 and 36 which required that the vessel head nozzles be uncovered are evidence that this was a good decision. The large variation in dose rate for different individuals while the actual fields remained constant showed that the dose rate was set by the manner in which the individual conducted himself around the beam from a control rod nozzle.

On recovery operations 35, 36, 37 and 38, the top of the reactor and the air space were uncovered and cleaned. On entry 37 the area under the seal coolant line access plate was cleaned and one garbage bucket reading 50 R/hr was collected. After this bucket was removed the dose rate went down markedly.

The individuals involved in recovery operations 39 and 40 were preparing for the trial lift of the pressure vessel and spent large portions of their time near the outer edges of the operating room floor, hence their low dose rate.

It can be seen from this summary of exposure rates that after the first few entries a man's exposure rate should have been predictable. This was the case and the predictions were used effectively to aid the health physicist in determining the working time of a man before checking his radiation dosimeters.

1.3.2 Radiation Surveys

The incident at the SL-1 scattered large amounts of radioactive contamination about the reactor operating room and fan room. It was decided to concentrate the initial cleanup on the operating room floor because abbreviated manual and remote radiation surveys showed the major source to be in the operating room and because the fan room was relatively inaccessible. It was also decided that a series of remote radiation and photographic surveys should be conducted for the following purposes:

- To assess damage and locate equipment and debris.

- To insure the safe and efficient use of manpower by evaluating the radiological feasibility, risk and consequences of specific proposals during the planning stage.

- To locate the hottest sources in order to establish the methods and sequence for removing or shielding these sources.

- To check the effectiveness of the particular method used to remove or shield a source.

- To record the location of the items in the operating room and the progress of the cleanup.

- To assist in briefing of personnel and in estimating potential dose rates for specific assignments.

Of the three doors leading into the operating room, the best for conducting remote operations through was the cargo doors. These doors extended the full height of the operating room and opened to a width of 8'-4". The area between the doors and the reactor was fairly clear of obstructions.

Due to the height of the operating room floor above ground an Austin-Western hydraulic crane, described in Section 1.2.1, was used to position the instruments within the reactor building. Since it was desirable to be able to duplicate traverses on subsequent entries, the following procedure was used. The crane was located on the centerline of an entry by the use of pointers on the crane and a guide rope on the ground. The horizontal distance of the end of the telescoping boom from the edge of the building and the elevation of the horizontal boom were determined by hanging a plumb bob from the telescoping boom and then positioning the crane and boom such that the plumb bob just touched the lower edge of the cargo doors.

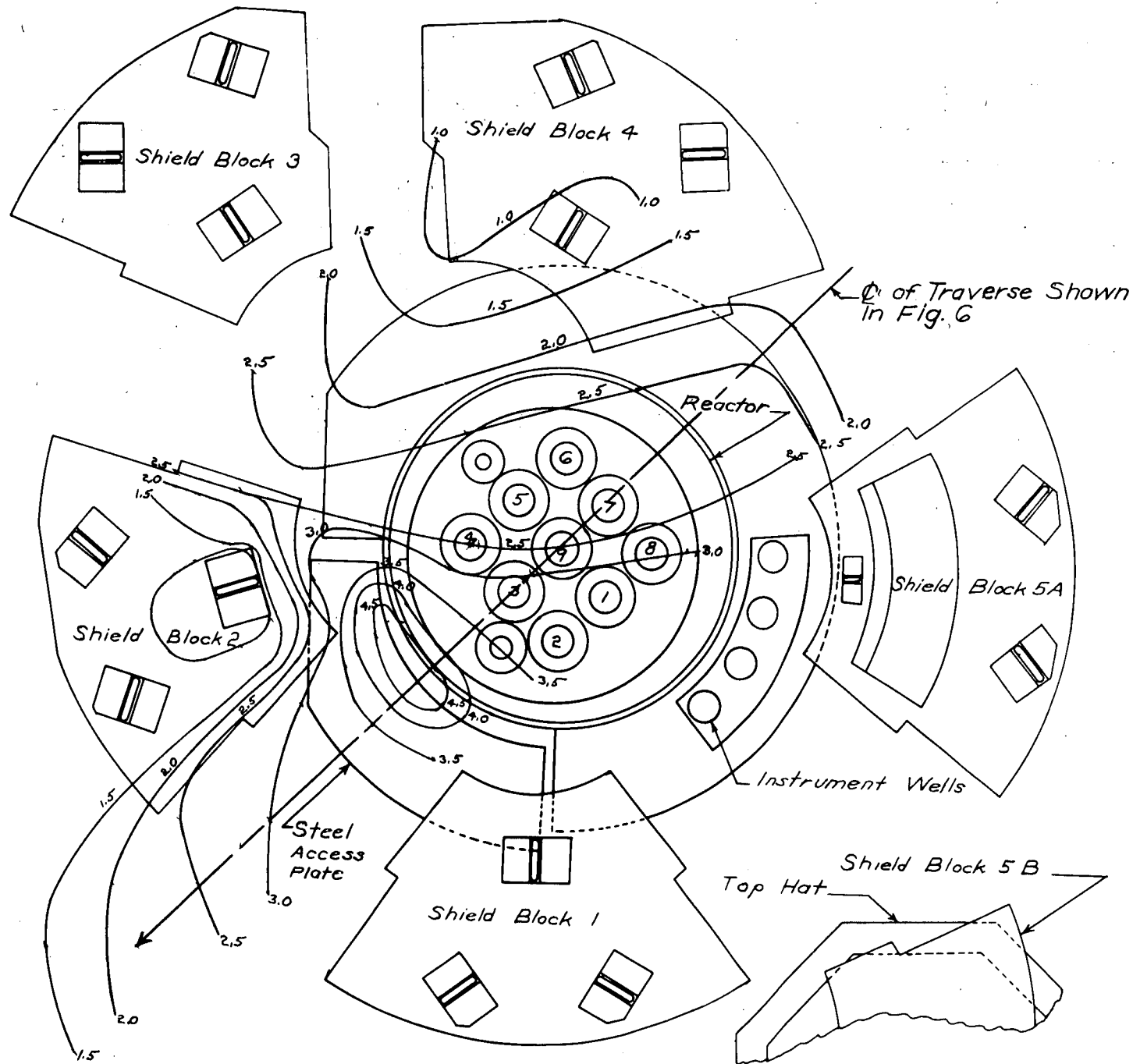
The boom was leveled by the use of a small spirit level mounted on the lower end of the telescoping boom. At the time of mounting, this level was adjusted so that it indicated level when the end of the horizontal boom was at the same elevation either fully withdrawn or fully extended. This method of leveling and positioning the boom was independent of the slope of the ground and of the deflection of the loaded boom.

The system was calibrated initially using a well type of calibration rack. The calibration rack and source were calibrated with a Victoreen Model 570 Condenser R-meter. The ion chambers used with the R-meter were Models 552 and 553 which had an accuracy of $\pm 5\%$. A cobalt 60 source was used for the calibration.

After the calibration well had been calibrated with the standard dosimeter, the collimator to be calibrated was placed so that its center of detection was in the same location formerly occupied by the standard dosimeter. The Jordan system was then calibrated to read the same over its range as the standard uncollimated dosimeter had read in the calibration rack. Over the period of several days between calibrations, the Jordan system drifted quite badly. As a result of this, a portable calibration rack was built so that the Jordan system could be calibrated in the field.

A check of the angle of collimation of the collimator revealed that the reading from a point source was reduced by a factor of six as the source was moved off the centerline of the collimator a distance equal to its distance from the center of detection.

The equipment was assembled on the Austin-Western crane and checked out at the shop and maintenance area. The crane was then driven to the SL-1 area and power connections and connections to the radiation detection equipment were made. At this point in the proceedings, on the entries



Note: Readings in R/hr

Figure II-11
ISODOSE MAP
OF ROOM FLOOR
SURVEY 6-14-61

subsequent to the July 14, 1961, entry, the ion chambers were calibrated with a portable calibration rack. After complete operational checks had been performed, the entry into the building with the crane boom was made.

For a particular traverse, the boom was rotated to a pre-selected angle from the entry centerline and the horizontal boom extended by jogging so as to feel for obstructions. All of the operations within the buildings were observed on a television monitor that had its remote controlled camera mounted in the operating room.

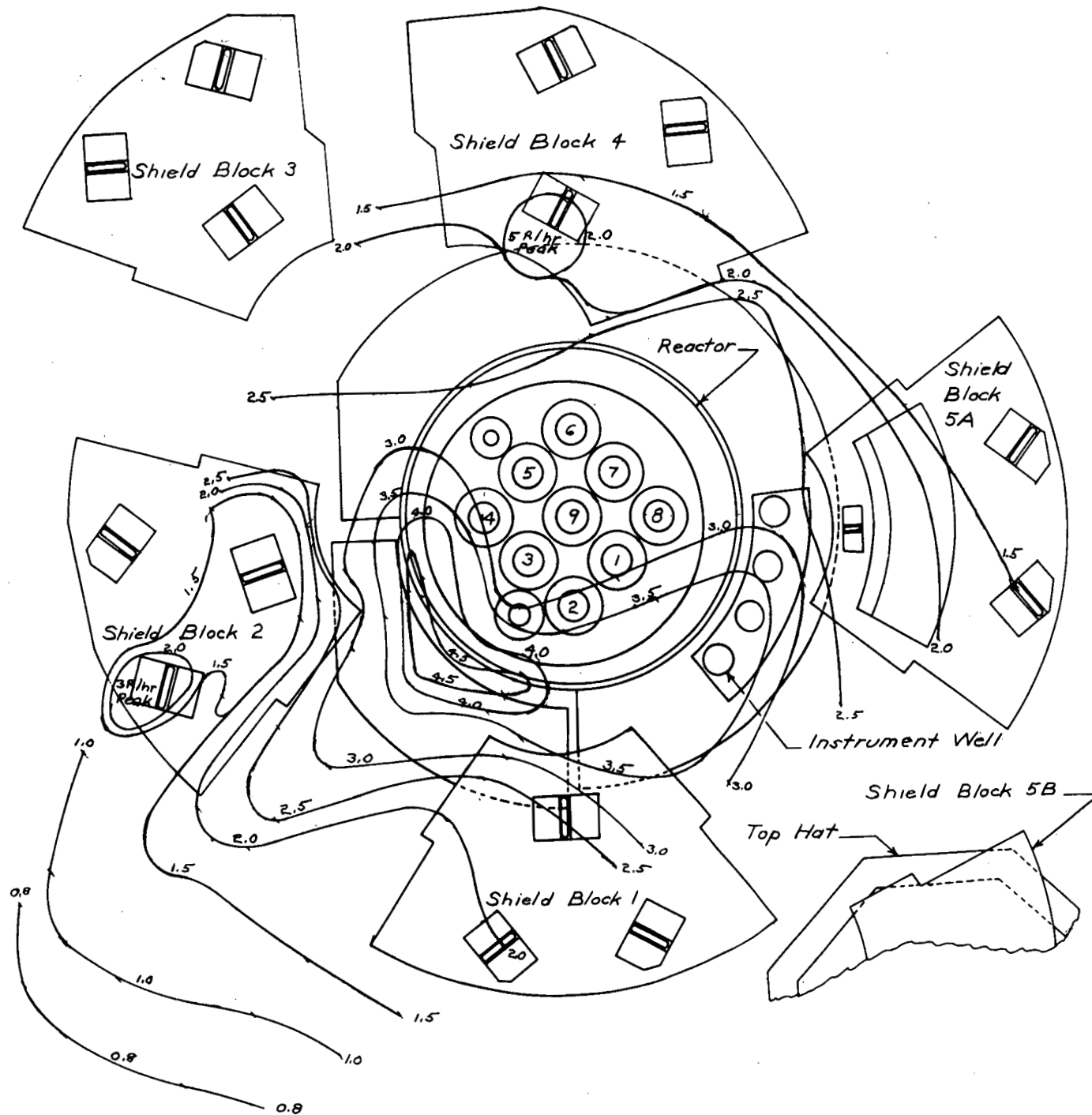
After the horizontal boom had been fully extended, the instrument control circuits and the boom withdraw switch were energized. Energizing the boom withdraw switch simultaneously started the recorder chart drive, turned on the lights, and started the camera drive motors. Once started, the horizontal boom was withdrawn at a constant speed until its limit of travel was reached at which time it was stopped and all instruments turned off.

The above procedure was repeated for four traverses at which time the crane was backed away from the building and the cameras reloaded for another entry of four traverses.

Although the above procedure for positioning was used in order to be able to repeat approximately the location of the traverses from entry to entry, the location of the traverses for plotting the isodose maps could be determined more accurately from the motion pictures.

An isodose map for the first radiation survey of the operating room floor is plotted in Figure II-11. This survey confirmed that the highest level source was within the area enclosed by the shield blocks. Within the confines of the blocks the source was fairly well distributed except for a peak in the area where the 3" thick steel access plate for the seal coolant header was blown back. The fact that the radiation level in this area had a fairly high, sharp peak imposed on a fairly broad base would indicate that there was a high intensity beam coming from the space between the pressure vessel head and the steel plate as well as a distributed source due to fission products being expelled through the opening as the plate was pushed back.

It is not possible to tell from the radiation survey if the beam was coming from fission products in the space between the support vessel and the pressure vessel or from the core itself. At the time of the survey this particular beam appeared to be the only one coming from the reactor itself, indicating that bags of shot that were placed on the control rod nozzles at the start of the cleanup were effective in stopping streaming from the nozzles.



Note: Readings in R/hr

Figure II-12

ISODOSE MAP
OP. ROOM FLOOR
SURVEY 7-5-61

The photographs revealed quite a bit of debris scattered across the operating floor in the spaces between the shield blocks. The isodose curves also indicated that the amount of visible debris was a good indication of the degree of contamination of an area.

Individual traverses exhibited peaks over some of the lifting lug wells on the shield blocks. This accented the impression that wherever water could collect the degree of contamination was high.

Figure II-12 is an isodose map for the operating floor obtained from a survey taken on July 5, 1961. This survey covered more area than the previous survey. Although some of the individual isodose lines are shaped slightly different in the two plots, the plots in general are quite similar.

Figure II-12 shows a decrease of a factor of between 1.5 and 2 in the radiation intensity emanating from the floor in the area between shield blocks 1 and 2 and the cargo doors as compared to that shown in figure II-11. This is due to the fact that the floor in this area was vacuumed between entries. The greatest reduction came in the area that read the hottest before cleaning.

Figure II-13 is an isodose plot for the ceiling of the operating room. There are two main points of interest concerning this curve. The first is that except for the hot spot from the displaced plate, the operating room floor was only twice as radioactive as the ceiling. This indicated that vacuuming the operating room floor would lower the dose rate to a point where the portion contributed from the fan room would become limiting.

Secondly, the valley in the isodose curve between the reactor and the cargo doors indicates that the major portion of the downward streaming radiation was coming from the fan room floor rather than from the ceiling of the operating room. If most of the contamination had been deposited on the ceiling it would have been deposited on the crane also and the collimator would have seen no valley. Also, the radiation levels would have been lower on the side of the bridge crane away from the reactor because that portion of the ceiling would have been protected by the bridge crane from contamination.

Figure II-14 is an isodose plot of the operating room floor after the debris had been scooped up and vacuumed from the floor around the reactor and bags of shot had been piled over the top of the reactor. A steel plate and bags of shot had been placed over the hot spot next to shield block 2. This shielding was responsible for the reduction in source strength in the area directly over the reactor. Cleaning reduced levels in the area surrounding the reactor by a factor of 6 in the hottest areas and by a factor of 1.5 in the areas that had been vacuumed previously.

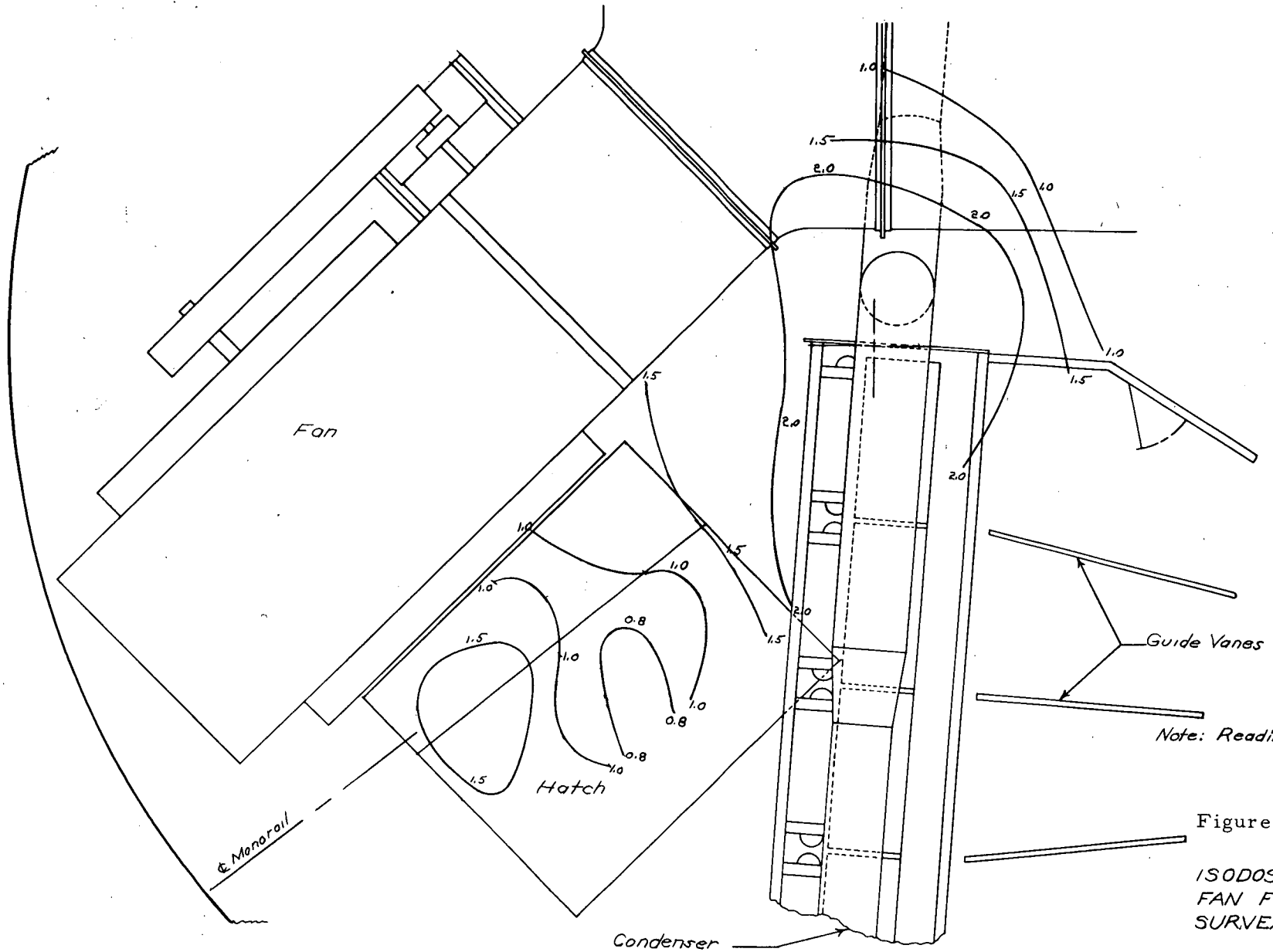
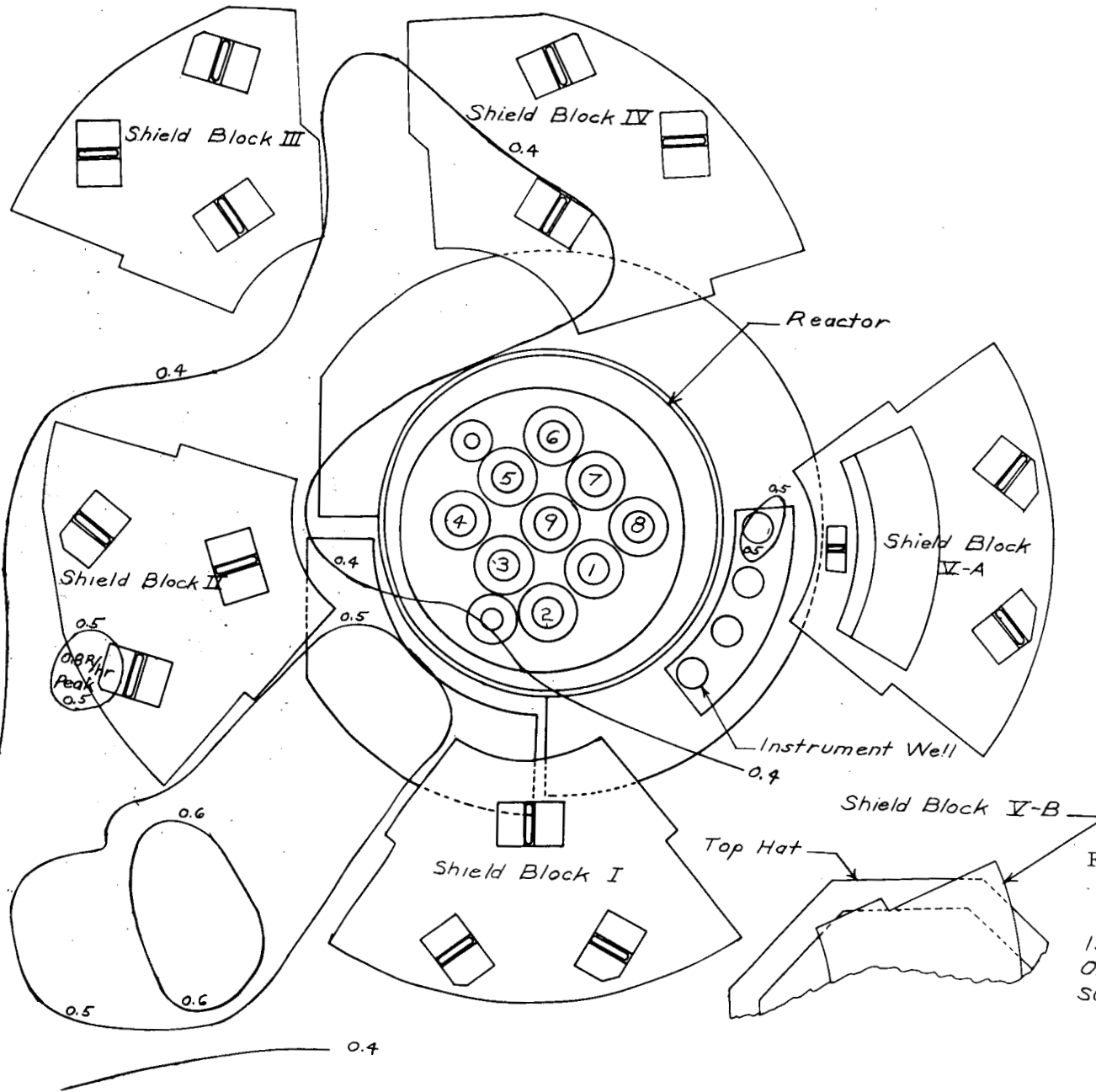


Figure II-13'

ISODOSE MAP
FAN FLOOR
SURVEY 6-14-61

II-291

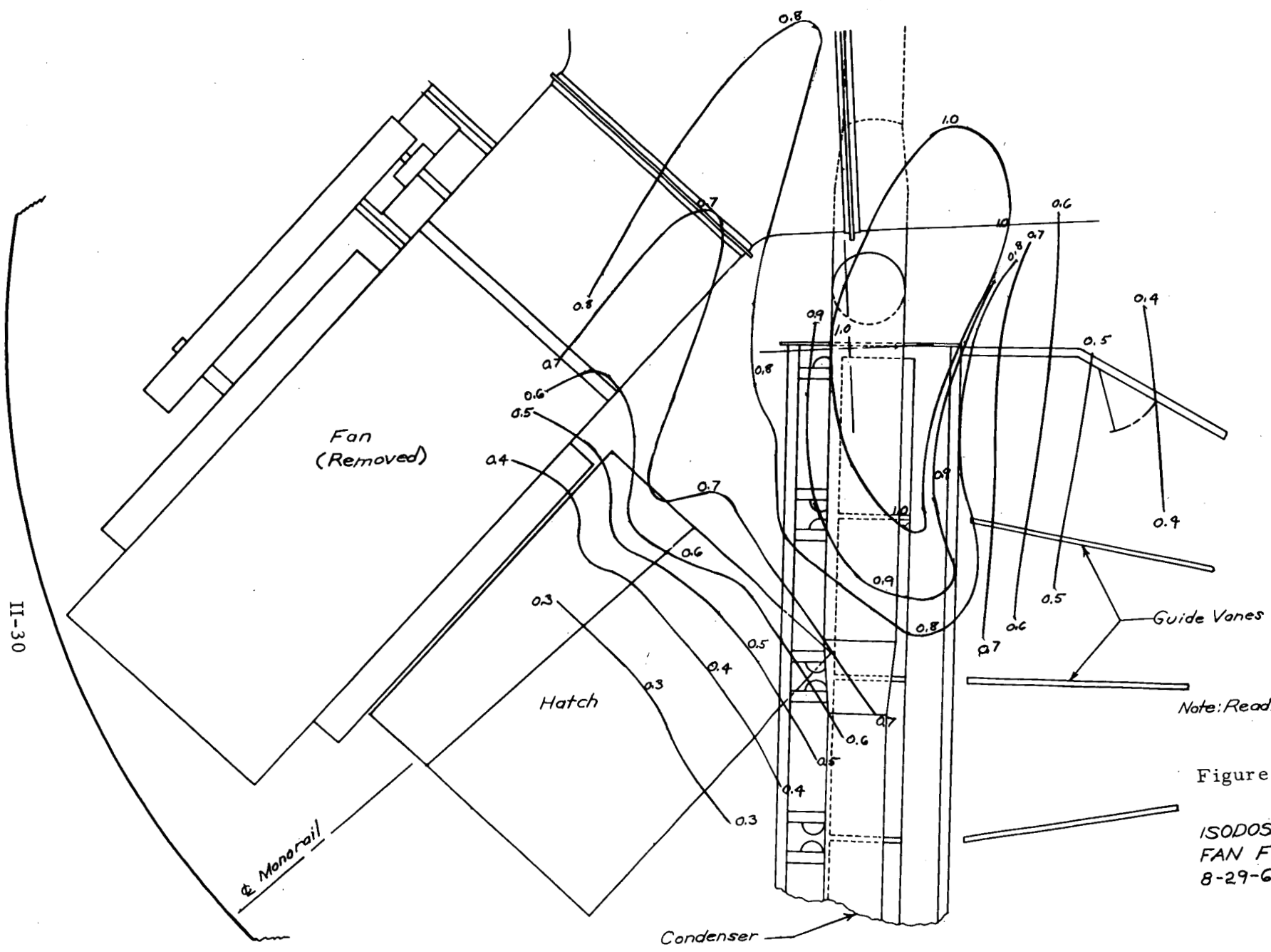


Note: Readings in R/hr

Figure II-14

ISODOSE MAP
OP. ROOM FLOOR
SURVEY 8-29-61

II-30



Note: Readings in R/hr

Figure II-15

ISODOSE MAP
FAN FLOOR
8-29-61

The hot spot just outside of shield blocks 1 and 2 was over a trench in the concrete floor. This indicated that the cover should be removed and the trench cleaned. Note that the cleaning tended to reduce the contamination of the floor to a uniform level over the floor. This would seem to indicate that the remaining contamination was a surface contamination, the magnitude of which was determined by the characteristics of the particular surface.

Figure II-15 is an isodose plot looking at the operating room ceiling after the fan floor had been vacuumed in the open areas. The significant things about this plot are that it shows a hot spot in the vicinity of the condenser and that the fan room floor was a factor of 2 hotter than the operating room floor. Whether the hot spot was on the floor under the condenser or on the condenser itself cannot be told from this plot. Also, there appeared to be a hot spot in the vicinity of the Gyrol Unit and relatively little contamination behind the condenser. Based on this survey it was decided to discontinue cleaning in the operating room until more work had been done in the fan room.

The collimated ion chamber system as designed and used did a good job of defining the relative intensity of the radiation field in the horizontal plane of the traverses. It did not give any information as to the elevation of the sources creating this field. This was a rather serious limitation, as it would have been helpful to know if the radiation from the fan room as seen in the operating room was coming from the operating room ceiling, the fan room floor, or from sources above the fan room floor. It would also have helped to know the relative proportion of the radiation field contributed by contamination on the vertical surfaces in the operating room.

The chief value of the information gained from the collimated ion chambers was that it aided in planning the order of the work on the operating room floor and in deciding when to stop work in the operating room and concentrate on the fan room.

1.3.3 Fan Room and Roof

When it became apparent that the operating room floor was cleaned to the point that the radiation from the fan floor would govern the radiation doses, the cleanup of the fan room was begun. It was judged to be unwise, if not impossible, to use the existing fan room entry provisions, due to the difficulty of any rescue operations or removal of material. Therefore a new entry was cut into the fan floor.

It was first necessary to construct a stairway and a working platform outside the building. The stairway was built at the General Electric shops and transported to the SL-1 site.

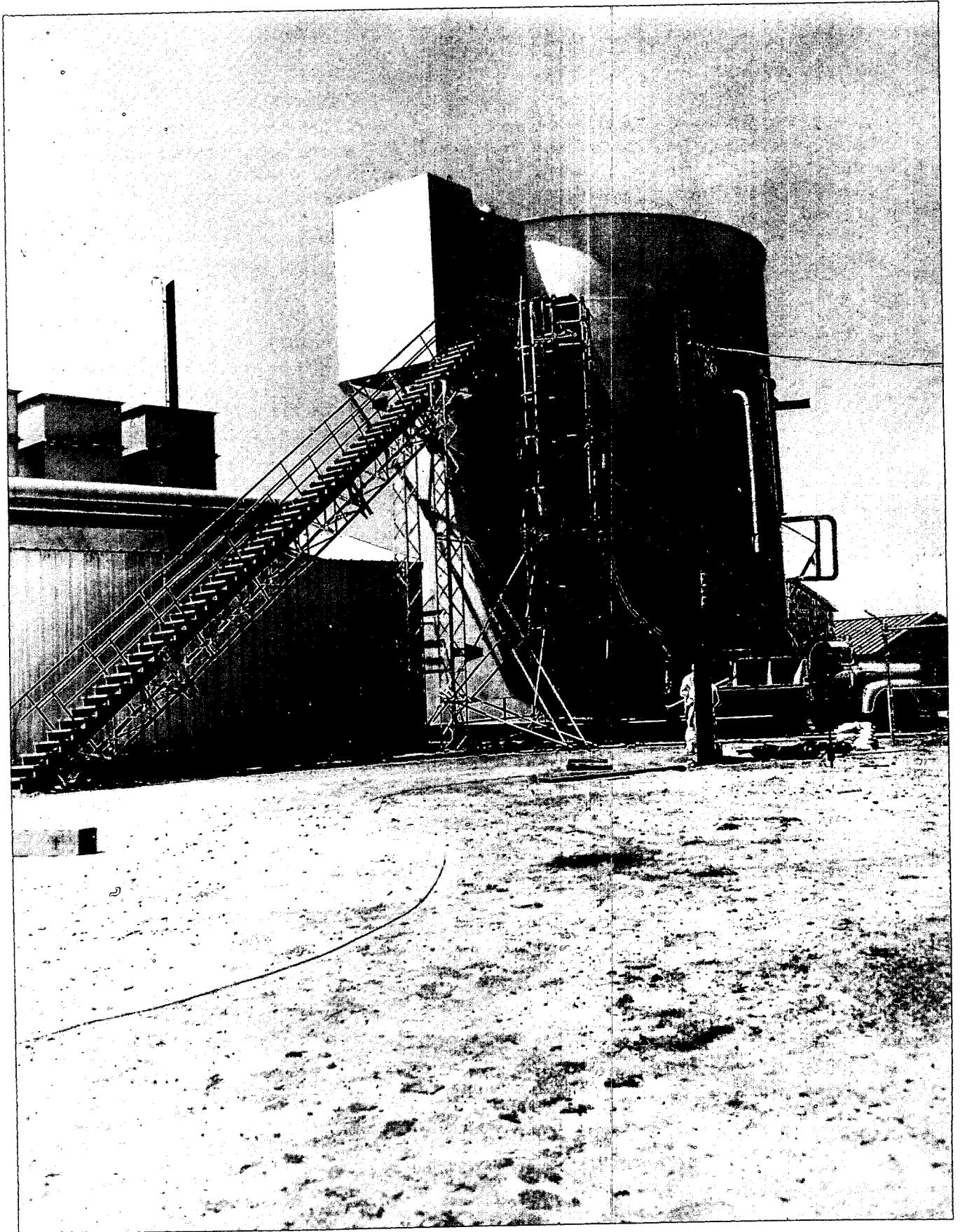


Figure II-16 Stairway to Fan Floor
II-32

The entrance platform was built up of scaffolding assembled in place. The stairway was positioned and secured to the entrance platform and to the ground. It was necessary to remove a small amount of yard piping for clearance. Shielding for the workman was placed on this platform and a shield plate attached to the piece of building wall to be removed. Figure II-16 shows the stairway and entrance platform in place.

Previous tests of SL-1 reactor building insulation had indicated that the insulation adhesive and paint would smoulder and smoke excessively but would not burn. With the crane holding the shield plate and the attached piece of wall being cut away, the entrance into the fan floor was rapidly cut using an oxygen-acetylene torch. The piece of wall was removed and a carbon dioxide fire extinguisher used to quench any smouldering insulation and paint.

The first entries into the fan room were for radiation surveys and photographs. The greatest radiation was in the center of the fan room near the end of the condensers, around the fan drive unit and at the canvas-covered hatch leading to the operating floor. See Section II, 3.0 for radiation dose rates encountered.

Two shielding plugs had penetrated the fan floor in the center of the building through the torn up flooring seen in Figure II-17. One was lying on the hatch cover, Figure II-18, while the other was hung up in the fan discharge duct. There were also pieces of control rod rack, "C" - clamp, a shoe, steel punchings and other debris.

The larger pieces were removed manually as soon as they had been recorded photographically. Here, as in the operating room, emphasis was laid on carefully recording the initial condition and the position of each item with photographs.

Starting at the entry way, the debris was scooped up, the floor and equipment vacuum cleaned with the equipment described earlier and several layers of 1/4 inch thick steel plates laid on the floor. These plates shielded personnel from the beta emitting contamination remaining on the floor and, to some extent, the radiation from the operating room.

A hole in the roof for crane access became necessary to allow the larger pieces of equipment to be removed. A pie shaped segment of the roof was cut out and replaced by a movable pie shaped segment pivoted about the center of the roof. The Link Belt crane could open or close the roof in a very few minutes.

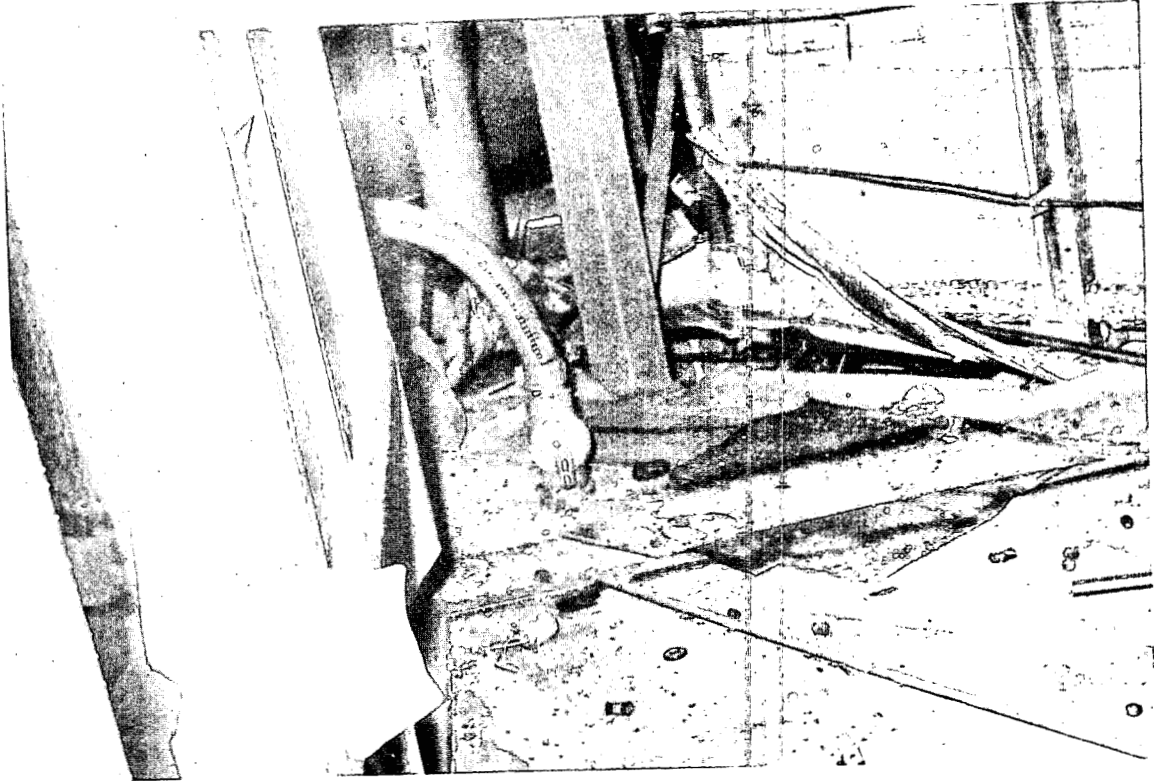


Figure II-17 Hole in Fan Room Floor

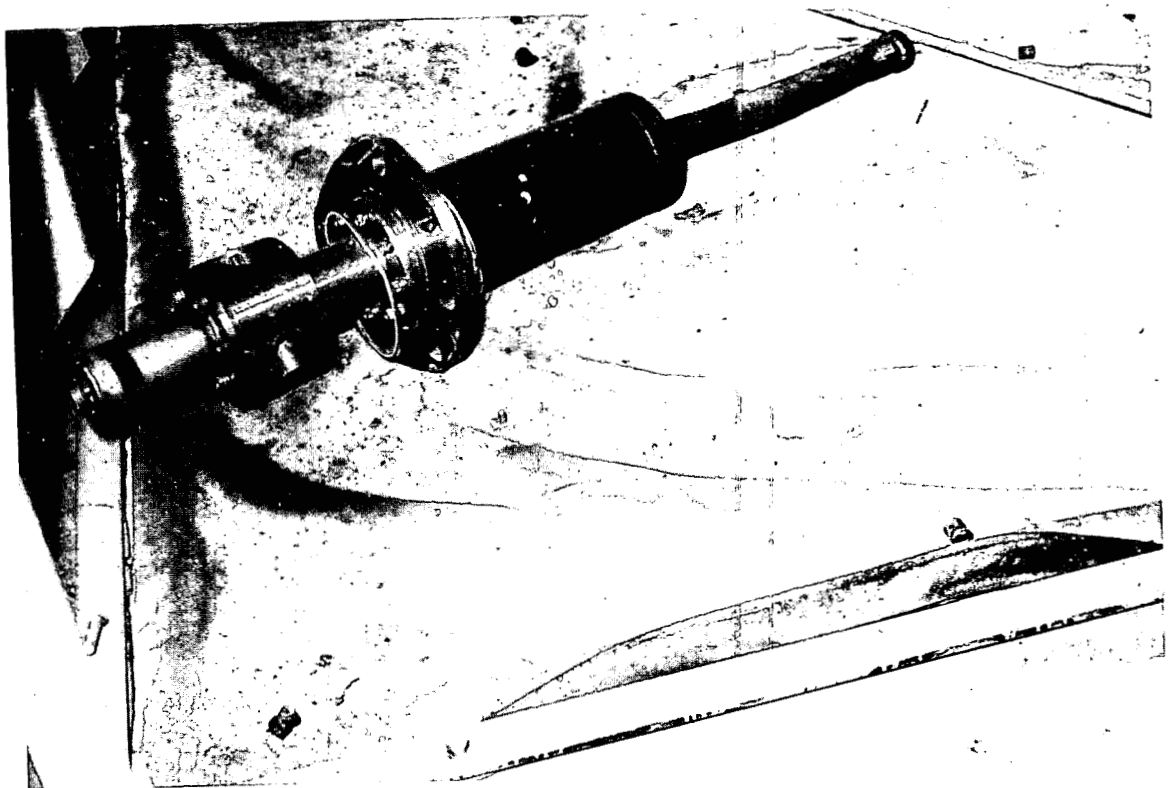


Figure II-18 Shield Plug on Fan Room Floor

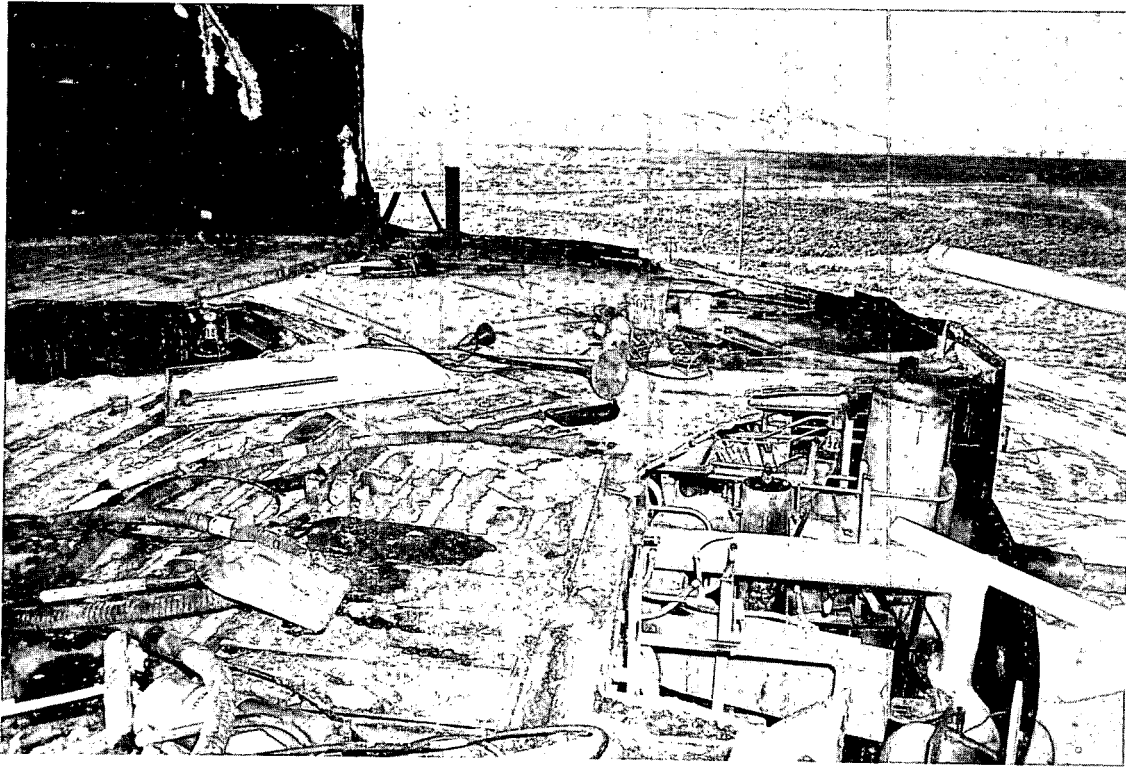


Figure II-19 Remaining Fan Room

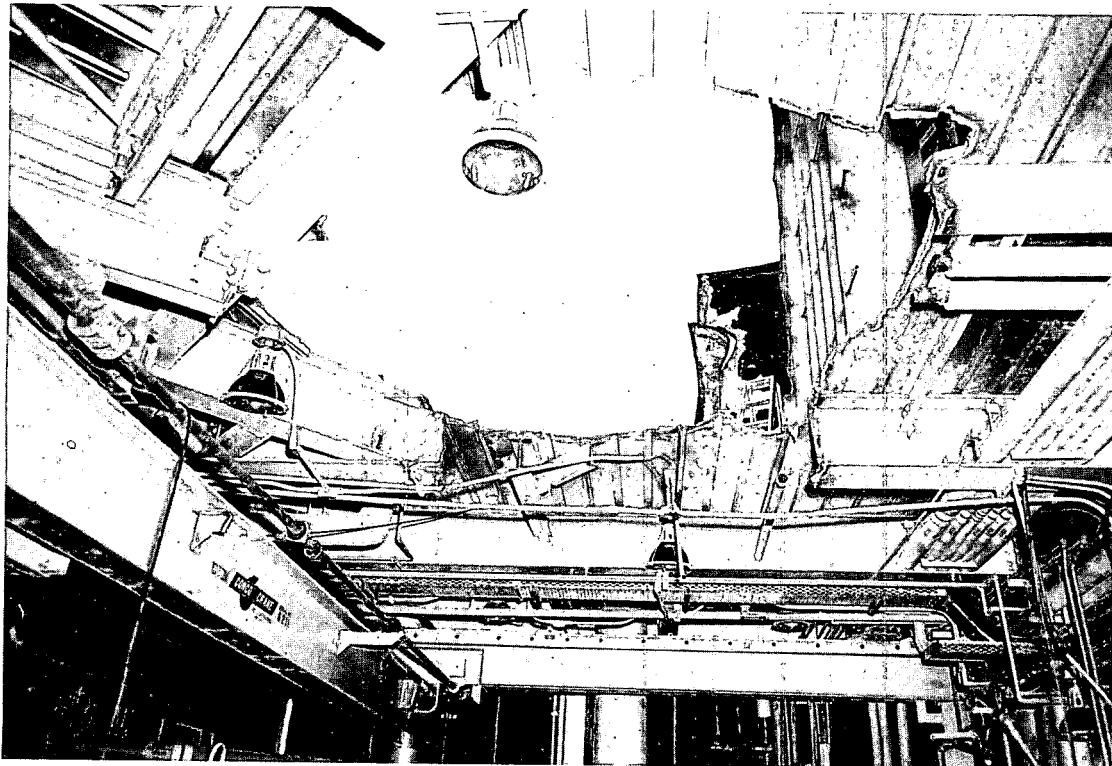


Figure II-20 Operating Room Ceiling

The air circulation fan was then removed from the building, followed shortly by the fan drive unit, which resulted in a noticeable reduction in radiation level.

The two sections of condenser nearest the center of the building were cut loose, pulled over and lifted out of the building with the crane. Removal of the other three condenser sections as well as heaters, oil coolers, baffles, piping and other parts and accessories continued until area was cleared sufficiently to allow clearance for the reactor pressure vessel and to allow the reactor building roof to be removed.

The remainder of the roof was then removed and lifted to the ground with the crane. A part of the fan room wall and the edge of the fan room floor were removed to allow crane boom clearance. A hole was cut in the fan room floor for passage of the pressure vessel. Figures II-19 and II-20 illustrate the fan room and the operating room overhead at the time the pressure vessel was removed.

1.3.4 Core Access Hole

The core access hole was drilled horizontally from outside the reactor building into the pressure vessel at a point about one foot below the reactor core. It was necessary to penetrate the steel building shell and approximately sixteen feet of gravel to reach the support cylinder. Drilling then proceeded through the various layers of material: 1/4" steel, 1 1/4" lead with copper tubing, 7/8" steel, 1/4" steel, 3" insulation, 3/4" steel, 3/16" stainless steel and 3/4" stainless steel layers, in that order, to reach the space in pressure vessel under the reactor.

The first operation was to cut a hole with a torch in the steel building shell at the location chosen as having a low radiation field and being located on a right radial line which was clear of fuel storage wells and structural members from the pressure vessel penetration point. A drill motor holding fixture was then welded to the building shell in proper relation to this hole. A driving bit support and guidance fixture was set up so that the centers on these two fixtures were located on the right radial line from the pressure vessel penetration point.

The hole through the gravel was then driven using a 1.9 inch O. D. steel pipe with a driving point assembled inside a 2.067 I. D. steel pipe. This assembly was inserted through the support stand and the drill motor holding fixture and driven through the 16 feet of gravel until the point contacted the first metallic layer surrounding the pressure vessel. Driving was done with a 500 lb. weight suspended from the Austin-Western crane.

With the driving completed, the inner pipe was withdrawn leaving the outer pipe in place as a casing giving a clear hole through the gravel. The hole was checked for straightness with a surveyor's transit sighting through the fixtures at a lighted target inserted into the bottom end of the casing. This showed that the casing had drifted sufficiently to displace the bottom end 1-1/2 inches in 16 feet of length. The driving operation was repeated in an effort to improve this alignment. The measurement of the second hole showed the same results, therefore the rest of the drilling operation was carried out with the casing in this position.

The drilling of the metallic layers used a 3/4" diameter twist drill connected by a long drill stem to a Gardner-Denver air powered drill motor. This was supported in the fixture on the outside wall of the building. Twist drills were selected for use because of their high rate of metal removal. Air was supplied by the compressor on a "Le Roi" tractor parked near the site. After drilling for a depth of 5-1/2 inches, the 3/4 inch drill jammed and broke off. Efforts to extract the broken drill were of no avail. A 2 inch O. D. core drill bit was quickly fabricated and used to cut around the broken 3/4 inch drill bit. The hole was completed in this fashion, albeit slower than originally expected due to many withdrawals of the drill bit necessary to clear chips and lubricate the cutting points. The cores of each layer, including the broken end of the 3/4 inch drill bit were retrieved in the process.

The intended centerline of the hole was to have been below the thermal shield. Due to the drift of the casing the hole passed through the 3/4 inch stainless steel thermal shield.

An important benefit of the access hole was its function as a drain, thus absolutely preventing the inundation of the core volume with water.

With this hole in place, a detailed inspection of the bottom of the core could take place since the man looking through the borescope was in a relatively low radiation field while obtaining a closeup view of the underside of the reactor. Two series of photographs were made, covering the field of view of the boroscope. Figures II-21 and II-22 are representative of conditions on the bottom of the core. In Figure II-21 can be seen a support structure bar and its attachment to a "T" stanchion, a portion of #5 control rod, a fuel element support box and fuel element end boxes. Figure II-22 shows a portion of fuel element side plate, support box, end box and ends of fuel plates.

.3.5 Vessel Removal and Transit

The SL-1 reactor was removed from the test building on November 29, 1961, and was subsequently transported from the SL-1 area to the ANP

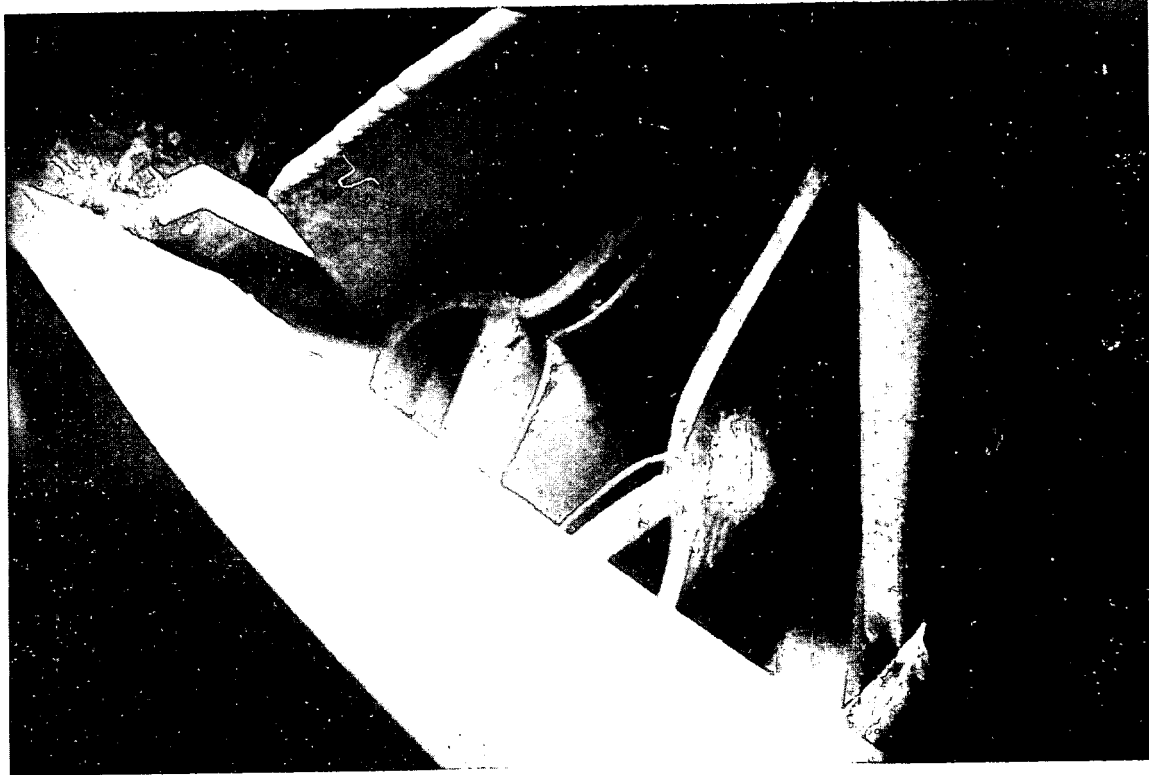


Figure II-21 Bottom View of Reactor

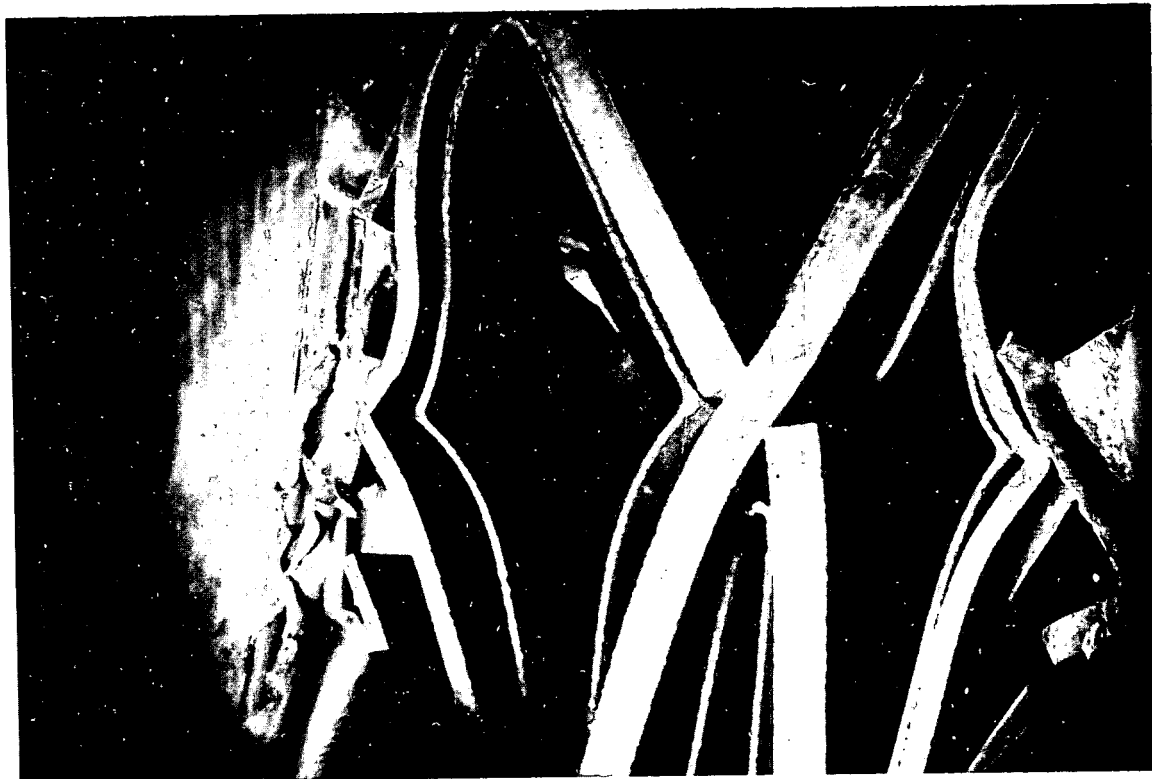


Figure II-22 Bottom View of Reactor

area on November 30, 1961. The planning and execution of removal and transit operations proceeded as planned with essentially no difficulties encountered. Prior to the final removal and transit, a considerable amount of careful preliminary work and trial operations were performed. These included: a trial lift of the reactor using the building crane; preparation of the test building, area and route of transit; and design, and fabrication, and where possible, checkout of special equipment.

Evidence strongly indicated that hydraulic impact forces had been exerted on the SL-1 pressure vessel of a nature and magnitude sufficient to have caused the entire assembly to be lifted out of its support cylinder. If, indeed, relative motion had occurred, it would result in shearing these connecting pipes and freeing the pressure vessel from the support cylinder. As a positive means of determining if this was the case, an attempt was made to lift the pressure vessel using the existing bridge crane. A further purpose was to enable inspection of the upper portion of the pressure vessel which had been subjected to extreme hydraulic impact loads. Equipment was designed such that the vessel could be lifted using both hooks of the overhead bridge crane. The connection to the pressure vessel was made through control rod holes 4 and 8 using dog latches which, after insertion, contacted the under surface of the pressure vessel head at these two locations. Prior to undertaking the lift all shielding material which had been placed around the head of the vessel was removed and the area cleaned to reduce the dose rate. Some shielding material was then replaced in this area to further reduce the radiation dose. Concurrently with these operations, a considerable number of photographs were taken of the vessel interior above and below the core in order to establish the location of all components prior to the lift. These photographs revealed an unexpected gap between the vessel head and flange. This was (correctly) attributed to flange or stud distortion and was not believed to have materially reduced the strength in this region.

The lower lifting fixture was inserted and secured in holes 4 and 8. Attached to this assembly was a dial type load indicator to indicate lifting load. The calculated load was 23,000 lbs. plus an undetermined amount due to the additional shielding placed on the head. The load indicator was connected to a spreader bar which was in turn connected at each end to the crane hooks. Using this arrangement the first trial lift was undertaken on November 2 and was successfully accomplished. The vessel was lifted 16 inches such that the lower surface of the head just cleared the cell floor. The lifting occurred at an indicated load of 26,000 lbs. and was limited at this stage to 16 inches due to limited crane hook travel. This lift demonstrated that the pressure vessel was not restrained by the connecting pipes but the lift did not accomplish the secondary purpose, namely, inspection of the vessel below the flange. It was necessary to use the two hook configuration without the load indicator to get an additional 18" of lift. This

II-40



U-5073-15

Figure II-23

Upper End of Pressure Vessel

was done on November 3 and the vessel successfully lifted until the lower edge of the flange cleared the floor by about 36 inches. The flange was found to be severely distorted such as might be explained by extreme internal pressure. A distortion of this nature could account for the gap mentioned above which was detected in the photographs of the interior of the vessel. It was, also, found that the insulation cover plate was not lifted with the pressure vessel. This cover plate was in the form of a cylinder around the pressure vessel and served to enclose the 3 inch layer of magnesia insulation which surrounded the vessel. In its normal configuration it was an integral part of the vessel, being welded to it at the underside of the pressure vessel flange. The welds at this location had failed, allowing the pressure vessel to lift out of the insulation and cover plate assembly. The large blocks of insulation seen in the photograph of the operating room floor, Figure II-4, Section II, 1.1, had apparently been lifted out with the pressure vessel and spilled out upon the floor during the incident.

This effort terminated the initial series of lifts. It was, however, decided to again lift the vessel before final removal in order to remove the insulation material around the flange and to inspect the vessel in the region of the pipe entrances. In order to do this, modifications to the lifting assembly were required to obtain the additional height required. This lift was successfully accomplished on November 27. The vessel was lifted approximately 49 inches. Figure II-23 shows the vessel in the lifted position after it had been cleaned. This photograph clearly shows a bulging of the vessel below the flange as well as the flange distortion noted above. Also shown are the ends of the cleanly sheared off pipes. The upper pipe is the steam line out of the vessel and the lower, smaller line is the line to the upper spray ring. As may be seen the shearing was relatively smooth with very little distortion to the pipe or vessel wall.

Upon completion of the lift the vessel was lowered. However, at this time, it did not return to the original position, but remained about 12 inches above the normal position. Further settling took place during the next several hours bringing the final location to about 4 inches above normal. It was prognosticated (and later verified) that some of the insulation had fallen below the vessel during the time it was lifted, and that the vessel was resting on the insulation.

Lifting operations with the bridge crane were terminated at this point. The lifting fixture was left in position since it was to be used for the final removal.

Several fairly substantial pieces of equipment were designed and fabricated for use in various aspects of the final removal and transit operations. These are described below.

A mockup of the SL-1 pressure vessel was built to be used for trial operations, crane positioning and operator practice. It was fabricated out of three sections of standard 48 inch concrete drain tile and closely duplicated the overall height and diameter of the pressure vessel. Correct total weight was attained by partially filling the assembly with gravel.

A transport cask was provided for use as a shielded container for the vessel during transit to the ANP area. The cask used was a modification of an existing ANP cask. The modifications included fabrication of an upper ring to mate with the SL-1 vessel flange, removal of existing frame members below the cask so that it could be placed on a lowboy-type trailer, and drilling holes through the cask walls and installing screw type centering pins. Miscellaneous guide rails and tie-down hooks were also installed. The cask was placed on a 60-ton capacity lowboy trailer and secured at four locations with double strands of 3/4" cable. Prior to placing the cask on the lowboy, the lowboy surface was covered with plastic sheeting in order to prevent contamination to the trailer bed. The cask was equipped with a sheet metal cover which served to totally enclose the pressure vessel when in position. Trial runs over the proposed route were made with the lower portion of the cask on the trailer in order to check road width and familiarize the driver with the route. A simple shield was placed on the tractor trailer combination to further protect the driver from radiation while in transit.

A rubberized fabric shroud was provided to contain the pressure vessel and minimize the spread of contamination while the vessel was exposed. The shroud consisted of a cylinder having dimensions slightly larger than the pressure vessel and having six garter-like elastic bands sewn in at equal intervals. The shroud was nested on a support assembly immediately above the vessel such that as the vessel was lifted it picked up the shroud automatically.

The crane used was the Manitowoc described in Section II-1.2.4.

Final building dismantling operations which were conducted just prior to vessel removal included: removal of all fan room equipment over the approximate north 1/3 of the fan floor, removal of the fan room wall over the north 1/3 of the building, cutting a hole through the fan floor to allow passage of the vessel, and cutting a notch below the fan floor for crane boom clearance.

Prior to removal operations, a level area was provided adjacent to the test cell in order to insure that the cask would be in the vertical position. Fill material was brought in and spread in this area to achieve the desired

elevation. In addition to this, clean fill material was spread inside the SL-1 area extending from the front gate to the loading position to minimize contamination to the vehicle tires.

In order to provide unobstructed transit from SL-1 to ANP, work was done to remove all overhead lines below 25 feet. There were 45 overhead crossings along the proposed route including: power lines, telephone lines, guy wires and gate tracks. Of these, 12 were below 25 feet and required raising or, in one case, placing on the ground.

To provide entrance into the ANP area, a portion of new roadway was constructed extending from Lincoln Boulevard, through the ANP security fence to one of the existing roads within the area.

In order to facilitate entrance into the Hot Shop at ANP, it was necessary to build a ramp over the door sill.

The pressure vessel was removed and placed in the transport cask on November 29, 1961. Operations performed on this day up through the final removal are summarized below.

The desired positions of the crane cask were established using scale layouts. These positions were then marked in the area by driving stakes into the ground. The crane and the cask containing the vessel mockup were driven to the area and positioned to the marking stakes.

The crane was then connected to the mockup and the mockup positioned over the center of the pressure vessel above the fan room floor. Positioning was done using a plumb bob fastened to the bottom of the mockup. The crane boom angle and elevation were altered until the mockup was within 1/2 inch of the vessel centerline. The boom location was then marked by an index stake clamped to the wall of the building. The mockup was then returned to a position over the cask. As it was swung over the fan floor, it was noted that minimum clearance (about 8 inches) occurred between the bottom of the mockup and a portion of the cell wall which protruded about 6 inches above the fan floor level. In order to gain additional clearance this portion of the wall was cut down to floor level.

With the mockup suspended over the cask, the cask position was then altered to match the mockup position. This entailed moving the vehicle about 4 inches. The mockup was then lowered to the ground and placed on the concrete pad adjacent to the test building.

Concurrently with these operations, T.V. cameras and a remotely operated movie camera were installed and checked out. One T.V.

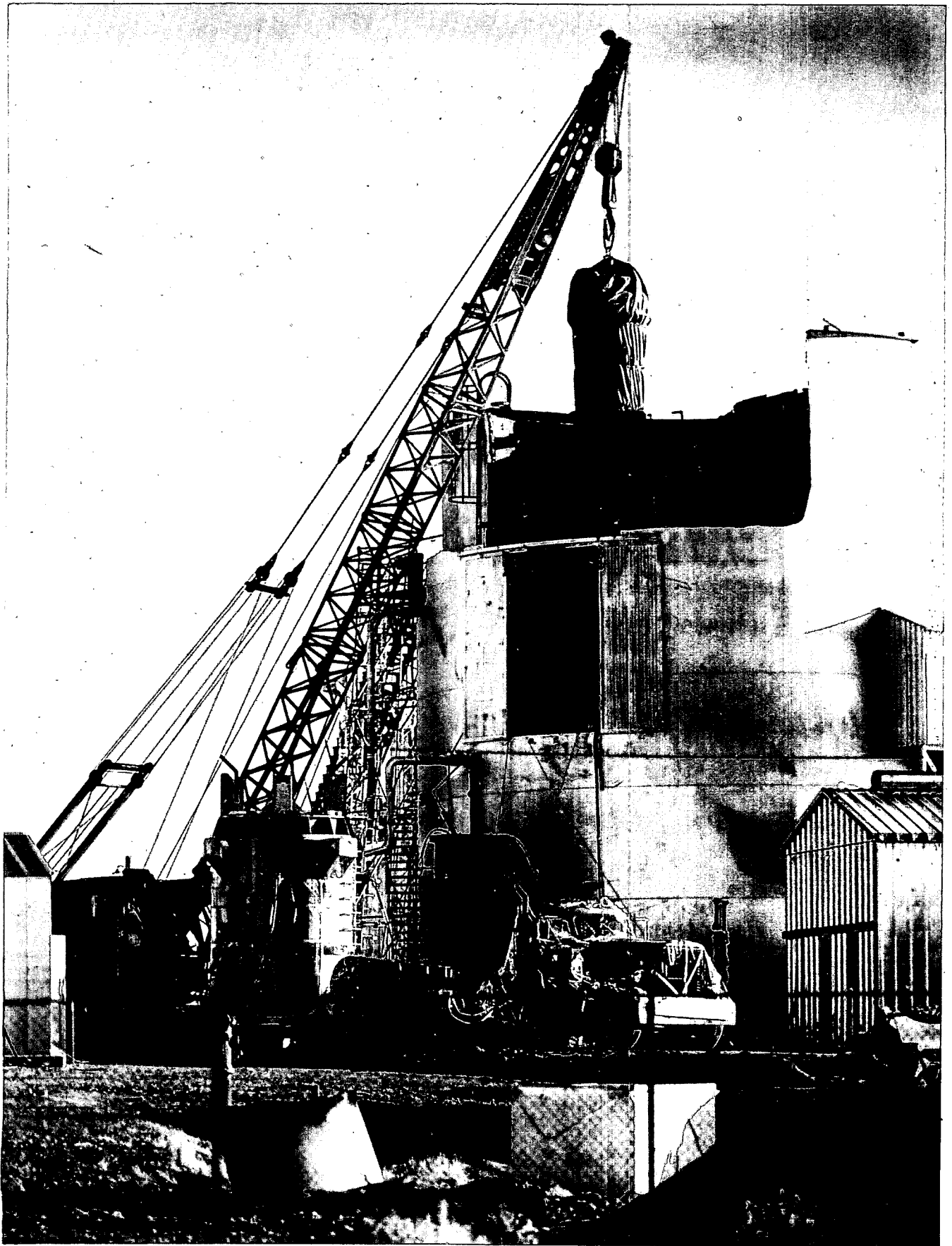


Figure II-24 SL-1 Reactor Removal
II-44

camera and the movie camera were placed in the test building in order to view the vessel as it was lifted. The other T. V. camera was placed on top of the SL-1 area water tank viewing the top of the cask. This camera was to be used to assist the crane operator during insertion of the vessel into the cask.

A command post was established in a trailer placed behind the water tank (to provide shielding). This command post contained the monitors for the two T. V. cameras and the controls for the remotely operated movie camera. It also contained two-way radio equipment to maintain contact with the crane operator and the control point. One remote observation station was established and provided with radio communication with the command post. This station was situated outside of the security fence approximately 120 yards north of the test cell. Other observation stations (without communications) were established at various locations. Two portable radiation survey meters were placed in the test cell such that they could be viewed with binoculars from the observation posts.

The crane boom was positioned to the index stake and the hook lowered to a position above the pressure vessel. The deviation between the loaded and unloaded hook position appeared to be about 12 inches. The crane hook was connected to the lifting fixture and a light load taken by the crane. The lifting fixture was then inspected to assure proper engagement with the vessel.

The test cell was cleared and instructions given to the crane operator to lift the vessel approximately 6 feet. Personnel accompanied by a health physicist entered the test cell to inspect the vessel, fixture and shroud. All was found to be in good order so the cell was again cleared and instructions given to lift an additional 4 feet. This was done and personnel again entered the cell and repeated the inspection. No difficulties were noted and instructions were given to remove the vessel and place it in the cask. Figure II-24 shows the vessel above the fan room floor.

The vessel was lowered into the cask with no difficulty. The hook was then disconnected and the crane used to position the cask cover. The vessel clamp pins were then tightened. The transport vehicle was then driven from the cell area to a location adjacent to the front gate where it was left until the next morning when preparations for transit were undertaken.

Results of the various radiation measurements obtained during these operations are summarized below.

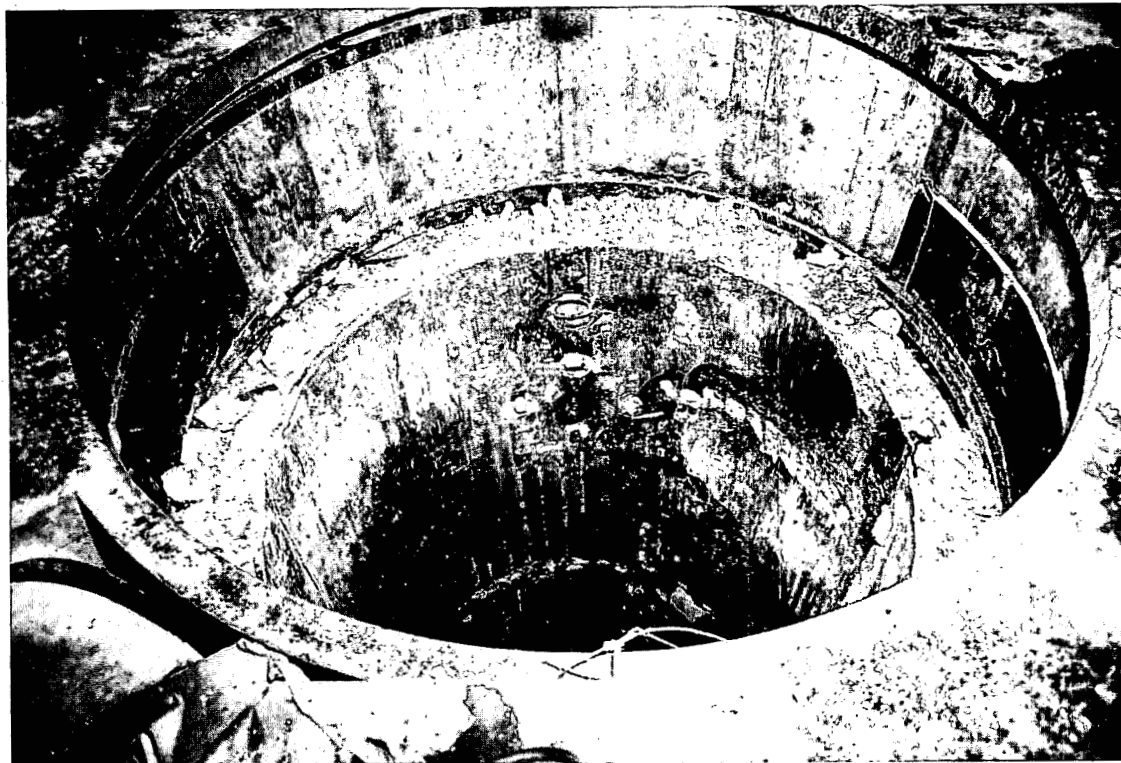


Figure II-25 Inside of Support Cylinder

U-5076-8



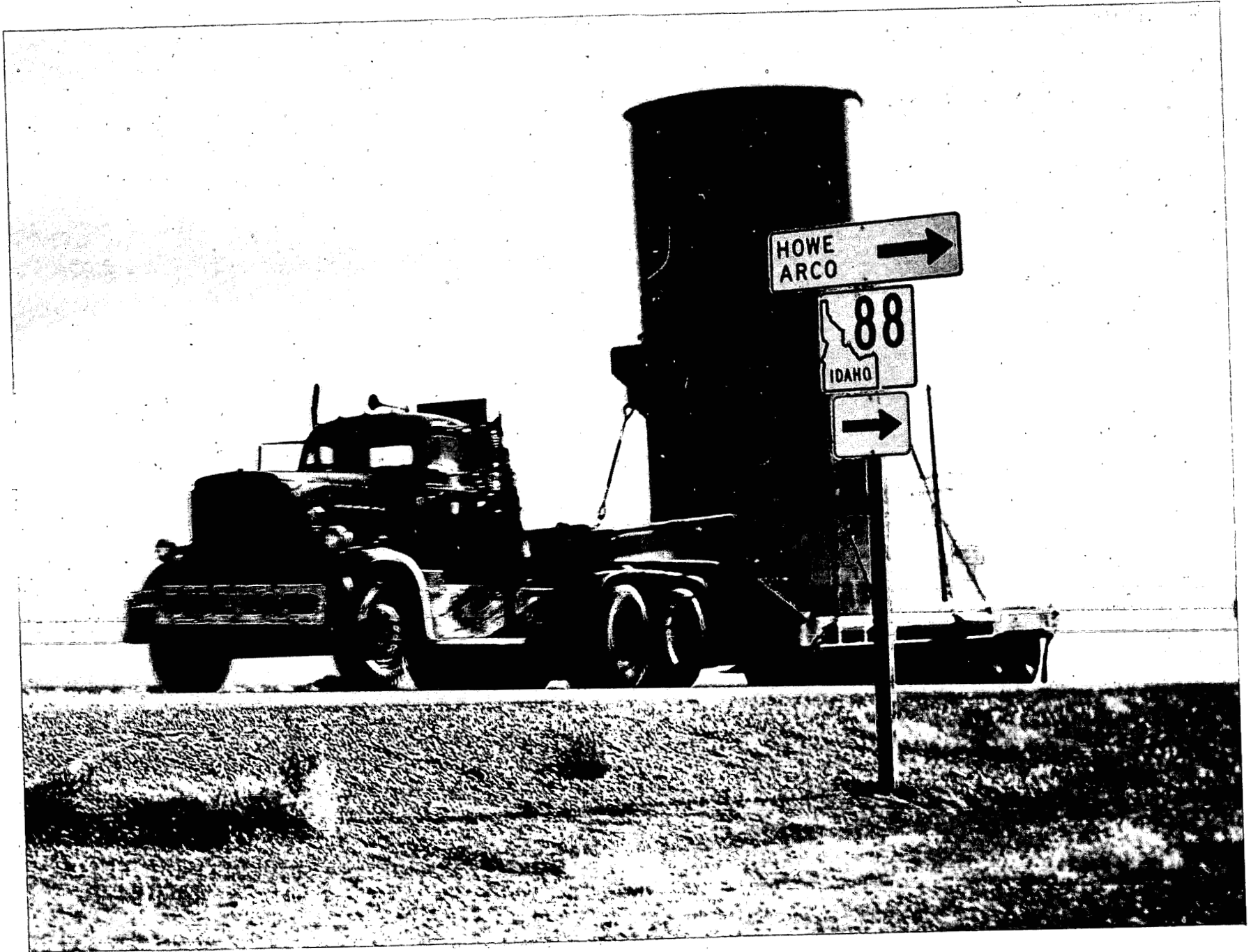
Figure II-26 Bottom of Support Cylinder

<u>Location</u>	<u>Predicted R/hr</u>	<u>Measured R/hr</u>
25' from bare vessel	14	9
At crane location (bare vessel)		7
Vessel in cask		
Contact with cask	1.0	0.042
25' from edge of cask	0.05	0.045
50' from edge of cask		0.021
Maximum dose rate (9' from edge of cask)		0.060
Truck cab		
Shielded portion	.005	.008
Unshielded portion	.050	.030

Of interest was the condition of the vessel support and containment structure. Figure II-25 is a photograph looking into the support vessel. The upper surface is the operating floor, and the change in diameter about 2 feet below this is the upper edge of the insulation cover plate and the support vessel. The lower surface of the pressure vessel flange rested on this surface. The cylinder seen extending below this is the inner surface of the insulation cover plate. Protruding through this surface may be seen the sheared off ends of the five pipe entrances. The debris seen on the support vessel flange is predominantly insulation which became lodged there at the time of the incident and during the lifting operations. Figure II-26 is a photograph looking into the bottom of the support and containment vessel. As was anticipated essentially all the insulation had fallen into the bottom of the vessel. The metal straps seen in this photograph were placed around the insulation blocks to secure them to the pressure vessel. Cracks and warpage to the insulation cover may be seen in this photograph.

On November 30, 1961, the SL-1 pressure vessel and core were transferred from the SL-1 area to the ANP area. Prior to removing the transport vehicle from the SL-1 area, decontamination of the assembly was undertaken. The outer plastic covering was removed and the vehicle was advanced out of the contaminated zone in steps. At each step the tires on the tractor and trailer were cleaned using a spray type steam cleaner. After several steps in this manner, radiation surveys indicated that contamination had been reduced to a permissible level and transit to ANP began.

The various support vehicles were lined up in proper order and briefed as to transit procedures. Included in the convoy were four security patrol cars, two site survey vehicles, one GE-HP vehicle, one emergency service vehicle, one GE control vehicle and assorted other vehicles bearing photographers, etc.



The convoy left the SL-1 area at about 11:30 a. m. and proceeded to the ANP area without event, arriving at about 3:30 p. m. The route was traversed at about 10 mph and several stops were made to inspect equipment and rest the drivers. Figure II-27 is a photograph of the transport vehicle and cask on the portion of State Highway 88 used for this operation.

The vehicle was driven onto the concrete pad outside of the Hot Shop and then backed into the shop. The cask was then lifted off the trailer and the vehicle driven out of the shop. The cask was then placed on the floor in preparation for subsequent operations.

- 1.3.6 Following the removal of the reactor vessel, the remainder of the fan room components, the rest of the wall at this level, and the remainder of the fan room floor were removed. Some of this work involved entry into the operating floor zone as components were supported from the fan room floor and miscellaneous piping, etc., penetrated the floor.

When the second phase of the fan room floor cleanup was complete the efforts were directed toward the operating floor. On the operating floor, the first step was to remove the equipment on or above the floor. Following this the building wall sections were removed after being retained as long as possible to give weather protection to personnel. The floor plates were then lifted and major sections of structural supports were cut away. Next, piping, etc., below the floor was removed, and as soon as the structure became accessible, the turbine-generator base was lifted and removed.

Several vessels set in the floor had to receive attention before the floor plates were lifted, among which were the fuel storage wells which contained two hot fuel elements. The SL-1 Reactor Building was equipped with three reactor fuel storage tanks which were located with their covers forming a part of the operating floor, the tank portion being in the shield gravel zone. Since water was the radiation shield for the elements in storage, the tanks were now solid with ice, as this portion of the work was done in mid-winter. An electric immersion heater was made up to melt its way into the ice column.

Within the storage tank there existed a family of seven divider tubes, a portion of whose lengths were Boral tubes. These were in turn welded to aluminum tubing. Through some mishap this joint had failed causing misalignment of the two tube portions, hence when an effort was made to lift out an element it fouled and it was necessary to first lift out the nest of dividing tubes of one well to permit the element to be raised.

A shielded cask was threaded with the recovery cable and when the element was hooked, the cask was placed over the well opening and the

element pulled by hand into the bottom opening. When the element was within the cavity of the cask the sliding cask door was closed and the cask transported to the ANP Hot Shop for unloading.

One of the most difficult operations on the operating floor was the removal of the central slab which had an estimated weight of eighty tons. This slab was reinforced concrete section with heavy steel shielding plates attached. The assembly was mounted on six columns (10" WF 49#) approximately 15 feet high. This slab had been cast in place during construction of the Reactor Building. The heavy weight located at the center of the 38 foot diameter building made it impractical to consider lifting with cranes. Before this slab could be removed, it was necessary to cut the reactor support vessel and the instrument wells adjacent to it. A good deal of the shielding gravel was also removed, as will be described shortly.

It was proposed to use explosives to cut the support columns and to turn the slab over for handling. Demolition experts from Fort Belvoir, Virginia, placed the explosives which wereshaped charges attached to the flanges and webs of the columns by small permanent magnet clips. Wooden boxes were placed over these charges to minimize danger of flying fragments. The turning operation was to be accomplished by a pair of charges fired after the main severing blast. On the actual blast, however, the leads to these "kick" charges were cut. It was necessary then to fire these separately, and the slab was dropped from its support columns and rested at about 45°.

After the slab was deposited on the shield gravel at approximately 45° several tasks remained: first, to turn the slab the rest of the way into a horizontal attitude; second, to have it clear the Reactor Building shell; and finally to transport it to the Burial Ground.

To gain the necessary mechanical advantage required to overturn the slab a set of blocks was used. A "deadman" anchor was fabricated out of structural steel salvaged from the building and placed outside the enclosure. Using this anchor and the set of blocks, a bulldozer was used to turn the slab.

Initial reeving of the block set resulted in severe twisting as the dozer load was applied. It was necessary to "cross reeve" the blocks following which the slab was overturned.

Efforts to move the total assembly proved fruitless in the soft terrain of the early spring thaw. It was noted that there was some separation between the concrete slab and the steel shield plates. This was exploited to remove the 20-tons of steel plates from the concrete, but even this was not enough weight reduction to allow the concrete slab to be dragged to the Burial Ground.

A crack was noted in the concrete slab. This was opened to split the slab into two parts, and each of these was then dragged into the Burial Ground pit.

Although only partially successful, the explosive method for lowering the slab was considered satisfactory.

Some concern was raised prior to removal of the shield gravel that enough water might have drained into the gravel to cause it to be frozen into a solid mass. An exploratory cut showed only a small amount of moisture remained with generally free flow of the gravel.

Panels of the building were removed and gravel was moved with a front end loader into a dump truck and hauled to the burial ground. A small scraper was made up to move the gravel from the central section of the building to where it could be reached by the front end loader. As the gravel level fell the vessels located in it became accessible and were removed.

Final gravel removal did not take place until after the operating floor slab had been dropped and removed, and after the lower section of the support vessel was removed.

Removal of the base plate and structural ribbing completed the removal of the steel section of the Reactor Building.

The Reactor Building assembly was supported on reinforced concrete columns projecting from a concrete slab below grade. Several proposals were made for the removal of these columns among which were: (1) the spalling of the concrete by thermite charge to expose the reinforcing steel, cutting the steel, and then finishing the concrete removal; (2) battering the columns with a "headache ball" and cutting the steel; and (3) the breaking of concrete in bending by use of a bulldozer and then cutting the steel. Method No. 3 was finally used with success.

1.3.7 Area and Other Buildings

The Cadre Building was a steel framed and shelled structure used for classrooms and instruction. It contained a very large amount of furniture, text and reference books, miscellaneous supplies and equipment. The furniture was first given a preliminary cleaning at the Cadre Building and delivered to the control point where it was given a detailed decontamination and check. When a sufficient quantity was accumulated, the material was transferred to a warehouse for holding. A survey of the insulation in the attic of the building showed it to be low enough in

radiation level to leave it in place. Fluorescent light fixtures were dismantled for decontamination and treated in the same way as the furniture. Books were vacuumed and wiped down. The outside wrappers of supplies were discarded and the contents saved. Interior walls were vacuumed and scrubbed down, with floor scrubbing completing the inside work. Exterior walls were scrubbed and hosed.

Turco Fabrifilm Remover was found very effective in removing surface contamination. The liquid was applied, the area scrubbed, followed by flushing with a hose. This compound also worked well as the detergent in the steam cleaner unit.

The Support Building was a steel framed and enclosed Butler-type building which housed the control panels, chem lab, machine shop, locker rooms, diesel electric set and a considerable supply of material and tools. Lights and furniture were treated as in the Cadre Building. Many of the tools and supplies were loaded into a dumpster box and delivered to the ANP site for decontamination. This was done to expedite the completion as the decontamination facilities at the SL-1 were occupied with cleanup of furniture, etc.

A radiation survey on samples of insulation in the attic showed this to be too highly contaminated to be retained. The material was removed, bagged, hauled to the Burial Ground, and replaced with new insulation.

One building section damaged in the explosive removal of the operating floor slab was replaced. Floors, walls and exterior were handled as in the Cadre Building. Instruments were removed from the control panels, packed and shipped to the ANP site for decontamination. The panels were buried.

The Administration Building was a two-story cinder block building. No special procedures were required. Heating radiators and covers were removed and cleaned up. The furnace had been damaged by freezing; one section was repaired; one replaced.

The Condenser Building, Laydown Building and Pump House were steel Butler-type buildings which presented no special problems.

The work at the SL-1 site was completed by cleaning up the load bank, transformer station, chlorination shed, fuel tank areas, and the general terrain of the whole enclosure. Depending on radiation levels, 3 to 6 inches of earth were removed from the all exposed soil surfaces inside the security fence and dumped in the Burial Ground. Clean dirt was

placed around buildings to bring radiation levels below 1 mr/hr in these areas. Since some areas outside the fence are contaminated, with readings as high as 20 mr/hr, no attempt was made to spread dirt throughout the area at this time. Further details are recorded in Section II, 3.

1.4 Recommendations

The problems encountered in the SL-1 cleanup lead naturally to design suggestions which are pertinent to the general case.

Rigid enforcement of cleanliness and housekeeping standards would minimize the clutter in the work spaces and facilitate any necessary cleanup.

Where possible, surfaces inside the building should be smooth and water-tight. Surfaces and equipment should be painted to ease decontamination.

Convenient means of emergency access to all spaces should be provided.

Any cranes should have all motions electrically powered. This would allow easy conversion to remote or semi-remote operation and would greatly increase the usefulness of the equipment.

Use of non-inflammable building insulation and elimination of oil lines by piping cooling water to the equipment rather than oil to the coolers would reduce the fire hazards greatly. Fire is one of the most severe hazards in a clean-up operation.

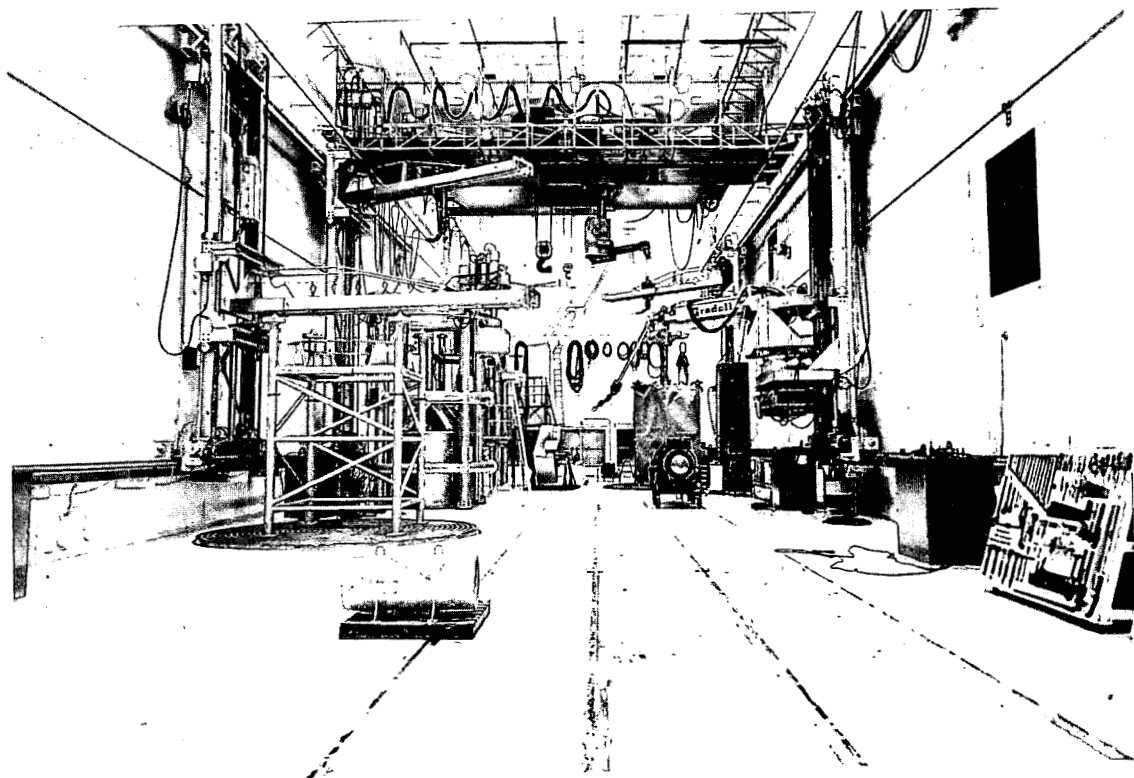


Figure II-28 Hot Shop

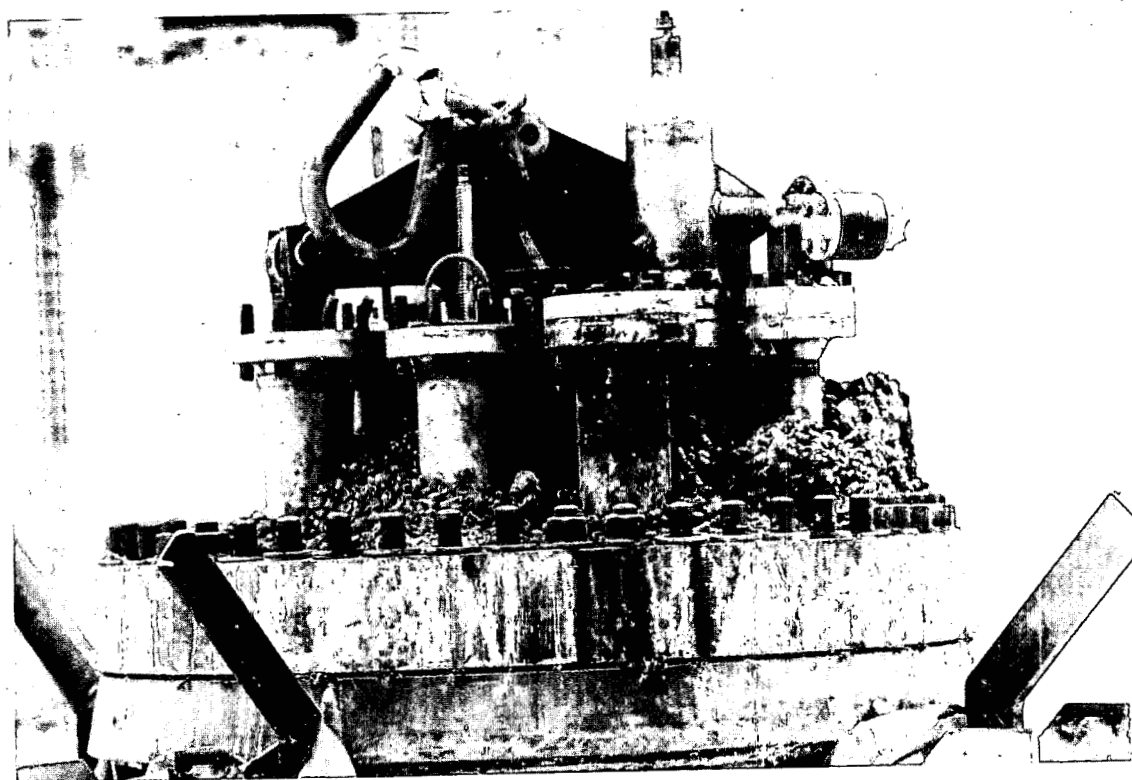


Figure II-29 Shielding Material
II-54

2. SL-1 Hot Shop Operations

2.1 Preliminary Operations

On November 30, 1961, the SL-1 pressure vessel and reactor, enclosed in the transport cask, were received at the ANP Hot Shop for disassembly and further investigations. The requirements were to record or preserve all evidence and information, to determine the integrity of the remaining core and structure, to preserve the core for a critical experiment, and completely dissect the core subsequent to the critical experiment.

The Hot Shop is a shielded cubicle 165 feet long, 51 feet wide and 55 feet high, (see XDC 58-9-112, Section 2.1) and is illustrated in Figure II-28. The basic equipment consists of an overhead crane, a heavy duty overhead manipulator, wall mounted manipulators, and services such as water, power, compressed air, etc. This is a general purpose shop, built to handle a wide variety of remote operations. Equipment of particular importance to the SL-1 operation included:

- 2' x 3' elliptical first-surface mirror
- 1' x 1' square first-surface mirror
- Light bar containing three 500 watt bulbs
- Stand for pressure vessel cutting operation
- Air powered disc grinder
- Overhead manipulator
- Wall-mounted manipulators
- Crane
- Air powered drill motor, core drill, twist drills
- Floor mounted milling machine head
- boroscope, 2" diameter with right angle objective
- Binoculars for observing core
- Remote actuated 4" x 5" press camera
- Remote repeating 35 mm camera
- Quartz lamps for small, high intensity light source

The SL-1 reactor and pressure vessel were received at the Hot Shop in the transport cask and the cask off-loaded onto the Hot Shop floor where it was to be used for shielding the subsequent operations.

The rubberized contamination cover was stripped off the pressure vessel and the pressure vessel examined. The #7 control extension rack had shifted to a position approximately 5 inches lower in its nozzle during transit. This extension and rack had been completely separated from its control blade during the incident and had shifted slightly during lifting or transit. All major components stayed in place during transit, as far as could be determined.

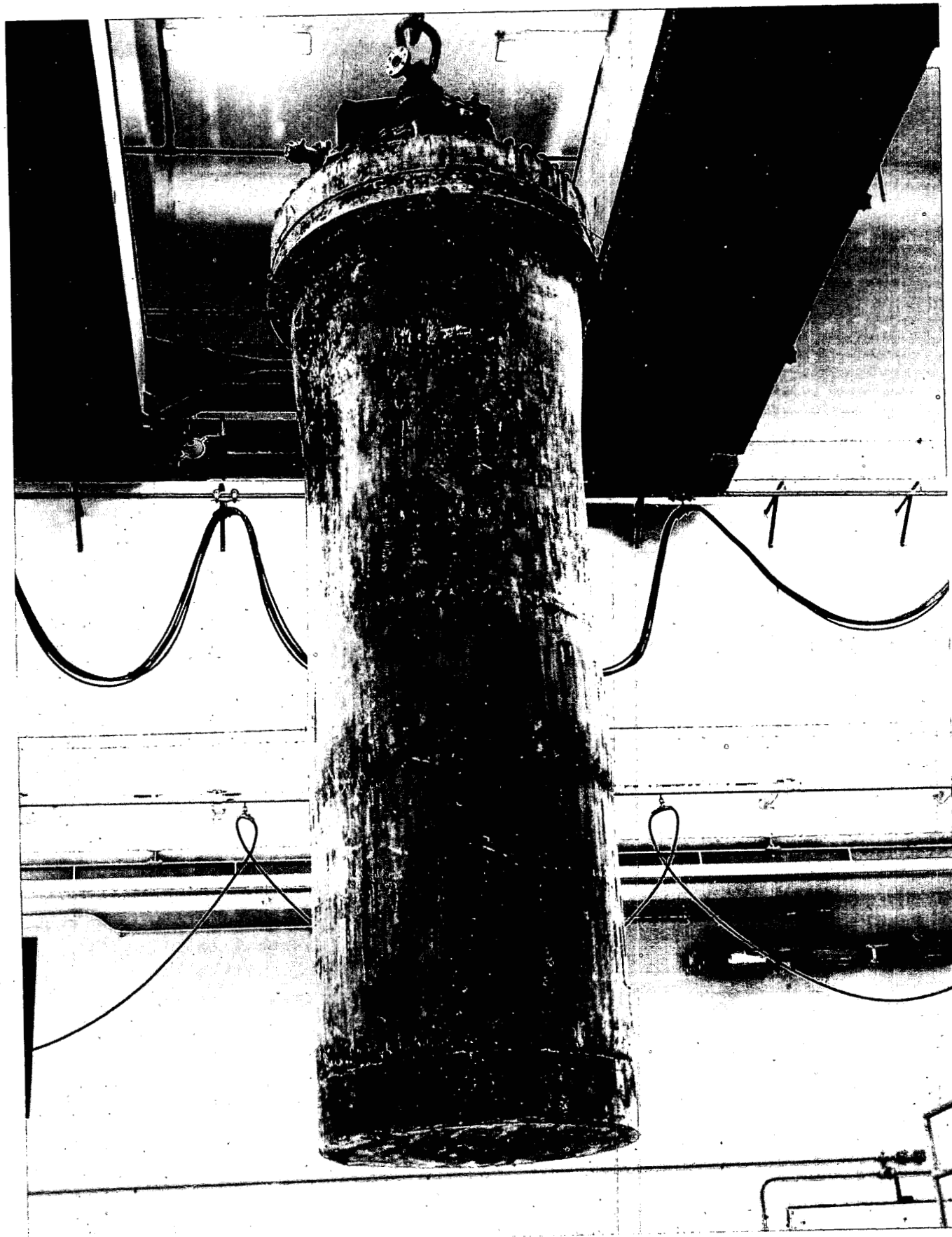


Figure II-30

SL-1 Pressure Vessel
II-56

The earliest work done was to remove the gravel fines, boron oxide, and steel punching shield material and its retainer from the top of the pressure vessel head. This material had been contaminated during the incident and its removal lowered the radiation field for the necessary contact work to follow. There was approximately twenty-cubic feet of this material removed by the twin "Tornado" three horsepower vacuum cleaner, using a 2" I.D. or a 3" I.D. suction hose. This system worked well for removing the loose material. In some parts of this material the combination of water, boron oxide and gravel fines had hardened into a weak concretion, seen in Figure II-29, which had to be broken up with an iron bar and a manipulator before the vacuum cleaner could pick it up.

With the head cleaned, the eleven nozzles in the pressure vessel head were open for inspection. This inspection is covered in Section III-1.5 of this report.

The portion of the pressure vessel volume above the core was thoroughly inspected and photographed using the two inch diameter boroscope with a right angle objective, 1000 watt quartz lamp and an Exakta 35 mm camera using Plus-X film at shutter speeds from 5 to 15 seconds. This inspection established several things.

The lifting fixture toggles were still engaged and would not accidentally disengage when the crane was disconnected.

The #5 control rod extension appeared to be disconnected from its poison blade.

The main water level still well float-rod (Nozzle #11) was disconnected from the pressure vessel head.

The secondary water level still well (#10) was collapsed but was still connected to the head and not entangled with the core.

The steam baffle and upper spray ring had broken loose from the pressure vessel and fallen down onto the core.

The handle from an auxiliary cadmium poison strip (probably the one missing from the #6 shroud) was lodged in the gap between the pressure vessel flange and the head.

The #9 poison blade was connected to its cruciform extension and the ball-joint connection between the cruciform and the control rack extension was intact.

The pressure vessel head could be removed without disturbing the core.

The gap between the pressure vessel flange and the head was photographed by installing a bright light inside and photographing the bright spots where the light was shining through.

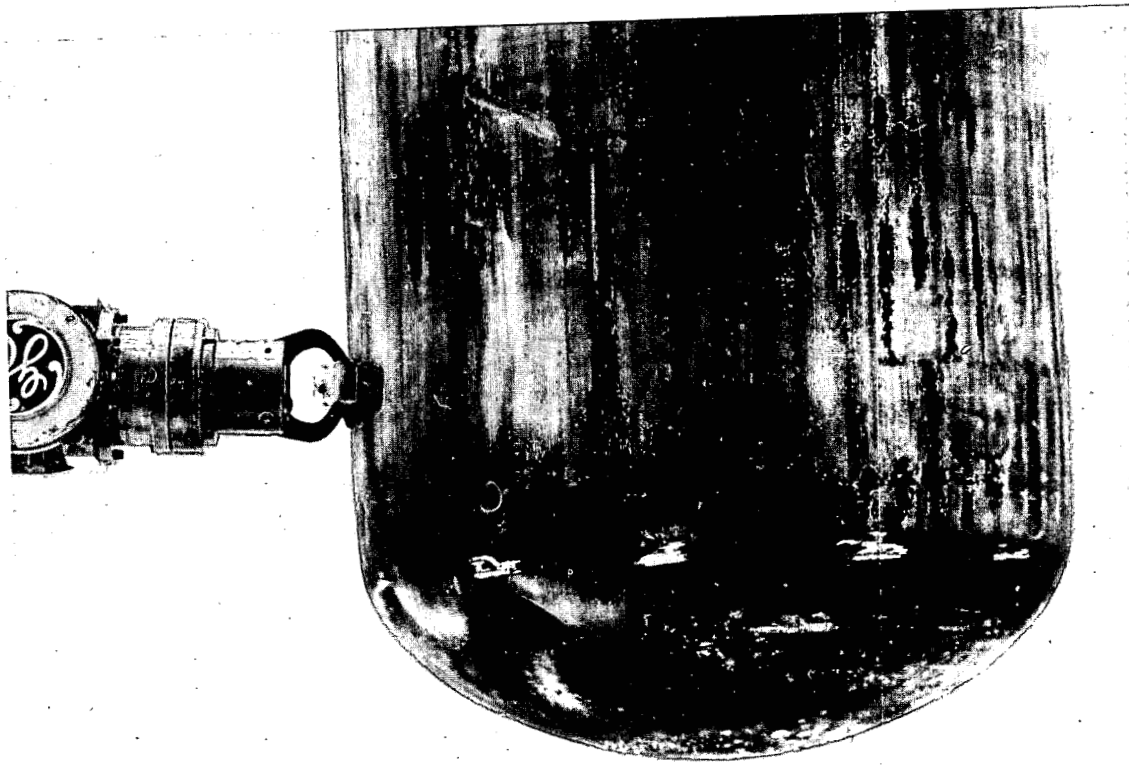


Figure II-31 Pressure Vessel Dished Head

U-5103-1

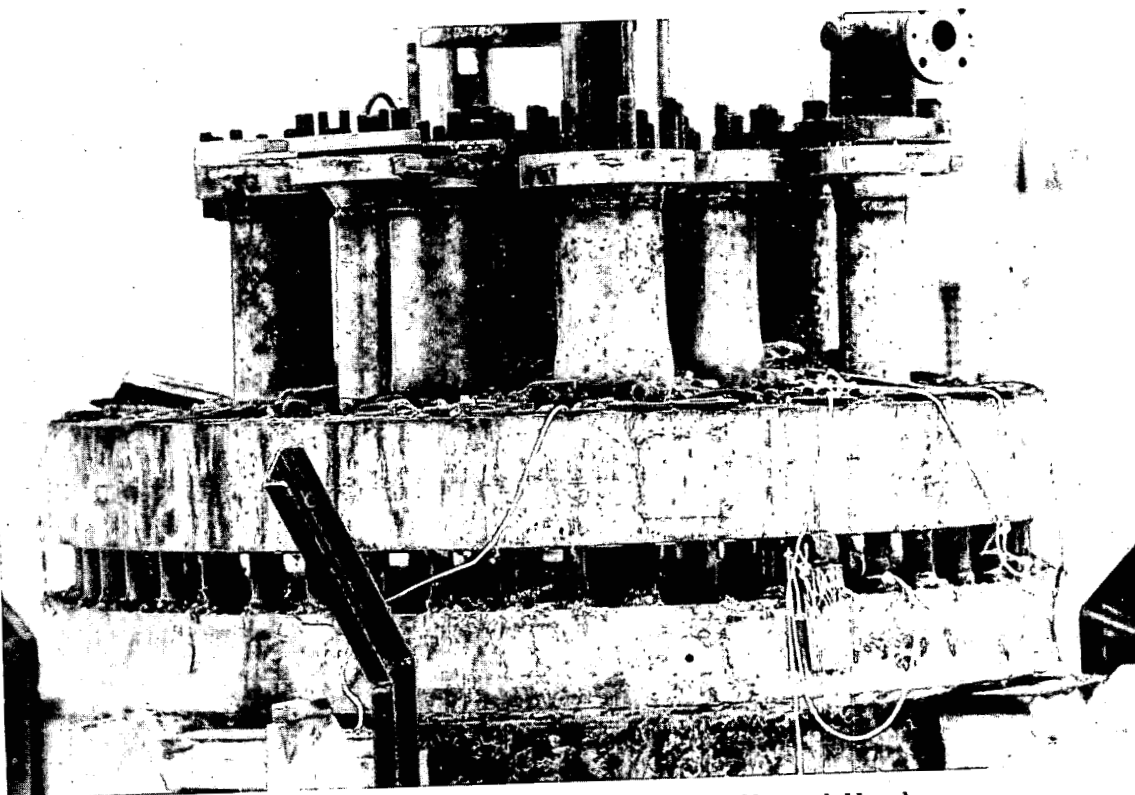


Figure II-32 Pressure Vessel Head II-58

The pressure vessel assembly was removed from the shielding cask, photographed and inspected. See Figure II-30. No marks which would indicate the height the vessel had risen were observed. The insulation fairing around the dished head was removed by grinding through the tack welds. This exposed the dished head, seen in Figure II-31, which appeared to be more spherical than the drawings indicated. The hole in the pressure vessel is the one drilled for boroscope inspection at the SL-1 Site.

The sides of the pressure vessel were brushed off remotely to remove particulate contamination and to allow a somewhat better inspection. An orientation stripe was painted down the side of the pressure vessel.

2.2 Head Removal

Prior to the pressure vessel head removal it was desired to remove all parts which would project below the head in an effort to prevent handling damage. An attempt was made to remove the auxiliary water level still well (#10 nozzle) but it was bound by the collapsing of the still well inside the nozzle. The #5 shield plug assembly was bound to its control rod rack by the collapse of the guide tube. The shield plug, control rack and extension rod were withdrawn as a unit (after removal of an inactive portion of the lifting fixture which interfered). This lifting operation was performed with the crane hook coupled through a weighing device to the shield plug. The expected load was 217 lbs. while the indicated load was 215 lbs. This confirms that the remaining parts of the core were not disturbed by this operation.

Other facts uncovered at this time were:

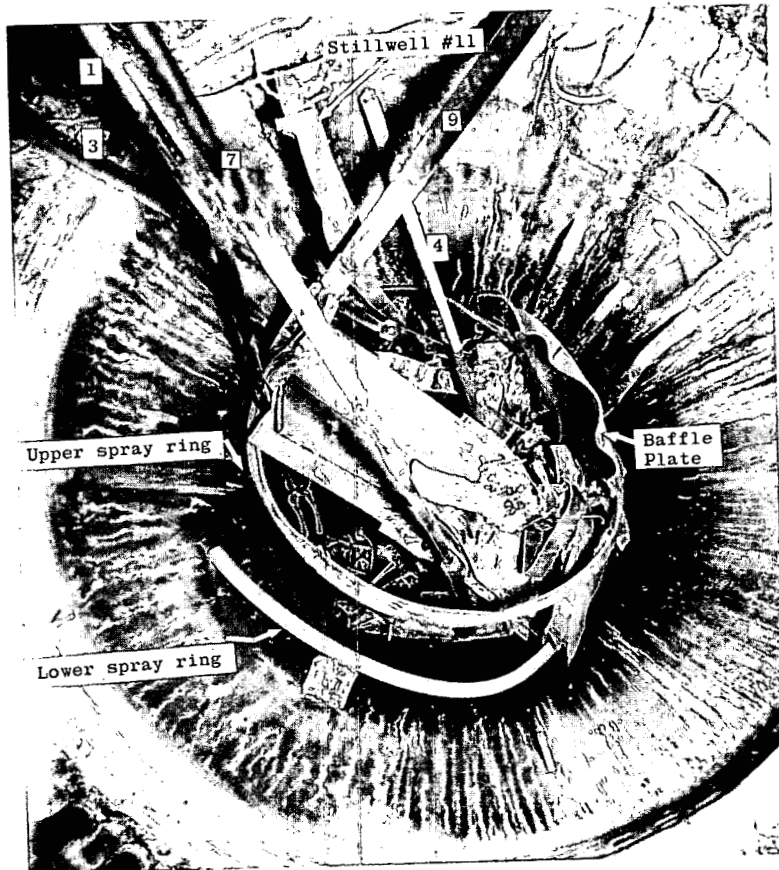
The #10 nozzle flange nuts required the 1-1/2 inch square drive impact wrench to loosen the nuts. This implies a higher than normal torque value.

The #5 bell housing pinion drive extension was bent down slightly. The #5 pinion spline was broken off, allowing the spline adaptor to turn over.

The nut on the end of the #5 control rack could not be removed.

The pressure vessel head hold-down nuts were to have their torque values checked before removal. Due to the radiation field, only five nuts were checked. The torque required to move these bolts was 400, 300, 370, 150, and over 400 ft-lbs. There was no noticeable difference between tightening and loosening the nuts. The remainder of the nuts were removed remotely with the 1-1/2" square drive impact wrench. The washers could be easily picked off with the manipulator.

Figure II-33 SL-1 Core



U-5123-7

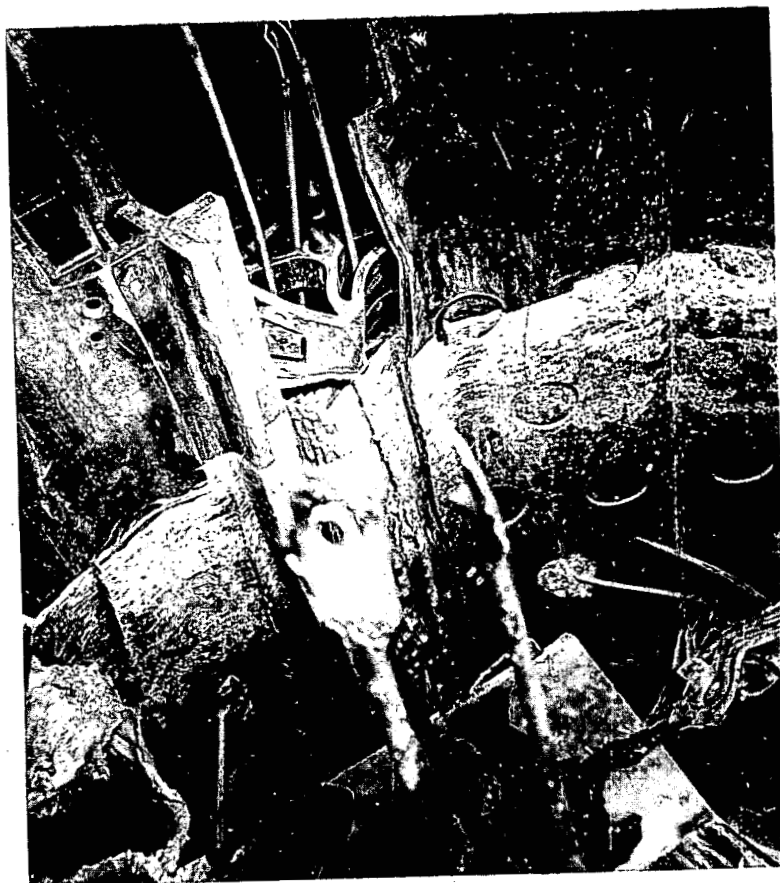


Figure II-34
Deposits on Core Parts

II-60

The pressure vessel head could not be removed with the crane. This was due to its being pinched firmly by the studs as a result of the cupping deformation of the pressure vessel flange. The head was removed by driving steel wedges between the pressure vessel flange and the head as shown in Figure II-32. The wedges were tied to the studs in an attempt to prevent losing the wedges inside the pressure vessel. The driving was done with a 200 lb. battering ram suspended by a cable from a manipulator and swung by a man on the boom of another manipulator. After 5-1/2 inches of wedging the head was free and was removed the rest of the way with the crane. The bottom of the head was covered with a white deposit, identified as boric acid crystals, some of which were scraped off for chemical analysis.

The number 10 still well was cut off a foot below the head, the head decontaminated, and delivered, with all pieces, to the laboratory for detailed examination.

2.3 Initial Parts Removal and Inspection

The core condition when the pressure vessel head was removed is clearly shown in Figure II-33. The #9 control rod shroud, the spray rings, steam baffle, etc. can be clearly seen. The #1 and #3 control rod extensions and racks were still attached to the poison blades. All loose inert pieces and fueled pieces more than six inches above the remaining core volume were removed to make ready for a critical experiment. An inventory of all pieces removed was kept and checked off against photographs of the core. These operations were performed with a long armed manipulator while observing the work in a mirror. Photographs were taken at each significant stage of the dissection using a remotely operated 4 x 5 press camera and electronic flash held over the core with a manipulator. On several occasions two photographs would be made in such positions as to form a stereo pair. This assisted greatly in understanding the conditions inside the core.

The white deposits seen in the upper portion of the pressure vessel were sampled and the samples sent to the laboratory. Other deposits in the top of the active core such as those in Figure II-34, were also sampled. The samples were obtained remotely with a spoon-shaped scraper.

The #1 and #3 control rod extensions were removed by cutting through the connecting rods with the remotely operated cut-off grinder. This allowed the finger disconnect to operate and the extensions were removed.

The reactor was now in condition for the critical experiment.

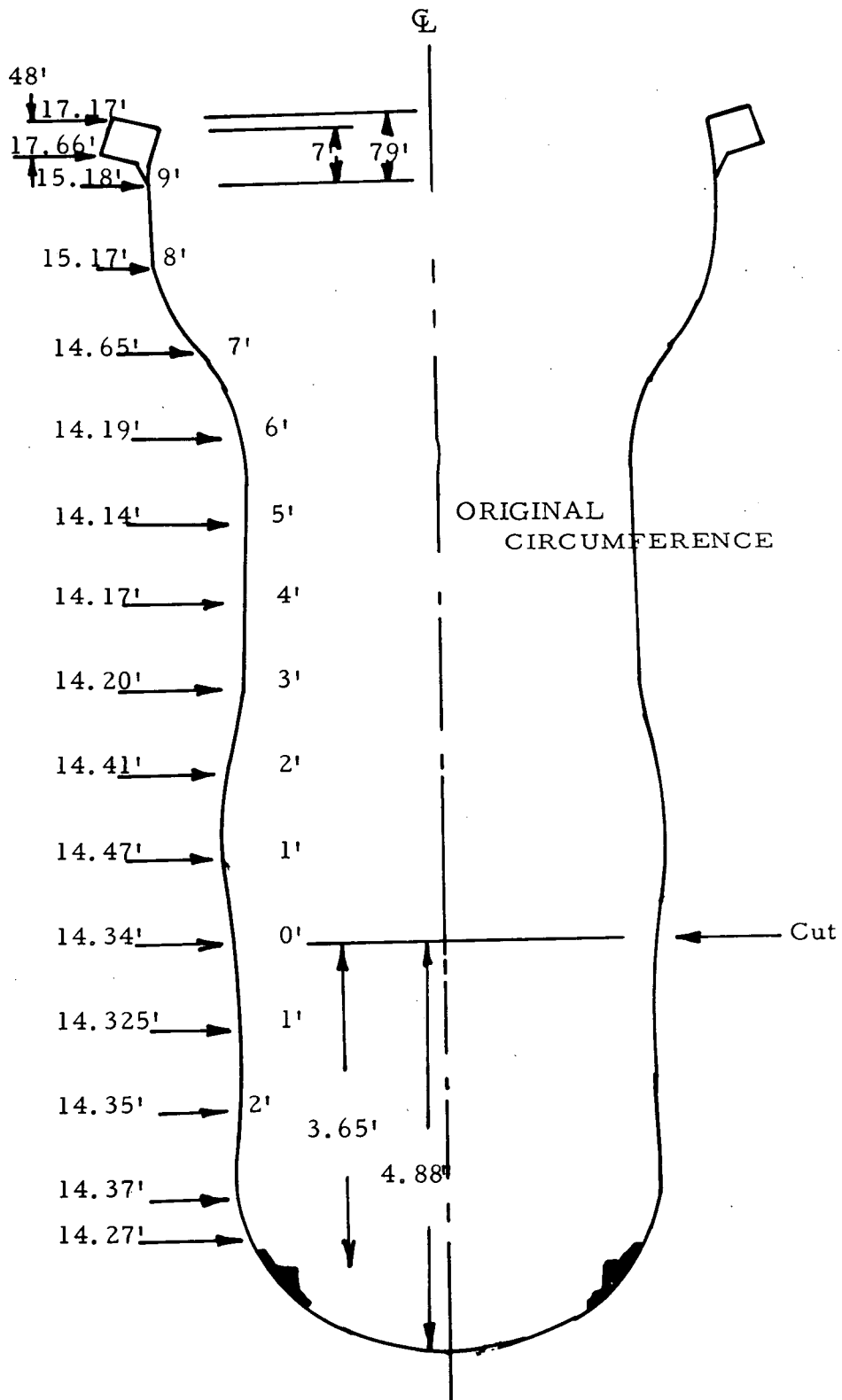


Figure II-35 Pressure Vessel Measurements

2.4 Pressure Vessel and Core Measurements

The parts of the core and pressure vessel were measured several times and in different ways. The first measurement of the pressure vessel was done by triangulation with a theodolite from a distance of approximately 100 feet. This was an effort to measure the deformation of the pressure vessel, previously seen in Figure II-30, at the earliest possible date.

For precise sizing of the criticality tank, a remote measuring device consisting of a 5 foot by 16 foot piece of light gauge sheet metal formed into a cylinder about 5 feet in diameter was made. This cylinder had a measuring tape and a tightening screw attached at top and at bottom and was suspended by springs from a frame. The pressure vessel was removed from the cask and placed inside the cylinder. The adjusting screws were then tightened with a manipulator and the circumferential distance read with binoculars. This reading gave an average diameter of 55.1 inches (173" circumference) for the bulge in the core region of the pressure vessel compared with a 54 inch diameter on the drawings.

After the reactor was completely removed from the pressure vessel, the pressure vessel and thermal shield were measured manually. The thermal shield had bulged from an original 13.22 feet to 13.37 feet circumference at the midline. The pressure vessel circumferential dimensions are given in Figure II-35.

In an effort to define the relative locations of various core components, the core was surveyed using the pressure vessel flange and its bolt circle as a base. The bolt circle was measured to be 62 inch diameter (3 measurements of 62", 61-1/2", 62"). The survey was made using a plumb bob suspended from a tape measure. With the plumb bob at the point to be measured, the elevation was read by sighting across the top of the flange studs. The plan position was then determined by the intersection of two sights across the bolt circle referenced to the numbered studs. These measurements were confirmed by the relative offsets seen in other photographs. Figure II-36 shows the points at which measurements were taken and Table II-1 gives the tabulation of survey measurements. The four critical experiment rod positions shown in Figure II-44 were located from this survey.

2.5 Lower End Inspection

The inspection of the lower end of the pressure vessel and the underside of the reactor accomplished several things.



Figure II-36 SL-1 Core

TABLE II-1

TABULATION OF CORE MEASUREMENTS

Reading Number	Location (Ref. U-5112-1)	Depth below studs (inches)	Intersection of lines between stud numbers Plan Position
1	Off #8 "Tee" to left	143 1/2	(22-42) & (16.5-33.5)
2	In from right edge of #7	150 1/2	(22-40.5) & (16-36)
3	Straight out #8 shroud	146	(20-44) & (14-36.5)
4	Top of #8 shroud	95	(23.5-40.5) & (19±31-)
5	End of connector on #7	87 1/8	(24-40) & (16-35.5)
6	Off end of #6	152	(23-41) & (15.5-35)
7	Same as position 3 on picture	142 5/8	(21-44) & (15.5-35)
8	In front of #1 rod	146 1/8	(20-46) & (15.5-36)
9	Between #1 and #8	128	(22-43.5) & (17.5-32.5)
10	Between #7 and #8	116 1/2	(23.5-41.5) & (17.5-33)
11	On cross in front of #6	117 1/2	(23.5-41.5) & (31.0-1)
12	Hole in front of point 11	147 1/4	(23.0-42) & (31-1.0)
13	~ Center (toward center in line with 11 and 12)	145 1/4	(21.5-44) & (29.5-3)
14	Close to point 7	147 1/2	(20.6-45) & (15.5-34.0)
15	On corner of #3 shroud	98 1/4	(18-48) & (8-45)
16	Back of center of #3 shroud	125 3/4	(16-3) & (27-6)
17	Check on point 15	89 1/4	(18-48.5) & (29-4)
18	On top of #2 shroud	97	(16-3) & (25-8)
19	Hole off point of #2 shroud	143 1/4	(16.5-49) & (25-8.5)
20	On top of #1 shroud	97 1/2	(18-1) & (16-34)
21	On top of #7 shroud	95 1/4	(24.5-41) & (16.5-34)
22	On top of stanchion between 6 & 7	117	(16-35.5)
23	On top of #6 shroud	96 3/8	(25-40) & (23-39.5)
24	On top of #6 cad fixture	96	(23.5-43) & (13-38)
25	On top of #5 shroud	96 5/8	(23-43) & (40-11)
26	On top of #5 connector	88 1/8	(22-43) & (11-40)
27	Top of #4 connector	89 1/4	(19-47) & (9-43)
28	Top of #4 shroud	98 3/4	(20-46) & (10-41)
29	Top of T stanchion between 3 & 2	97 1/2	(15-3) & (10-41)
30	Top of T stanchion between 1 & 8	116 3/4	(21-42) & (19-31)
31	Hole off point of #3 shroud	139 1/2	(18-48) & (12-39)
32	Hole in center	142 1/8	(21-45) & (14-37.5)
33	Side plate center	135 1/4	(21-42.5) & (28.5-4)

Studs extend $11 \frac{3}{8} \pm \frac{1}{8}$ " above flange.
Bolt circle is 62" at top.



Figure II-37 Core Support Bracket



Figure II-38 Bottom of Core

The conditions of the underside of the core were established.
The integrity of the support structure was established.
The bottom of the pressure vessel was cleaned out.
A water flow passage for the critical experiment scram function was made.

With the pressure vessel in the shielding cask, a 3" diameter hole was core drilled through the two foot thick concrete of the shielding cask and liner just below the level of the thermal shield, using an air powered drill motor. This hole was then sleeved down to two inches with a metal sleeve which was used as a guide for the subsequent drilling and boroscope operations. Eight 2-1/2" holes at 45 degree intervals were then drilled through the pressure vessel wall. These holes penetrated on a plane approximately 15 inches below the active core. One hole was blocked by a fuel element which had fallen down and stood in front of the hole.

The boroscope used was 2 inches in diameter and 7 feet long with a right angle objective. A 1000 watt quartz lamp was attached to the end of the boroscope and projected about one foot beyond the objective. A camera adaptor which allowed a choice of either visual inspection or photographic recording was attached to the ocular end of the boroscope together with a 35 mm Exakta camera. Kodak Plus-X film at shutter speeds of one second to five seconds was used.

At each of the seven open holes twelve photographs were taken as follows:

With the boroscope objective 3 inches inside the thermal shield: straight up, 45° left of up, 45° right of up, straight down.

With objective at 9 inches inside: the same four angles were photographed.

With objective 16 inches inside: straight up and straight down only.

With the objective at 23 inches inside: straight up and straight down only.

Since the radiation field at the boroscope ocular was relatively low, a great deal of visual inspection was done and additional photographs of particular points of interest were made.

Figure II-37 shows one of the core support structure to thermal shield attach points and the support boxes and lower end boxes as well as the ends of some fuel plates, as photographed through the boroscope.

In Figure II-38 can be seen an upside-down fuel element with its flux wires, an X-stanchion, melted fuel plates and part of the support structure.

From the visual inspection and an examination of the photographs, the integrity of the arbitrarily numbered support structure brackets was assessed as follows:

Bracket #1

No structure attached, stanchion seemed to be in place. Remaining pieces appeared solid.

Bracket #2

Structure not attached and had dropped down several inches. Bar from 2 toward 1 ran down toward bottom. Stanchion is in place. Remaining parts seemed solid.

Bracket #3

Stanchion and structure appeared to be in place. Bracket pin was bent. Remaining pieces appeared solid.

Bracket #4

Bracket could not be seen due to piece in the way. The support bars did not appear to be damaged or displaced.

Bracket #5

Block was on top of guide pin. Support bars and stanchions appeared to be attached.

Bracket #6

Support bars appeared to be in relatively good condition.

Bracket #7

Long support bar seemed torn loose and dropped several inches. Stanchion and remaining parts seemed solid.

Bracket #8

Block appeared to be raised up on guide pin but support bars and stanchions appeared to be attached and solid.

It was concluded that the integrity of the support structure was sufficient to prevent any collapse or movement during the critical experiment.

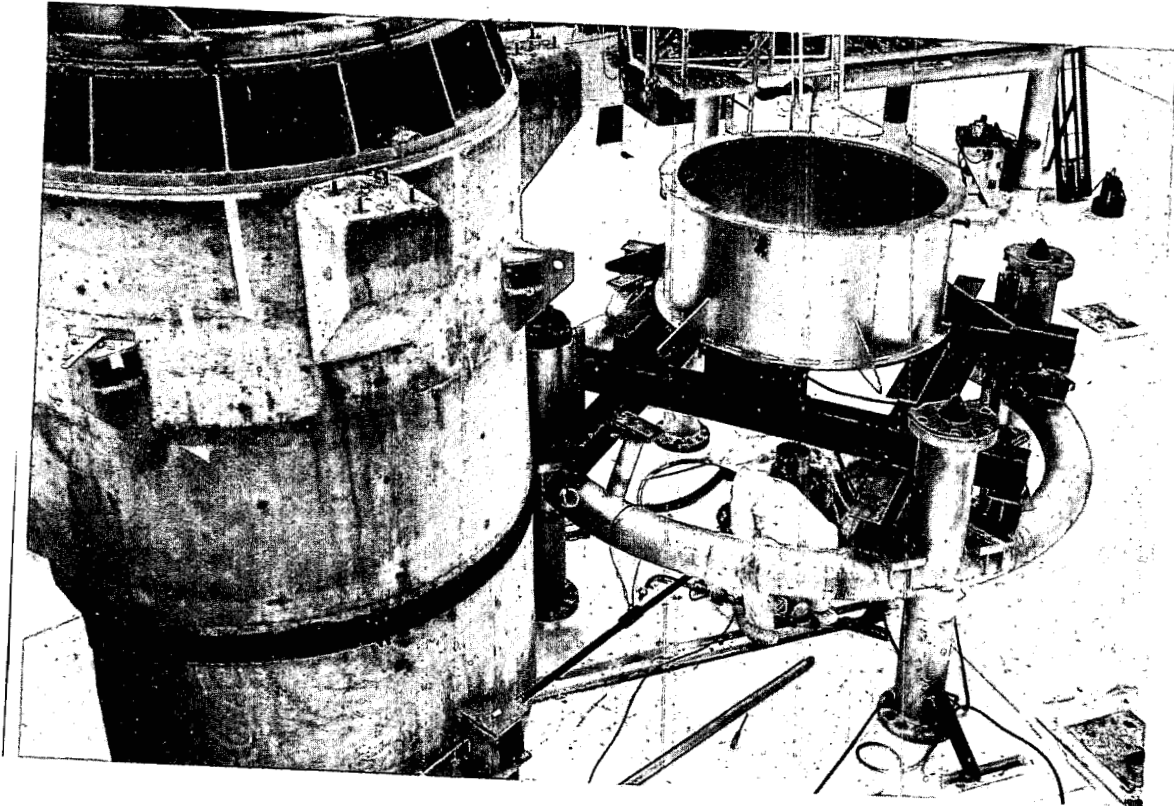


Figure II-39 Equipment for Hole Cutting



Figure II-40 Inside Bottom of Pressure Vessel
II-69

It was necessary to cut a hole in the bottom of the pressure vessel for a water flow passage and to clean out the bottom of the pressure vessel prior to the critical experiment. It was also desired to obtain a stratified sample of the deposit in the bottom of the pressure vessel. To cut the 8 3/4" diameter hole required for these operations, a multi-toothed carbide-tipped, hole-saw was mounted in a milling machine secured to the floor. The machine head was turned so that the axis of the cutter was vertical and centered in the 4-legged pressure vessel stand. This stand restrained the pressure vessel radially by means of four pair of lock bolts while the pressure vessel weight was carried by the crane. Figure II-39 shows this equipment. The tool feed was operated by a long, universal jointed shaft from a shielded position. The cutting action was observed from outside the shop, in a mirror positioned on the floor. The sample from this operation was delivered to the laboratory for detailed examination.

The remainder of the deposits in the bottom of the pressure vessel were scraped out into a tray using a specially built hoe-shaped scraper held by a manipulator while the operation was observed with television. Figure II-40 shows the inside bottom of the pressure vessel near the completion of the cleaning operation. During the cleaning operation the manipulator was also used to check the rigidity of the core support structure, shown in Figure II-40. No motion or deformation of the support structure could be observed, upon applying forces of approximately 50 lbs., thus verifying the adequacy of the support structure for the critical experiment.

The bottom of the pressure vessel was then vacuum cleaned and rinsed out with water. The rinse was performed using a curved 1/4 inch tube inserted through several of the eight boroscope holes. The water was caught in a barrel and delivered to the laboratory along with the scrapings and other loose material.

2.6 Post-Incident Critical Experiment

The SL-1 critical experiment test stand was installed in the Hot Shop on March 15, 1962. Installation of additional equipment, connection of services and final checkout was done during the next two and one half weeks and the reactor was inserted into the test assembly on April 4, 1962. The initial filling occurred on April 5 and test operations continued until April 13, when the test series was terminated. During the test, the tank was filled five times in an attempt to achieve criticality but the reactor remained grossly subcritical throughout the test period. A dilute acetic acid solution was used during three of the fillings in order to

dissolve and remove from the core the boric acid contaminant without dissolving the B-10 enriched metallic boron present as a burnable poison. The unwanted boric acid entered the core when water drained back into the reactor through the sheared steam line and blown head gasket after picking up some of the boron oxide from the top of the pressure vessel head. During the final filling with acetic acid, the system was heated to approximately 160°F to assist further in dissolving the boric acid. At the termination of the test, the core was removed from the test tank and the test tank again filled with water with the source in place, in order to examine source neutron attenuation at various water levels.

The critical experiment equipment performed in a satisfactory manner throughout the test. The nuclear instrumentation was essentially noise free. A continuing problem of maintaining the minimum acceptable count rate of two counts per second existed throughout the entire test. This was due to increasing attenuation with water level with no significant compensating increase in multiplication. The gamma compensation of the ion chambers was not complete in the high core gamma fields, creating difficulty in obtaining the required reading of a factor of two above background during checkout. By using a 35 curie Polonium-Beryllium neutron source, however, the required reading was obtained. The fill, drain, level indication, and water heating systems operated satisfactorily.

The control and source actuators operated in a satisfactory fashion throughout the test; however, upon removal of the number three actuator, the poison tip was found to be severely bent, indicating interference with a core component.

During the test, seven non-significant deviations to the test program were written as provided for in Idaho Test Station Standard Practice J80-81. Essentially all these deviations were written on the basis of two experimental developments. Namely:

The reactor was found to be grossly subcritical indicating that a revised filling procedure could be used.

The low solubility in water of the boron compounds contained in the core indicated the advisability of using an acetic acid rinsing solution.

Figure II-41 is a schematic of the test stand, tank and pressure vessel, including all lines, valves, etc. used to fill, drain and heat the system. Figure II-42 shows the entire system in its operating configuration. With

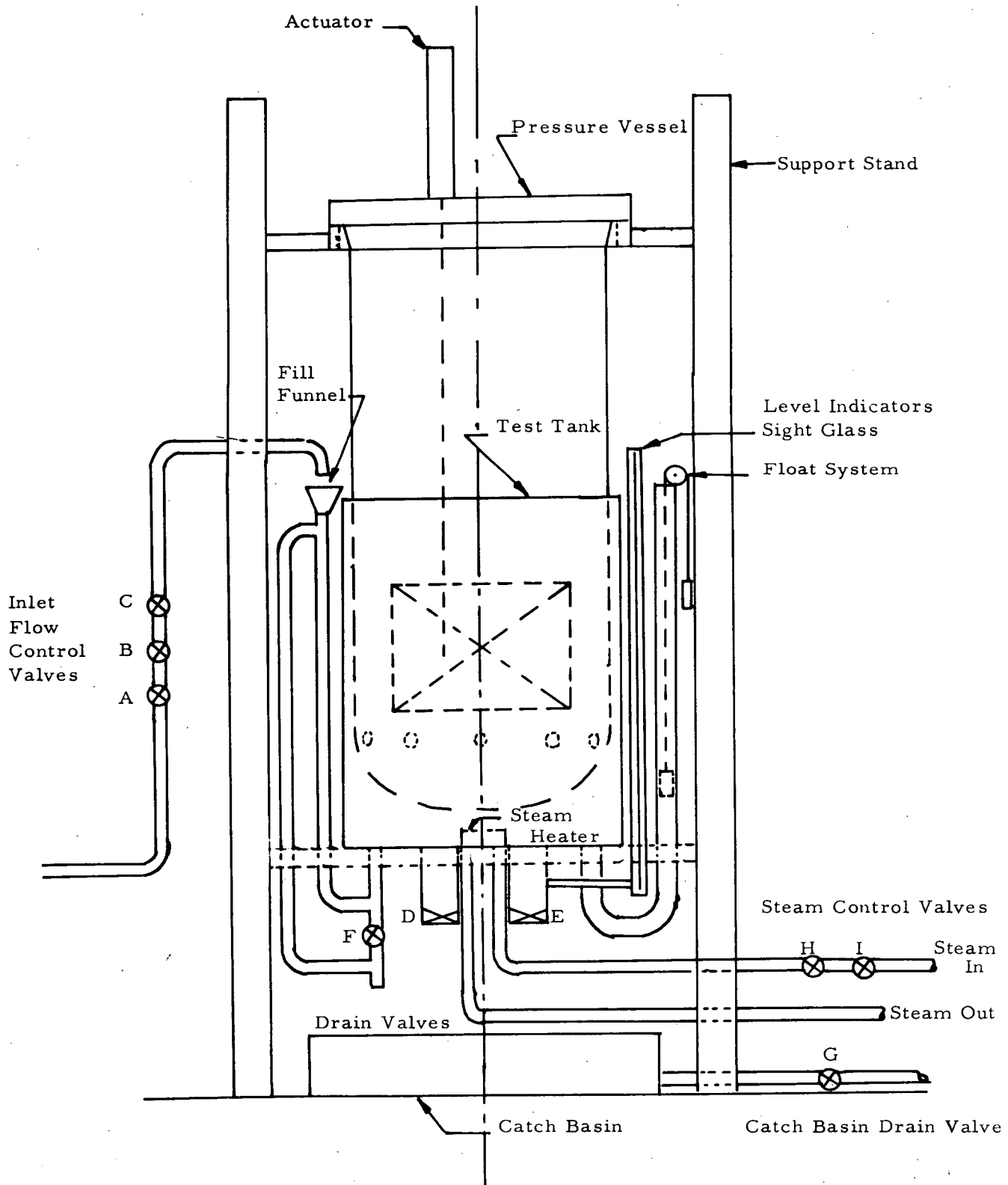
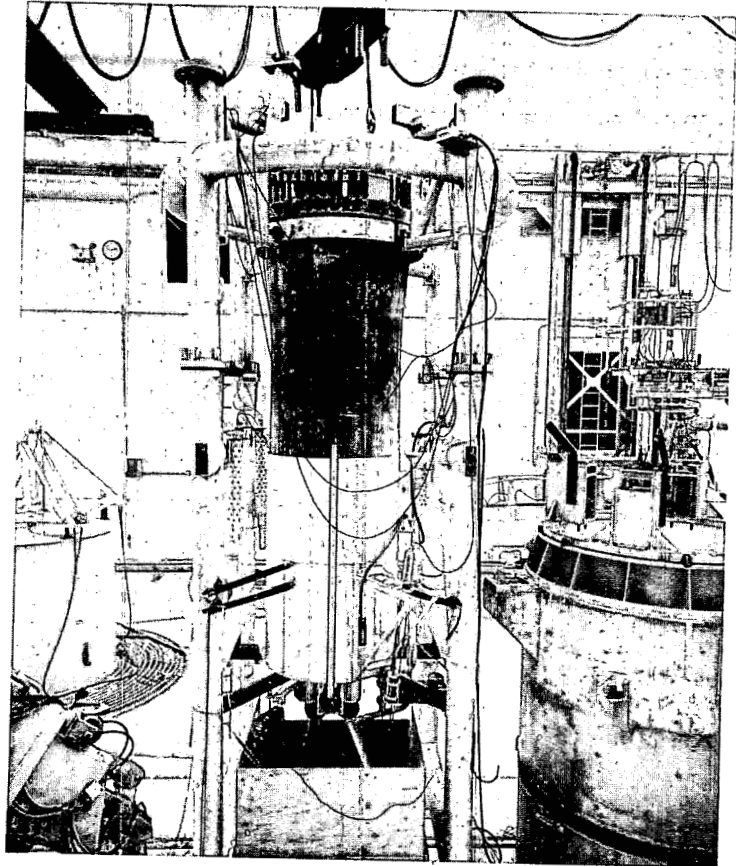


Figure II-41 Test Assembly

Figure II-42
Core in Critical Experiment Tank



U-5112-3A



Figure II-43
Critical Experiment Rod Position

the aid of these figures the system is described as follows. The pressure vessel was supported from its top flange by a machined ring attached to the support stand. When placed in this fixture the pressure vessel extended down into an aluminum tank which served as the water containment vessel. To allow passage of water from the containment vessel into the pressure vessel, a hole 8-3/4 inches in diameter had been bored through the bottom of the pressure vessel as described earlier. Additional entrances were provided by the eight, 2-1/2 inch holes drilled through the pressure vessel wall for the boroscope examinations. To reduce side loads on the containment tank, the pressure vessel remained connected to the 100-ton overhead crane so that the crane bore a portion of the weight of the pressure vessel.

Filling was accomplished using three remotely operated solenoid valves. Valve "A" was the primary control valve, valve "B" was a backup valve, and valve "C" was actuated by a key operated switch so that the fill system could be secured in the closed position. As an additional means of control, a manipulator was used to position the fill line over the fill funnel. In order to prevent overfilling, a standpipe arrangement was provided to limit the water level to the desired maximum height (six inches above the top of the active core).

Two eight inch dump valves were situated on the bottom of the containment tank to provide scram protection. These valves consisted of gasketed blind flanges held against the bottom of short sections of eight inch pipe. The primary dump valve (D) was actuated by a modified safety rod actuator. The withdraw action of the actuator was used to close the valve and the scram action was used for quick opening. This actuator employed an electromagnetic latch and was spring actuated on scram. The secondary dump valve (E) served as a backup for valve D. It was closed remotely using a manipulator and was held closed by an electromagnet. Both valves D and E were connected to the safety circuitry so that dumping automatically occurred in the event of a high flux level or short period. A third motor driven drain valve (F) was used when small amounts of water were to be drained. All drainage water dropped into a open rectangular catch tank below the containment tank, and a manipulator operated valve was used to drain the catch tank to the Hot Shop drain.

The water level was indicated by two devices. A direct indication was obtained from a 100 inch sight glass mounted so that it could be viewed with binoculars from the control point. A second indication was obtained from a float device which operated a 10 turn "Helipot" providing a signal to a recorder at the control console.

In order to perform elevated temperature experiments, a "Platicoil" steam heat exchanger was placed in the bottom of the containment tank. Steam flow was controlled by valves "H" and "I" and the steam was discharged into a trap with the condensate being discharged to the Hot Shop drain system. Two chromel-alumel thermocouples were inserted into the core to monitor water temperature. One thermocouple was inserted to a position below the core between shroud number six and the thermal shield. The other thermocouple was inserted to the top of the active core adjacent to shroud number eight.

An additional means of controlling reactivity other than by the addition or draining of water was provided by three control rods inserted into the core from the top of the pressure vessel. These rods had no scram capability, and were used only for control purposes. Core locations for the rods had been determined by examination of photographs and by measurements of core void areas. The rod actuator mounting fixture had been marked such that when the actuators were positioned to the appropriate index marks the rods would be above the desired locations in the core. The actuators were installed and the rods individually driven into the core while being observed in a mirror above the pressure vessel. Some readjustment of position was required to achieve maximum penetration of the rods. Locations and depth of insertion of the three control rods and the source rod are shown on Figures II-43 and II-44.

The source rod actuator was identical to the control rod actuators described above, and was positioned as shown on Figure II-43. The startup source was 13 curies of Polonium-Beryllium.

Figure II-45 is a schematic of the nuclear instrumentation and safety circuitry. Figures II-43 and II-46 illustrate the locations of the various sensors and Figure II-47 shows all control and nuclear instrumentation in the installed configuration.

Neutron flux was measured by three scintillation detectors and three compensated ion chambers. The scintillation detectors consisted of boron impregnated plastic crystals coupled to RCA C555A photomultipliers and connected to TMC DC-12 preamplifiers. Victoreen AID linear amplifiers (model 672-A) were used to drive the count rate and period amplifiers and the TMC scalars. These three channels were used to generate an automatic scram signal on high count rate and to provide a visual signal for the Reactor Operator.

Compensated ion chambers provided log flux and period signals. The chamber output was amplified and visually displayed on Log N and Period Amplifiers (Engineering Specialities Model K-2 and J-2). These amplifiers were equipped with automatic period trips which provided short period scram protection.

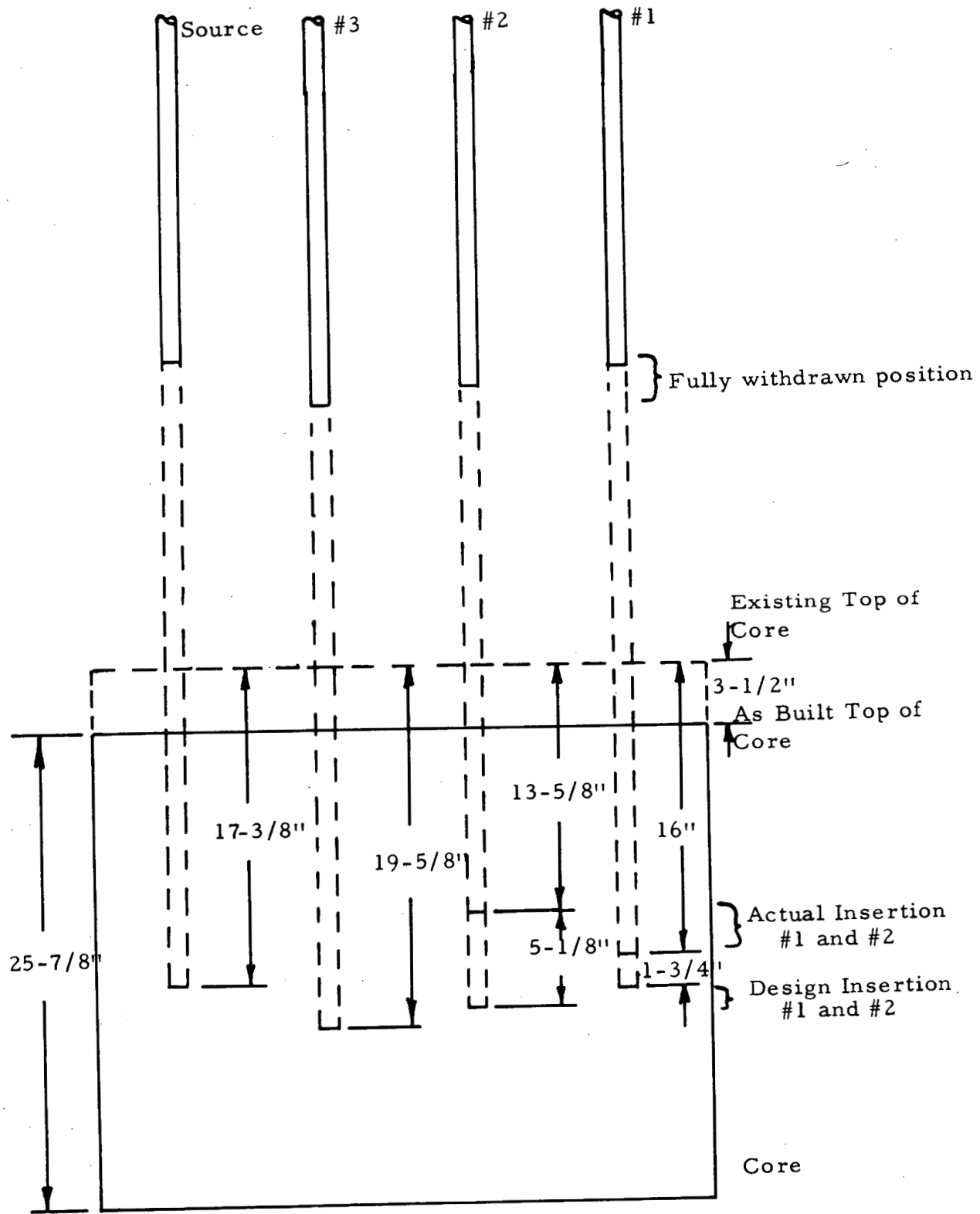


Figure II-44 Location and Travel Distance of Control Rods and Source

II-77

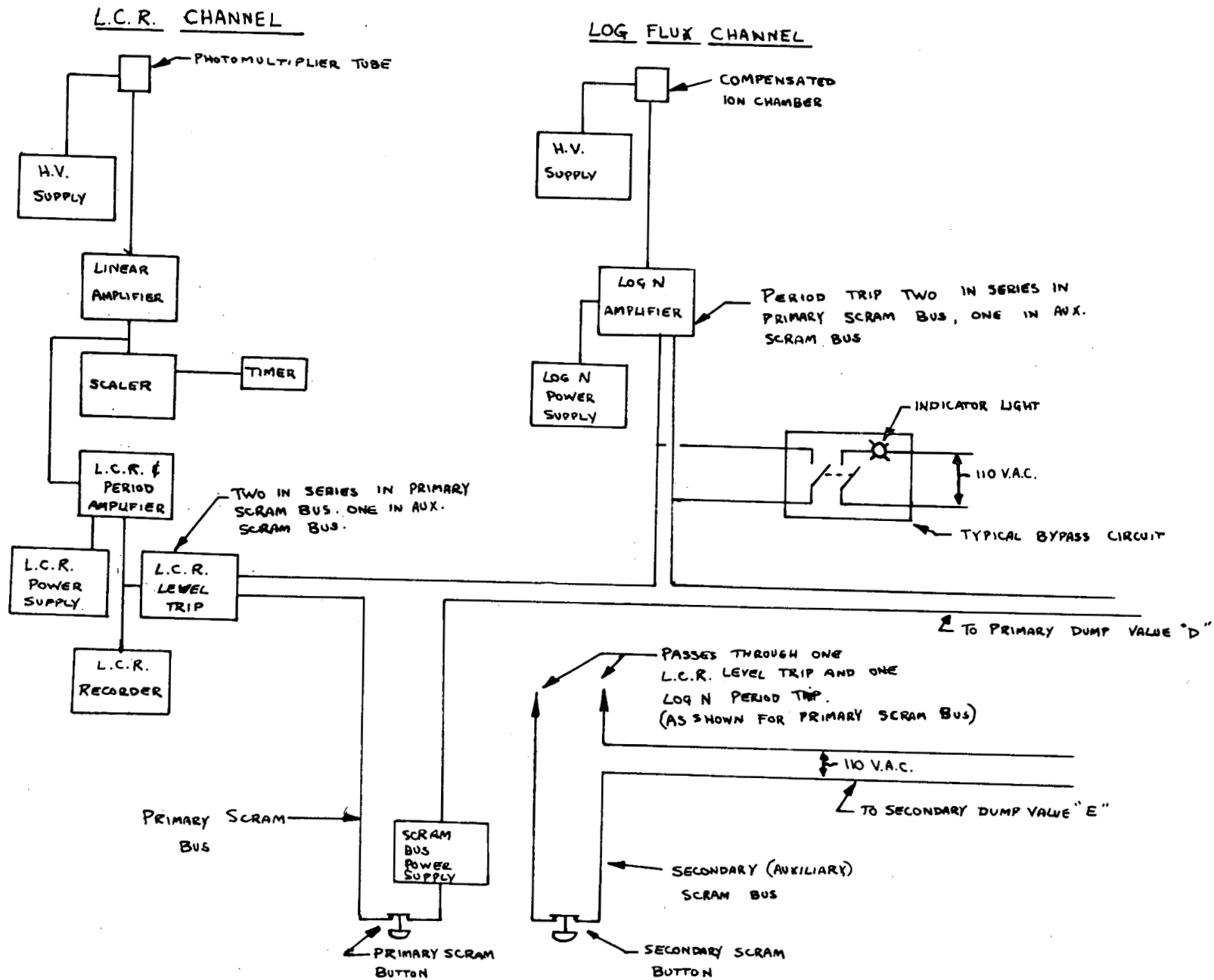


Figure II-45 Nuclear Instrumentation Schematic

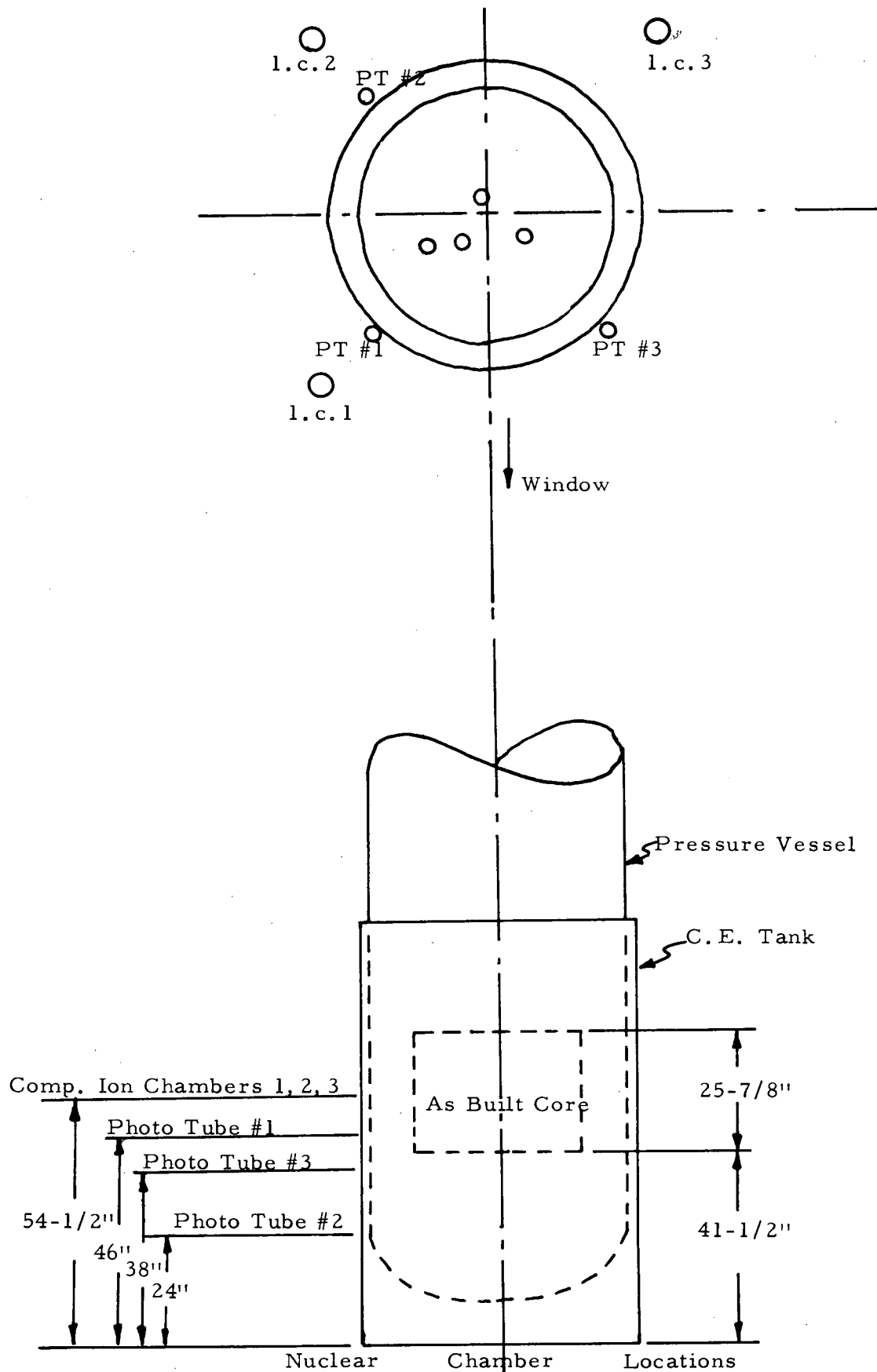
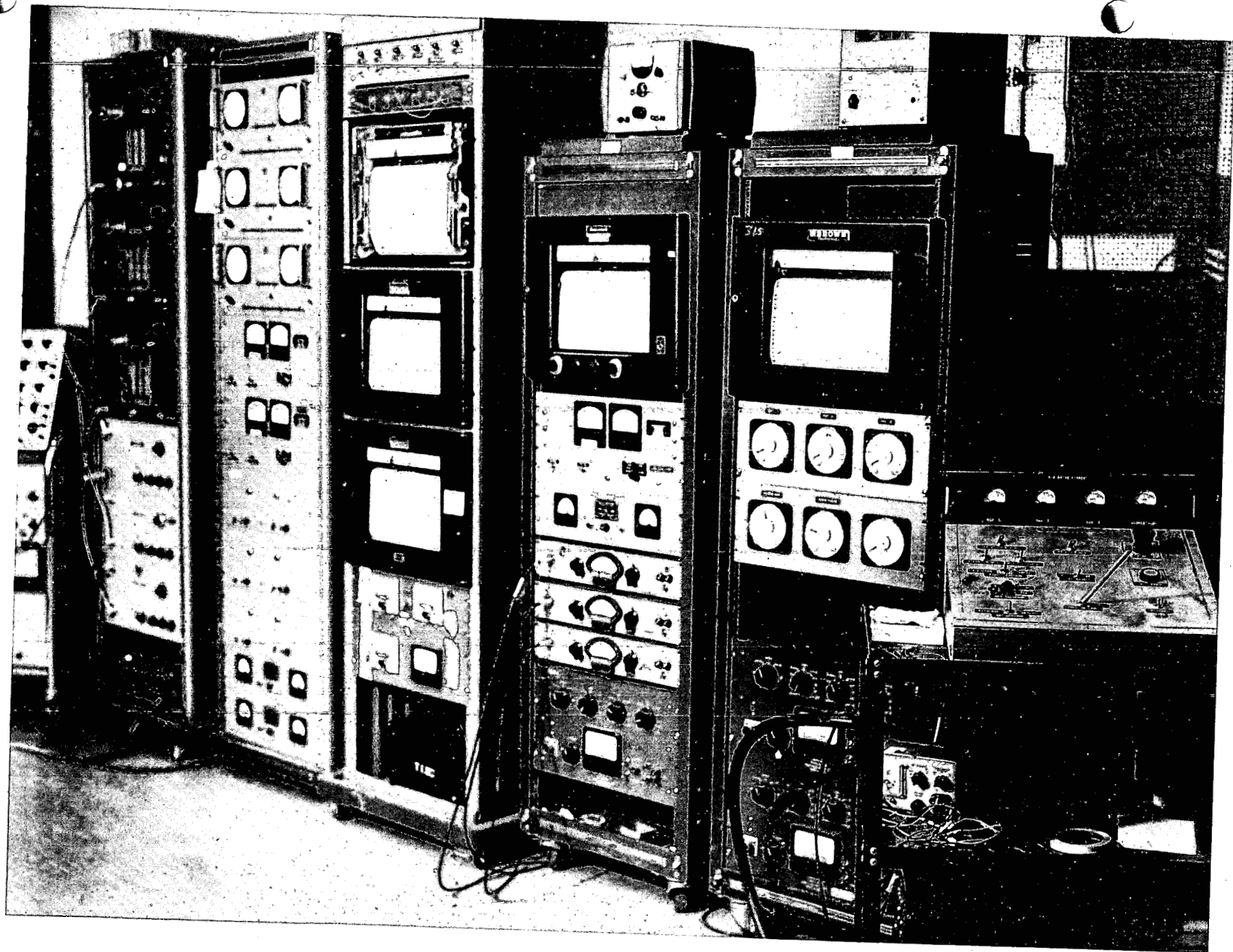


Figure II-46 Nuclear Sensor Locations



U-5144-1

Figure II-47

Nuclear Instrument Panel

Rod Drive Current



1



2



3



Source

115V, 400~ Power

28 V.D.C. Power



Steam Valves



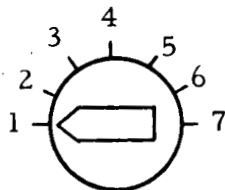
1



2

Source Drive

With.  Insert



Rod Selector

With.  Insert

Rod Control



(Valve C)

(Valve B)

Off  On

Fill Enable

(Valve A)

 Fill

Hold to Fill



Scram
(Valved)



Aux.
Scram
Valve (E)



Setback
(Valve F)

II-80

Figure II-48 - Control Console for Critical Experiment

The actuator control circuitry consisted of a drive control switch and a seven position selector switch. Control rods one, two and three could be selected individually by positions on the selector switch and were driven using the rod drive control switch. A fourth switch position provided for motion of the scram-valve actuator. A fifth switch position selected the source rod for precise position indication only, with source drive control provided by a separate switch. A sixth switch position connected all three control rod actuators to the drive control switch so that they could be driven in unison. A precise indication of rod position was provided by a digital voltmeter which indicated the position of the selected rod, and in addition, rod position was indicated by individual panel meters for the three control rods and the source rod. Individual meters were also provided to indicate rod drive current for the three control rods and the source rod.

Also included on the control panel were the fill and drain valve controls and the steam valve controls. Figure II-48 illustrates the relative position of all controls on the Reactor Operator's control console.

Checkout of Nuclear Instrumentation at the Shield Test Facility - All six channels of nuclear instrumentation were assembled and checked out at the Shield Test Facility using the "Susie" reactor as a neutron source. The purpose of the checkout was:

To determine if all components were in operating condition and were compatible with each other.

To identify any tendency to saturate or lose sensitivity in high neutron and gamma fields.

To insure an adequate overlap between the log count rate and ion chamber channels.

Pre-operational Checkout - Prior to insertion of the vessel into the test assembly, a rigorous checkout was made to assure the proper operation of all instrumentation and controls.

Upon installation of the vessel into the test assembly additional checkout operations were performed and the system was ready for operation on April 4, 1962.

A detailed summary of the operation is presented below in chronological order.

Thursday, April 5 - Vessel filled to overflow with demineralized water
Log Count Rate channel #1 showed large increase in count rate (order of 10^6) while the two other counters showed a net decrease in count rate from water level at bottom of core to water level at top. This was believed to be due to radiation sensitivity of some electronic component in channel #1.

Friday, April 6 - Vessel filled with demineralized water to 5 inches above bottom of fuel (54.5 inch level) when a scram occurred due to dip in line voltage.

Monday, April 9 - Vessel filled with dilute acetic acid to within several inches of top of fuel (72.3 inches above bottom of tank) when a scram occurred due to faulty adjustment on one of the trip circuits. Again Log Count Rate channel #1 showed a large increase in count rate, while the other two channels showed a net decrease.

Tuesday April 10 - The solution of dilute acetic acid from the previous day's filling was pumped back through the fill system. The vessel was filled and the solution was heated slightly. Log Count Rate #1 again showed the same large increase in count rate.

Wednesday, April 11 - The Log Count Rate #1 channel was replaced with identical components. The vessel was filled with a fresh acetic acid solution. The water level was lowered to the top of the fuel and the solution heated to about 160°F. The water level was then raised to the overflow and the solution temperature maintained for several hours at a high temperature. All Log Count Rate channels showed a net decrease in count rate as the vessel was filled and no significant change in count rate during the heating process.

Thursday, April 12 - The vessel was filled with demineralized water. All Log Count Rate channels showed a net decrease in count rate.

Friday, April 13 - The vessel was removed from the aluminum tank, and this tank was filled so as to obtain a count rate vs. water height curve for the case of no reactor or pressure vessel but with the source in its equivalent position as during the other fillings.

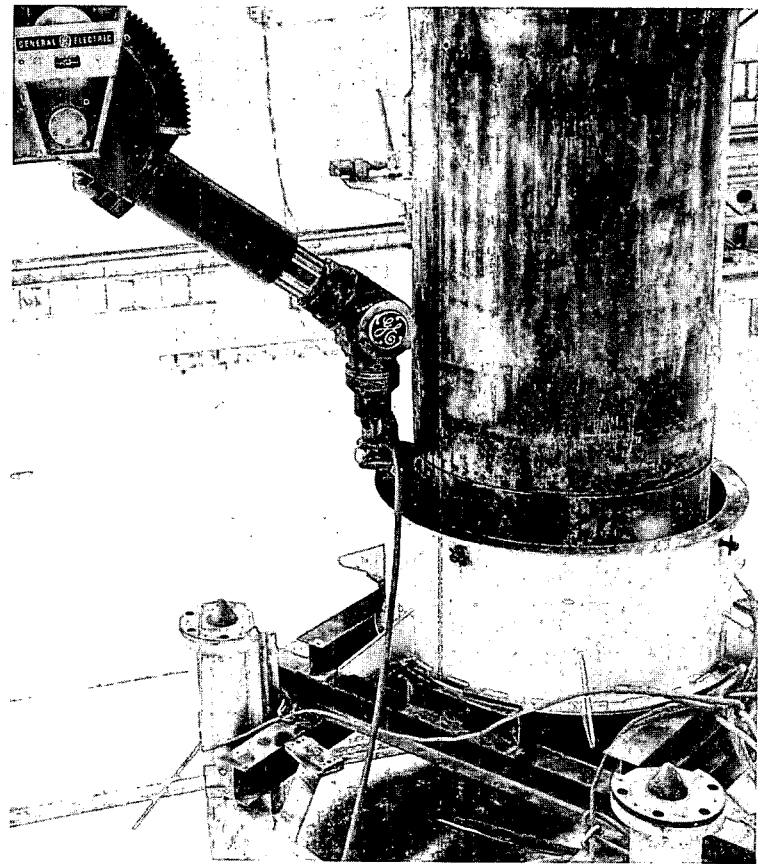
2.7 Final Disassembly and Disposal

After the conclusion of the critical experiment, preparations were made to completely dissect the remainder of the core and pressure vessel for detailed laboratory examinations. As a first step, the upper end of the pressure vessel was cut off to improve access to the core region.

The critical experiment equipment was removed from the pressure vessel and the four remaining pipes (lower spray ring, purification system, spare and main water level still well) were cut to sever all connections between the upper and lower ends of the pressure vessel. At this time it

Figure II-49

Cutting Off Pressure Vessel



U-5147-5

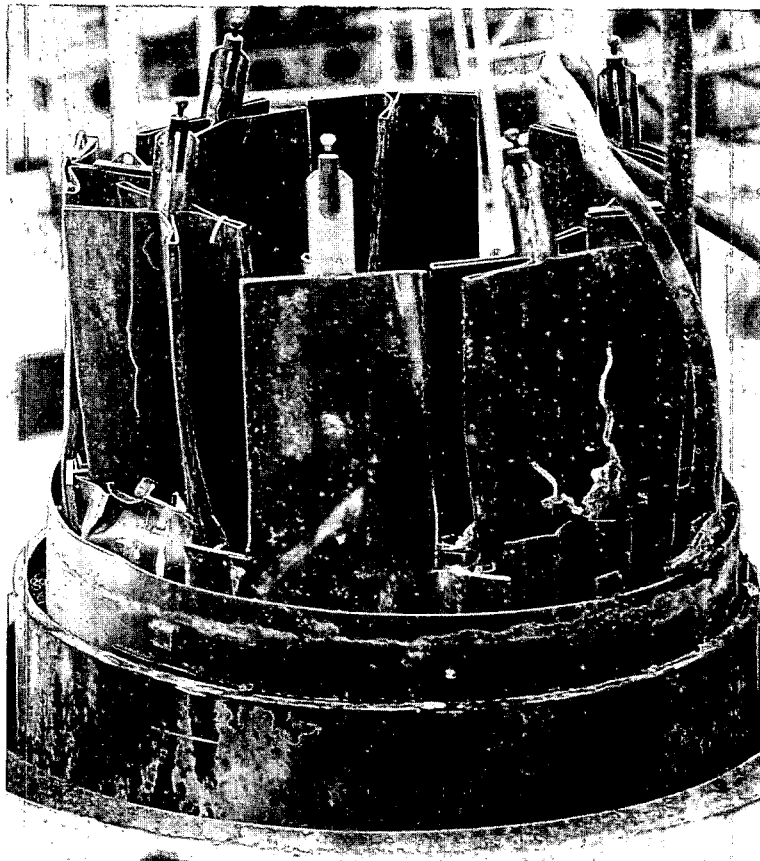


Figure II-50

Upper Control Rod Shrouds

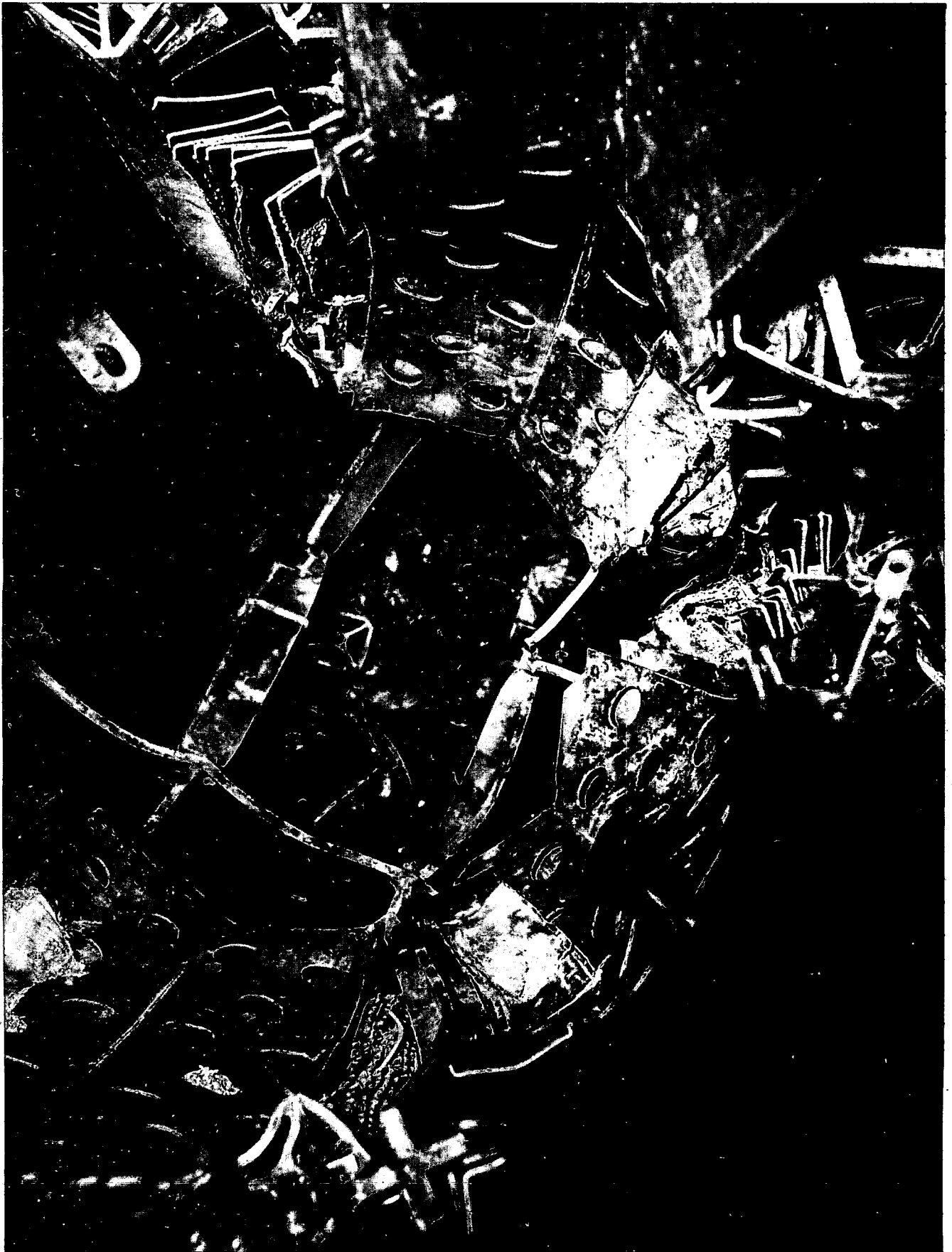
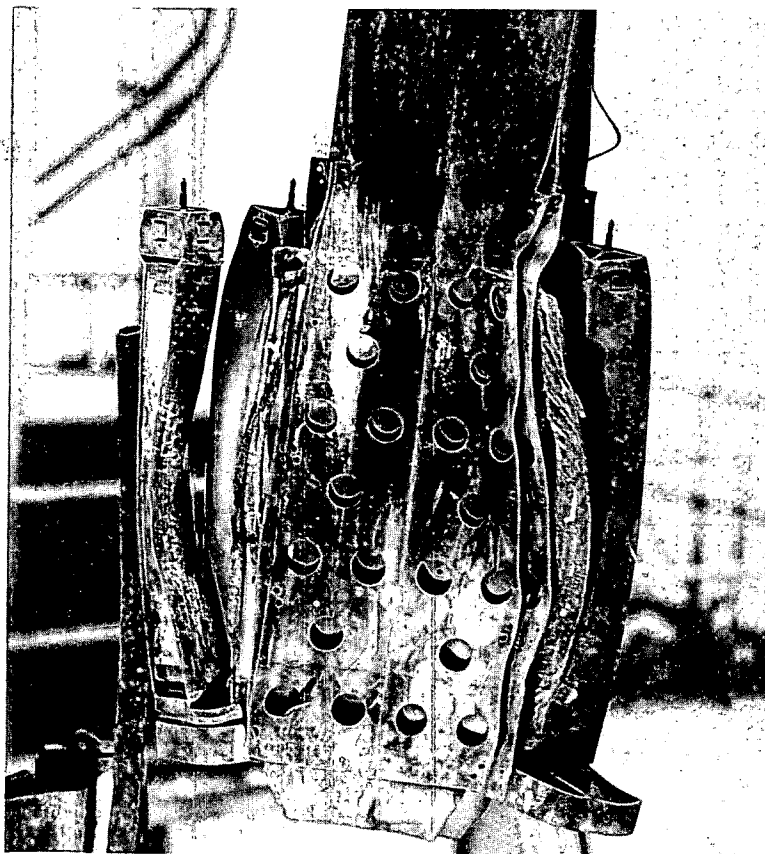


Figure II-51 Remaining Core

Figure II-52

No. 1 Control Rod and Shroud



U-5150-1



Figure II-53

Thermal Shield

was discovered that the 2 inch connection to the lower spray ring was broken inside the pressure vessel wall penetration. All loose pieces which might fall out when the pressure vessel was removed were picked out with the manipulator and put into the accumulation trays.

With the pressure vessel suspended in the cut-off fixture, a circumferential cut was made through the pressure vessel wall at a level approximately 5 inches below the top of the thermal shield. The cut was made with an air powered cut off grinder held in the overhead manipulator. Figure II-49 shows this operation. The upper pressure vessel was then removed leaving the lower end and core shown in Figure II-50. Here the lower spray ring can be seen lying across shrouds #1 and #2 and around the water level still well. The sheared rivets in the T-stanchions where the shrouds and baffles have been pulled loose can be clearly seen.

Loose pieces of fuel elements and core structure were then removed from the central portion of the core gradually emptying this volume. Three of the four x-stanchions were loose and were removed. The fourth, in front of shroud #6, was left in place.

The #1 control rod and shroud were lifted out with the manipulator, and brought with them the support boxes and fuel elements seen in Figure II-52. This grouping was completely free of the remainder of the core. The #2 shroud, also free of the core, was then removed, leaving the remainder of the core in the condition shown in Figure II-51.

The #3 and #4 shrouds were still tied together and were removed as one unit.

At this time the last X-stanchion was removed by breaking its one or two remaining rivets. Two of the remaining T-stanchions required the same treatment to allow the rest of the shroud assemblies to be separated. The remaining shroud and control blade assemblies were then removed.

The core support structure was removed. The thermal shield, Figure II-53, was lifted out with the manipulator and examined. The mid-point of the cylinder had increased its diameter by about 1/2 inch. There are eight support structure brackets attached to the inside of the thermal shield. Two of these have guide pins, three have broken hold-down studs and three have intact hold-down studs.

The remaining small pieces were removed from the bottom of the pressure vessel with a manipulator and vacuum cleaner, completing the core dis-assembly.

All parts removed were sent to the laboratories for detailed investigation. The pressure vessel was then decontaminated and samples for metallurgical investigation cut out according to the accumulated requests.

3. Health Physics

At the beginning of Phase 3 of the SL-1 recovery operations (May 23, 1961) between 3,000 and 4,000 curies of gross fission product contamination were estimated to be distributed in the reactor building and environs (plus that in the reactor itself). The radiation field within the reactor room varied from 20 R/hr to over 100 R/hr and readings of 1 R/hr were obtained as far as 25 feet away from the reactor building. In accomplishing the dual task of rehabilitating the SL-1 site and recovering the remaining evidence, about 475 individuals made 3240 entries into the SL-1 area, spending a total of 9325 man-hours in protective clothing and respiratory equipment. These individuals received a total accumulated dosage of 3481 rads to the skin and 998 rem to the whole body within the SL-1 area.

Radiological safety control procedures were established to provide the maximum amount of protection consistent with the requirements of the operation. In spite of the fact that dose rates were extremely high and variable, less than six percent of the individuals involved received radiation doses in excess of the radiation protection guides recommended by the Federal Radiation Council for exposure to external sources of radiation. The highest of these technical over exposures exceeded the applicable limit by only 16 percent. Less than four percent of the participants were found to have statistically measurable internal contamination and the highest of these was less than four percent of the established maximum permissible body burden.

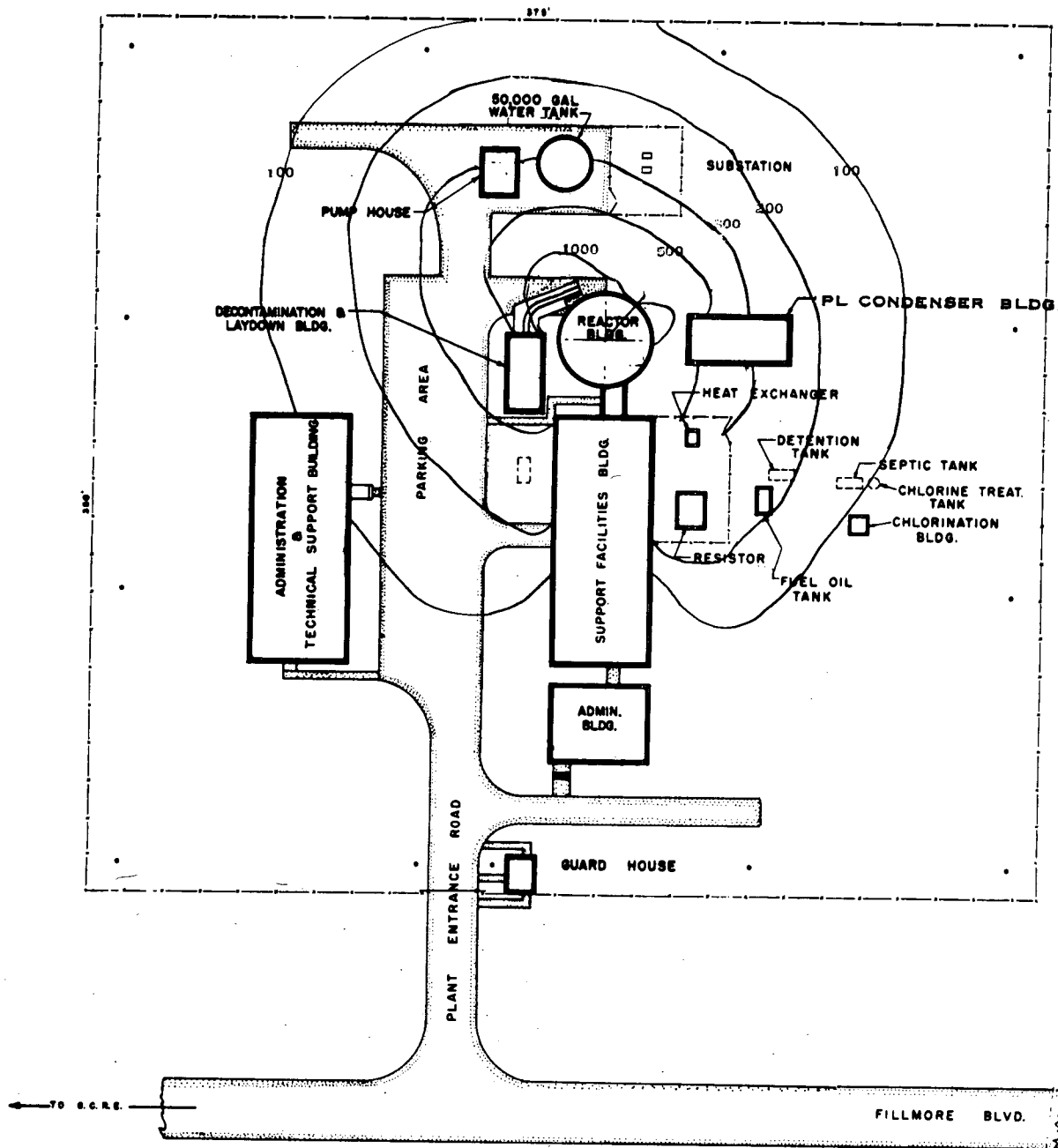
3.1 Radiological Conditions

3.1.1 Initial Radiation Levels

Radiation levels on the grounds, as measured on May 19, 1961 by Combustion Engineering, are presented on Figure II-54. Radiation levels in and around the reactor and support buildings as measured on June 1, 1961, by G-E health physics personnel were as follows:

Administration Building (SL-1 613)	10-15 mr/hr
Support Facilities Building (SL-1 602)	
Machine Shop	20-25 mr/hr
Outside access door in corridor from control room	150 mr/hr
Reactor Building (SL-1 603)	
Bottom of reactor building south stairs	200 mr/hr
First stair landing	325 mr/hr
On stairs midway between first and second landings	650 mr/hr

Instrument SR Juno IDO HP 1246
All Readings in MR/hr



SL-1 SITE ISODOSE SURVEY

May 19, 1961

Figure II-54

Reactor Building (SL-1 603) Continued

Middle stair landing	1.7 R/hr
Top stair landing	40 R/hr
Reactor room just inside SW door	45 R/hr
Near hot well tank	60 R/hr
Near raw water and deionized water piping	50-60 R/hr
Front of motor control board (west end)	75 R/hr
Front of motor control board (center)	80 R/hr
Front of motor control board (east end)	90 R/hr
Near west end of shield block 5A	105 R/hr
Bottom of outside (north) stairway	1 R/hr
Halfway up outside stairway	250 mr/hr
Top landing of outside stairway (door closed)	20 R/hr
About three feet inside NE door	40-50 R/hr
Six to eight feet inside NE door	75 R/hr

Calculations, based upon initial radiation surveys in the reactor room and subsequent surveys in the third floor fan room, indicate that 3,000 to 4,000 curies of fission product activity were distributed throughout the reactor building at the beginning of the Phase 3 operation.

3.1.2 Reactor Building

The extremely high initial radiation levels in the operating room made necessary the use of very short working time limits. The magnitude of the problem is emphasized by the fact that while only 3% of the time in the SL-1 area was spent in the reactor building, 80% of the total exposure was received therein. As a result, decontamination efforts were made in the early stages of the operation in order to allow more effective use of the available manpower. Removal of debris with scoop shovels and brooms followed by dry vacuum cleaning of all accessible surfaces as described in Section II, 1.3, reduced the radiation levels significantly.

These decontamination efforts also reduced the beta to gamma ratio; an important result since the beta + gamma skin dose was the limiting factor in establishing time limits. Significant reductions in the local beta doses, resulting from gross contamination on protective clothing, were also achieved.

The effectiveness of this method of cleaning is indicated by the fact that, after a total expenditure of only 11.9 man-hours in the operating room, the average gamma radiation level was reduced from 60 R/hr to 4 R/hr.

Radiation levels were not reduced as effectively by vacuum cleaning in the fan room as in the operating room because the crowded installation of equipment resulted in a number of inaccessible surfaces. Here, attempts to obtain longer working time limits were made by laying steel plates on the floor. This was somewhat effective since it essentially eliminated the beta contribution from the covered areas as well as partially shielding the gamma radiation from the operating room, below. The extent of the decontamination effort applied, prior to the actual removal of equipment, was jointly determined by health physics personnel and project supervision in an attempt to achieve the minimum possible total exposure to personnel.

Since the major decontamination work within the reactor building (excluding equipment removal and building destruction) was completed by the end of October, the following statistics for the period from May 22, 1961, through October 26, 1961, can be used to illustrate the magnitude and effectiveness of these efforts.

Total number of working days	114
Total entries into reactor building	335
Total man-hours in reactor building	83
Total accumulated dose in reactor building	395 rem (whole body) 1709 rads (skin)

Average dose rate for first 30 entries into reactor building:

809 mrem/min (48.5 rem/hr) gamma

2807 mrads/min (168 rads/hr) beta

Average dose rate for last 30 entries (prior to October 26) into reactor building:

29 mrem/min (1.74 rem/hr) gamma

48 mrads/min (2.88 rads/hr) beta

Approximate dose rate reduction factors:

Gamma: 28

Beta: 58

Weekly average skin and whole body dose rates within the reactor building are shown in Figures II-55 and II-56. These values, calculated from film badge results, show the reduction in dose rates as a function of time as the work progressed. The accumulated total weekly exposures for Phase 3 are presented in Figure II-57 and Figure II-58.

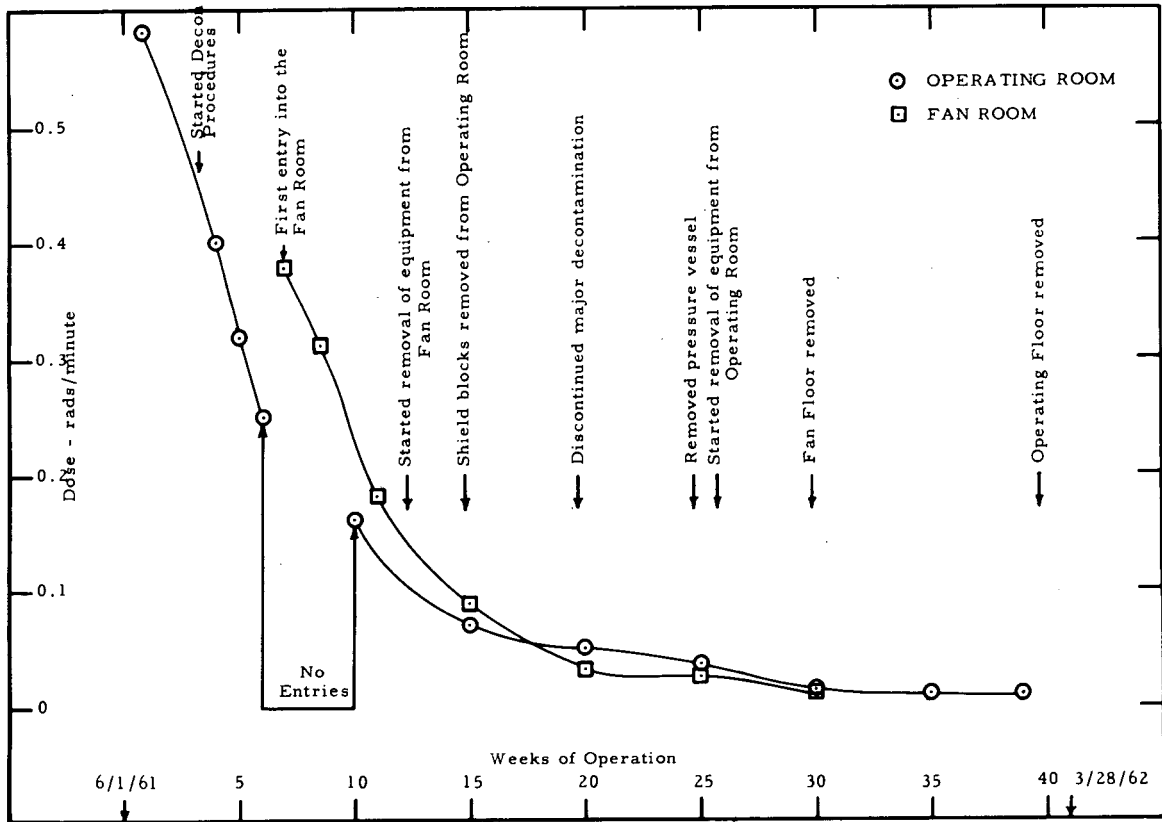


Figure II-55 Dose Rate to the whole Body (γ only), SL-1 Reactor Building

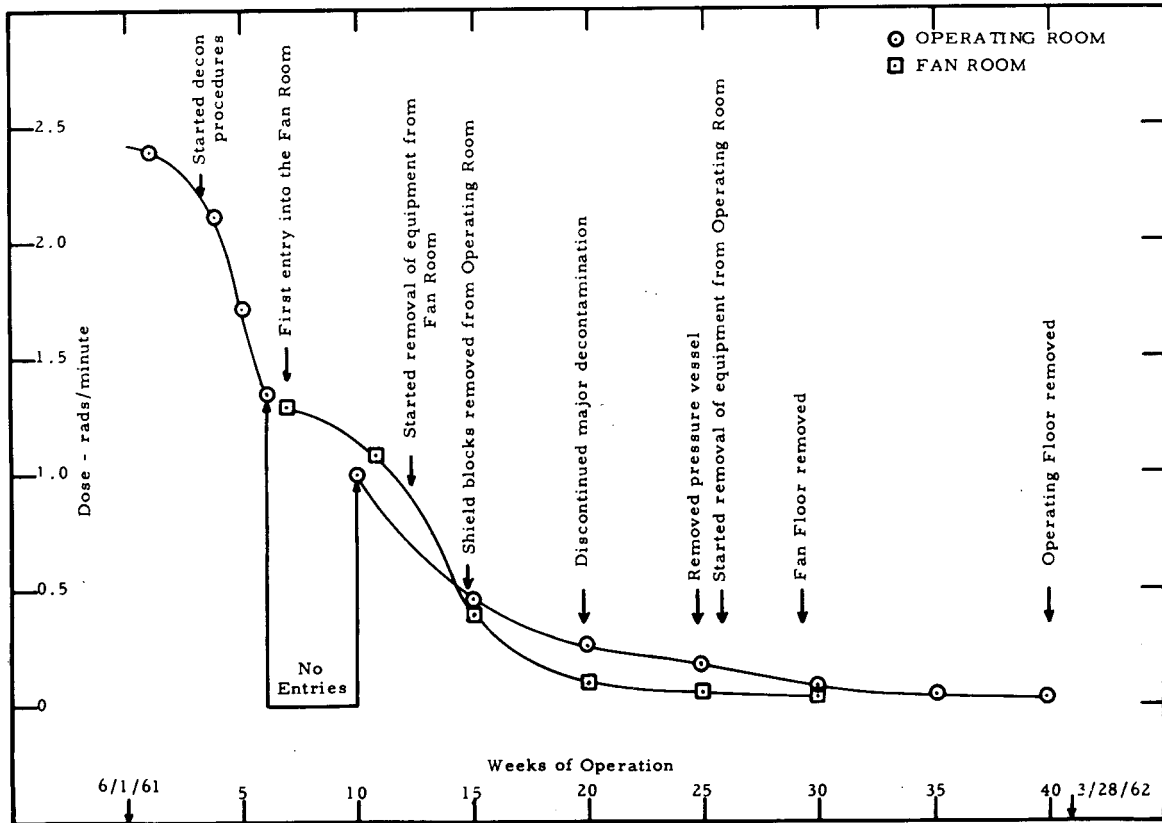


Figure II-56 Dose Rate to the Skin ($\beta + \gamma$), SL-1 Reactor Building

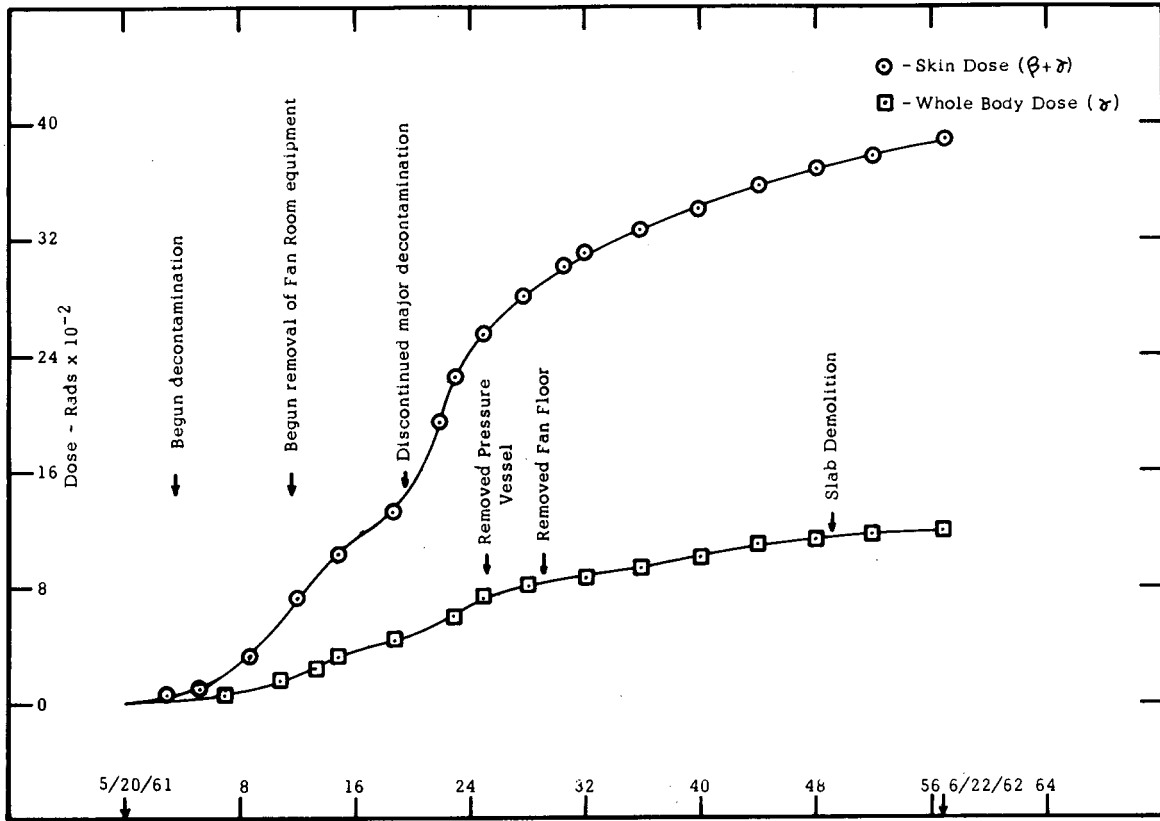


Figure II-57 Accumulated Radiation Dose, SL-1

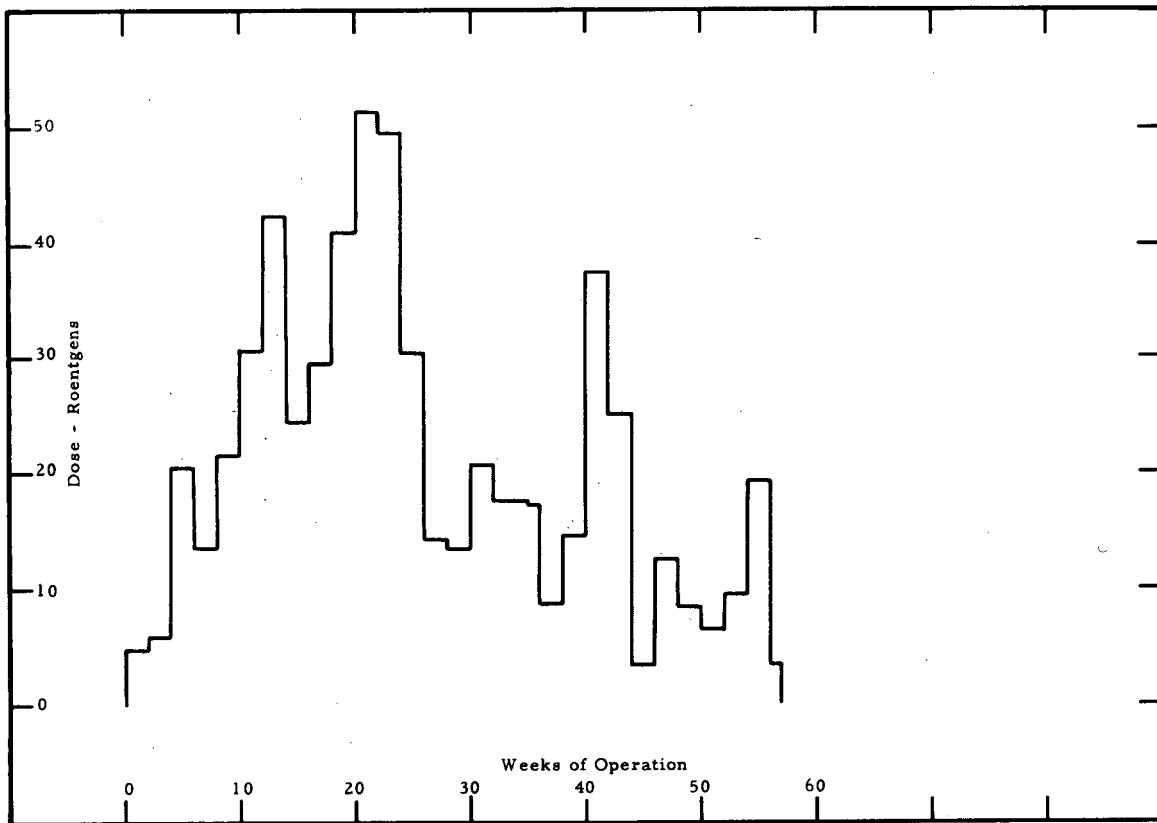


Figure II-58 Weekly Whole Body Dose, Gamma Only

Gamma radiation levels in the operating room after initial decontamination, removal of the reactor vessel, and removal of most of the equipment are presented in Figures II-59, 60 and 61 respectively. Radiation levels in the fan room after initial decontamination and removal of equipment are presented in Figures II-62 and 63. Other radiation levels measured at various stages of the operation are shown in Table II-2.

TABLE II-2

Radiation Levels at SL-1 Site

Date	Location or Activity	Radiation Level R/hr
7-20-61	Scaffold outside fan room behind personnel shield	1
	Near fan room wall (no shielding)	9
7-21-61	Fan room, general field	10-50
	Hole in center of floor (torn by shield plug)	200
	Edge of fan floor by scaffold	10
	Outer edge of scaffold	5
	Three feet from top of steps	1
8-16-61	Ten feet inside fan room	10
	Center fan room (at waist level)	60
January 1962	Body dose rate to personnel cutting up fan floor	1-3
	Support beams removed with fan floor (at one foot)	3-6
	Center section fan floor torn by the accident, at three feet (after steam cleaning)	5
	Three feet above ground where floor was cut up (after burial of floor)	1-5
February and March, 1962	Under operating floor	
	During gravel removal	2-3
	During removal of storage wells	4-5
April, 1962	Cutting up operating floor slab after demolition	.1 - 3
April, 1962	Steel support plate for operating floor (at one foot)	6-50

TABLE II-2

Radiation Levels at SL-1 Site (Con't)

Date	Location or Activity	Radiation Level R/hr
5-10-62	Dose rates to personnel removing foundation	.03 - .08
6-22-62	Reactor building site after removal of building	<.001

3.1.3 Support Facilities

Standard decontamination methods such as detergent washing and steam cleaning proved sufficient to reduce contamination in most areas to acceptable occupancy levels (see Table II-3). In the control room, access corridor, and on the exterior surfaces of the end of the support building (SL-1 602) exposed to demolition blasting, removal of floor tile, paint and repainting were required.

Samples of insulation from the ceiling of the support building read from .5 mr/hr to 20 mr/hr. Since the background in the building at the time of sampling was 5 to 10 mr/hr, calculations were relied upon to determine whether this insulation should be removed. These calculations indicated that the contaminated insulation would create a field averaging 1.25 mr/hr 6 feet above the floor of the support building. The insulation was therefore removed. Measurements showed that insulation removal was unnecessary in the Administration and Technical Support Building.

A summary of removable contamination levels prior to decontamination is tabulated below. All values are in d/m - 100 cm².

Support Facilities Building (SL-1 602) Shop Area	
Floor, tables	1.5 x 10 ⁶
Light fixtures, etc.	2.0 x 10 ⁵
Interior Walls	4.0 x 10 ⁴
Administration Building (SL-1 613) First Floor Offices	
Floor	1.5 x 10 ⁶
Tables and Desks	4.0 x 10 ⁵

Administration Building (SL-1 613) Second Floor Offices	
Floor	1.2×10^5
Desks, Cabinets	2.0×10^5
Walls	1.0×10^4
Administration Building Roof	
	5×10^4 to 2×10^5
Administration and Technical Support Building (SL-1 606)	
Interior	5×10^2 to 5×10^4
Exterior Walls	1×10^3
Roof	5×10^4 to 2×10^5
Guard House (SL-1 604)	
Interior	1.5×10^4
Exterior	5×10^3
Power Extrapolation Building (SL-1 615)	
Interior	1.5×10^4 to 1×10^5
Roof	5×10^4 to 2×10^5
Decontamination Building (SL-1 614)	
Interior	1×10^5 to 1×10^6
Exterior	1×10^5

Final contamination levels, after decontamination, are given in Table II-3.

3.1.4 Grounds

Whole body radiation levels on the grounds near the perimeter fences were generally in the range of 5 to 20 mr/hr after removal of the reactor building. Radiation and contamination levels in areas of concentrated recovery activity reached a maximum of 5 R/hr at 3 ft. above the ground. Radiation doses were minimized by intermittent scraping and removal of the surface in areas where protective clothing was removed and where highly contaminated equipment had been placed on the ground. During the winter months when the ground was frozen, this type of periodic contamination removal could not be accomplished effectively and localized hot spots contributed significantly to the personnel doses.

TABLE II-3
Final Contamination Levels in Support Facilities
mr/hr

Location	Removable Contamination (d/m/100 cm ²)	Radiation Levels (GM-OW)		Notes (Readings in d/m-100 cm ² unless otherwise noted.)
		Max. 1'	Avg. 3'	
SL-1 - 606, Interior	<500	20	0.2	Hot particle imbedded in tile
SL-1 - 606, Exterior	500 - 1000	--	--	Roof contaminated. 500 - 5000
SL-1 - 604, Interior	<500	2	0.2	
SL-1 - 604, Exterior	<1000	--	--	Roof contaminated. 500 - 1000
SL-1 - 613, Interior	<500	20	0.2	Several hot particles imbedded in tile greater than 20 mr/hr.
SL-1 - 613, Exterior	<1000	--	-	Roof contaminated. 1000
SL-1 - 602, Interior	<500	20	0.2	Several hot particles imbedded in tile greater than 20 mr/hr.
SL-1 - 602, Exterior	<1000	--	--	Roof contaminated. 3000 - 5000
SL-1 - 602, Interior - Control Room	<500	1.5	0.5	Power Equipment inside. 500 - 10,000
SL-1 - 615, Interior	See Note	2.0	1.0	Floor, equipment and walls are < 500 d/m to a height of 8 ft. Above 8 ft. 5000 - 10,000
SL-1 - 615, Exterior	<1000	--	--	Roof contaminated. 5000 - 10,000
SL-1 - 614, Interior	<1000	10	1.0	
SL-1 - 614, Exterior	<1000	--	--	Roof contaminated. 500 - 10,000
SL-1 - 605, Interior	<500	0.5	0.2	
SL-1 - 605, Exterior	<1000	--	--	
SL-1 - 601, Interior	<500	0.5	0.2	
SL-1 - 601, Exterior	<1000	--	--	Roof contaminated. 3000 - 5000
SL-1 - 702, Exterior (Water Tank)	<1000	--	--	
SL-1 - 701, Substation	<2000	3-5	--	Area posted as to radiation and contamination levels. Clean gravel in yard.
SL-1 - 703, Resistor	<2000	5-10	--	Area posted as to radiation and contamination levels. Clean dirt put in yard.
SL-1 - 705, Fuel Oil Tank	<1000	--	--	Contaminated dirt removed.

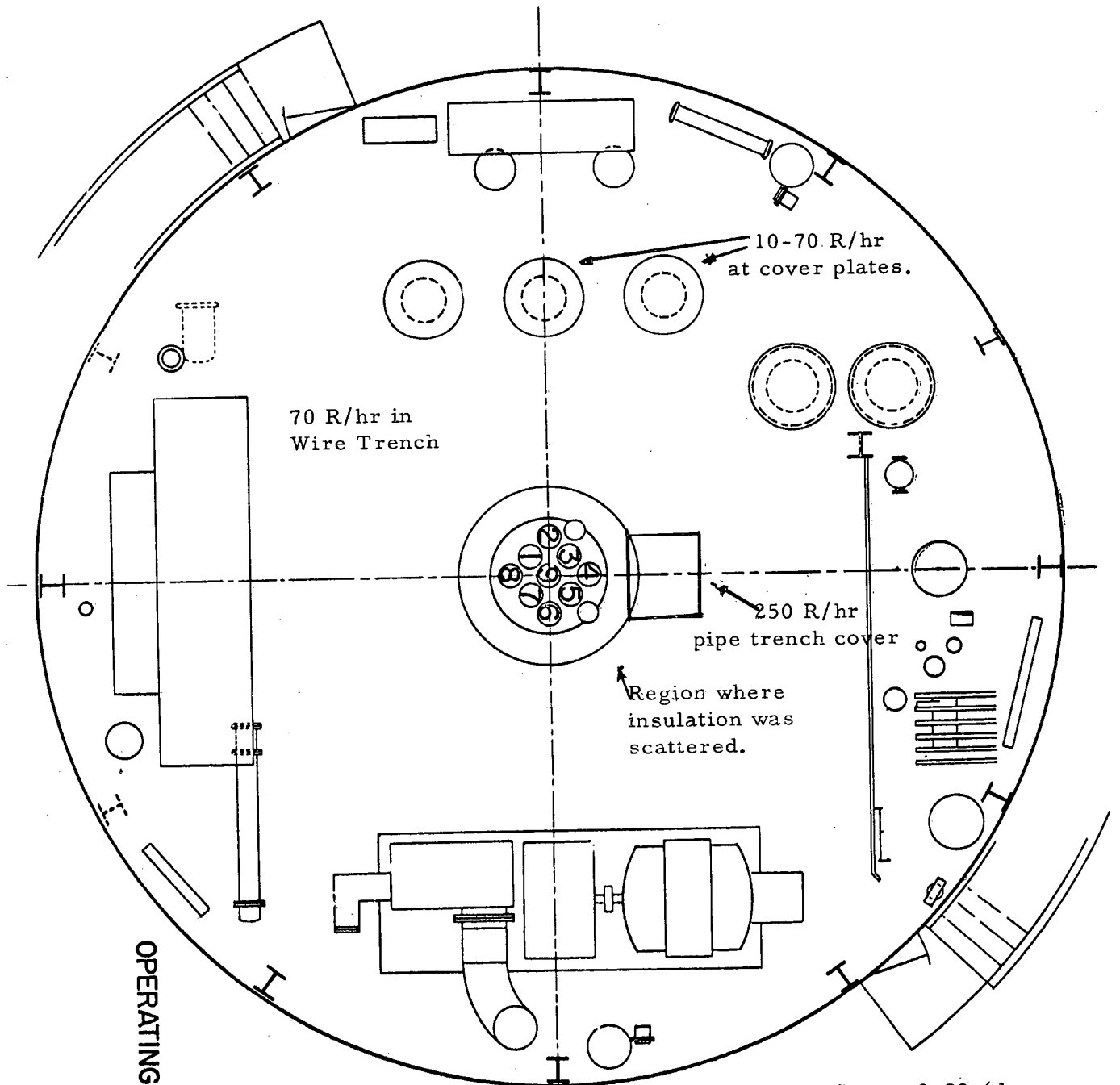
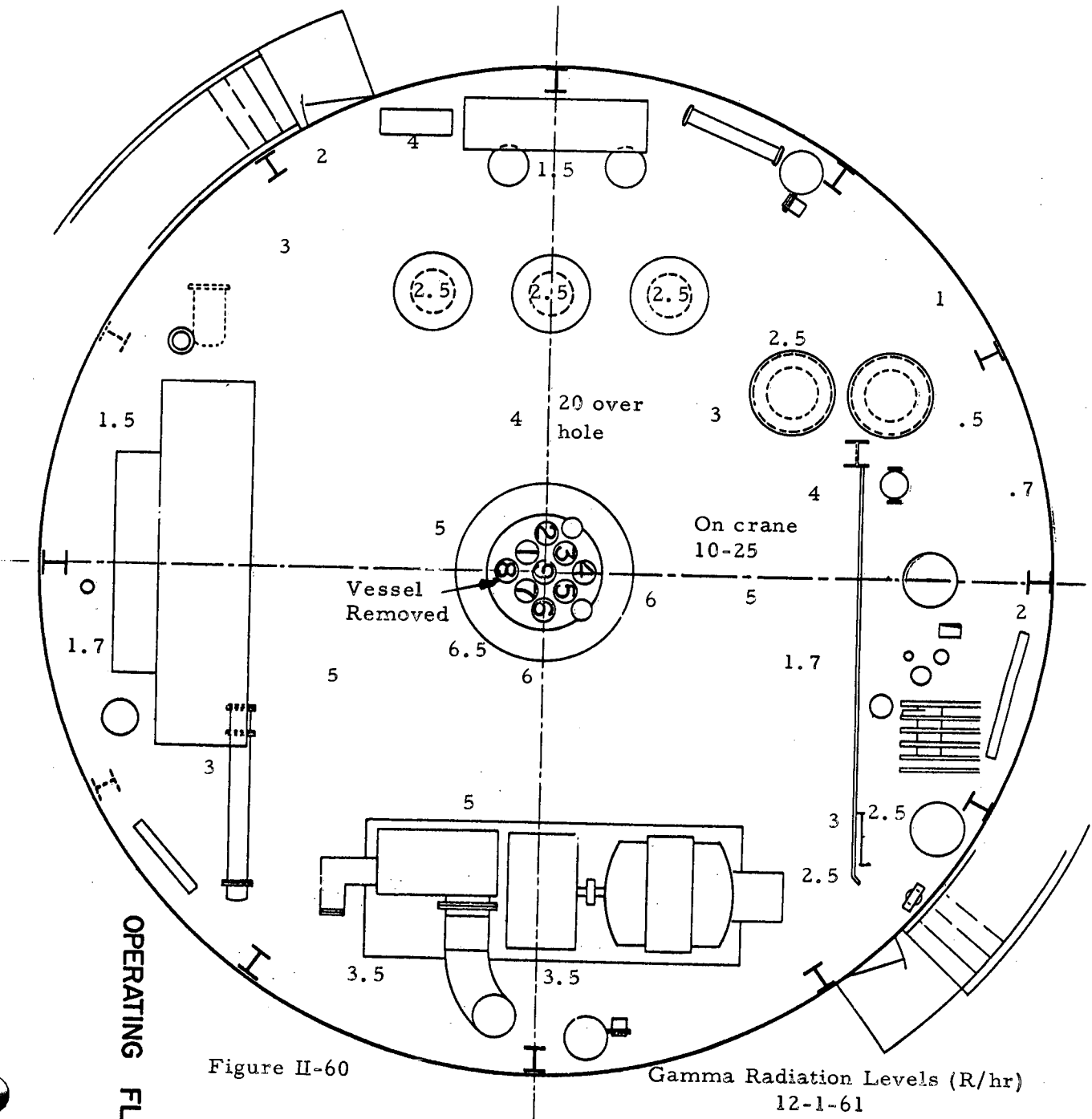


Figure II-59

Radiation Hot Spots, 9-29-61.
Average waist high
Level \approx 4 R/hr



OPERATING FLOOR

Figure II-60

Gamma Radiation Levels (R/hr)
12-1-61
Readings at 4' above floor.

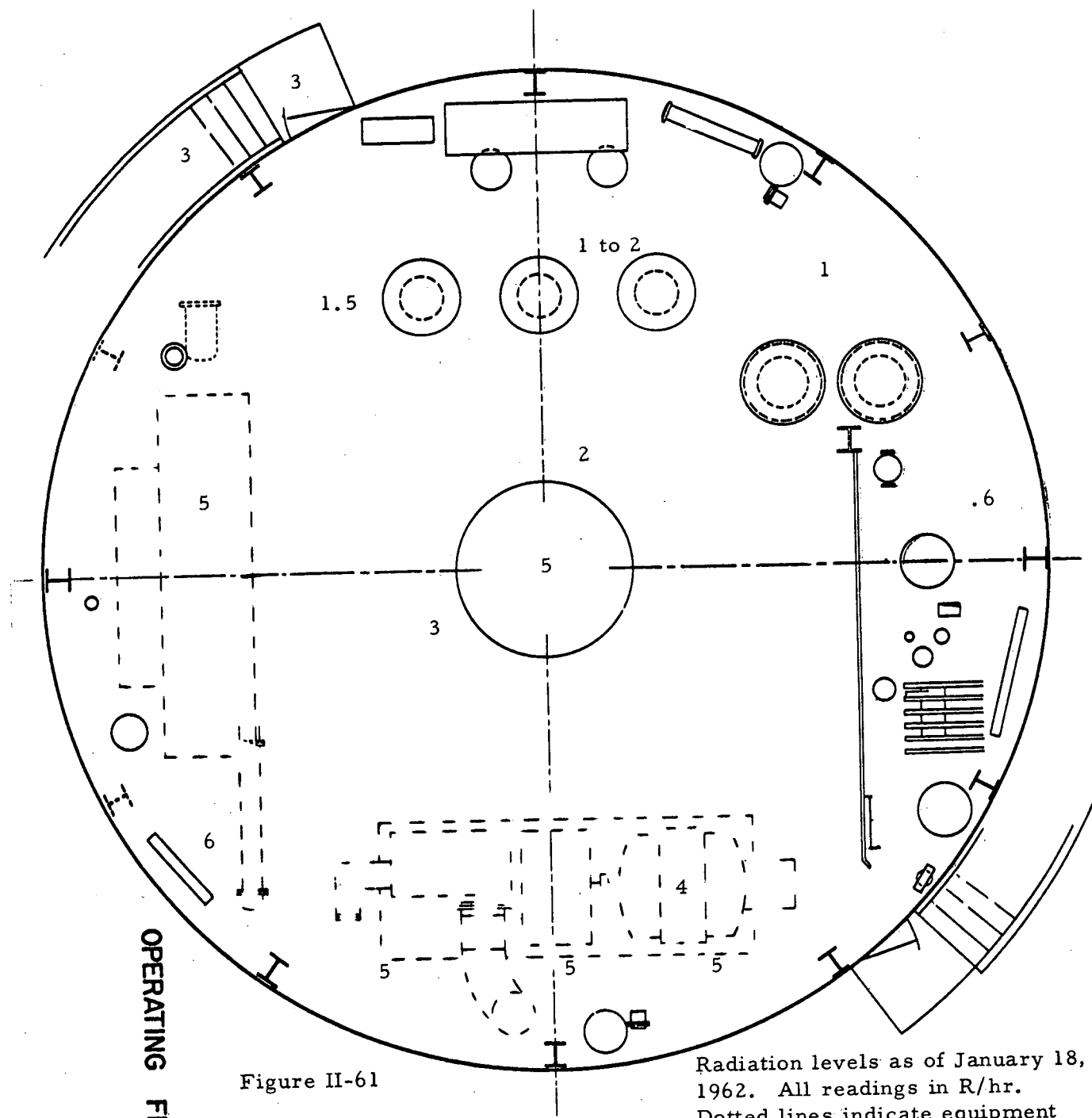
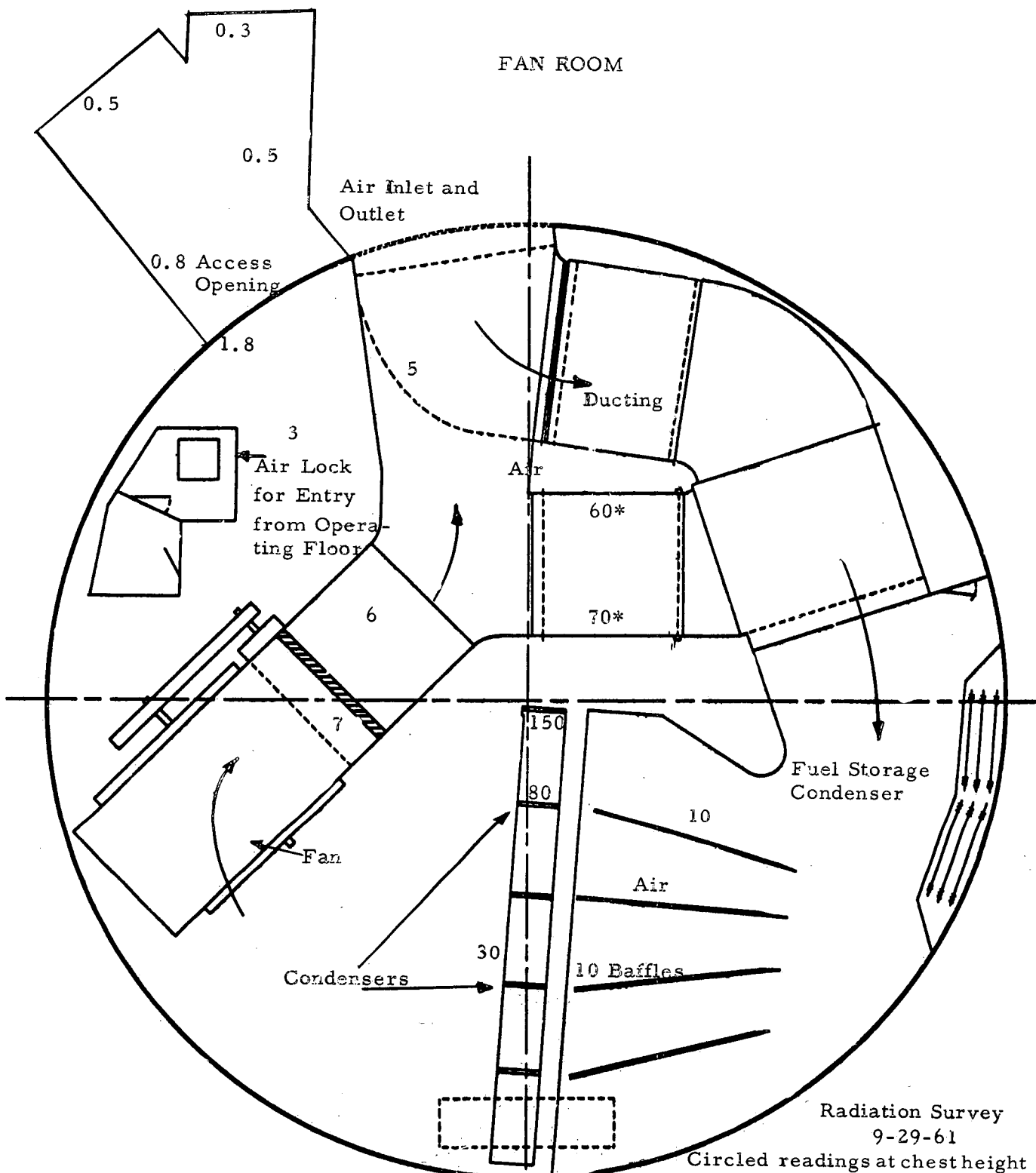


Figure II-61

Radiation levels as of January 18, 1962. All readings in R/hr. Dotted lines indicate equipment which has been removed.



General Field \approx 8R/hr
Figure II-62

Radiation Survey
9-29-61
Circled readings at chest height
*Readings at 12 to 18 inches.
All other readings at 3 to 6 inches.
All values in R/hr.

On March 28, 1962, after demolition of the reactor building support structure, radiation levels in the SL-1 area were primarily a result of ground contamination. Radiation levels at this time are presented in Figure II-64.

In order to minimize cross contamination between the buildings and grounds during final cleaning of the building exteriors, a layer of dirt was removed. The exterior surfaces of the building were then cleaned, and a second layer of dirt was removed. The surface soil was removed to an average depth of 4" within the entire fenced area. Replacement of the soil in the fenced area was delayed because of expected cross contamination from the uncleaned area outside the fence, but a layer of clean gravel was spread over the normal vehicle and pedestrian traffic lanes. Radiation levels in three separate areas, where emergency and recovery operations had caused gross contamination, were still as high as 30 mr/hr 3 feet above the ground at the time of this report. However, when the soil is replaced, radiation levels are expected to be less than 1 mr/hr. The condition of the grounds as of June 22, 1962 is presented in Figure II-65. No work was done after this date.

Core samples, taken before and after removal of the top soil, indicated that significant penetration of contamination into the ground ranged from 5" to 20". Peak activities from the samples were at the surface or a few inches below the surface, indicating that the remaining radioactivity will probably not reach the water table for hundreds of years. Typical activity gradients from two core samples are presented in Figure II-66.

3.1.5 Hot Shop

The SL-1 recovery required 302 entries into the ANP Hot Shop involving 318 man-hours of radiation exposure. A total integrated dose of 113.5 rads beta and 59.6 rem gamma was accumulated by personnel engaged in non-remote Hot Shop operations.

Unloading and sorting of the material transferred to the Hot Shop from SL-1 caused gross contamination within the shop. A two foot plastic barrier stretched across the floor of the shop helped to control the spread of contamination from the highly contaminated east end to the west portion where unloading from trucks was accomplished. Even so, surface contamination levels on the "clean" side of this barrier periodically reached 10^6 d/m-100 cm², and frequent cleaning was necessary. Contamination remaining on the Hot Shop floor, after removal of the sorted debris to the Special Equipment Service room for temporary storage, created maximum radiation levels of 5 R/hr at the barrier and average levels of 100 mr/hr on the "clean" side of the barrier. Prior to receiving the pressure vessel, a complete decontamination of the Hot Shop reduced the above radiation levels to between 50 and 100 mr/hr.

Radiation Survey SL-1 Area
 March 28, 1962. All readings
 in mr/hr at 3' above ground.

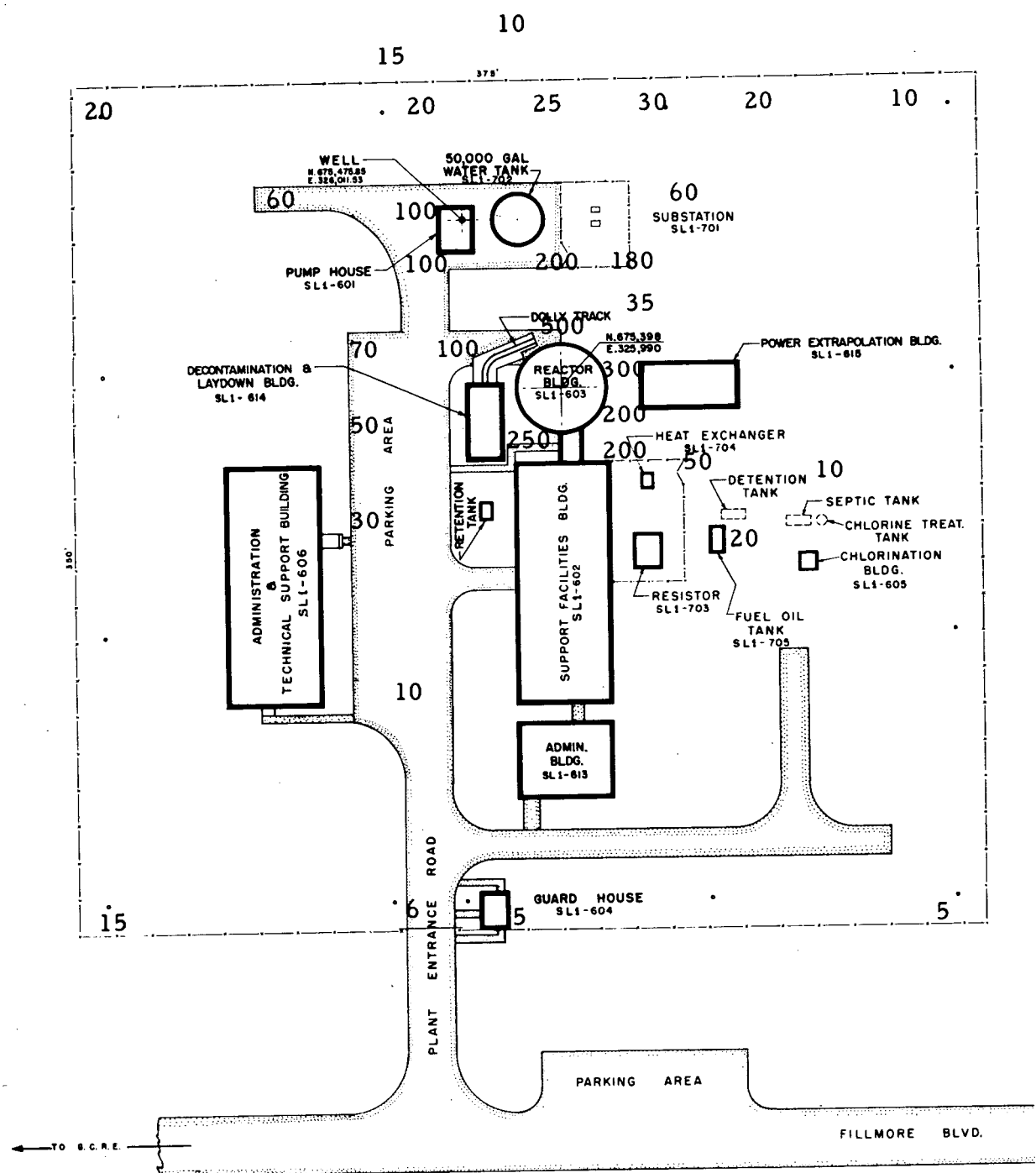


FIGURE II-64
 II-104

SL-1 AREA RADIATION LEVELS
 JUNE 22, 1962

PLOT PLAN
 of
SL1 AREA
 (FORMERLY ALPR)
 NATIONAL REACTOR TESTING STATION

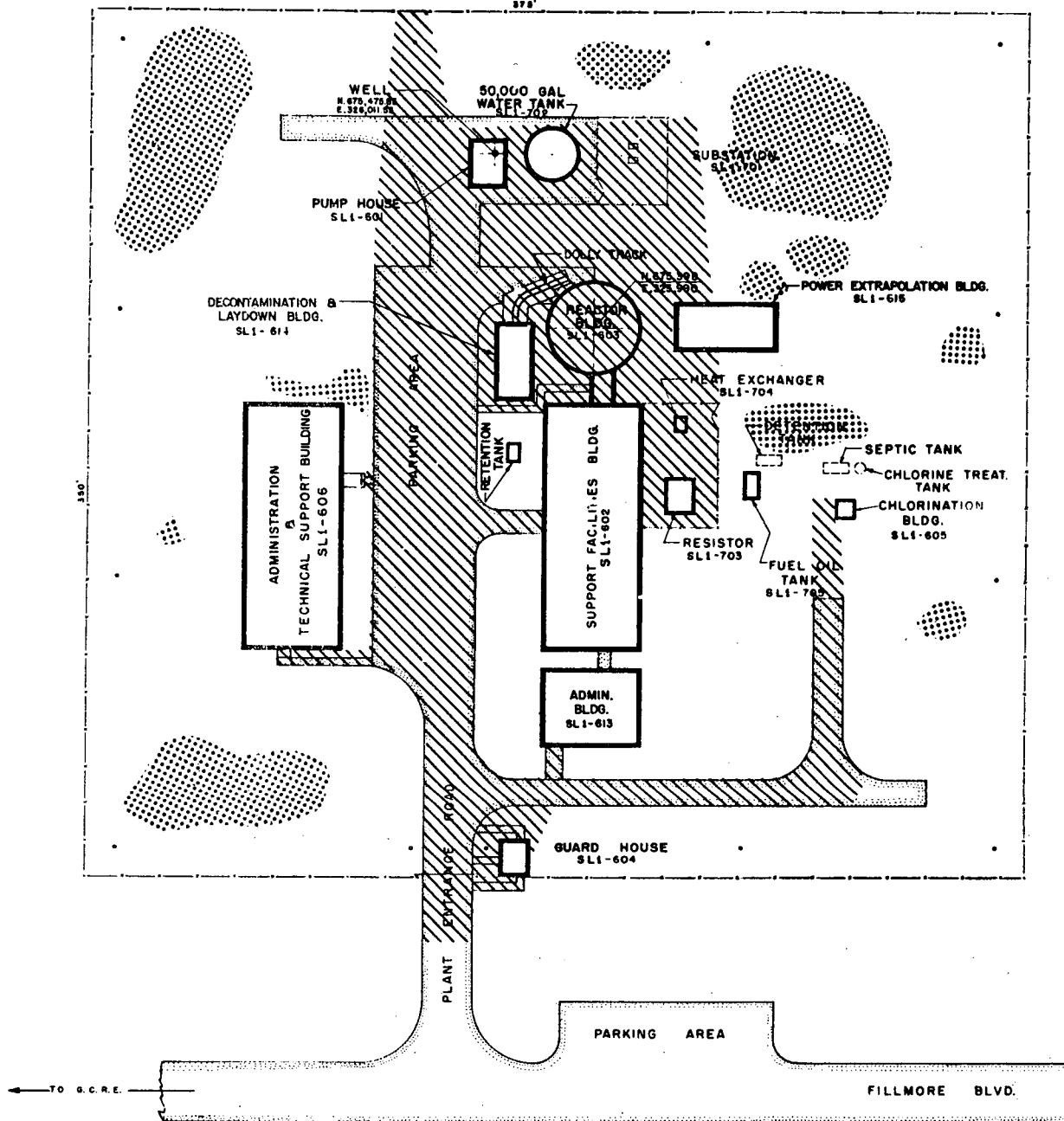


Figure II-65 Cross hatched area: Clean dirt replaced (< 1 mrad/hr, at contact, G.M.). Dotted area: 3" to 6" dirt removed; Radioactive particles still remain. 5 mrad/hr to 5 rad/hr at 3" above ground. All other areas: 1 mrad/hr to 30 mrad/hr at 3" above ground.

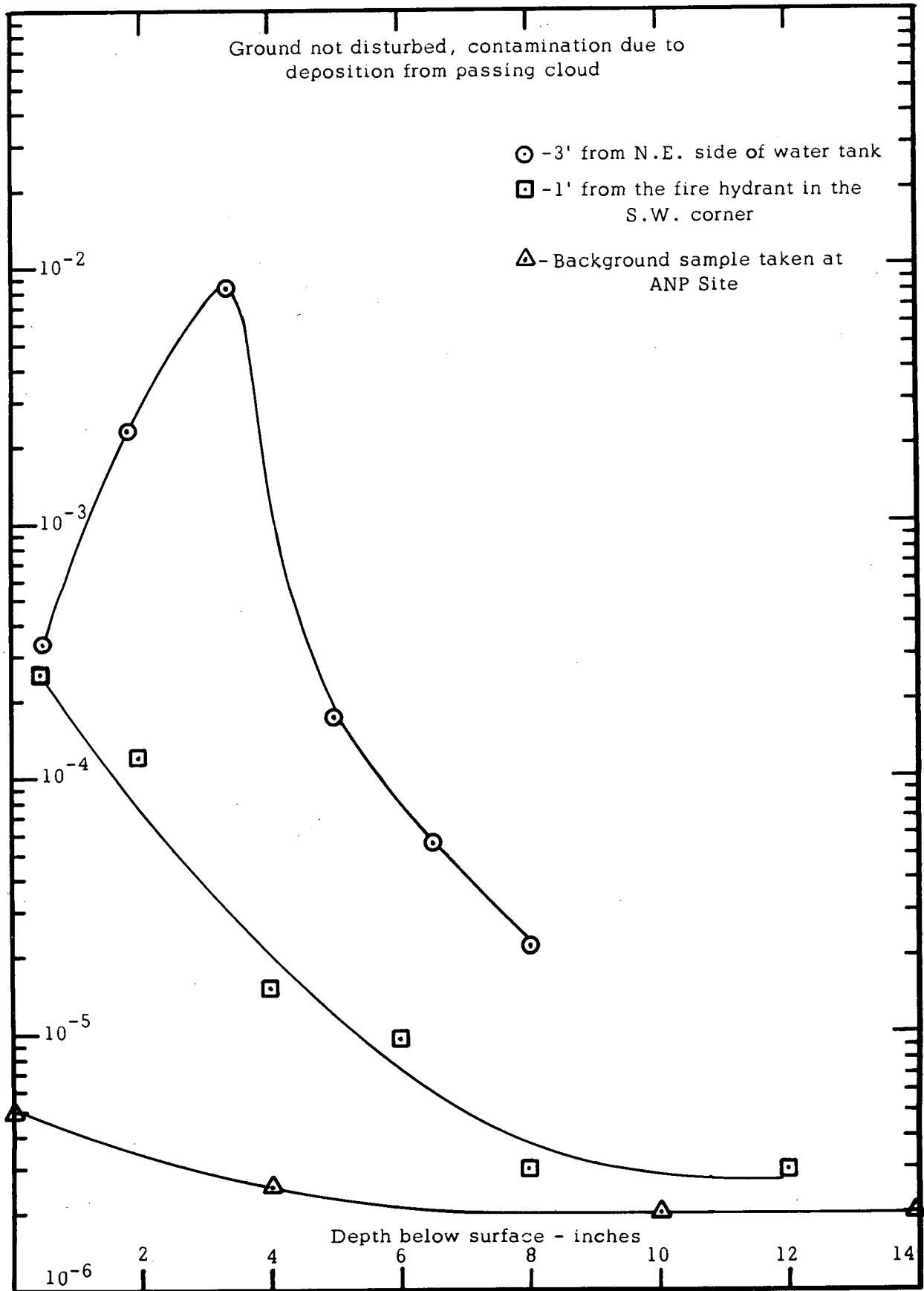


Figure II-66 Soil Samples Taken at SL-1 on May 23, 1962

Persons engaged in removing the pressure vessel head worked in radiation fields of 3 to 6 R/hr. During this period the significant radiation levels within the Hot Shop were:

Average Field	150 mr/hr
Three feet from edge of pressure vessel head	5 R/hr
Top of pressure vessel head	12 R/hr
Between pressure vessel and top edge of cask	40 R/hr

Over the top of the vessel after removal of the pressure head, a reading of 450 R/hr was obtained.

Significant radiation levels 3 feet above the floor during preparation for the critical experiment were:

14' from the edge of the pressure vessel	20 R/hr
3' from the edge of the pressure vessel	60 R/hr

Gross floor contamination undoubtedly contributed significantly to these high readings.

Individuals engaged in cutting the holes in the pressure vessel worked behind shields in radiation fields of 100 to 200 mr/hr. The maximum dose rate to which any individual was exposed in the Hot Shop was about 20 rem/hr occurring while the pressure vessel was being secured in the support fixture. Radiation levels at 3 feet above the floor in the Hot Shop at the conclusion of the critical experiment on April 13, 1962, were as follows:

	<u>mr/hr</u> <u>Core in Cask</u>	<u>mr/hr</u> <u>Core out of Cask</u>
At main doors	110	120
Window B	110	160
Window C, 14' from vessel	300	750
End of Pool	1500	1500

Radiation levels at 3 feet above the floor in the shop after the pressure vessel and reactor core were remotely dismantled and transferred to a storage area on May 19, 1962 were:

	<u>mr/hr Gamma</u>	<u>mrad/hr Beta</u>
Zone #1 (west 1/3 of shop)	125-175	750-1050
Zone #2 (central 1/3 of shop)	200-500	1200-3000
Zone #3 (east 1/3 of shop)	10,000	25,000

On May 28 and 29, partial decontamination of the Hot Shop reduced radiation levels to 200 mrad/hr beta and 100 mr/hr gamma.

During the last few months of SL-1 work in the Hot Shop, contamination problems were severe and maximum protective clothing and respiratory protection were used. For example, shoe covers worn within the shop read as high as 10 R/hr gamma and 25 rads/hr beta at contact.

Approximately 500 curies of fission product activity were collected as liquid waste during the SL-1 work. Approximately 300 curies were obtained from reactor washings during the critical experiment. This activity is presently contained in 40,000 gallons of liquid in an underground holding tank.

3.2 Control Procedures

A small support building, approximately 500 feet from the SL-1 reactor, containing shop equipment, two offices, a shower room, and work benches, was utilized as a control point for all operations at the SL-1 site. In order to minimize the transport of contamination into the control point, a trailer was located adjacent to the building and used for the removal of contaminated protective clothing. Plywood windbreaks were constructed between the trailer and building and around the outer trailer door to control airborne contamination. Since the radiation level inside the control point building was substantially above natural background (1 mr/hr maximum) a steel cubicle was located in the building, adjacent to the trailer entrance, to provide a lower radiation background for personnel monitoring. The floor from this area to the hot side of the trailer was covered with blotting paper, which was changed daily, or more often when necessary. The rear portion of the building and surrounding yard were established as a contaminated area. This area was used as a staging area and parking lot for vehicles and equipment used within the SL-1 area.

All access to and from the SL-1 area was controlled through this control point. Material being removed from the SL-1 area was surveyed here before release. Careful preparations for each task were made at the control point. Before each entry, a person was carefully dressed and briefed. His name and time of entry were logged on a special work permit which described his job and special precautions for the job. Both the health physics representative and operations supervisor were required to validate this document by signature before access was permitted. In most instances, a health physics representative accompanied the person or team to the SL-1 area where he assisted in procuring tools and equipment, gave final precautionary instructions, and, when radiation levels were high, timed the worker during actual work performance.

The time limits were established from prior radiation surveys, knowledge of the operation, and previous exposure experience. The fact that exposure limitations prevented health physics personnel from accompanying each man into the highly varied radiation fields, coupled with the requirement to accomplish as much as possible without over exposure, taxed the skill of the health physicist.

The checkout procedure at the control point consisted of careful removal of protective clothing, personnel monitoring, and showering. Estimated dosages, exposure time, and time of departure was recorded for each individual at this time.

SL-1 entry logs containing the date and time of entry, job description, personnel involved, areas entered, and estimated doses were compiled and recorded.

3.3 Protective Clothing and Equipment

The conventional types of protective clothing already on hand for use in the GE-ANP program proved to be adequate for the SL-1 operation, although significant increases in quantity were made. The following protective clothing and equipment were used:

- Canvas twill coveralls
- Disposable plastic coveralls with hood
- Canvas head covers
- Surgeon's operating cap
- Canvas shoe covers with elastic at top
- Rubber boots
- Cotton gloves
- Rubber gloves
- Half face respirator with twin, high efficiency particulate filters
- Army M9A1 Assault Mask with cannister
- Commercial full-face masks of several types with high efficiency particulate filters
- Masking tape, 2 inch

The approximate number of items of protective clothing and equipment decontaminated or discarded are tabulated below:

	<u>Laundered</u>	<u>Discarded</u>
Coveralls	7,000	750
Plastic coveralls	0	500
Head covers	3,500	500
Canvas shoe covers	9,000 pr.	1,500 pr.
Rubber boots	7,000 pr.	250 pr.
Rubber gloves	7,000 pr.	1,500 pr.
Half face respirators	3,000	-
Full face	500	-

Since there were many volunteers who did not have experience working in high radiation and contamination areas, the following dressing sequence was carefully observed and directed by the health physics representatives, prior to all work within the reactor building.

Remove all personal jewelry, etc. and all personal clothing except shoes and stockings.

Don one pair of coveralls, shoe covers, rubber gloves and surgeon's cap.

Seal wrist and ankle regions with masking tape.

Place three self-reading dosimeters and one film badge on chest pocket and film badge belt containing 15 to 18 badges around waist.

Don second pair of coveralls, rubber gloves, rubber boots and an outer pair of canvas shoe covers.

Don assault mask; test for air leaks.

Don canvas hood and seal all openings around neck and mask.

Don two piece plastic suit.

Tape self reader encased in plastic to the chest near film badge.

Attach filter cannister to face mask before entering SL-1 gate.

After each individual left the reactor building, it was necessary for an experienced health physics inspector to undress him according to the following sequence in order to minimize skin contamination.

At the base of the reactor building the inspector removed the man's outer shoe covers and cut the plastic suit around the neck, wrists, waist, ankles, and down the front peeling it off gently. In this step, extreme care was taken by the inspector to prevent contamination of his person even though he was fully dressed in a respirator and protective clothing. At the SL-1 gate he helped the man to remove masking tape, hood, assault mask, outer gloves, and coveralls. At the control point the inspector on the "cold" side of the trailer (an 18" high plastic barrier separated the "cold" and "hot" sides of the trailer) carefully removed the film badge belt and dosimeters. The individual removed his own rubber boots, surgeon's cap, inner gloves and inner pair of coveralls. The individual removed the last pair of shoe covers while stepping across the plastic barrier to the clean side.

The individual entered the steel cubicle in the control point building and his entire body was scanned carefully with a GM count-rate meter equipped with a loud speaker for audible monitoring. (Levels of approximately .1 mr/hr above background could be detected.) The individual showered; if contamination was formerly detected he then returned to the cubicle for a further survey and repeated this process until no further contamination could be detected.

Shoes or other articles of personal clothing which could not be decontaminated were replaced after a written report was filed.

The above procedure proved very effective. A total of 653 entries were made into the highly contaminated reactor building, in which the airborne activity reached 10^{-2} to 10^{-3} uc/cc during cleaning operations. Even so the maximum internal contamination was less than 4 percent of the maximum permissible body burden and no cases of serious skin contamination occurred.

3.4 Dosimetry

Planned doses for all personnel engaged in SL-1 operations were to be within the occupational radiation protection guides recommended by the Federal Radiation Council (10 rads/quarter or 30 rads/year to the skin and 3 rem/quarter to the whole body, eyes and gonads). Beta absorption studies showed that the full face masks provided effective beta shielding for the eyes and that the gonads would not receive an appreciable beta dose. Therefore, the measured beta plus gamma dose was applied against the skin dose limits while only the gamma dose was considered as contributing to the whole body dose.

Film dosimeters worn during initial entries into the reactor building indicated very high beta doses with wide variations in the beta to gamma ratio. As was expected for these conditions, discrepancies also existed between self reading pocket dosimeter and film badge results. In order to report more accurate beta doses to individuals, a series of test badge exposures were undertaken. Badges and pocket dosimeters were exposed to a source comprised of general contamination from the reactor room floor. A beta absorption experiment was also run, using this same source, which indicated a maximum beta energy at 23 inches of approximately 2.5 Mev.

For exposures to this source, beta readings were reasonably consistent from badge to badge. Badges exposed without interposed absorbers at 23 inches from the source, having beta readings in the three to four rad range, indicated very erratic gamma readings, varying by a factor of three or more. However, when the betas were absorbed by a 1400 milligram per square centimeter absorber, the gamma readings were consistent within about 5 percent and were in agreement with ion chamber readings with an average error of less 5 percent. Unfortunately, the radiation spectrum of the source utilized in the test exposures did not appear to be sufficiently related to the overall spectrum inside the reactor building to permit meaningful correlation between the two conditions. It is believed that the

vast difference in geometrical arrangement, between the test source and the source as seen by a badge worn within the reactor building, accounts for most of the discrepancy. Self reading ion chamber dosimeters showed a definite beta sensitivity of 10 to 30 percent, varying for different ranges and makes of dosimeters.

Beta film reports, based upon singly exposed badges worn by persons entering the reactor building, were highly inconsistent. These inconsistencies are partially attributed to the difficulty in separating the film darkening effects of degraded gamma radiation (below .025 Mev) and beta radiation although differences in the beta field caused by different badge orientation and partial body shielding may have been more significant. Gamma readings from badges worn in the reactor building were reasonably consistent and in good agreement with other methods of measurement. As a result of these difficulties, beta dosages to personnel were determined by equipping each person with a dosimetry belt containing 15 to 18 identical badges and recording the average beta reading for these multiple badges. The gamma dose was determined directly from the single badge worn on the chest.

An average beta to gamma ratio of 4.5 was determined from the initial belt experiments and was used to assign beta doses to those individuals who were exposed prior to use of the belts. It is believed that the soft gamma film darkening effects resulted in conservative beta reporting.

In other experiments, badges worn on the ankle, knee, hip, and chest of exposed individuals indicated that no one part of the body was receiving an appreciably higher dose than other parts. It was concluded that the badges worn at the waist or on the chest gave a reasonable indication of the whole body dose.

Skin dose, rather than whole body dose, was generally the limiting factor during decontamination and removal of equipment from the reactor building. In the fan room, steel plates laid on the floor as cleaning progressed reduced beta doses and permitted longer working time limits.

A number of different types of instruments were used in the health physics radiation and contamination surveys carried out during the SL-1 Phase 3 work. The type of instrument used depended upon availability and suitability for the existing conditions. A listing of this instrumentation appears below.

Direct Radiation Instruments

Use	Maximum Range a Units	Instrument
Gamma	500 R/hr	Victoreen Radector
Gamma	50 R/hr	Victoreen Radector
Gamma	1000 R/hr	Eberline Gadorà I
Beta-Gamma	25 R/hr	Technical Associates, Juno, Model 3
Beta-Gamma	5 R/hr	Technical Associates, C. P. Model 2
Beta-Gamma	5 R/hr	Technical Associates, C. P. Model 2
Beta-Gamma	5 R/hr	Technical Associates, C. P. Model 3
Beta	1000 rads/hr	Chalk River AECL (development inst.)
Beta-Gamma	20 mr/hr	Nuclear Chicago G. M. Model 2612
Beta-Gamma	20 mr/hr	Nuclear Instruments G. M. Model 2160-A
Beta-Gamma	20 mr/hr	Victoreen Thyac G. M., Model 398-C

Personnel Metering Dosimeters

AEC IDO Film Badge (Cd, Ag, and Al filters) with Dupont Type 558 film packet

Bendix Model 611 Self-Reading Dosimeter; 0-5 R

Radiacmeter Model 1 M-135/PD Self-Reading Dosimeter; 0-5 R

Landsverk Model L-51, Self-Reading Dosimeter; 0-5 R

Landsverk Model L-50, Self-Reading Dosimeter; 0-0.2 R

Victoreen Model 541/A, Self-Reading Dosimeter; 0-0.2 R

Victoreen Model 656/A, Self-Reading Dosimeter; 0-0.5 R

Personnel Contamination Monitors

Sharp Monitor Ratemeter, Model LMR-168 with Amperex Type 90 NB GM Tube

Atomic Instrument Count Rate Meter, Model 410 with Victoreen Type 1B85 GM Tube

Removable contamination monitoring was performed by use of standard smear or wipe techniques using Whatman No. 1 filter circles. Smears were counted using shielded, end window gas-flow proportional counters (Atomic Inst. Co.) and decade scalars (Technical Measurements, Model 562A). All smear results were reported in units of disintegrations per minute per 100 square centimeters of surface (d/m-100 cm²).

3.5 Bioassay

Because of the extreme contamination levels resulting in air activity of 10^{-2} to 10^{-3} $\mu\text{c}/\text{cc}$ during cleaning operations in the reactor building, the existing bioassay program was expanded. All persons working at SL-1 submitted urine specimens monthly or whenever abnormal results were expected. All specimens were processed by the Health and Safety Division, Idaho Operations Office, AEC. Each specimen was placed in a deep well scintillation counter and gamma counted. Specimens showing statistically significant activity were chemically processed and beta counted. Repeat specimens were taken and whole body counts were made on all individuals showing positive results. The whole body counting procedure involved thorough cleansing of the skin before being placed in a shielded container for a five minute gamma scan of the whole body.

A total of 630 bioassay samples were processed during Phase 3 of the SL-1 recovery project. Less than 3% of these showed statistically significant results. The 15 individuals showing these positive results were given a total of 24 whole body counts. The results of this program showed that the maximum internal contamination of any individual was approximately 4 percent of the maximum permissible body burden as listed in National Bureau of Standards Handbook 69.

3.6 Material Transportation and Waste Disposal

3.6.1 Transportation Problem

A large quantity of debris, small equipment, and vacuum sweepings from the reactor building, containing several thousand curies, as well as the reactor itself, containing $\sim 50,000$ curies, were transported to the ANP Hot Shop 35 miles away from the SL-1 site. Approximately $26,500 \text{ ft}^3$ of grossly contaminated equipment and materials, reading up to 50 R/hr, were loaded and transported to the burial ground and buried. About $54,500 \text{ ft}^3$ of contaminated gravel and dirt were also buried.

3.6.2 Control of Contamination

The following general procedure was used to control contamination during loading of debris and equipment and transportation to the ANP Hot Shop. A steel box, 4 feet x 8 feet x 4 feet, (referred to as the liner) was transferred via the shielded crane to a point where buckets of debris and pieces of equipment could be loaded into it. This liner was placed in a second box (referred to as the cask) whose 1 inch steel walls provided some shielding. This cask was then closed, sealed with masking tape, and steam cleaned. It was next transferred to the control point and loaded onto the clean truck and final decontamination and monitoring were

continued until levels were below 500 d/m-100 cm². At times this procedure was varied by leaving the cask mounted on the truck and loading the liner directly into it. Other items too large for the cask, such as the shielded vacuum cleaner barrel, were wrapped in plastic at the intermediate point and again at the control point.

Unloading at the Hot Shop followed similar procedures. The truck was backed into the Hot Shop on a clean sheet of plastic and the liner was transferred to the "hot" side of a plastic contamination barrier for unloading. Reusable containers were then hosed down on the "hot" side, wiped down on the "clean" side of the barrier and then reloaded into the cask. No other work was permitted in the Hot Shop while the truck was being loaded or unloaded.

Steel plates totalling 2-3/8 inches in thickness were mounted on the truck to shield the driver. Although only two drivers were used to transport material to the Hot Shop and back to the burial ground, the maximum dose received by either, in any one quarter, was only 78% of the applicable guide values.

The extensive health physics precautions taken during the transport of the reactor vessel to the Hot Shop are included in the detailed description of that operation given in Section II 1.3.5, and will not be repeated here.

Waste Disposal

The personnel exposure expenditure required to cut up and package the large volume of contaminated material for safe transit over public highways to the common NRTS burial ground justified the construction of a new burial ground only 1600 feet from the SL-1 site. Two trenches were initially provided; one 12 feet wide, 10 feet deep, and 466 feet long, the other 6 feet wide, 10 feet deep, and 495 feet long. When it became apparent during the cleanup operation that this volume was inadequate, a third pit 20 feet wide, 10 feet deep, and 400 feet long was dug between the other two. Monuments were placed at the ends of each trench and markers were placed at 25 foot intervals along the sides to facilitate recording the burial locations of various items.

Disposal of the reactor building was generally made in this fashion: Small components were loaded into the 5 ton dump truck, driven to the burial ground, and dumped directly into a trench. On certain loads where the nature of the load was such that dumping was not feasible, the truck was accompanied by a crane which was then used to perform the disposal operation. Each load was monitored by a health physics representative who logged the items buried, their location, the radiation

levels, the volume buried, the estimated curie content, and the date of burial. The top two feet of the trenches were filled with clean dirt as disposal progressed in order to control the spread of contamination and to reduce the radiation level to <1 mr/hr.

The use of this burial ground eliminated a great deal of labor and exposure, possibly saving a total of 300 man-roentgens.

The total quantity of waste disposed at the SL-1 burial ground was approximately 80,000 cubic feet containing about 600 curies of fission product activity. Material taken to the ANP site for inspection prior to burial comprised 900 cubic feet and 190 curies of this total. Collected during the SL-1 recovery were 40,000 gallons of liquid waste containing approximately 500 curies. At present this is contained in a large underground holding tank at the ANP site. Approximately 300 curies of this liquid waste were collected from the reactor washings during the critical experiment. Maximum concentrations measured before disposal were about 27 $\mu\text{c}/\text{cc}$ of gross fission products from reactor core flushing and 5 $\mu\text{c}/\text{cc}$ from decontamination of the Hot Shop.

3.7 Exposure Statistics

During Phase 3 of the SL-1 recovery, 463 individuals made 3240 entries into the SL-1 area. There were 285 working days at SL-1. The doses and exposure times for men are recorded in Table II-4. Exposure statistics for SL-1 work in the Hot Shop are also given, as well as the totals for the Phase 3 operation.

The total accumulated skin dose and whole body dose for the SL-1 Phase 3 recovery are presented as a function of time on Figure II-57. The weekly total whole body dose is presented in Figure II-58.

Exposure distribution breakdowns are presented on a quarterly basis in Figures II-67 and II-68 and an annual basis on Figures II-69 and II-70.

The number of exposures in excess of annual and quarterly limits are tabulated below:

	No. of Technical Overexposures		% of RPG For Maximum Dose	
	Quarterly	Annual	Quarterly	Annual
Whole Body Dose*	13	0	107%	92%
Skin Dose	15	3	115%	116%

*Based on the following limits:

Whole body 3 R/quarter, 12 R/year
Skin 10 rad/quarter, 30 rad/year

TABLE II-4

Exposures During Phase 3 of SL-1 Recovery

Location or Operation	Exposure Time (hours)	Number of Entries	Total Dose		Average Dose Rate	
			Beta (rad)	Gamma (rem)	Beta rad/hr	Gamma rem/hr
SL-1 AREA						
Fan Room	148.5	287	905	380	6.1	2.6
Operating Room	177.6	366	1158	327	6.6	1.9
Total in Reactor Building	326.1	653	2063	707	6.3	2.2
Cutting hole in fan room wall	19.1	11	4.5	5.7	.23	.3
Removing Roof Under operating floor	11.3	10	8.5	8.6	.75	.76
removing storage wells and gravel	55.6	112	47.0	48.3	0.84	0.87
Removing Reactor in Reactor Building	2.3	10	31.4	10.0	13.6	4.3
outside Building	70.0	20	0.0	1.8	0	.02
All work outside reactor building	8999.0	5677	420.0	291.0	.05	.04
TOTAL SL-1 Area	9325.0	6240	2483.0	998.0	.27	.11
HOT SHOP						
Removing Pressure Vessel Head	2.8	-	35.5	14.6	9.4	3.8
Cutting Hole in Bottom of Vessel	39.6	-	10.4	6.6	.27	.17
Other	174.6	-	20.1	19.3	.12	.11
Total Preparation for Critical Experiment	218.0	215	66.0	40.5	.30	.19
Dismantling Reactor and Decontamination	100.0	87	47.5	19.1	.48	.19
TOTAL HOT SHOP	318.0	302	113.5	59.6	.36	.19
Other*	-	-	103.5	82.4	-	-
TOTAL PHASE 3	-	-	2700.0	1140.0	-	-

*Includes work in Hot Shop prior to receiving pressure vessel.

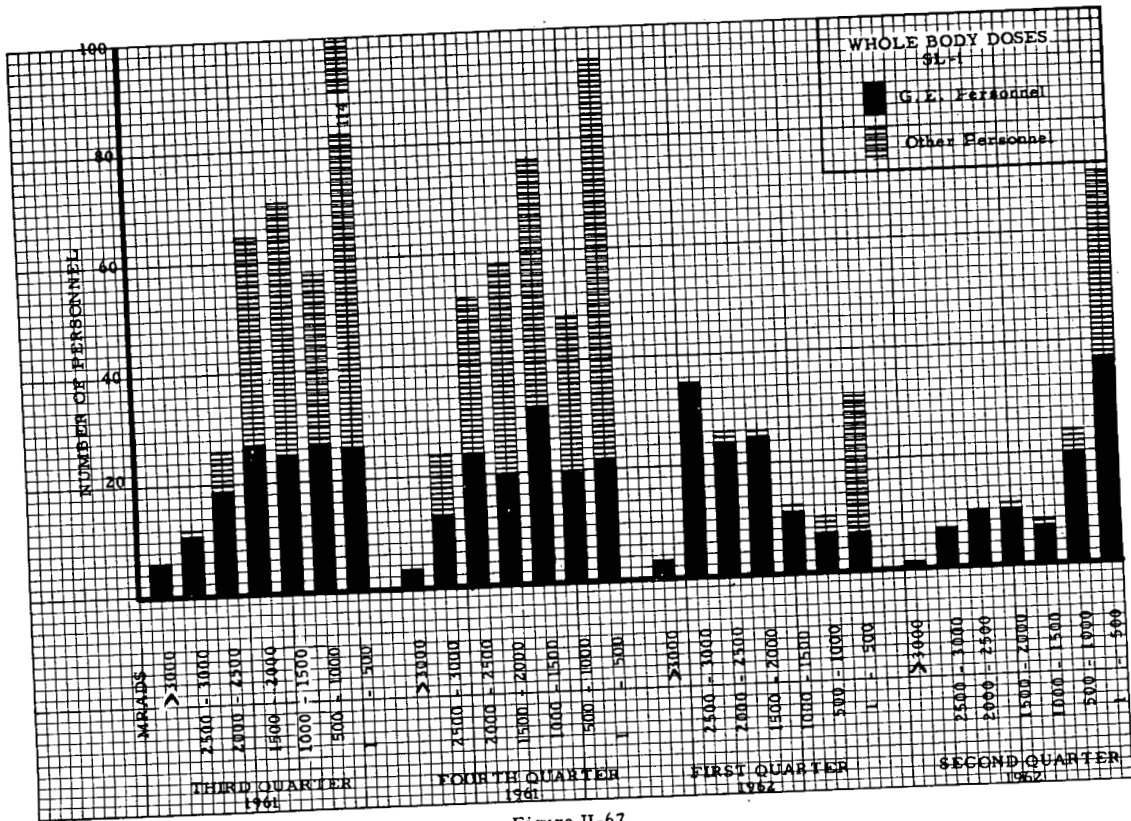


Figure II-67

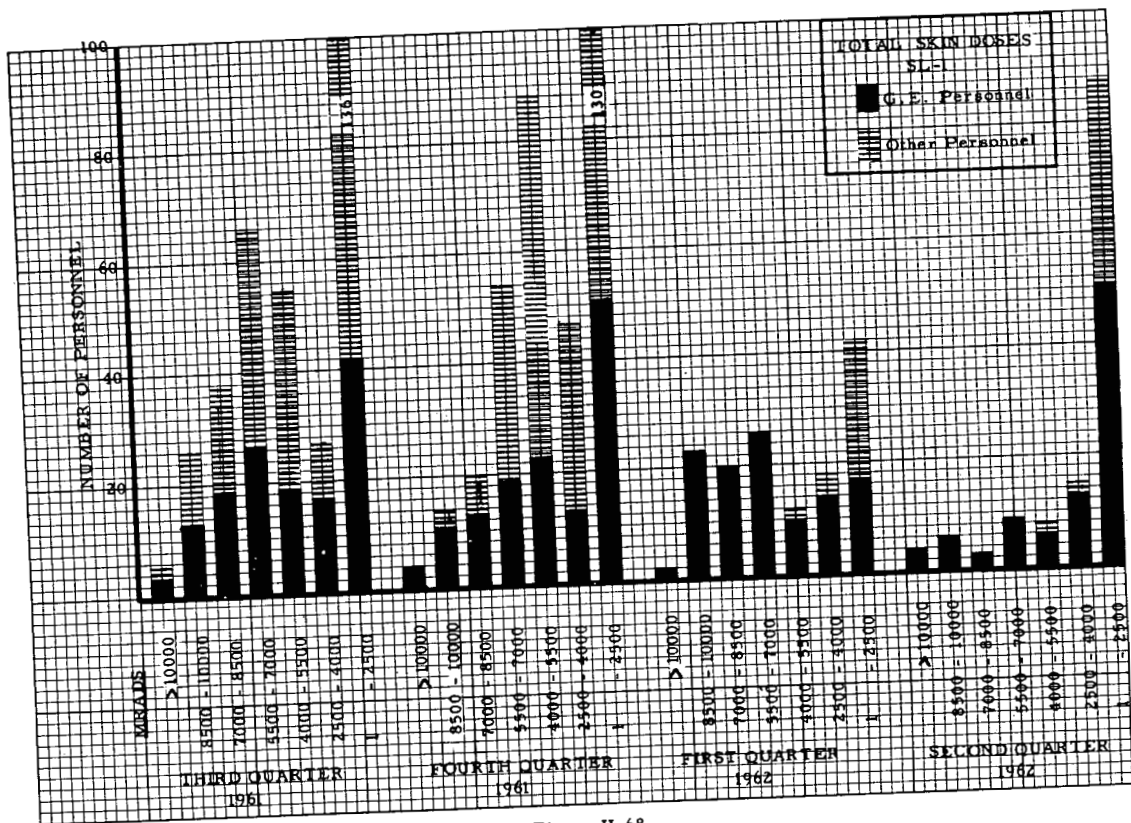


Figure II-68

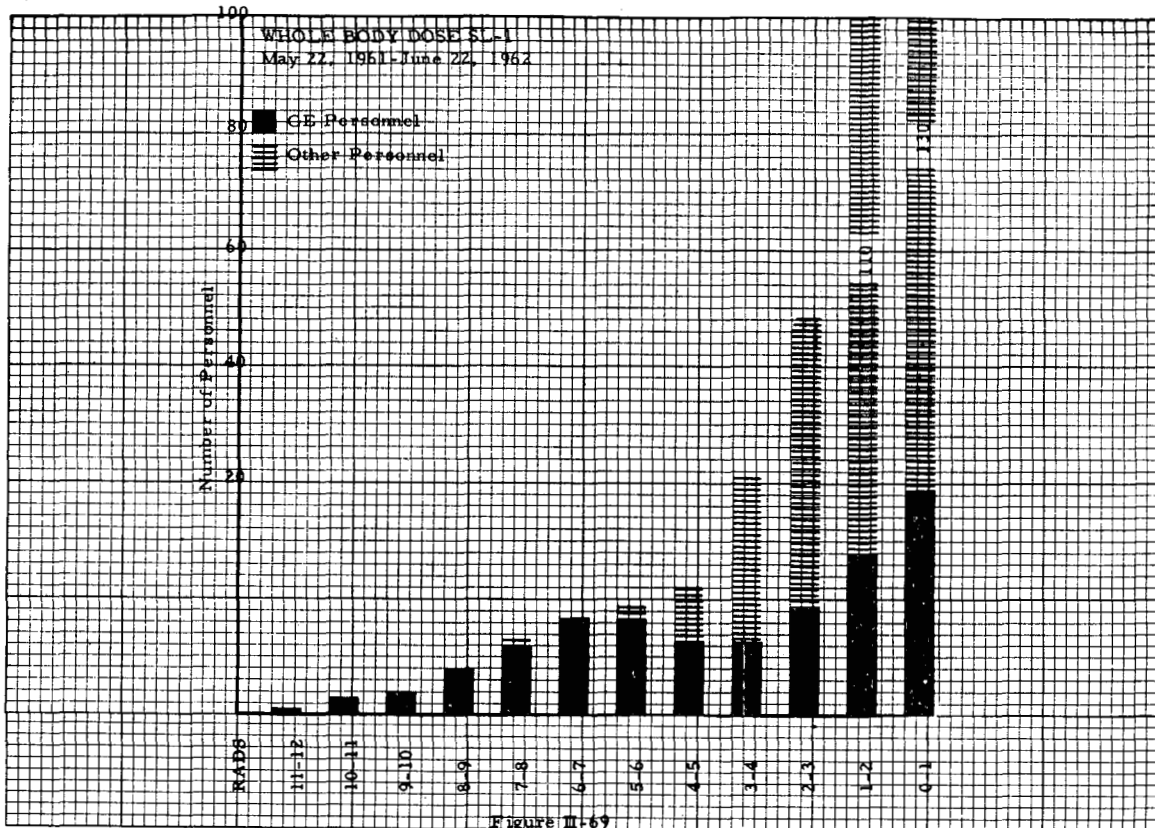


Figure II-69

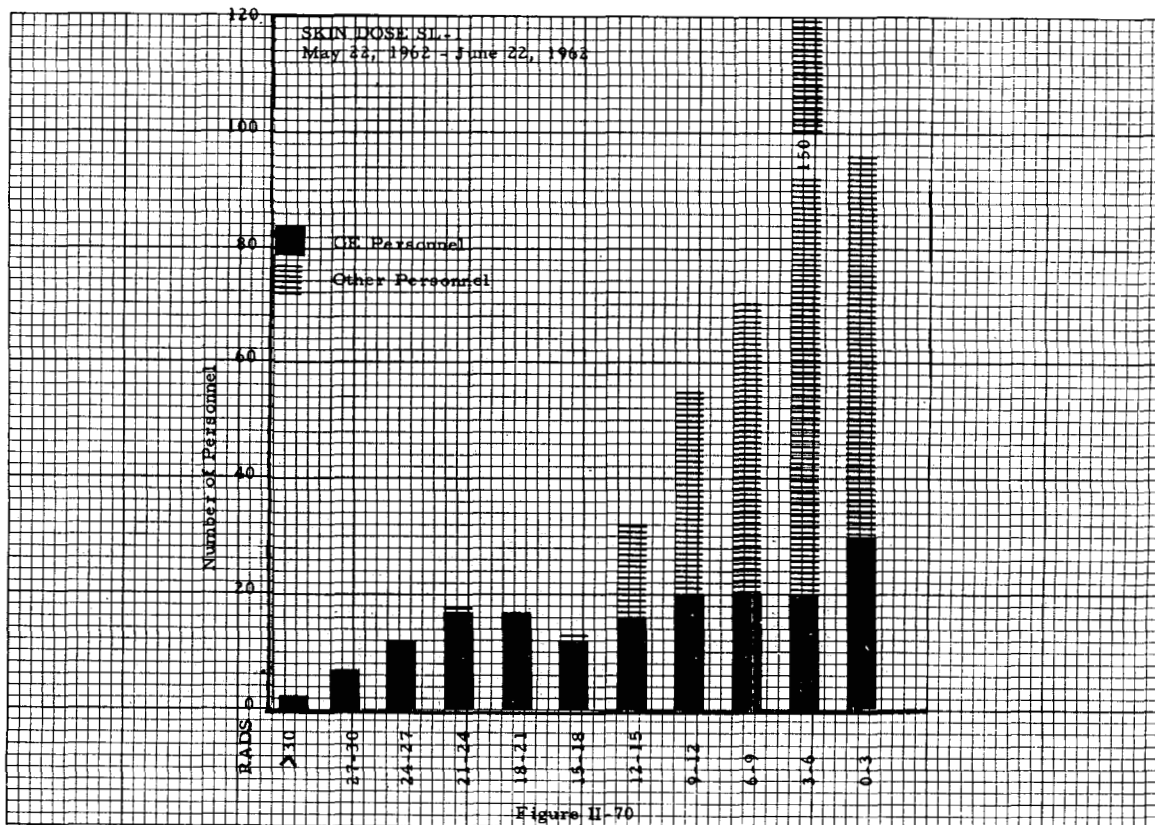


Figure II-70

III. EVIDENCE AND RELATED INVESTIGATIONS

Throughout the Phase III recovery effort great care was taken to preserve and study all possible evidence. This section covers the results of the investigation as related to mechanical, chemical and nuclear effects. Of particular importance was to establish the position of the central, or #9, control rod.

I. Mechanical Evidence

I. 1. Shield Plug Assembly #9, Central Control Rod Identification and Position

I. 1. 1. General

The importance of establishing the position of the center control rod at the time of the incident led to placing a greater emphasis on examination of these components compared with the other shield plug assemblies. Consequently, the discussion of this assembly is given in much more detail, although examination conducted on the other plugs followed a like pattern.

I. 1. 2. Initial Examination

In May of 1961 the central control rod shield plug mechanism (Figure III-1 and Figure III-2) was found lying across the top of the pressure vessel in such a position that it impeded access to Port #4. Shortly thereafter the plug mechanism was removed from the reactor building and taken to the ANP area for examination. The high radiation level (up to 25R/hr) required initial examination to be done remotely in the Radioactive Materials Laboratory (RML) where it was examined and photographed by use of through-wall periscopes. Figure III-3 shows the general assembly of a typical shield plug.

Initial examination disclosed that the guide tube was severely collapsed near the top where it joined the main plug body, and at the lower end of the tube just above the stellite bearing housing (Figure III-4). The latter collapse was the more severe and was sufficient to bind the extension rod firmly. The overall appearance of the guide tube and shield plug showed that it was coated with a non-uniform deposit. Examination confirmed that a substantial deposit, a white crystalline salt, was present on any surface which had been facing the reactor prior to its removal. This material was sampled and found to be normal boric acid.

A portion of the extension rod protruded from the guide tube and unsuccessful efforts were made to pull the rod from this tube. Additional efforts to pull the rod with heavy duty manipulators were also unsuccessful. The assembly was then disassembled in the RML by unbolting the pinion housing and removing the component parts. The guide tube was cut at the location where it joined the plug body two inches from the lower end, and again 6-3/4" from its lower end. These cuts isolated the seized

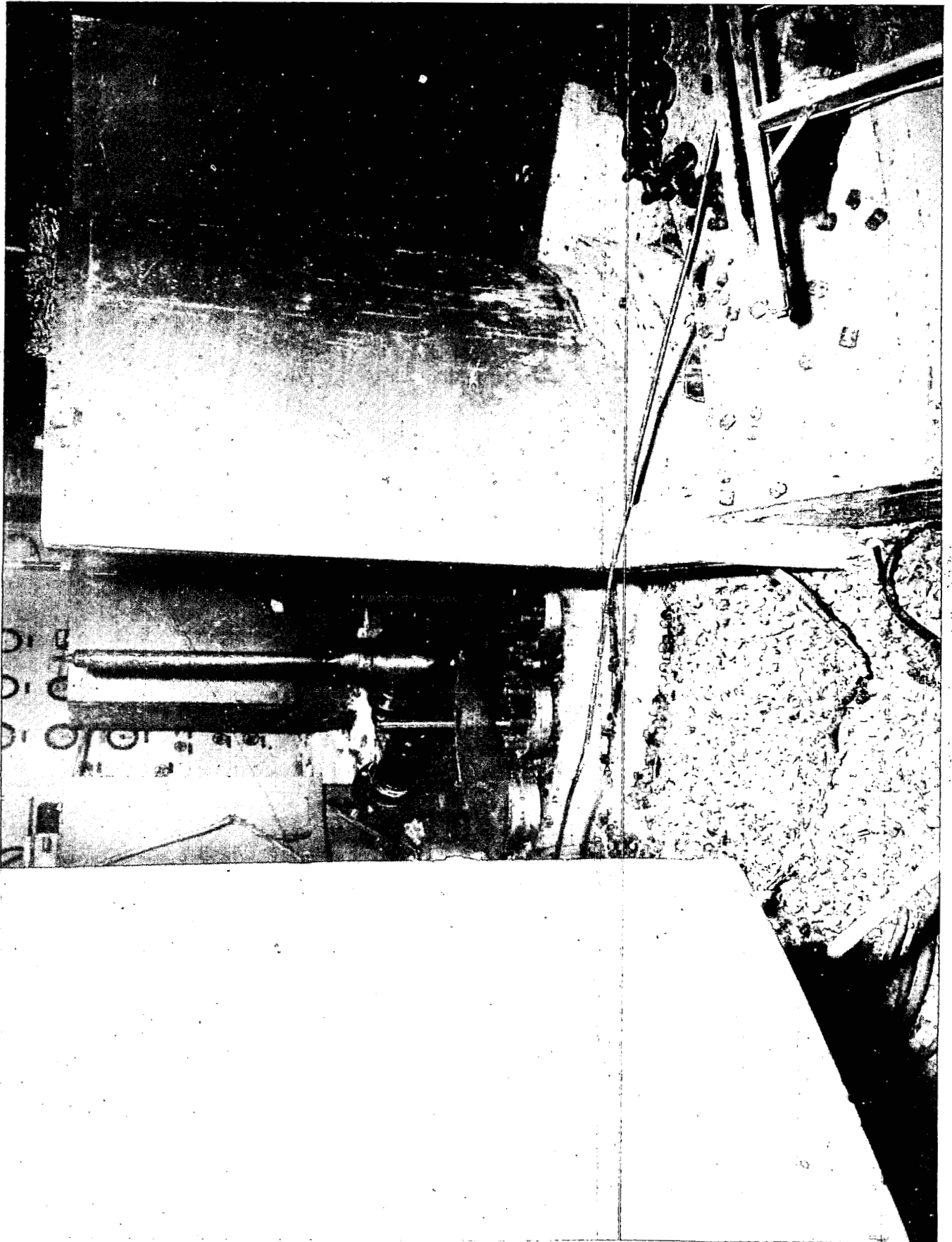


Fig. III-1, Shield Plug Assembly #9, lying across Reactor Head.

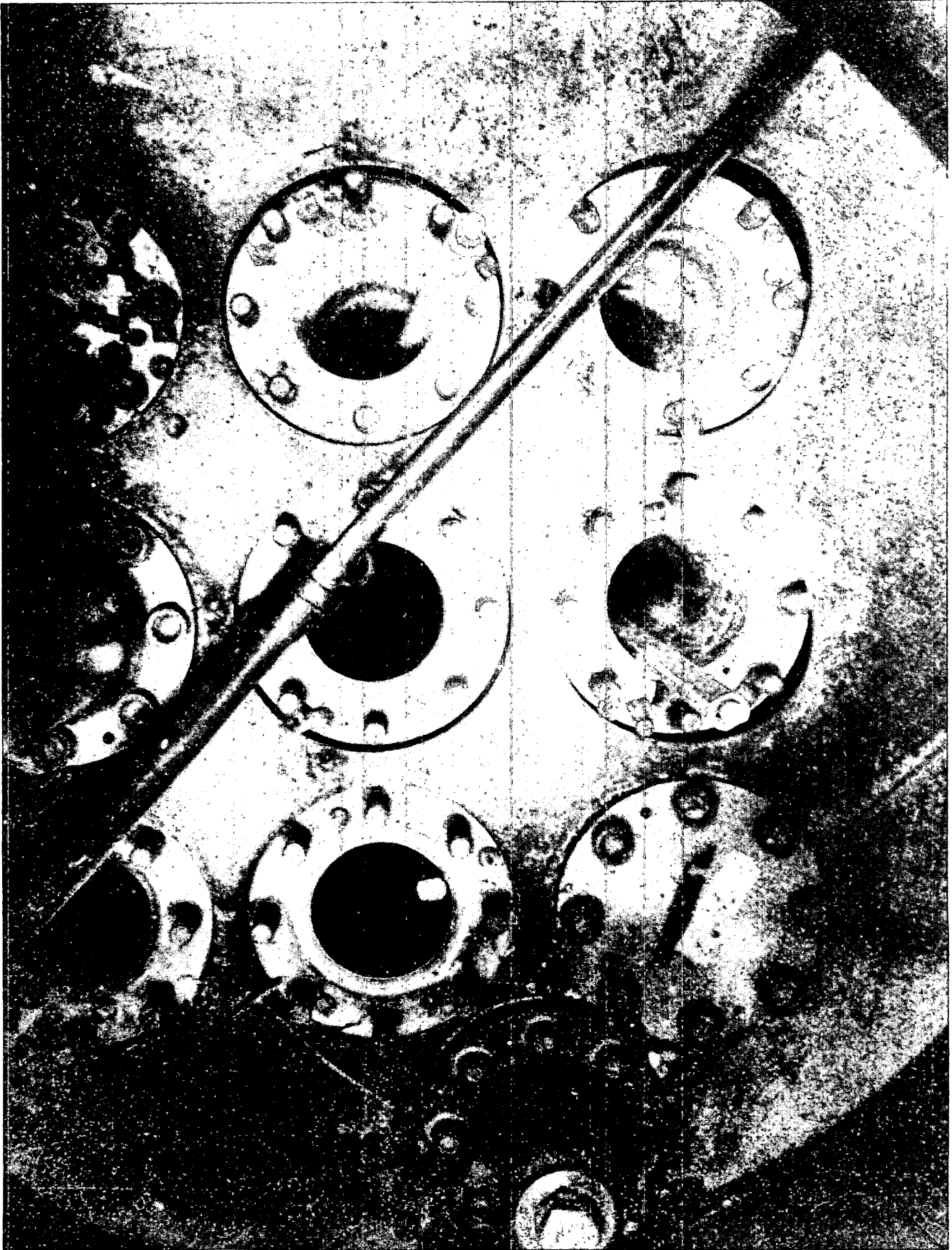


Figure III-2, Shield Plug Assembly #9 Lying
Across the Reactor Head Over Nozzles 4, 9 & 8

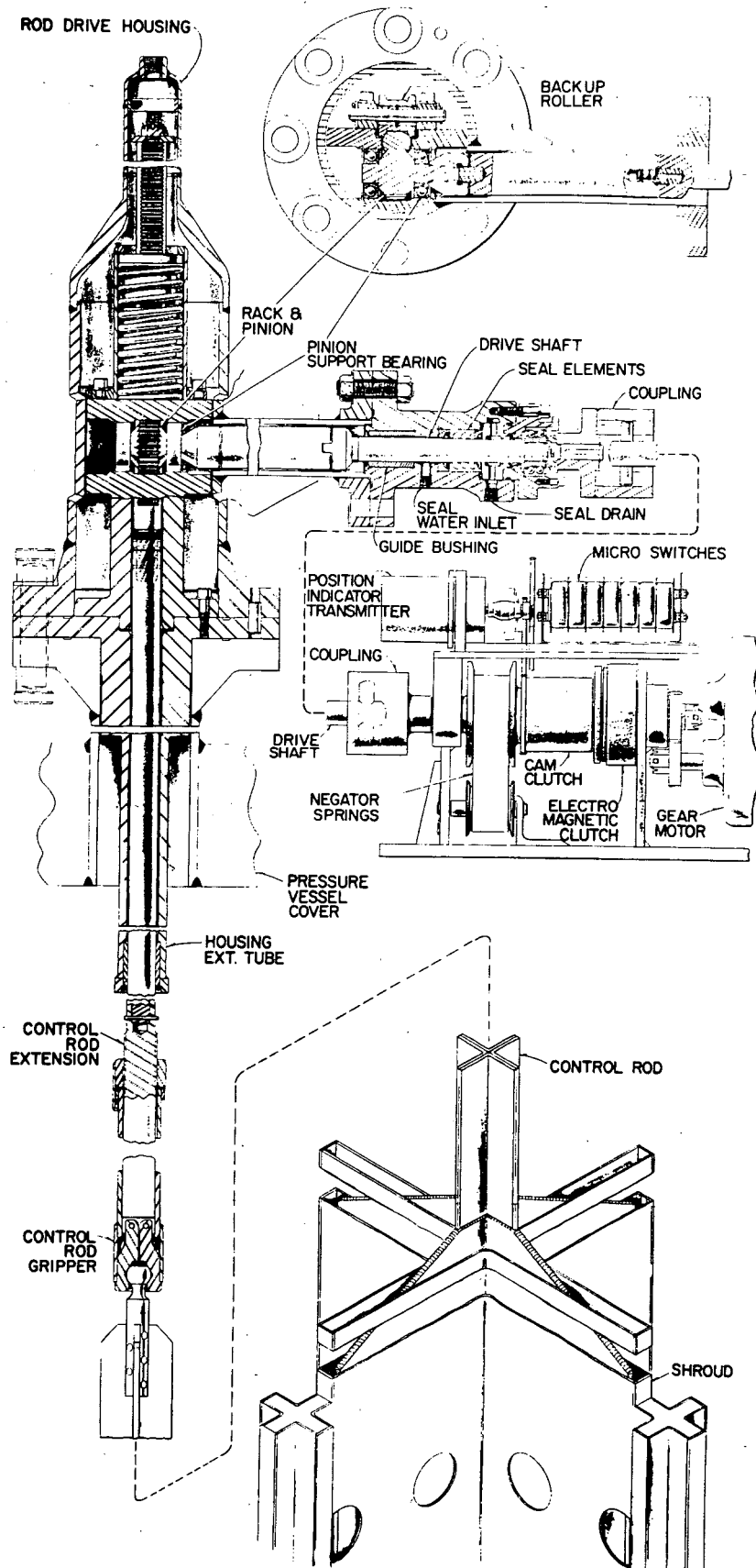


Fig. III-3, General assembly of a TYPICAL SHIELD PLUG.

region as a 4-3/4" long section. The cut closest to the seized section revealed the pinched guide tube on the extension rod, seen in Figure III-5.

The disassembled mechanism including the shield plug, pinion housing and spring housing, plus the entire extension rod and a section of attached rack, were then sent to the decontamination room. The parts were successfully decontaminated to radiation levels of less than 10 mr/hr., allowing further examination of the parts to be made by direct contact.

Following decontamination a detailed physical examination of all parts of the shield plug assembly was conducted. Results of that examination are as follows:

1. 1. 3. Spring Housing Assembly

No detectable damage was observed to either interior or exterior surfaces. Both helical springs were in good condition and free to operate.

1. 1. 4. Pinion Gear Housing

No damage to the housing was detected other than normal oxide film formation.

1. 1. 5. Pinion Gear

No damage other than normal operational wear was detected. The gear teeth were protected with a hard chrome plate and a small amount of chrome chipping was detected at the edges of several teeth. Such wear is considered normal for this service.

1. 1. 6. Roller Bearings and Housing

The back-up roller bearing was partially broken from impact. No damage to the back-up roller housing was noted. Both ball bearing assemblies were badly corroded and all bearings had sustained corrosion damage to the extent that they were seized in the races. Decontamination and cleaning freed the ball assemblies, but not sufficiently for normal operation.

1. 1. 7. Shield Plug

The 7/8" thick stainless steel shield plug flange sustained a permanent set deformation by impact in two diametrically separated areas. The maximum deflections were 9/16" at one edge and 1-7/16" at the other edge. Figure III-6 shows flange deformation, surface deposits and ruptured gaskets. Figure III-7 shows an imprint from impact. Severe distortion of the bolt holes occurred in each area of impact. Later reconstruction of the event and matching of the imprints with marks on

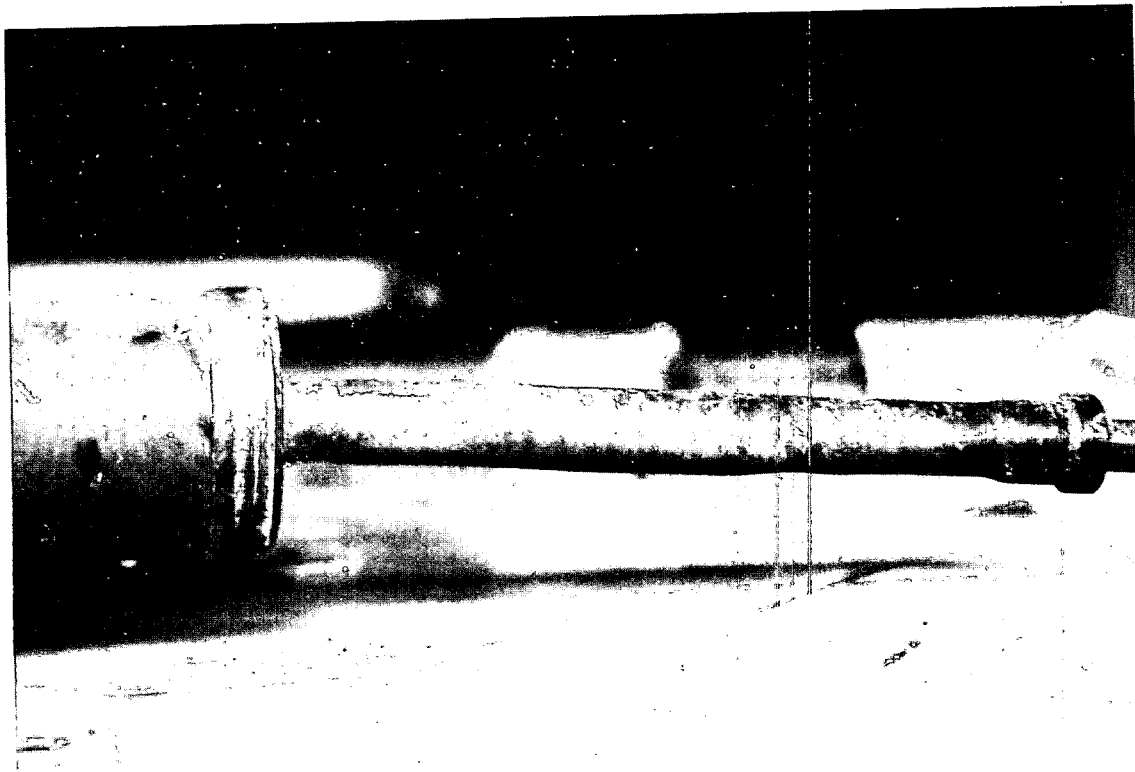


Fig. III-4, Shield Plug #9, guide tube collapse and white surface deposits.

U-5001-47

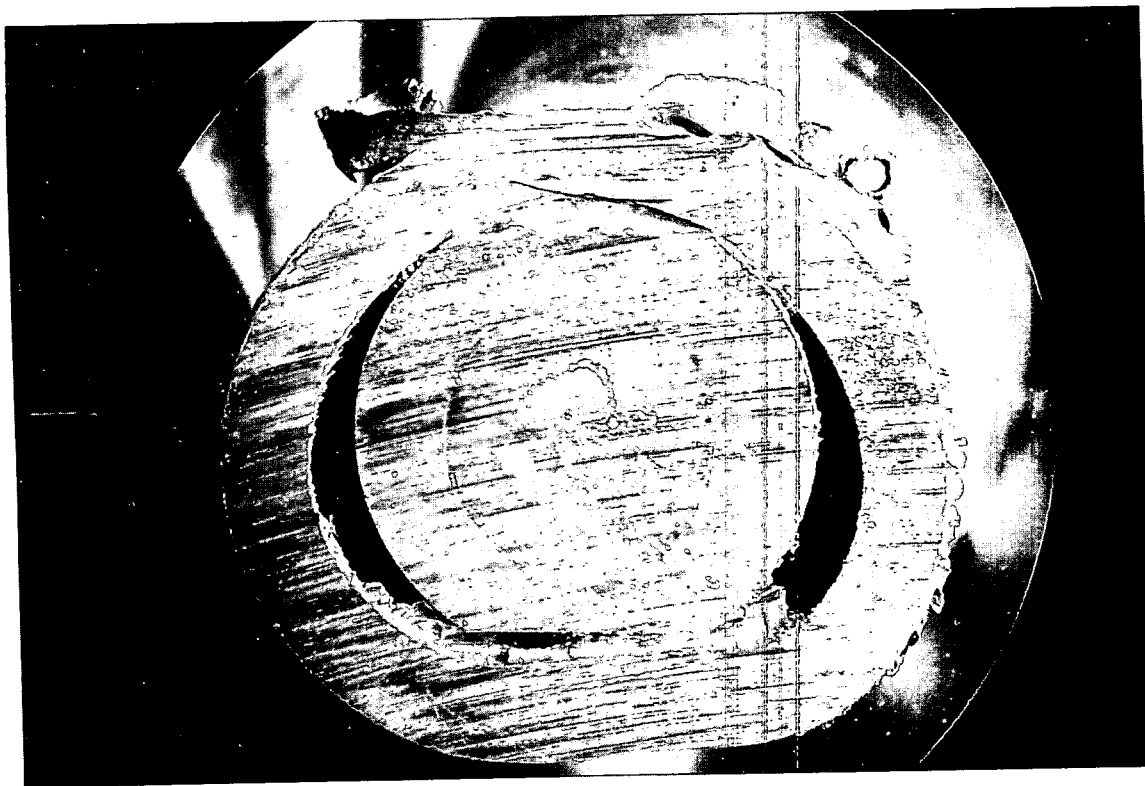


Fig. III-5, Shield Plug #9, cross section of seized extension rod by collapsed guide tube.

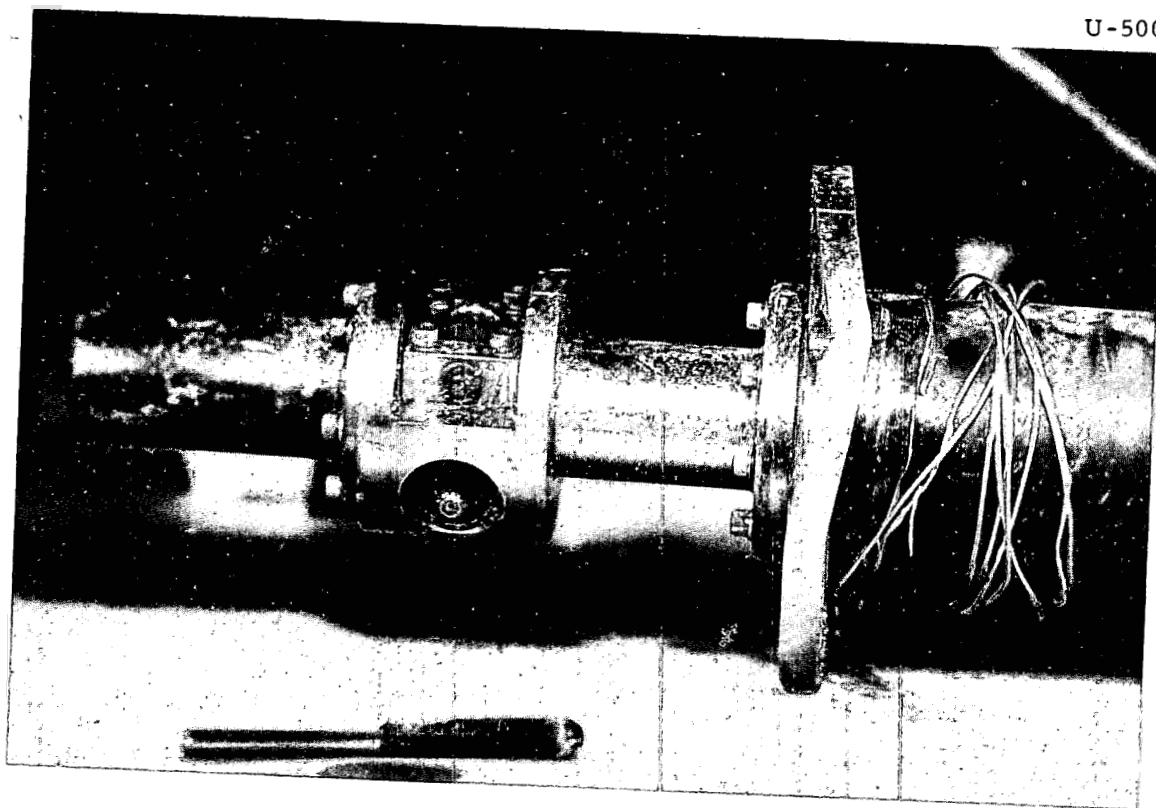


Fig. III-6, Shield Plug #9, upper section, showing flange deformation, surface deposit and ruptured gaskets.



Fig. III-7, Shield Plug #9, imprint on bolt hole from impact against corner of condenser.

other parts disclosed that one edge of the flange struck an angle bracket in the fan floor above the reactor and the other edge struck the corner of a condenser installed on the fan floor above the reactor. Examination of the plug body showed bright marks attributed to scraping on the midpoint of the plug. No significant physical damage was found that might have resulted from the forces causing this effect.

1.1.8. Guide Tube

Measurements show that the guide tube was elongated from the 18-1/2" length nominally specified to 18-3/4", an increase of 1/4". The guide tube was reduced in size by necking down and partial tube wall collapse at several points (see Figure III-4). The extension rod was firmly seized by the guide tube in the area of major tube collapse. Cuts were made at three locations, Figure III-8, leaving the seized region isolated as a 4-3/4" long section. This seized section of tube and rod was placed in a tension-compression testing machine and the extension rod pushed out of the guide tube. An initiating force of 5020 pounds was required to move the extension rod and a force of 3600 pounds was required to maintain sliding until the pieces separated.

Total deflection of the guide tube was approximately 2° from the centerline normal to the bottom face of the shield plug.

Visual inspection and stereomicroscopy of the surfaces of pieces cut from the section containing the seized extension rod disclosed the very important fact that the final travel of the rod was upward with respect to the shield plug after the seizing action started.

1.1.9. Extension Rod

The first examination of the rod surface downstream from the guide tube failed to show any metal rupture, burring, or scratches beyond normal wear. The extension rod had a hard black deposit, which was identified as chromous acid. There were some longitudinal scratches in this coating, but these were initially attributed to the sliding action of the Hot Shop manipulators during the attempts to pull the rod out of the plug.

Prior to forcing apart the extension rod and guide tube from the 4-3/4" bound section, a portion of the guide tube was cut away and removed without using any force. A portion of a slide mark extending onto this piece showed burring indicating predominantly upward movement of the rod with respect to the plug, although there was some evidence of downward movement as well. Because of the markings which the manipulators were suspected of making on the extension rod, this part was of little aid in identification of sliding which may have occurred during the incident. Inspection of the rod after removal from the guide tube indicated no appreciable downward movement had occurred after seizure.

Zylo, dye penetrant and stereomicroscopy inspections revealed no surface cracks in the rod material. Rockwell hardness measurements were taken longitudinally along the rod and an average of $38 R_c$ was measured as against a specified hardness of $44 R_c$.

6-III

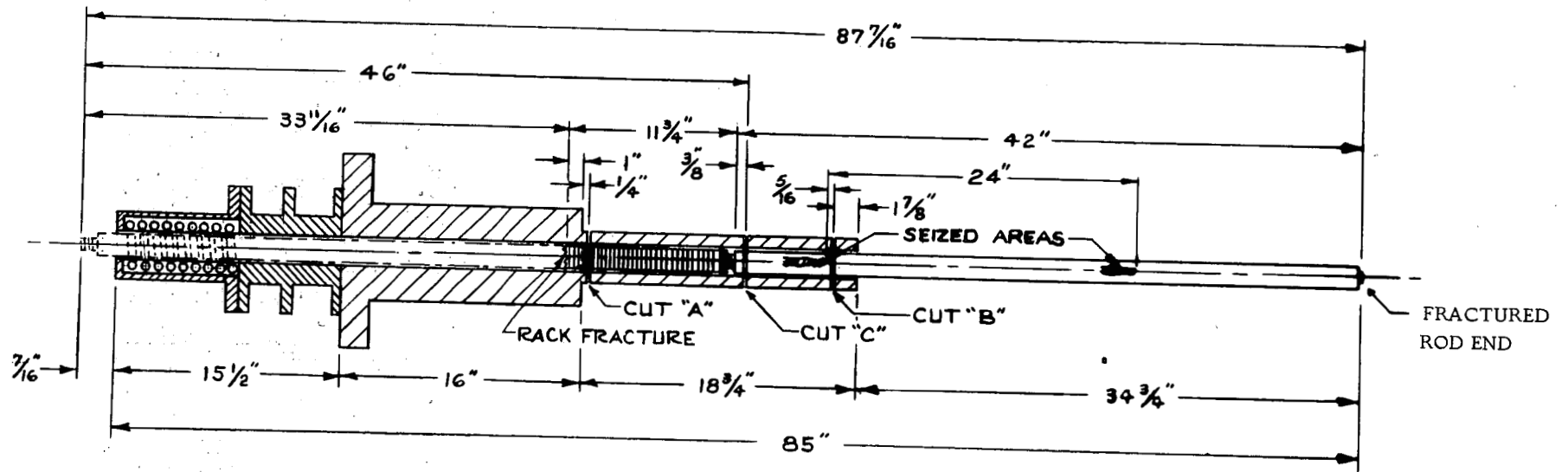


Figure III-8 Shield Plug #9 Assembly - Sectioning and positions of rod during seizure.

An impact-tensile-fatigue fracture occurred at the root diameter of the threaded stud. Figure III-9 shows that the fatiguing had started at the root diameter of the threaded stud and progressed inwardly. The crescent shaped dark area is the fatigue break and the bright area represents sound metal that was fractured by an impact-tensile action. Profilometer measurements show that approximately 46% of the cross-section area involved was due to pre-incident fatigue.

I. I. 10. Gear Rack

The section of gear rack remaining in the guide tube extended approximately 1" into the lower end of the shield plug. This section was threaded to the extension rod and measured 11" in length. Stereomicroscopy detected many transverse stress cracks on the rod flat along the entire length of the section (Figure III-10). The gear rack had sustained an impact fracture in a section weakened by fatigue.

Inspection of the lower section of gear rack indicates no burring or galling of the rack teeth and no seizing or rupture of metal other than that attributed to normal wear.

A 32-1/2" length of gear rack complete with washer and nut was recovered from the fan room floor. The fractured section at the lower end of the rod matched the short piece cut from the top of the extension rod in the plug assembly. The length of the section is within 1/4" of that expected. The underside of the washer was imprinted with an outline of the top of the rack section although there was no imprint of the nut on the top of the washer. The washer, however, was deformed downwards at one point by apparent impact (Figure III-11). The threaded end was broken off at the pinhole. This broken piece of stud (Figure III-12) was found in the control rod handling tool, imbedded in the fan room floor, and matches up with the pinhole. One thread in the section covered by the nut was sheared off the stud body (Figure III-11). Investigation indicated that this galling was a pre-incident event and served as a means to further identify the assembly as #9.

Additional studies were made of the fine cracks across the flat portion of the rack body in an attempt to determine their origin. Although dye penetrant and zygo techniques did not develop crack indications, the MAGNAFLUX method brought out the defects clearly. A metallurgical specimen prepared from one short section of the rack showed the crack indications to be of the type usually resulting from overstressing during the finish grinding or from some type of cleaning procedure prior to chrome plating. Discussion of this point with a representative of the fabricator led to the information that similar cracks have been noted in 17-4 PH alloy, after the use of certain cleaning procedures prior to chrome plating.

I. I. 11. Connecting Rod

The connecting rod was recovered from the top of the reactor vessel. This rod was broken from the extension rod at the base of the threads on one end, and through the hollow pins which retain the ball joint latching fingers on the other end, Figure III-14.

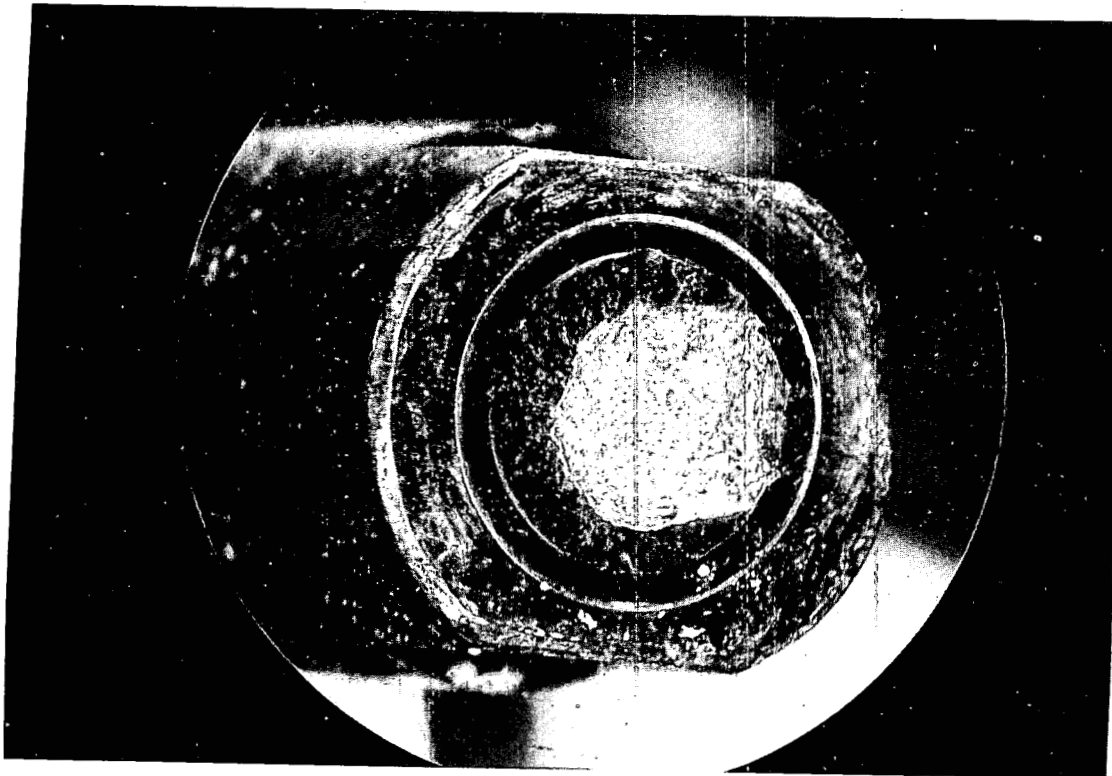


Fig. III-9, Shield Plug #9, extension rod, showing fatigue area and fracture.

U-5001-34

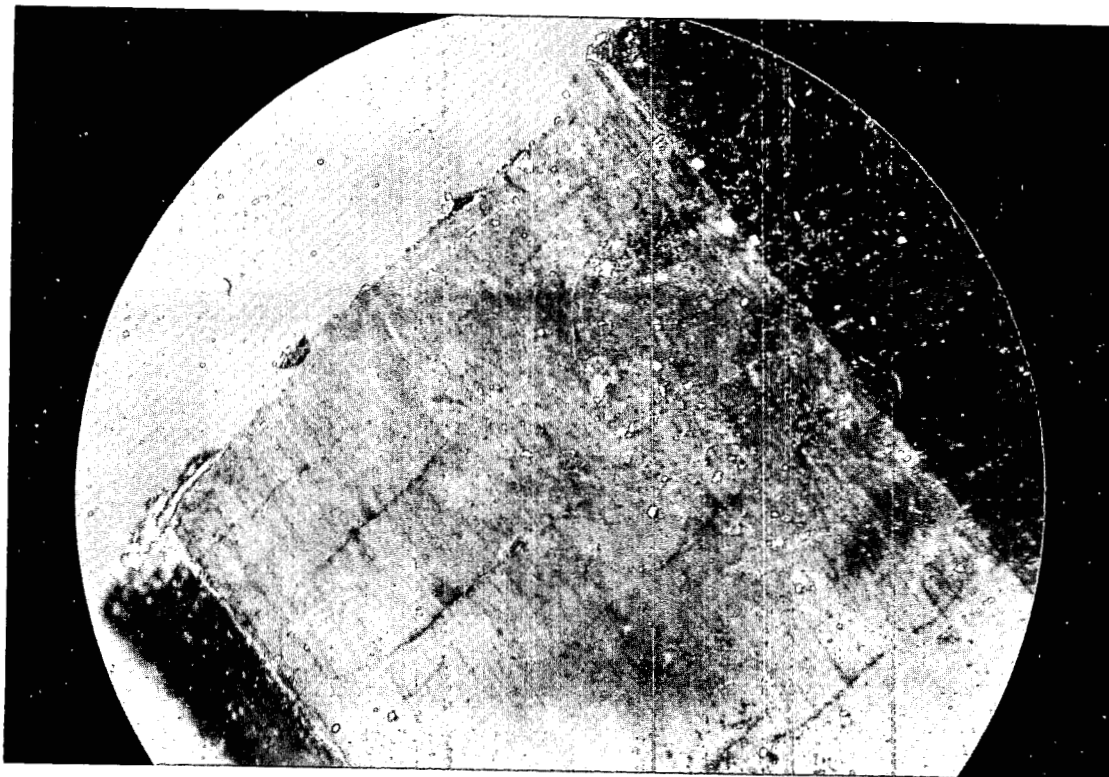


Fig. III-10, Shield Plug #9, transverse stress cracks in gear rack section.

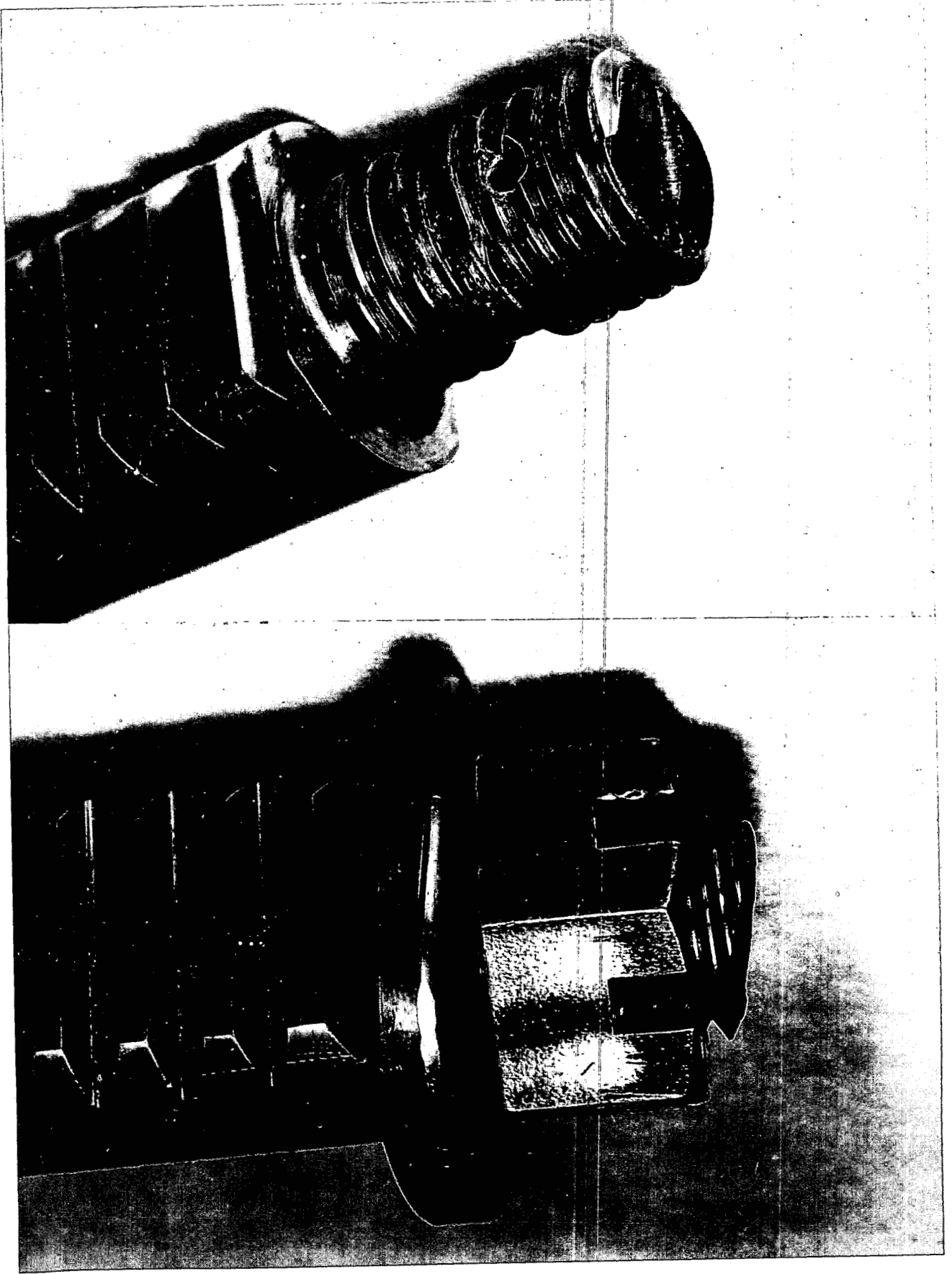
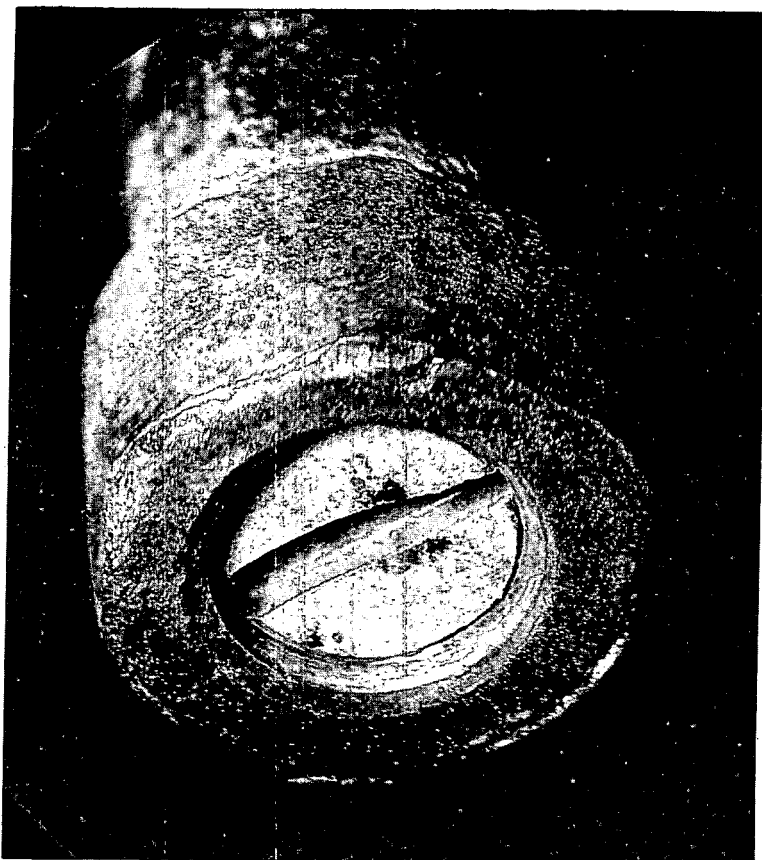


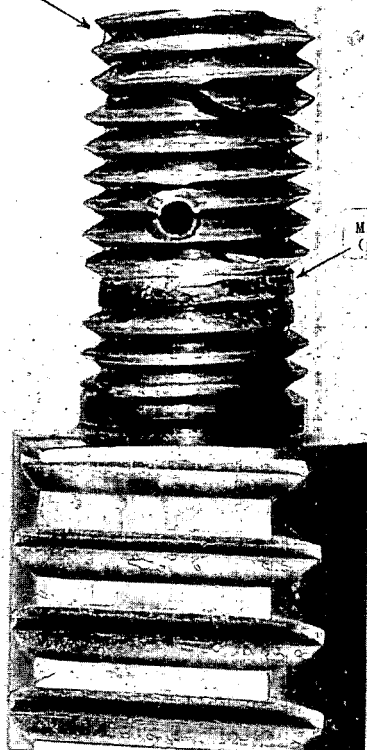
Fig. III-11, Shield Plug #9, top of rack, nut and washer. Galled thread (pre-incident) was one major identification feature.

Fig. III-12, Handling tool with broken end of #9 gear rack stud retained in tool which was found embedded in fan room floor.



U-5081

Stud section found
in control-rod
handling tool



Missing thread
(pre-incident)

Rack of central
control-rod

Fig. III-13, Matching of broken stud of central control rod rack.

1.1.12. Position of the Central Control Rod

Reconstruction of the severed pieces of extension rod and guide tube (Figure III-8) shows that, at the time the mechanism was recovered, the control rod was $2\text{-}1/2" \pm 1/4"$ withdrawn from its normal scram position, relative to the plug mechanism. In addition, a broken C clamp was recovered from the fan floor (Figure III-18). The C clamp was open to the diameter of the rack. Had the clamp been in place on the rack for the rod assembly operation, the rack would have been raised approximately $2\text{-}1/2$ inches. The control rod handling tool was, at the time of the incident, attached to the rack of the central control rod. Figure III-13 shows the matching of the broken piece of stud found in the handling tool with the broken stud of the rack. The handling tool penetrated the fan room floor in the region above nozzles 5 and 6 (Figure III-30).

Slide marks are evident on the extension rod as it was found sticking out of the guide tube. It is apparent that there are longitudinal marks in the black chromous acid deposit. These are shown in detail in Figure III-15. Though it was originally thought that these marks were produced by the manipulator hands, Figure III-15 shows that the marks extend well beyond the end of the housing, up inside where the manipulator hands could not have reached. Therefore, it is evident that this slide mark (as well as two similar marks spaced approximately at 120° around the rod) was not made by the manipulator hands. There are other less well defined markings on the extension rod, markings which did not extend up inside the guide tube and which do not extend down the rod a uniform distance. These marks can be attributed to the manipulator hands.

Impact impression - When the guide tube collapsed, the region of greatest collapse and seizure received the impression as shown in Figure III-16. Both the inside of the guide tube and the plaster cast of that region are shown in the photograph. At the end of the slide marks on the extension rod, $21\text{-}11/16"$ down from the end of the guide tube, an impression exists on the extension rod. This impression matches the plaster cast of the guide tube impression. The matching is virtually perfect, as can be seen in Figure III-17. These two impressions were $24 \pm 1/8"$ from each other in the relative positions in which the mechanism was found. The impression of the extension rod is at the end of the most prominent slide mark. This relative position can be noted in Figure III-8, which shows the extension rod in the position relative to the housing in which it was found.

In view of the facts as discussed above, the extension rod and plug at the time the guide tube collapsed, were in a relative position corresponding to $26\text{-}1/2 \pm 1/4$ inches withdrawn.

In the ensuing events of the incident the extension rod was forced through the collapsed guide tube to a final, securely clamped position corresponding to $2\text{-}1/2$ inches withdrawn. Preliminary analysis, therefore, revealed the relative position of the rod in the plug when these were recovered from the SL-1 building.

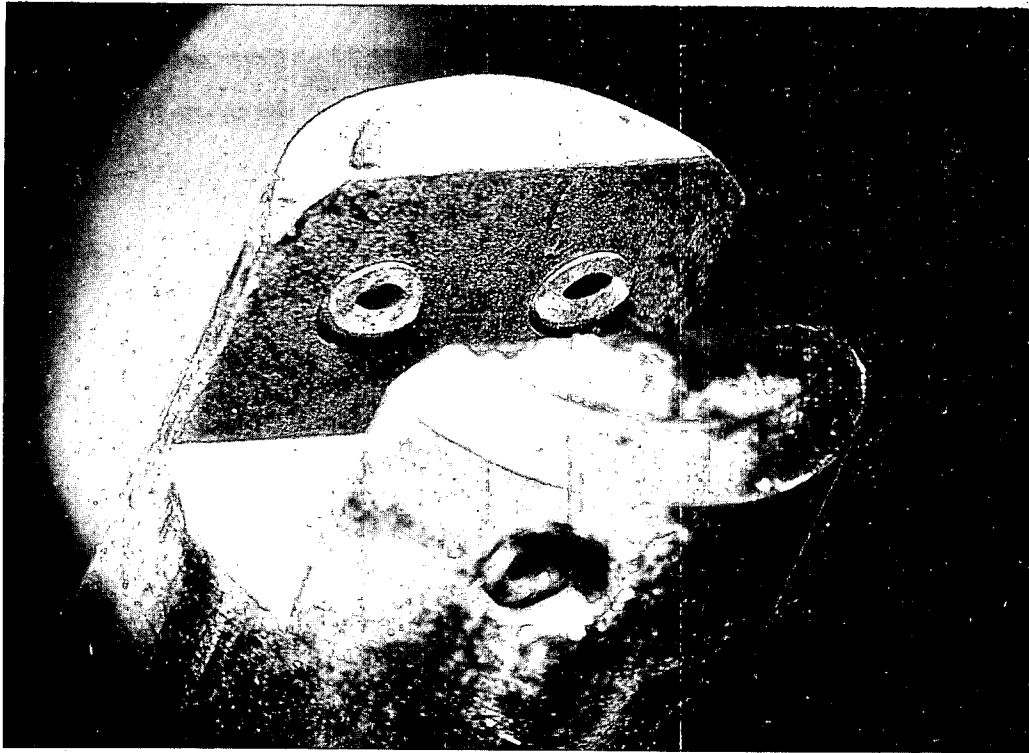


Fig. III-14, Shield Plug #9, connector rod, showing sheared roll pins.

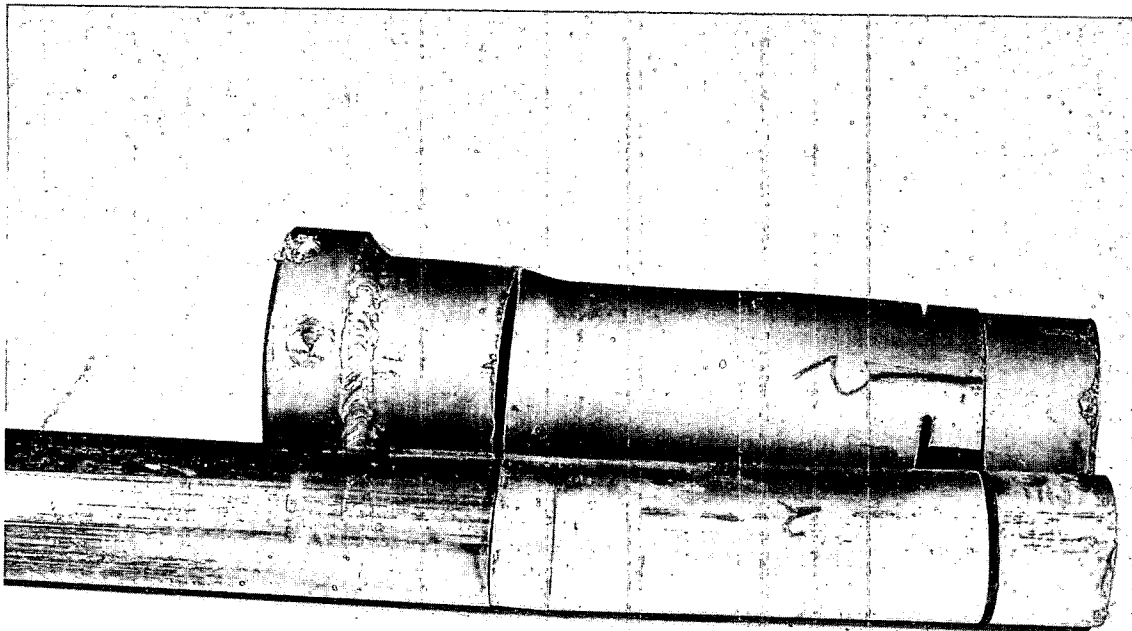


Fig. III-15, Shield Plug #9, relative position of extension rod and sectioned guide tube showing sliding marks.

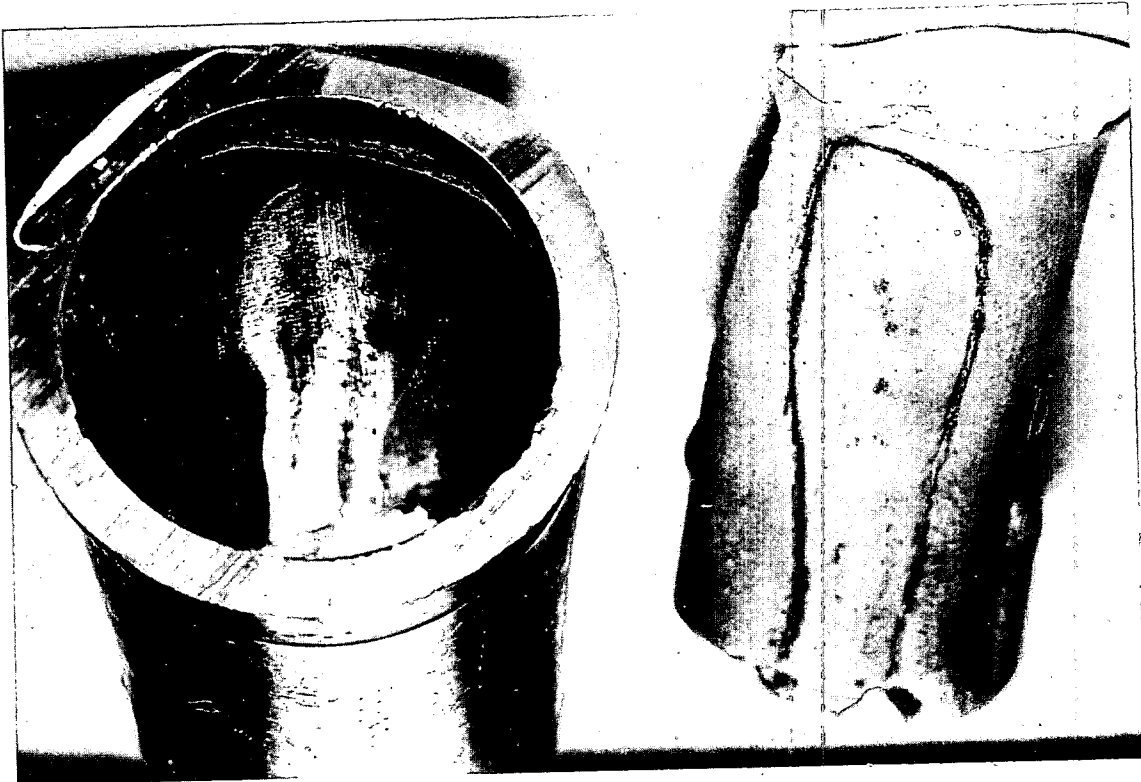


Fig. III-16, Shield Plug #9, seized region of the guide tube with plaster cast. Pencil line on plaster cast outlines impression area.

U-5048-2

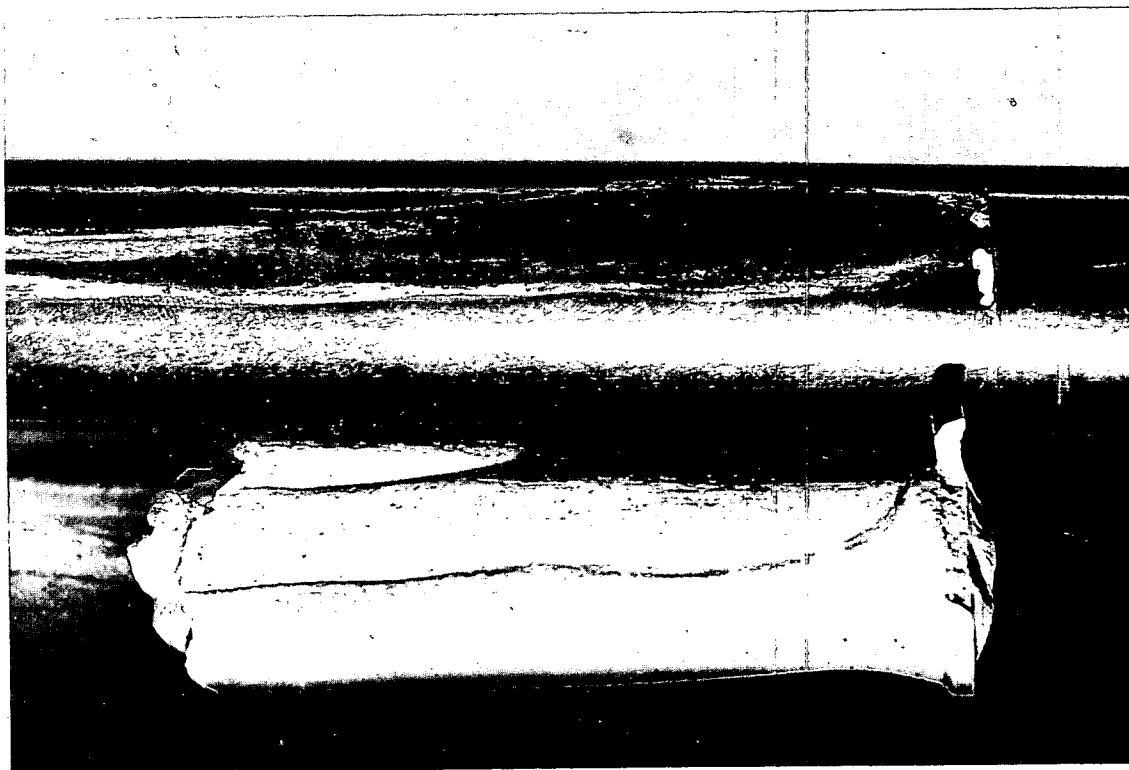


Fig. III-17, Shield Plug #9, plaster cast of guide tube impression and similar impression on extension rod.

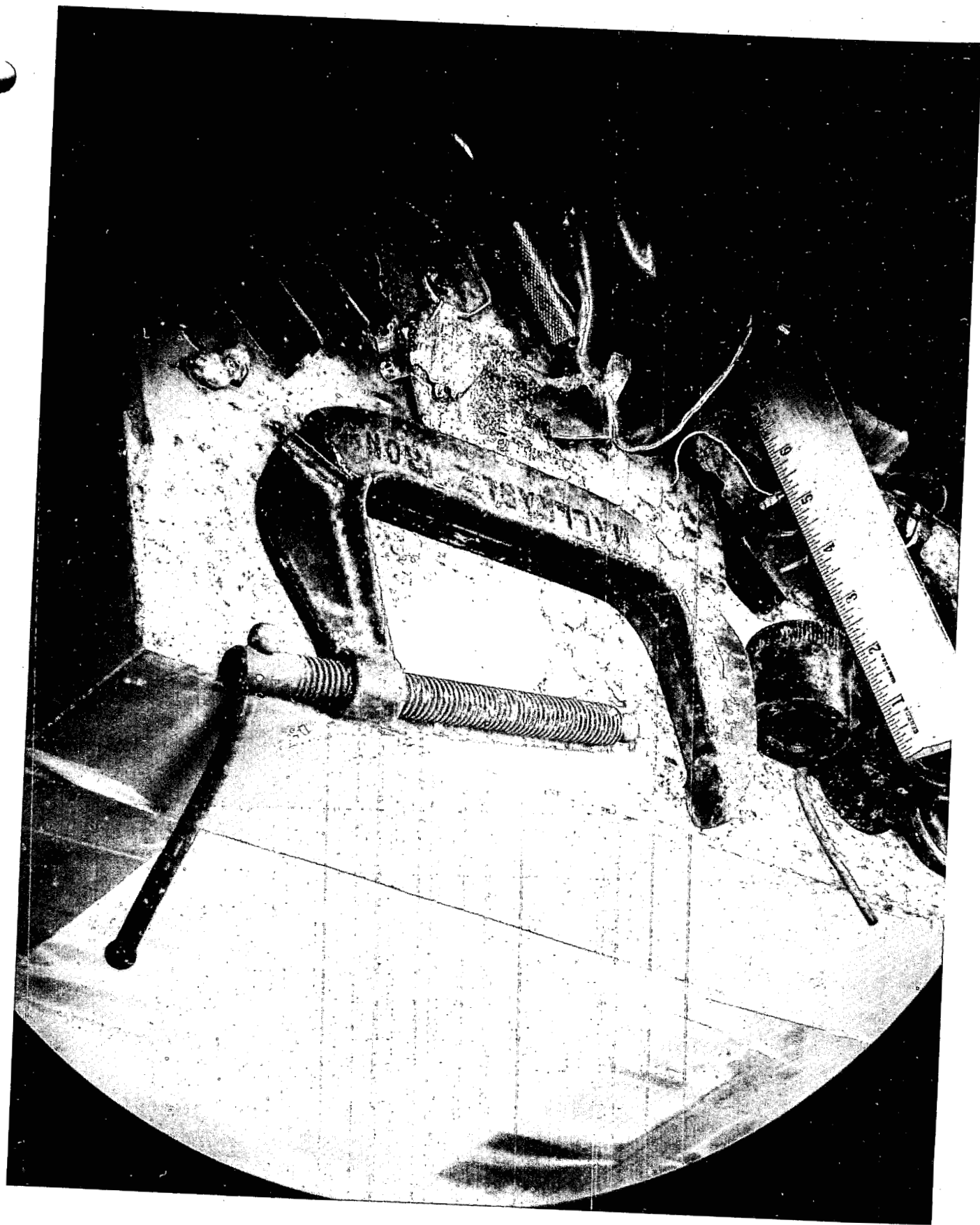


Figure III-18, Broken C-Clamp Recovered
from Fan Room Floor

III-17

The forces which drove the extension rod from the 26-1/2 inch withdrawn position, relative to the extension housing in which it was seized by the water hammer, to the 2-1/2 inch position in which it was found do not have a profound effect upon the conclusions which may be drawn about the accident. The pertinent evidence has been examined carefully, however, to make sure that a plausible explanation can be found connecting all the observations.

It is believed that when the high pressure from the water hammer ejected the #9 shield plug, the same pressure was also crushing the guide tube onto the extension rod. This crushing action permitted the transmission of forces to the extension rod greatly in excess of the 5020 lbs. subsequently observed. In addition, since the rod and housing were swaged together by the pressure, the force required to slide them apart initially would be expected to exceed that required to slide an undeformed portion of the rod through the housing. For these reasons, the extension rod was initially accelerated with the shield plug as a unit.

Although the central shroud, collapsed around the blade by the force of the explosion, was essentially torn free from the rest of the core and was moving upward at the time, the inertia of these parts was sufficient to prevent their acceleration with the extension rod and shield plug by the force which could be transmitted through the rod pins, estimated to be about 9000 lbs. These pins failed, consequently, but not without imparting some additional upward momentum to the blade and shroud. The connecting rod, moving up with the extension rod, did not leave the connector housing completely, as a result, until the latter had been guided into the nozzle in the head of the pressure vessel.

As the shield plug left the nozzle, the handling tool attached to the top of the rack was deflected and possibly bent by the operator holding the tool. The tool struck the ceiling at a point not directly over the shield plug, so that a moment was exerted on the handling tool and rack, which was presumably still at the 26-1/2 inch withdrawn position. The threaded end of the gear rack broke inside the end of the handling tool. The impact of the handling tool on the ceiling may have also provided the force necessary to separate the swaged regions of the extension rod and housing, and to break the rack 32 inches from its top, near the pinion gear location.

The rack, still moving upward with the shield plug, penetrated the fan room through the opening made by the #3 shield plug. The washer struck and was bent down as observed by an unidentified object, driving the rack, extension rod and connecting rod downward nearly to the completely inserted position. The rack, if not already broken, fractured at this time. Since the rack was made

of 17-4 PH, a brittle material, and had many pre-incident cracks, the exact position of fracture is of little significance. A static test on a washer showed that a force of 6500 lbs. produced deformation comparable to that observed.

When the shield plug struck the beams and condenser, as previously noted, the fractured section of the rack continued into the fan room from its momentum (it must be presumed to have passed the object which bent the washer) and fell on the fan room floor. The shield plug then fell back onto the pressure vessel head, a probable cause for the break between the extension and connecting rods and the 2° bend in the extension housing. From the burrs that indicated upward motion of the rod with respect to the plug, it can be inferred that the extension rod was driven upward slightly by this action to the 2-1/2 inch withdrawn position in which it was found.

Thus a possible sequence of events can be found to explain all the existing evidence. While extreme reliance should not be placed on any individual detail in the chain, there seems to be no reason to doubt the validity of the general argument.

1.1.13. Control Rod Blade and Shroud

The central control blade when recovered from the reactor vessel was bound by the collapsed shroud at a position of 20 inches withdrawn from normal scram position. The control blade had not moved after the shroud collapsed (see Section III-1.8 for details).

1.2. Shield Plug Identification, Trajectories and Damage

1.2.1. Shield Plug Assembly #1

This plug assembly was imbedded in the fan room floor almost directly above the reactor head nozzle #1. The spring housing bore the brunt of the impact against the ceiling and the bottom of the condenser in the fan floor. It was badly distorted and collapsed downward (Figure III-19). The flange showed no evidence of damage except for some distortion of one bolt hole, at which point it appeared that a sharp object had struck the under face of the flange.

The extension rod guide tube sustained partial collapse of the tube wall but not to the same extent that has been observed on other rod guide tubes. The deflection of the guide tube from its normal axis was more severe than was seen on other assemblies (Figure III-19). This deflection was caused by the body of shield plug #7 in its flight from the reactor head striking the stellite bearing end of the guide tube. The imprint marks matched perfectly (Figure III-20).

Both ball bearings in the pinion gear assembly were badly corroded and immovable.

The control rod assembly was removed from the pressure vessel by sectioning off above the gripper fingers through the connector rod and connector rod housing since the assembly was still attached to the control blade and held firmly by the collapsed shroud.

The gear rack top stud was broken off. Neither the washer nor the nut have been recovered or identified.

The extension rod sustained a fracture in the stud connecting the gear rack.

Metal abrasion was detected along the side of the gear rack and extension rod, which is attributed to the movement of the plug when ejected from the pressure vessel head.

1.2.2. Shield Plug Assembly #3

The shield plug assembly had penetrated the fan room floor and was found lying on the fan room floor with a section of gear rack inside the housing. Another section of rack, 6-5/8 inches long, was recovered near the shield plug.

Following decontamination, the gear rack section which was bound in the guide tube dropped out when the assembly was inverted. This proved to be the top end of the rack, 8-7/8 inches long, with all but 3/8 inch of the stud thread broken away (Figure III-21). The sections found in the guide tube and that recovered from the fan room floor matched perfectly (Figure III-21).

The extension rod guide tube was deformed, partially collapsed and deflected from its normal position (Figure III-22). There was no indication of an external impact mark.

The total guide tube elongation was measured to be 3/16 inch.

The flange was deformed on both sides due to impact (Figure III-22).

Several scoring marks apparently made by the rack teeth are visible inside the guide tube. These marks lead to the postulation that the impact-bending break of the rack occurred while it was bound in the collapsed tube as a result of the severe tube deflection. The bottom piece of rack subsequently fell out on the fan room floor. A broken nut and stud recovered from the reactor operating room matched the broken thread end of the gear rack (Figure III-23).

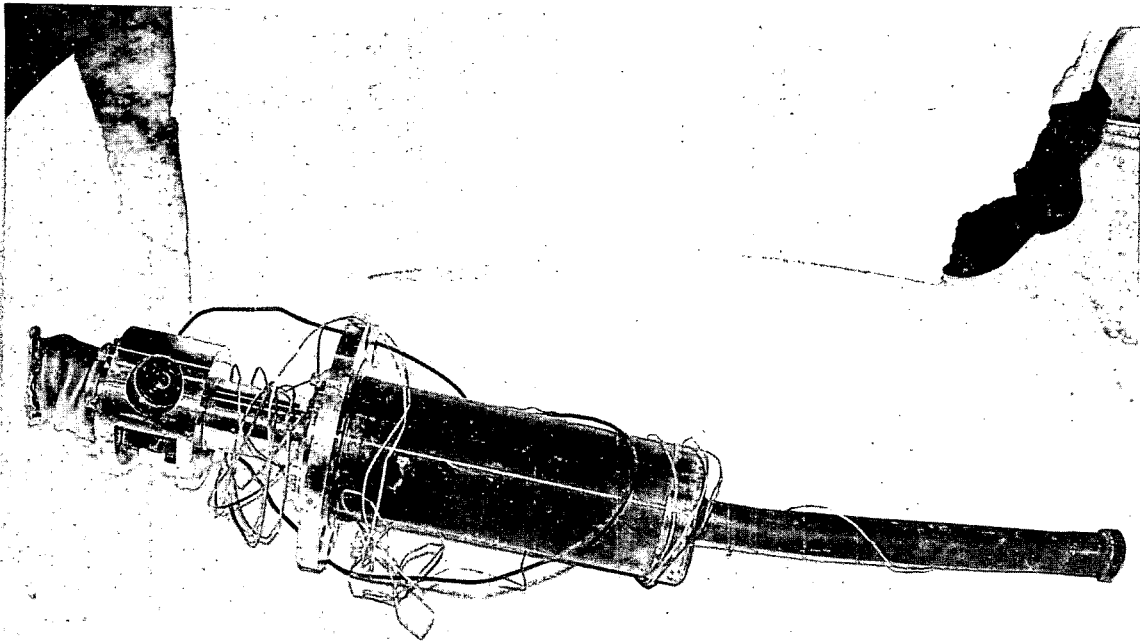


Figure III-19, Shield Plug #1, showing Damage to Spring Housing, Flexitallic Gaskets, and Guide Tube

U-5052-3

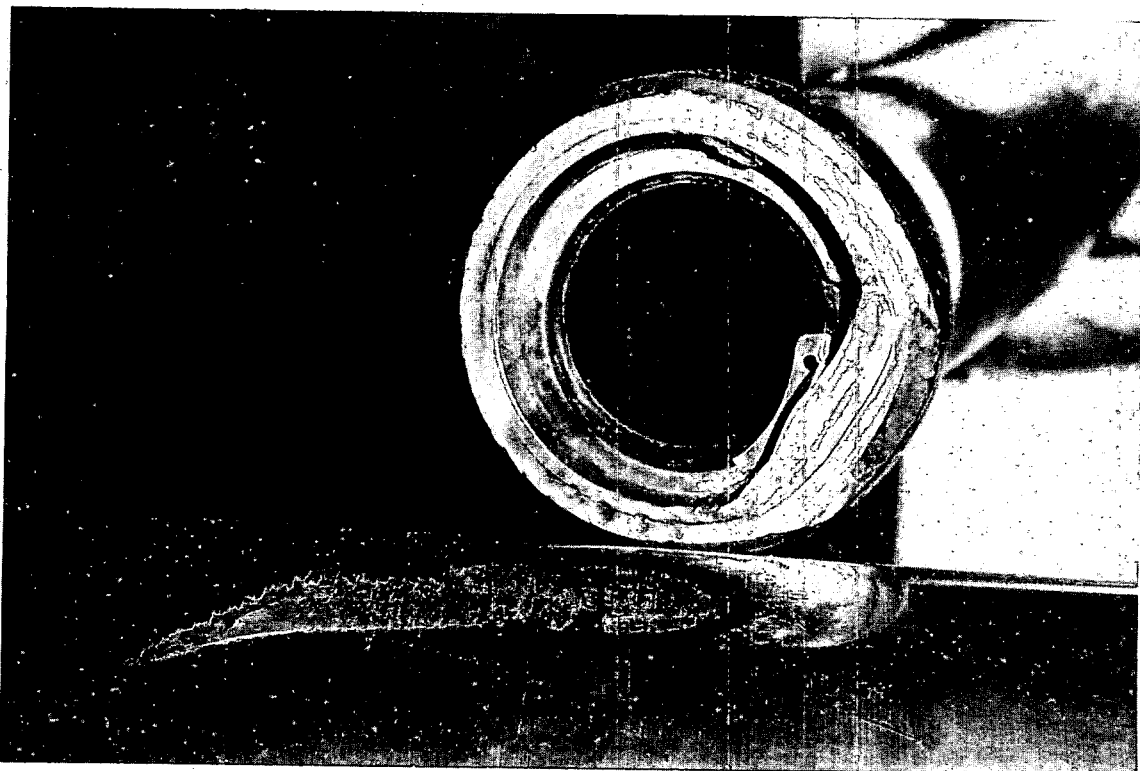


Figure III-20, Shield Plug #1, Matching Imprint of Shield Plug Body #7 with Imprint on End of Guide Tube, Shield Plug #1

The pinion gear ball bearing was badly corroded and frozen in place. Two of the pinion gear teeth were badly dented; the chrome plate coating, however, remained intact.

The frame of the back-up roller was badly dented by impact in a localized area.

The remaining components of the rod assembly, that is the fractured lower section of the gear rack, the extension rod, the connector rod and connector rod housing, were intact in the pressure vessel and attached to the control blade. This remaining assembly was removed from the pressure vessel by sectioning through the connector rod and housing just above the gripper fingers.

A part of the gear rack nut with a fractured section of the threaded stud and lock pin in place was recovered from the fan room floor. The washer was not recovered (Figure III-23).

1.2.3. Shield Plug Assembly #4

Shield plug #4 was imbedded in the ducting in the fan room floor (Figure III-24). There was slight flange deformation on one side caused by impact with a sharp rectangular object. This plug was a replacement for the original plug #4, which was damaged during the shutdown period prior to the incident. The surface appearance of the replaced plug was bright while the surface appearance of all the other recovered plugs showed dark discolorations which are attributed to surface oxidation under the environment of normal reactor operations.

The spring housing was undamaged although its surface had sustained severe scratches. The plug body was also undamaged although small superficial surface marks were detected.

The guide tube was deformed, deflected and had experienced severe collapse. No external impact marks were detected.

Neither gear rack nor extension rod was recovered with the plug assembly. These components were removed from the pressure vessel without difficulty. The control rod blade was a dummy with a stainless steel plug at the upper end of the connector rod. The upper



Figure III-21, Upper Section Retained in Shield Plug #3 and Matches Perfectly with Lower Section Recovered from Fan Room Floor

U-5031-9

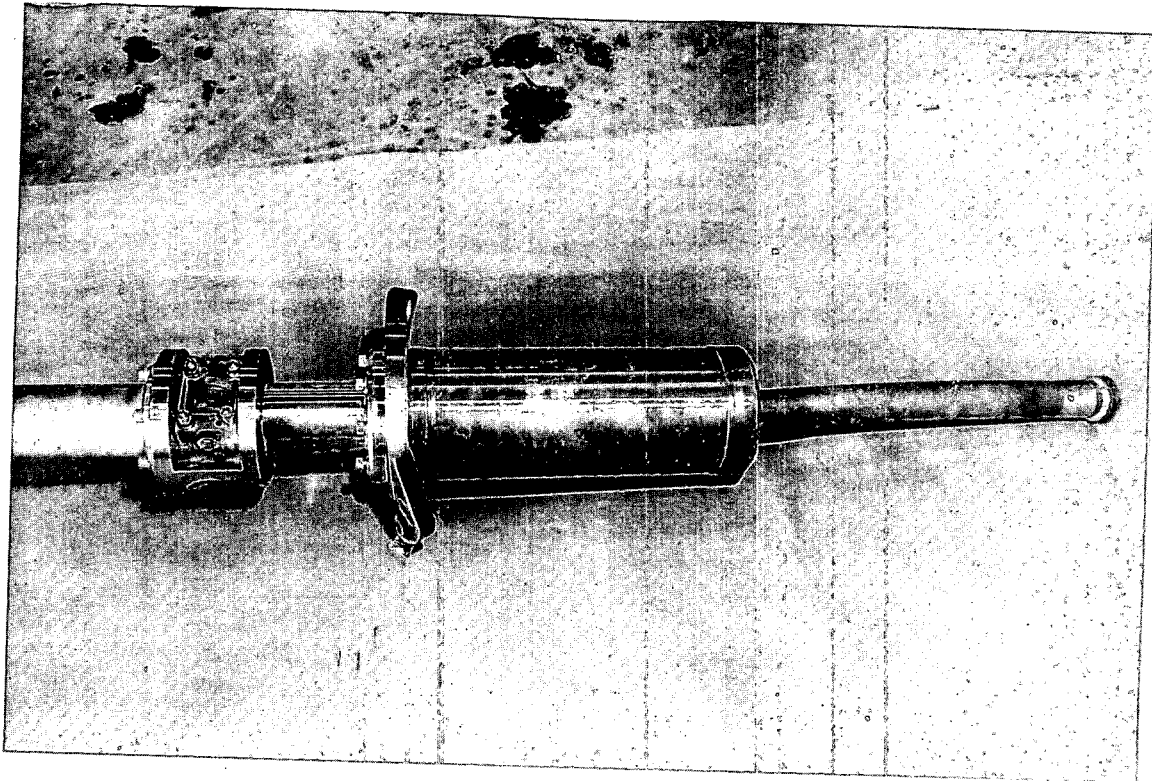


Figure III-22, Shield Plug #3, Showing Deformation of Flange and Collapse of Guide Tube

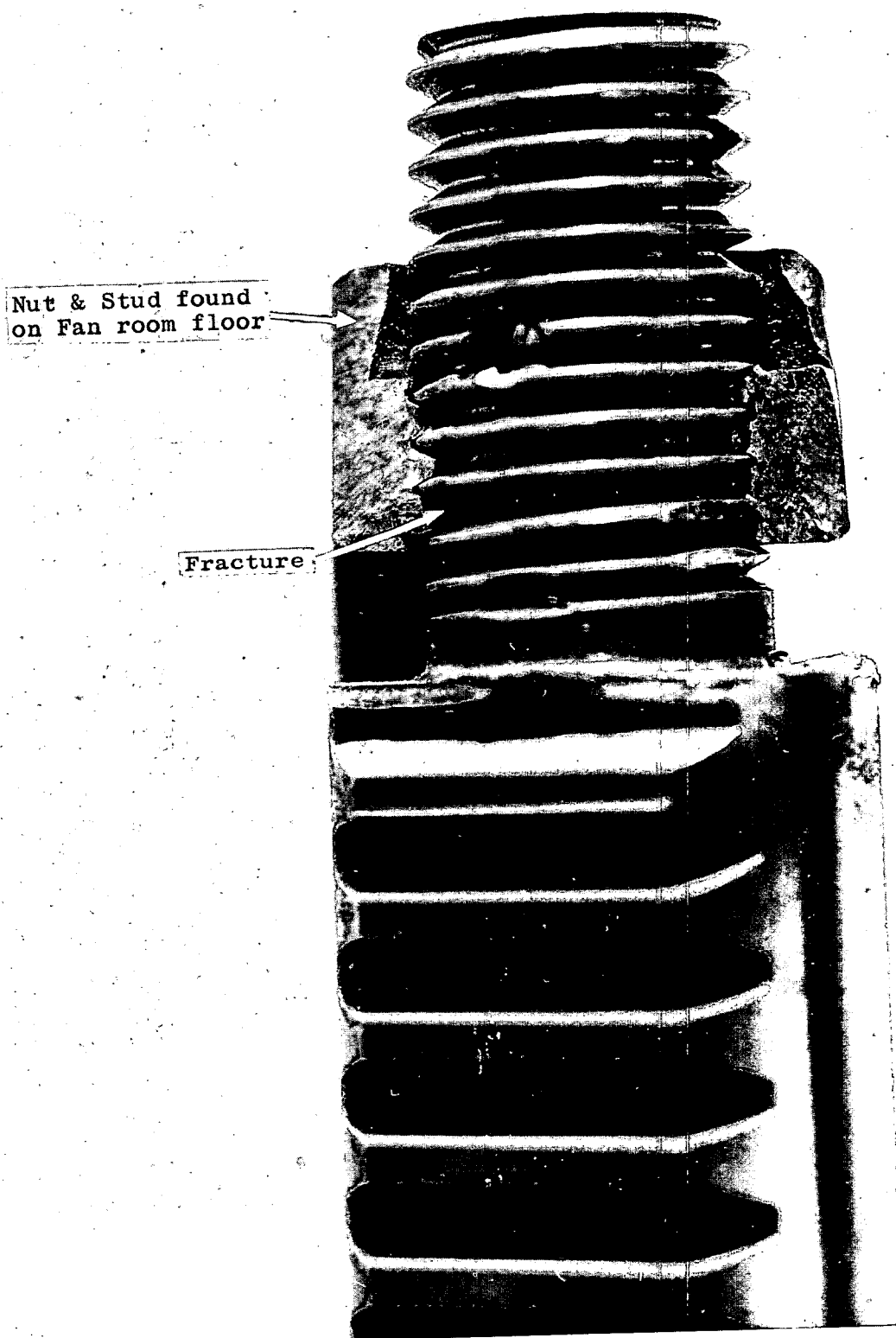


Figure III-23, Shield Plug #3, Mating of Fractured
Nut Retained in Stud with Fractured End of Gear Rack

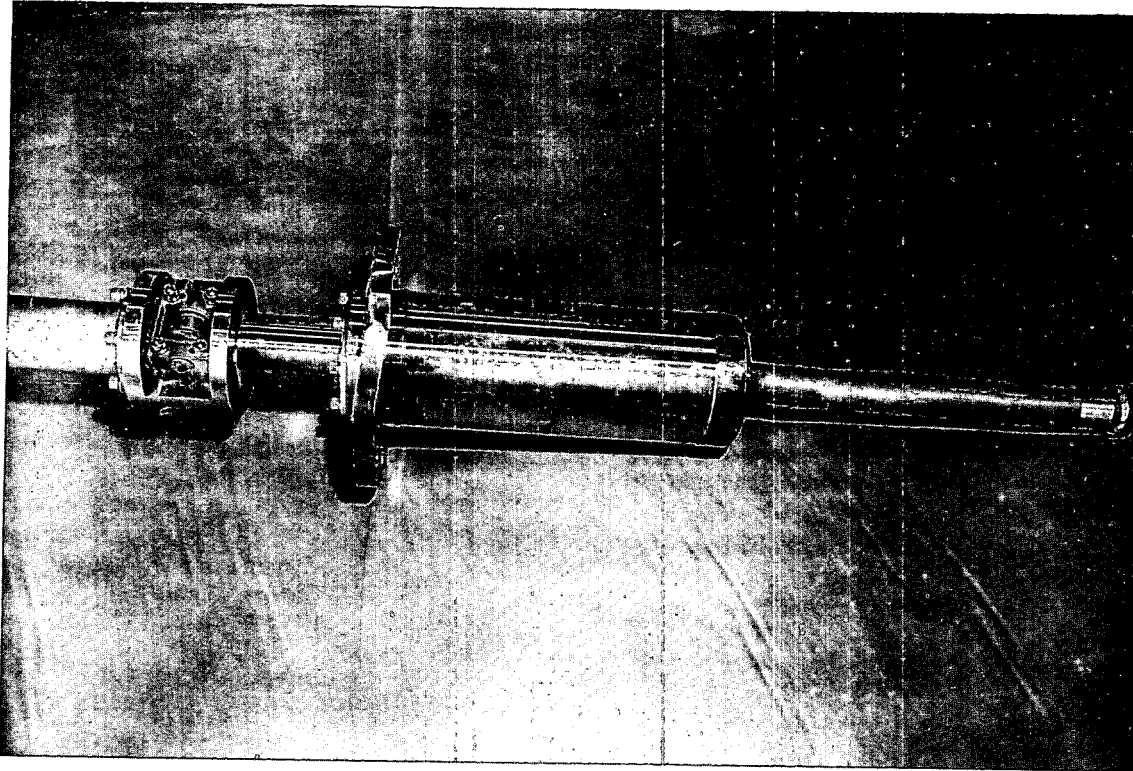


Figure III-24, Shield Plug #4, Showing Flange Deformation and Guide Tube Collapse

U-5001-150



Figure III-25, Number 5 Guide Tube and Rack Shown in Same Relative Position as when Received. Note teeth imprint marks and gouged metal.

III-25

threaded end of the rack was broken off (impact tensile) about half the distance along the threaded length. Some indentations were detected on the gear rack teeth and sliding marks visible along the curved sides of the entire length of rack.

The rack and extension rod were bent at their junction in the plane of the rack flats and a concentration of stress cracks was detected in the extension rod two to five inches from its upper end. A second concentration of stress cracks appeared at the lower end of the extension rod centering about the drill hole. The two hollow pins at the lower end of the connector rod were sheared in the same manner as in the other rods.

The dummy stainless steel plug was heavily coated with a scum-like deposit on a line which appeared to indicate a "water level" line similar to that observed on the shrouds and fuel elements.

The spring housing was intact and in good condition. The pinion gear bearings were made from stellite material and showed normal amount of oxidation and corrosion; otherwise, the condition of the component was excellent.

There were deep indentations in one pinion gear tooth. This component was in excellent condition otherwise.

The gear rack nut and washer were not recovered and identified.

Elongation of the extension rod guide tube was measured at 3/16 inch.

1.2.4. Shield Plug Assembly #5

This plug assembly with the bell housing installed was the only assembly bolted down and it remained in its nozzle during the excursion. This assembly was carefully removed from the reactor head. The rack, extension and connecting rod came with the shield plug, the rack being firmly bound in the guide tube. The connecting rod roll-pins were sheared at the gripper assembly of the rod which connects to the cruciform control blade assembly.

Investigation showed that the guide tube was collapsed along the greatest part of its length. The tube was cut from the plug circumferentially at the weld, and the gear rack, extension rod, and connector readily removed from the plug body. The guide tube was sectioned longitudinally at two positions 180° apart and removed from the rod. Impressions on the gear rack and tube definitely established the point of seizure which was 17-1/2 inches from the end of the guide tube. The seized area was approximately 3 inches long (Figure III-25).

Several rack teeth imprints were discernible on the interior surface of the sectioned tube. A gouge mark indicated downward travel of the rod, with respect to the tube, of at least 3/4 inch. Burred metal on the curved side of the rack extended continuously for approximately 5 inches from the shoulder of the rack. No scouring or sliding marks were detected on the extension rod below the extension guide tube (relative to the position at the time of recovery).

The tip-end of the gear rack was measured to be 6-3/4 inches above the shoulder of the spring housing when firmly held by the collapsed guide tube. Normally the tip-end is approximately 3/4 inch above the spring housing when in the scram position.

No severe damage was sustained to the gear teeth. However, there were many transverse stress cracks on the flat side of the rack. These cracks are similar to those observed on #3 and #9 racks.

Two pinion gear teeth had received an impact from the gear rack teeth while traveling up. No severe damage was incurred.

Chipping of the chrome plate along side of the gear teeth is attributed to normal wear.

The seal housing was connected to the bell housing which was bent slightly downward. The heavy coupling connector was sheared off from the seal housing shaft and was recovered from the operating floor.

The spline shaft in the bell housing was fractured by a torsional shear. The end remaining on the gear was badly burred due to rotation in the shoulder of the splined coupling.

Many cracks were detected in the splined shaft in the area of fracture.

The pinion gear ball bearings were carbon alloy steel. They were badly corroded and bound in the races. After decontamination the bearings moved freely, but pitting had occurred on all surfaces.

1.2.5. Shield Plug Assembly #7

This shield plug was ejected from its nozzle and was embedded into the bottom of the fan room floor between two I-beams in an approximately vertical position over nozzle #6. The plug was recovered without gear rack or extension rod (Figure III-26).

As this plug was one of the first recovered and brought to the Hot Shop for examination, beta and gamma radiation profiles were taken along the longitudinal axis. The contact radiation level varied from approximately 25 R/hr at the spring housing to 2 R/hr at the stellite bearing section at the lower end of the guide tube. The beta radiation contributed from 50% to 90% of the total.

The shield plug flange had sustained an impact-induced permanent set deformation on one side which had been attributed to the flange striking an overhead I-beam (Figure III-26). Examination of the plug surface showed an impact abrasion mark (Figure III-20), which was made by the plug body striking the end of the shield plug #1 guide tube during its flight.

Measurements showed that the extension rod had been elongated from the 18-1/2 inches nominally specified to 18-11/16 inches - an increase of 3/16 inch.

Visual examination showed that the guide tube had been deformed, necked down and partially collapsed. The tube showed no damage due to external impact.

At one period of time during the incident the extension rod was held in the guide tube as indicated by a macroscopic examination of its interior surfaces. During this examination it was determined that the travel of the rod with respect to the plug was downward. There was no indication of any upward travel of the rod.

The spring housing had incurred severe damage on the top face (Figure III-26). This damage is attributed to the use of a heavy sledge hammer used to dislodge the shield plug during Phase I operations.

The inner helical spring was easily removed and had sustained no damage. The outer helical spring was badly distorted and bound in the housing.

No damage was detected to the pinion gear housing assembly or to the pinion gear other than normal operating wear.

The back-up roller housing and graphite bearing were undamaged and in good operating condition.

Both ball bearings assemblies were badly corroded and bearing bound in the assembly. Decontaminating solutions partially freed the bearing, but not sufficiently for useful operation.

The control rod assembly was recovered from the pressure vessel with the gear rack, extension rod, connecting rod and connecting rod housing intact. The connecting roll-pins had sheared from the gripper assembly, freeing it from the cruciform blade assembly. The upper threaded end of the gear rack had retained the stripped threads of the nut. Neither washer nor nut was recovered.

The extension rod and connecting rod were bent at an angle of approximately 3° . The threaded section joining the rod was not broken though but had sustained severe cracking. There was no detectable indication of any surface damage to the components other than minor superficial abrasions.

1.2.6. Instrumented Flange-Nozzle #8

The instrumented blind flange recovered from the operating floor was examined and the following notations observed:

Three of the bolt holes were badly distorted and general deflection occurred across the face diameter of the flange. Sharp imprints were made by the flange nuts around the bolt holes. The sharp imprints indicate that the majority of the flange nuts were not overstressed prior to the incident. There is an apparent over stressing of two of the flange nuts as indicated by severe burring of the contact surfaces.

All of the 8 stud threads holding the flange down were sheared. Recovery of 6 of the 8 nuts showed that in each case the sheared thread of the stud was retained in the nut grooves (Figure III-31). The remaining two flange nuts have not been recovered.

1.2.7. Table III-I is a summary of the control rod components examined following the incident, and is self explanatory.

1.3. Reconstruction of the Fan Room Floor and the Pressure Vessel Head

1.3.1. General

The pressure vessel head and the fan floor section directly above the vessel were reassembled. The purpose of this reconstruction was to identify the damage caused by the shield plugs as they were ejected during the incident and to determine the height to which the pressure vessel rose. The sequence of events which took place during the incident was analyzed by matching up deformation marks caused by the shield plugs during their trajectories. This analysis appears quite complicated, but positive identification of the impact areas clearly established the trajectories of the plugs and the sequence of events.

Figure III-28 shows the fan room floor superimposed on the pressure vessel head. The dotted lines indicate areas where the impact of the plugs deformed the ceiling beams and punctured the fan room floor. The solid line on the plugs indicates areas of plug deformation caused by the impact.

Figure III-29 shows a reconstruction of the reactor head and the plug assemblies. Figure III-30 shows the location where the plugs hit the ceiling. Plugs #1, 3, 4, 7, 8 (blind flange) and 9 were ejected from the nozzles of the pressure vessel head as projectiles by water hammer

TABLE III-I - SUMMARY OF CONTROL ROD COMPONENTS FOLLOWING INCIDENT

	#1	#3	#4	#5	#7	#9
Control Blade - Location	Bound in shroud at normal scram position.	Bound in shroud at normal scram position.	Bound in shroud near normal scram position.	Bound in shroud 1" below normal scram position.	Bound in shroud at normal scram position.	Bound in shroud at 20" withdrawn position.
Damage	Bent nearly flat	Bent nearly flat	Little damage Dummy rod with aluminum blade	Bent Blade had moved 1-1/4" after impact.	Bent nearly flat	Bent nearly flat. Extension cross bent where it emerges from shroud.
Shroud - Location	Pushed outward against thermal shield	Pushed outward against thermal shield	Pushed outward against thermal shield	Pushed outward against thermal shield	Pushed outward against thermal shield	Lying across other shrouds
Damage	Collapsed around blade. Bent nearly parallel	Collapsed around blade. Bent nearly parallel	Collapsed around blade. Little damage	Collapsed around blade. Bent	Collapsed around blade. Bent nearly parallel	Collapsed around blade. Bent and distorted. Impact mark on top, on one edge.
Connecting Rod - Location	In vessel attached to control blade.	In vessel attached to control blade.	Inside reactor vessel.	Inside vessel. Attached to extension rod.	Inside vessel. Attached to extension rod.	Inside section recovered from vessel trench.
Damage	None	None	Broken at fingers of ball joint connection	Broken at fingers of ball joint connection.	Broken at fingers of ball joint connection.	Broken at fingers of ball joint connection.
Extension Rod - Location	In vessel attached to connecting rod.	In vessel attached to connecting rod.	Inside reactor vessel. Attached to rack and connecting rod.	Inside vessel. Attached to rack and connecting rod.	Inside vessel. Attached to rack and connecting rod.	Seized inside shield plug guide tube.
Damage	Broken near stud connection to rack.	None	None	None	None	Bottom stud broken
Rack - Location	Protruding from nozzle. Attached to extension rod.	Bottom in nozzle, attached to extension rod. Middle on fan room floor.	Inside pressure vessel. Dummy weight inside active core	Inside vessel. Attached to extension rod.	Protruding from nozzle. Attached to extension rod.	Bottom section inside plug. Top section in fan room.
Damage	Top stud broken off.	Top in plug. Broken in 2 places. Top stud broken	Top stud broken. Still attached to extension rod.	Bound by collapsed guide tube.	Stripped nut threads in the rack stud threads.	Broken. Top of stud found in handling tool which was embedded in fan room floor.
Washer - Location (only 4 washers have been recovered, 2 of these unidentified)	Unidentified	Unidentified	Unidentified	In place on rack	Unidentified	In place on rack
						Bent downward.
Top Nut - Location	Not located	2/3 found on fan room floor.	Not located	In place on rack	Not located	In place on rack
Damage		Broken; stud inside Lock pin in place		Undamaged during incident	Threads stripped	Essentially none
Shield Plug - Location	Embedded in end section of condenser.	Lying on fan room floor.	Embedded in fan ducting in fan room.	In pressure vessel head with bell housing installed.	Embedded in ceiling with victim	On top of pressure vessel head.
Damage	Spring housing severely squashed. Guide tube collapsed 3" from top. Impact mark on bottom of guide tube.	Flange bent downwards on opposite sides by 1-1/2" and 1/2". Guide tube collapsed 3" from top.	Slight flange deformation at one location. Severe collapse on guide tube 6" from top.	Guide tube collapsed near upper end. Seized rack. Bell housing and seal housing bent downward.	Flange bent 1" downward at one location. Guide tube collapsed rather uniformly.	Flange bent downwards 1-1/2" and 1/2" on opposite sides. Guide tube collapsed 3" from bottom and seized extension rod. Also collapsed near top.

Remarks (#8 blind flange was ripped off of studs (stripped nuts) and found behind turbine)

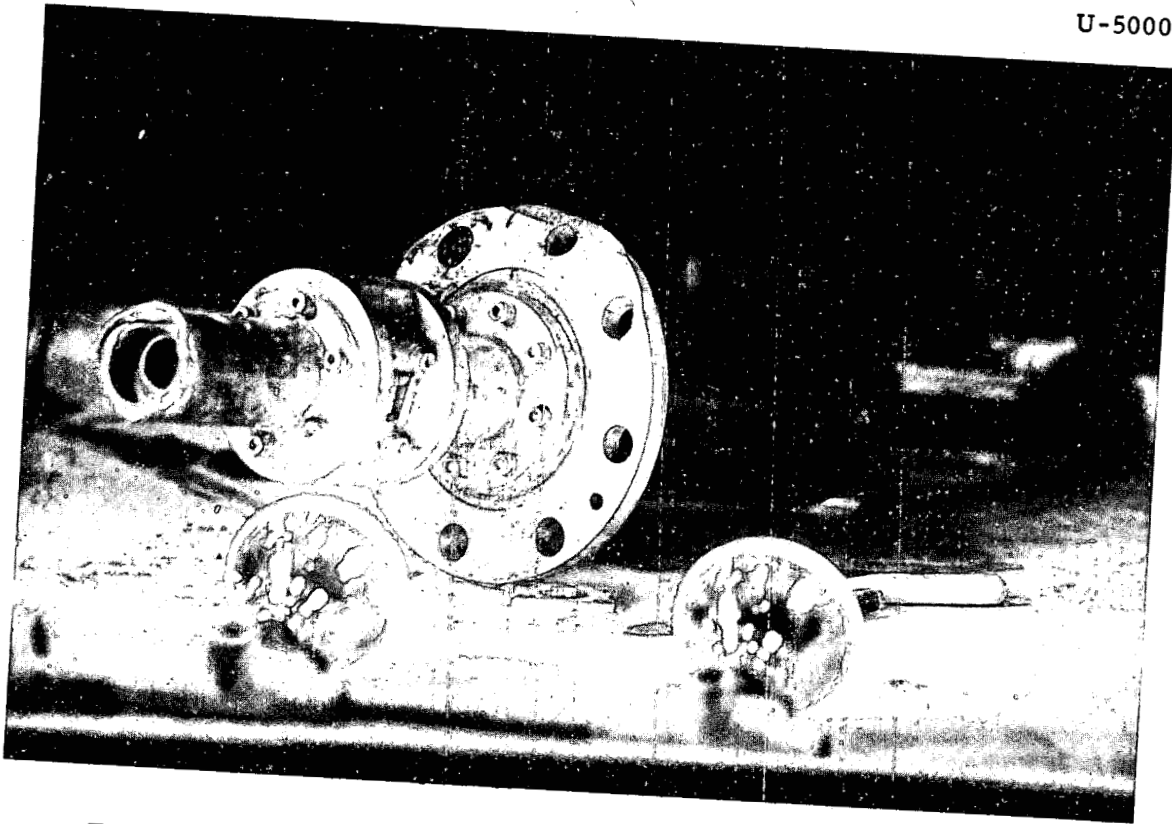


Figure III-26, Showing Spring Housing and Flange Deformation and Guide Tube Collapse



Figure III-27, Nut from Instrumented Flange #8, Showing Sheared Stud Threads Retained in Nut.

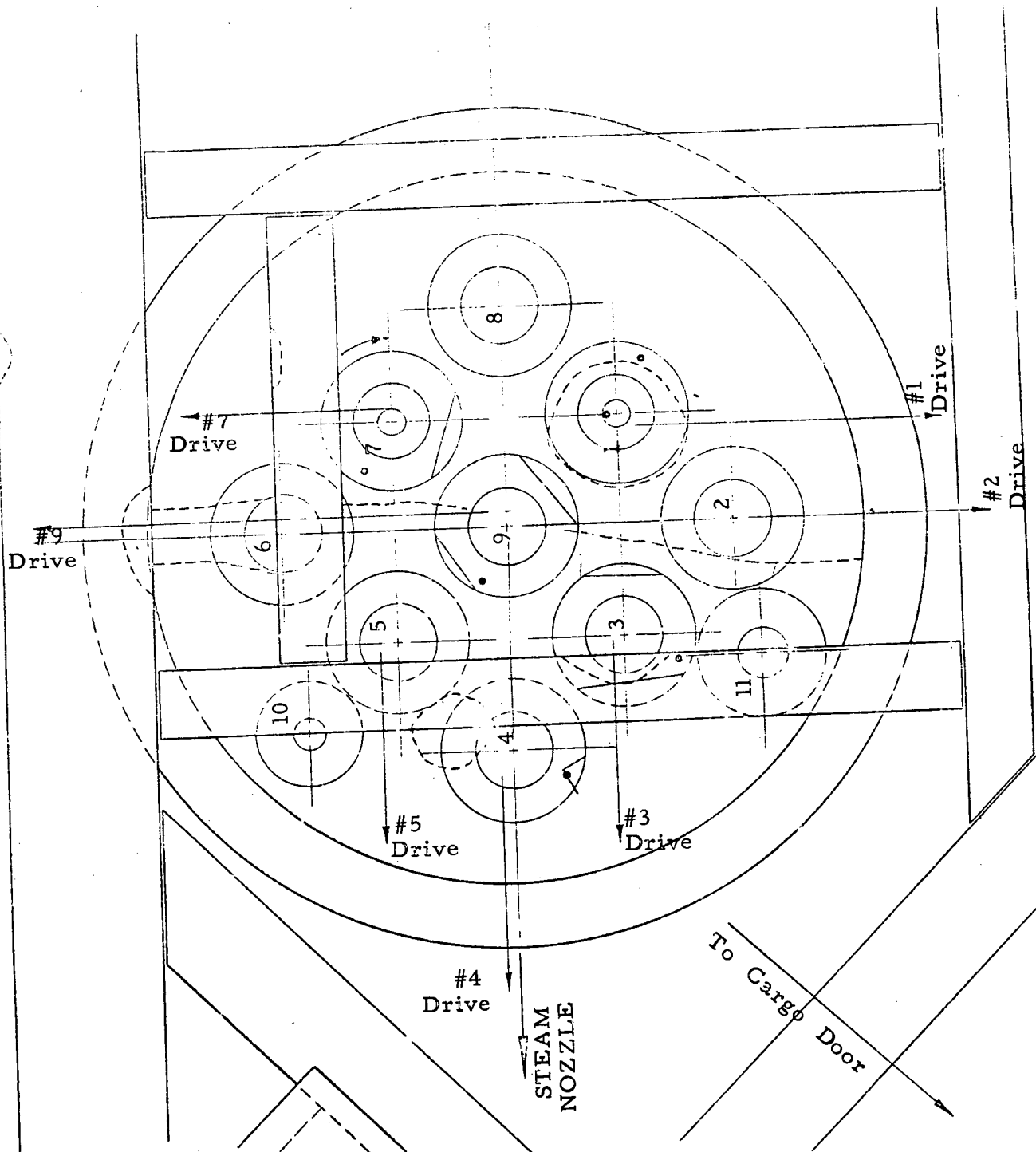


Figure III-28 Superimposition Fan Room Floor Section on Reactor Head.

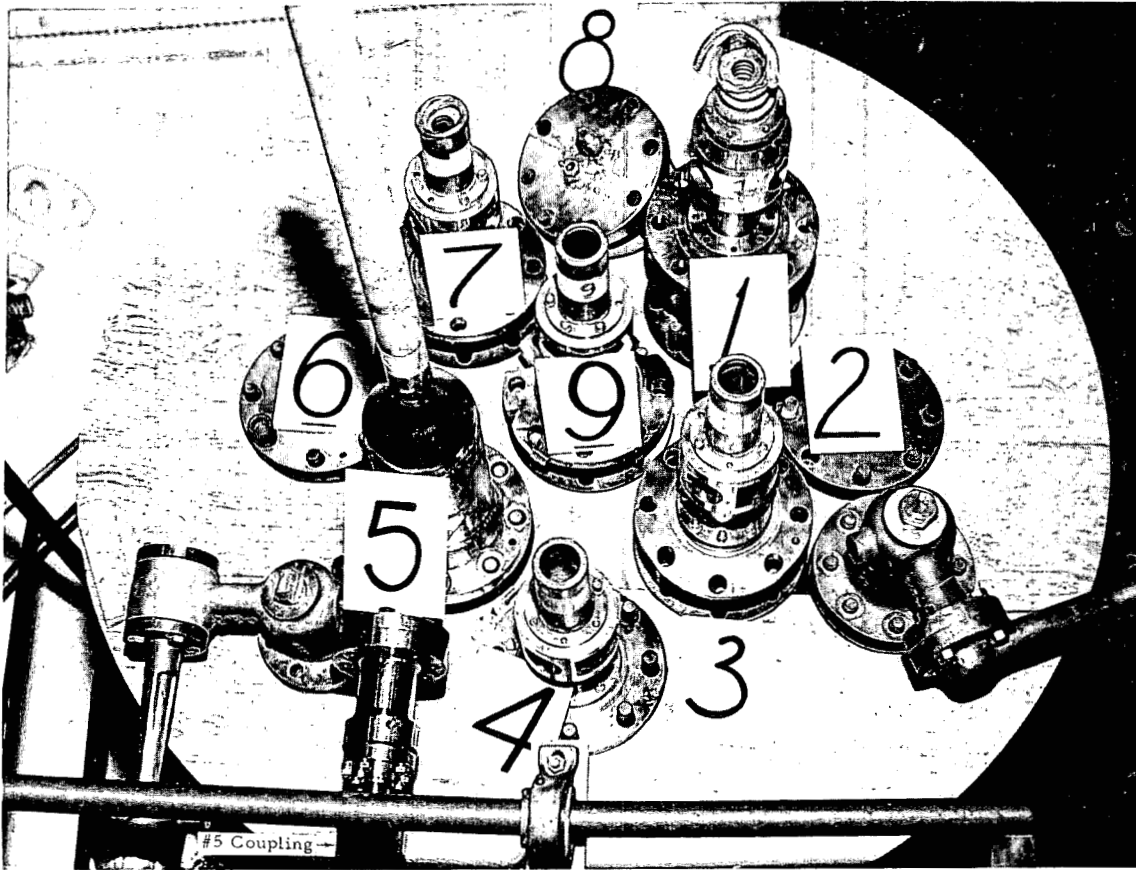


Figure III-29 Reconstruction of reactor head and plug assemblies



Fig. III-30, Section of fan room floor, showing areas of damage.

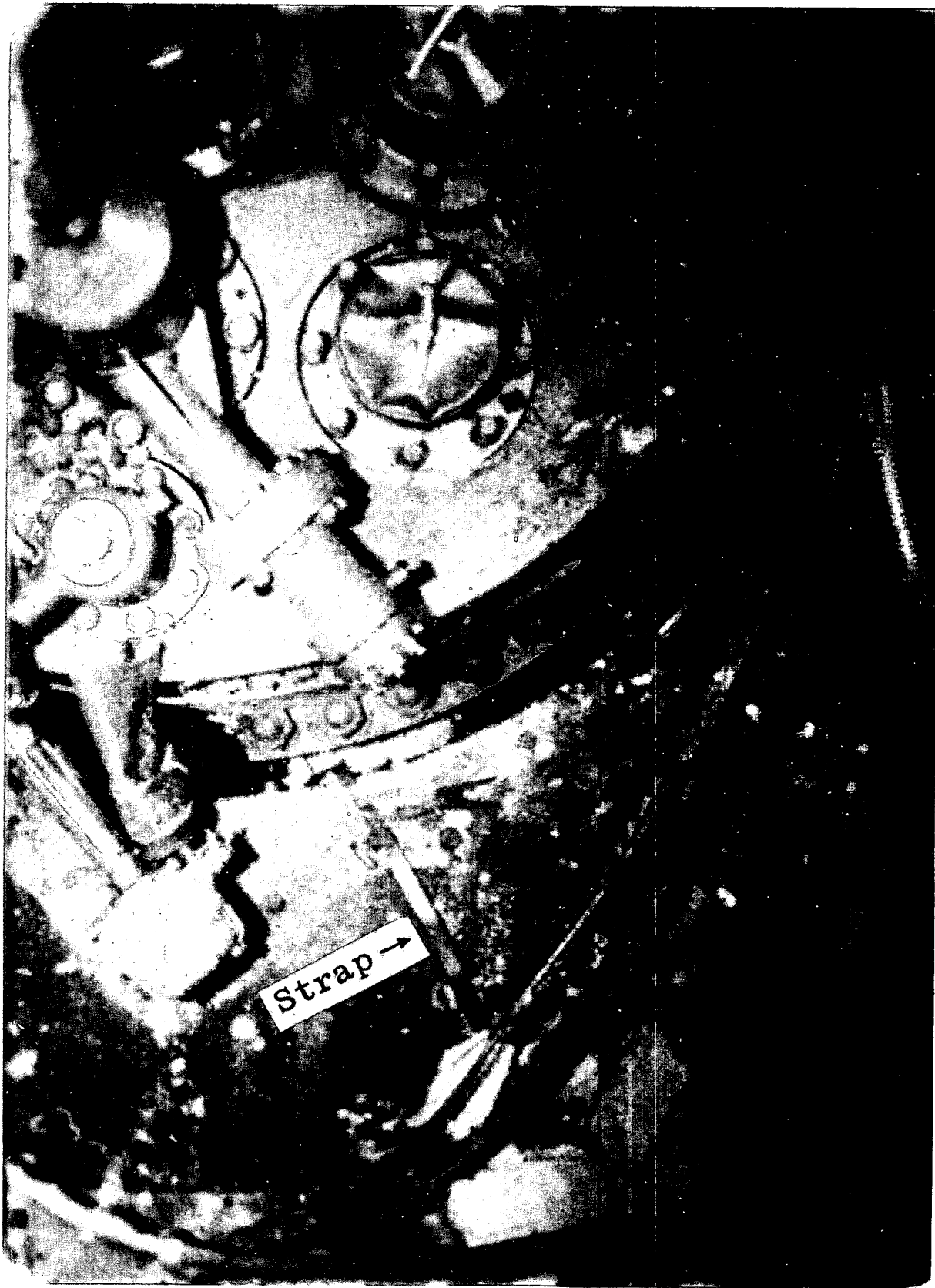


Fig. III-31, View of vessel head.

pressure caused by the incident. Plugs #3, 5, 6, 10 (liquid level nozzle) and 11 (auxiliary nozzle) remained in position. The conclusions drawn from the reconstruction and the events which took place are discussed below.

1.3.2. Shield Plug #1 Trajectory

Plug #1 shot straight up, pierced the fan room floor, hit the bottom of a condenser, and remained imbedded in the floor. The stellite bearing at the end of the guide tube on plug #1 was hit by the #7 shield plug body. Indentation marks found on both plugs match perfectly, as shown by Figure III-20. Plug #1 would have reached the ceiling first because #7 plug carried an operator and thus had its in-flight mass doubled. Subsequent tests, conducted on a 1/4 scale model at the Aberdeen Proving Ground in Maryland, verify this statement.

1.3.3. Shield Plug #3 Trajectory

Plug #3 shot straight up, glanced off a 6 inch I-beam and tore a hole through the ceiling. It was found lying on the fan room floor. The I-beam was badly deformed and the indentations match the deformation observed on the flange of #3 plug.

1.3.4. Shield Plug #4 Trajectory

Plug #4 was ejected straight up, collided with a 6 inch I-beam and tore a hole in the fan room floor. Deformation on the I-beam matches the markings found on the body of the plug. This plug was found to be lodged in the fan ducting.

1.3.5. Shield Plug #7 Trajectory

Plug #7, carrying the body of an operator, was ejected straight up from the pressure vessel nozzle. When the plug was free of the nozzle, it was tilted slightly by off-center forces and collided with the end of the guide tube on plug #1, which was already in the ceiling. This collision further deflected the plug and it glanced off an 18 inch I-beam and lodged in the ceiling. The deformations on the I-beam and the #7 plug flange coincide.

In an earlier analysis, the #7 plug was believed to have rotated 180° while in flight, perhaps due to the rotation imparted by the victim. The reconstruction analysis, however, indicated that the plug had been placed in the vessel 180° out of phase. If the drive mechanism had been assembled, this error would have been discovered. The Aberdeen tests indicated that the plugs used in the experiment did not rotate during ejection.

1.3.6. Flange #8 Trajectory

An instrumented flange cover had been secured on nozzle #8 by nuts on eight studs. This cover was blown off and later found behind the turbine -

generator unit. The threads of the studs were stripped and the nuts were ejected as missiles. One of the nuts hit a 6 inch I-beam leaving the impression of its knurl marks. Two of the eight studs were bent in the direction that the flange cover was blown off. Two electrical conduits were attached to the 18 inch I-beam at the point of impact. The I-beam was slightly deformed and the two conduits were flattened. Two impressions on the flange cover were observed which coincided with the impressions on the conduit.

1.3.7. Shield Plug #9 Trajectory

Plug #9 was ejected straight upward. It struck the ceiling and fell back on top of the vessel head where it was found. Deformation was observed on opposite sides of the plug flange. These deformations coincided with the damage observed on the ceiling. The flange was deformed on one side when it struck the corner of a condenser located on the fan room floor. The other side of the flange struck a structural angle curling a chip-like piece for a distance of four inches.

1.3.8. Pressure Vessel Rise

The pressure vessel rose out of its support cylinder and sheared the pipes connected to the upper and lower spray rings, purification system and steam separator. The drive shaft coupling on the #5 seal housing collided with the drive shaft on the overhead crane. The coupling was sheared and the crane drive shaft was bent approximately 3 inches (impact marks were lacking). No evidence could be found to indicate that the pressure vessel head had collided with the ceiling. When the fan room floor was lowered to the vessel head, the #5 bell housing was clear of any obstruction and was able to protrude through a hole in the floor torn by #3 and #9 plugs.

The pressure vessel was determined to have risen 9 feet 1-1/2 inches plus or minus one inch. Other pertinent facts substantiate the pressure vessel rise. The drive shaft coupling was found lying in front of the instrument panel in the operating room. As there were shield blocks between the vessel head and the instrument panel, the coupling would have had to shear when the vessel head was above this shielding. Also an insulation banding strip (Figure III-31) and a vessel head gasket leak-off line were found on the operating floor, which would not be possible without an elevated vessel. During the Aberdeen tests the vessel was also observed to rise during the explosion.

1.4. Steam Baffle, Spray Rings, Stillwells, Reactor Head

1.4.1. Steam Baffle

The steam baffle plate (Figure II-33) was recovered from the pressure vessel. It had sustained impact shear fracture along the entire length of the fillet weld. The plate was 19" long x 18" wide x 5/16" thick and was

fabricated from 304 stainless steel. The plate had been collapsed outward and toward the pressure vessel wall. The plate was deformed along the upper and bottom edges (Figure III-32). One of the support lugs was sheared from the plate and was found lodged between the vessel flange and reactor head. This lug was recovered after the reactor head was removed.

The side of the baffle plate facing the wall of the pressure vessel bore an impression of the four inch steam outlet pipe, caused by impact of the plate against the vessel wall. No sliding or scouring marks have been detected. A second impression is an outline of larger diameter and approximately 1-1/4 inches above the first impression. The second marking may have been created when the vessel fell back into its support cylinder.

The nominal position of the center line of the steam pipe is 4 inches from the horizontal centerline of the bottom fillet weld of the baffle plate. The center of the pipe's impression on the plate is approximately 4-1/2 inches above the centerline of the weld. The center of the deepest collapse of the plate is approximately 5-1/2 inches above the centerline of the weld.

All four drain holes in the lower edge plate were distorted, the center two the most severely.

1. 4. 2. Spray Rings

The upper spray ring was completely collapsed and had torn away from the pressure vessel water inlet line at the welded T-joint. The break was one of impact-shear. Figure II-33 shows the upper spray ring settled down in the lower section of the pressure vessel. The lower spray ring had not collapsed but was broken at the welded T-joint and elbow section of the spray ring feed pipe. The fracture in the welded section was due to impact on underside of the elbow. Figure II-33 shows a section of the lower spray ring displaced partly above the core section and reveals the severed section.

1. 4. 3. Stillwells

The liquid level stillwell pipe installed in nozzle #10 had collapsed and was firmly bound in the nozzle. The collapsed length from the underside of the reactor head to the line was 36 inches, indicating the height of water in the pressure vessel. The pipe was sectioned a distance of 8 inches from the underside of the reactor head and the remaining section was transferred to the RML. Figure III-33 shows the cut-off section of the stillwell pipe, the collapsed end and the transition area between the collapsed tube and the undamaged tube.

The compensating liquid level float was bound in the stillwell pipe and can be seen in the pipe where it was sectioned (Figure III-34).

A force of 12000 lbs. was required to relieve and remove the upper section of the pipe which was bound in the nozzle.

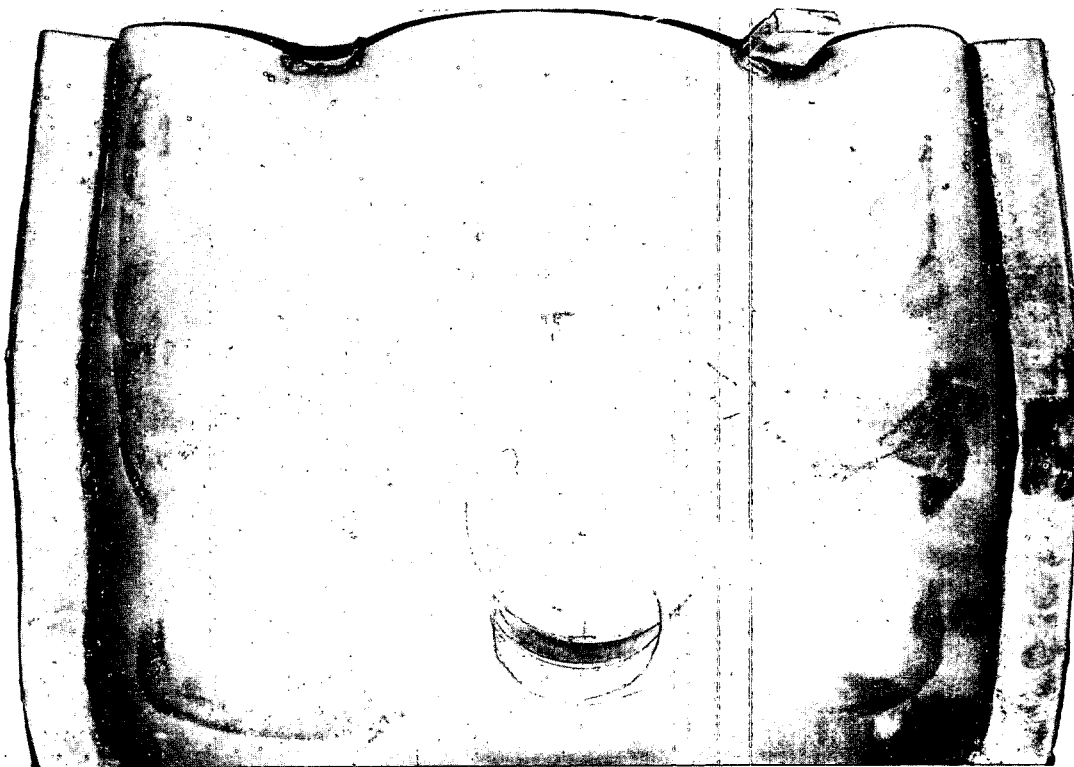


Fig. III-32, Baffle plate showing areas of impact and deformation.

U-5001-144

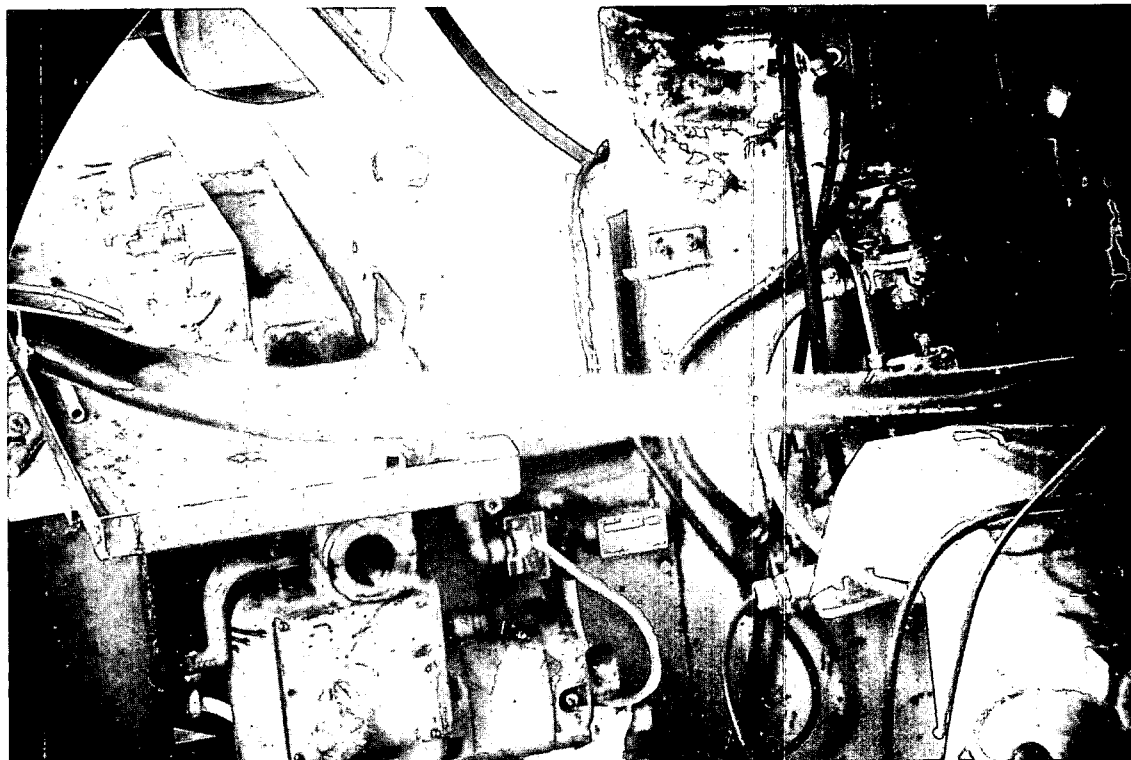


Fig. III-33, Collapsed stillwell pipe.

The auxiliary stillwell was broken off from its bracket and had suffered complete collapse a distance of 36 inches from the underside of the reactor head (Figure II-33). Also the guide pin support which was welded to the vessel above the thermal shield was deformed upward and the fillet weld partly broken (Figure III-35). Shearing of the welds was attributed to the thermal shield striking the lower spray ring and its striking the underside of the support bracket.

1.4.4. Pressure Vessel Head

The pressure vessel head was decontaminated using standard decontaminating solutions and procedures. Each bolt hole had a high radiation field ($> 5R/hr$ at contact) primarily due to retention of contamination in the heavy corrosion scale visible in these holes. Analysis of the scale showed it to be an anti-galling compound used on the threaded studs. Most of this scale was removed mechanically using a wire brush and emery paper. Removing the scale reduced the radiation level low enough so direct observation could be made.

The bolt holes appeared to have been elongated, but later investigation indicated that in the manufacture each bolt hole in the head bolt circle had been re-drilled to provide proper mating with the stud bolts. All inner surfaces of the holes at the underside of the head toward the center of the vessel showed a substantial metal upset due to bearing of the stud bodies.

The gasket seating surface was smooth and undamaged except for gouge marks caused by the steel wedges pounded in during the head removal operation.

The #2 and #6 dummy plugs were easily removed from the nozzles. The removal of the nuts from the nozzle flange studs was accomplished without difficulty.

Dye penetrant inspection of all the nozzles in the reactor head indicated many vertical stress cracks on all exterior surfaces of nozzles which had sustained bulging or deformation. The cracks did not penetrate through the nozzle walls. The dye penetrant inspection of the deformed or bulged nozzles did not indicate stress cracking on the interior surfaces.

1.5. Pressure Vessel Bulges, Nozzle and Flange Deformation and Studs

Figure II-30 shows the pressure vessel after it was removed from the SL-1 building and transported to the ANP Hot Shop. The bottom of the vessel, after the pan was removed, is shown by Figure II-31. The reactor head and the pressure vessel flange is shown in Figure III-36. Note the magnitude of the bulge near the vessel top and the extent of the flange tilting. The bulges in the lower regions of the vessel, (Figure II-30) were caused by the large pressure increase in the core

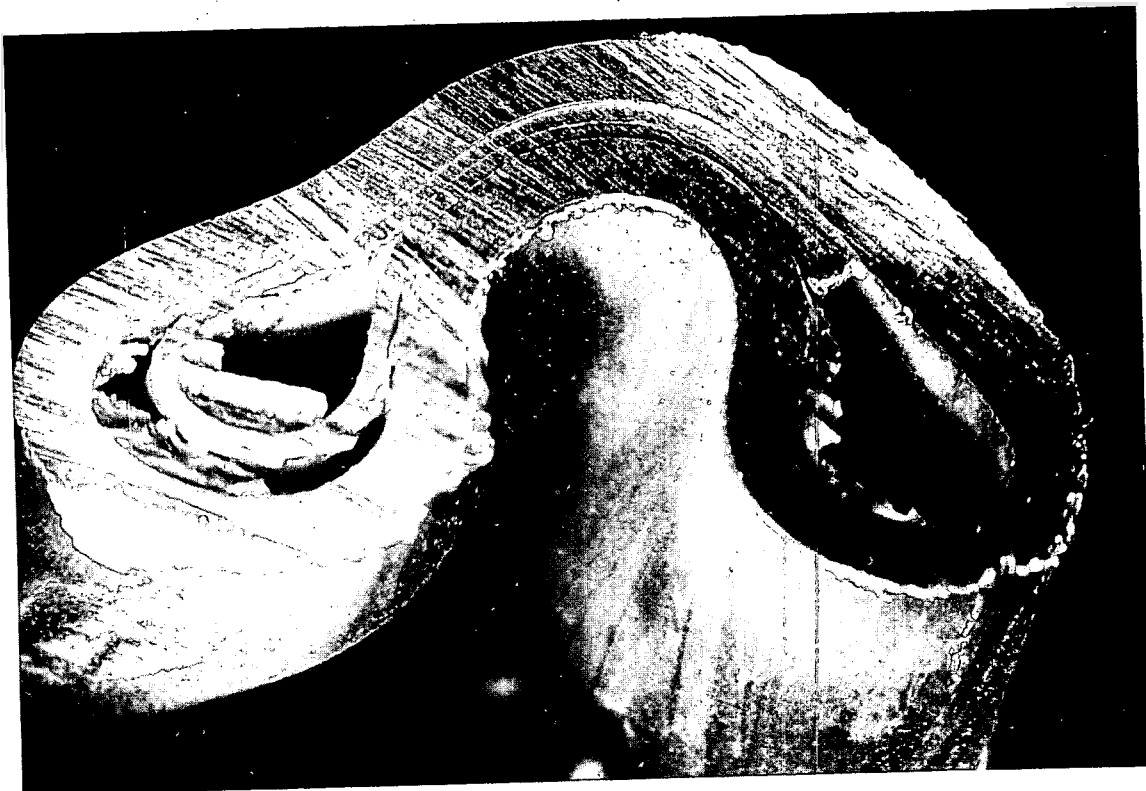


Fig. III-34, Cross-section of stillwell pipe.

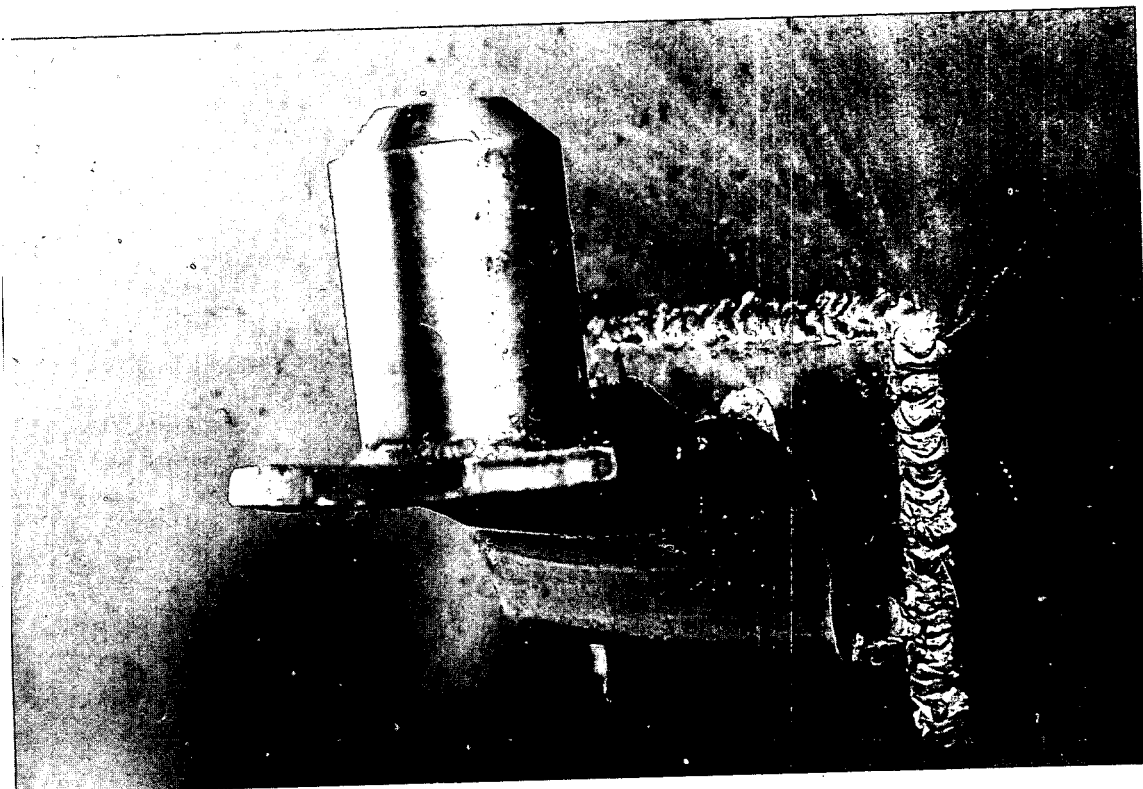
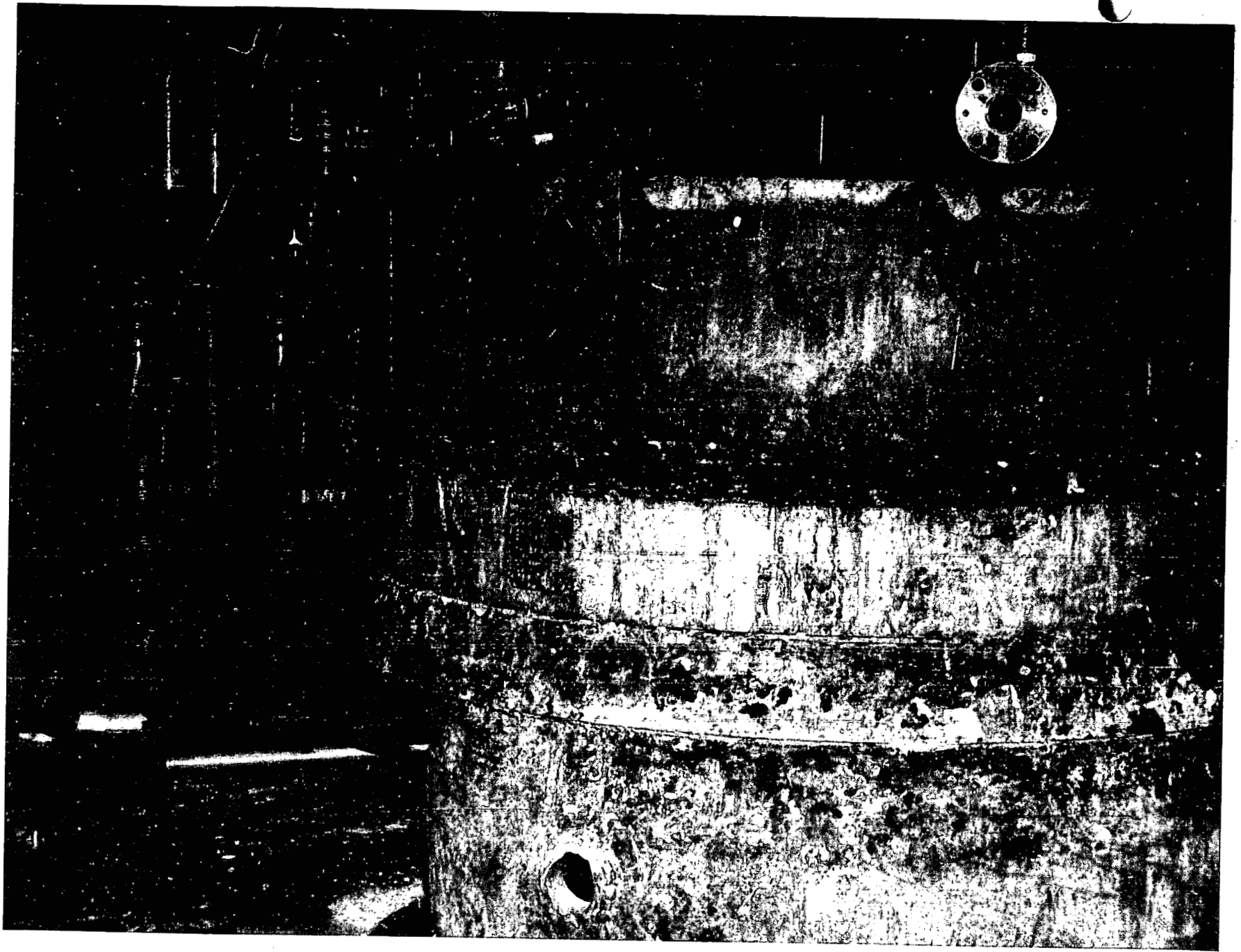


Fig. III-35, Fractured weld, auxiliary stillwell guide pin support bracket.

III-41



U-5073-15

Figure III-36, Deformation of Flange and Vessel

section during the excursion and the large bulge near the flange at the top resulted from the subsequent water hammer.

In Figure II-32, the tilting of the top flange can be seen. This flange was tilted at a 10° angle with respect to the vertical axis of the vessel. Severity of the flange tilt was indicated by the fact that light was visible between the flange and the top head, suggesting that the gasket had blown out. After the head was removed, the gasket was found to be ruptured and numerous sections were missing. Also the 48 studs were bent at an angle of 10° toward the outside of the flange.

The effects of the water hammer caused an expansion deformation of the #1, 3, 4, 7 and 9 nozzles adjacent to the head (Figure III-37 and Figure III-38). All plugs were installed but not bolted down.

Nozzle #5 had the shield plug assembly and bell housing in place and bolted down. It experienced deformation adjacent to the head but to a lesser degree.

Nozzles #2 and #6 had blind shield plugs fastened in place. These plug bodies were 7 inches longer than the others and extended into the reactor head.

Liquid level nozzle #10 and auxiliary nozzle #11 were smaller in diameter than the shield plugs and of heavy wall thickness.

Nozzles #2, 6, 10 and 11 did not bulge or deform.

1.6. Aberdeen Tests

A series of model tests was conducted for General Electric Company by the Army Ballistic Research Laboratory at the Aberdeen Proving Ground, Aberdeen, Maryland, to verify the water hammer hypothesis. These tests used a 1/4 scale model of the SL-1 pressure vessel shown in Figure III-39. The objectives of these tests were: to verify the postulated causes of the mechanical damage observed by achieving equivalent damage to the simulated reactor vessel; to measure the pressure-time history, the final velocity of the water column accelerated above the core, and the velocity of the shield plugs as they were propelled from the nozzles; to determine the energy released into the water from the excursion. The test series, which took place in May and June, 1962, used high explosives to simulate the energy released by the nuclear explosion. There were four separate phases.

Phase I: One index of the mechanical damage observed was the collapse of the #9 guide tube which seized the extension rod. In order to establish the order of magnitude of the forces required to accomplish this, the guide tube and extension rod combination were exposed to shock waves in air from high explosive charges which were positioned at an appropriate distance. The charge size was to be successively increased until the required deformation was attained. This phase

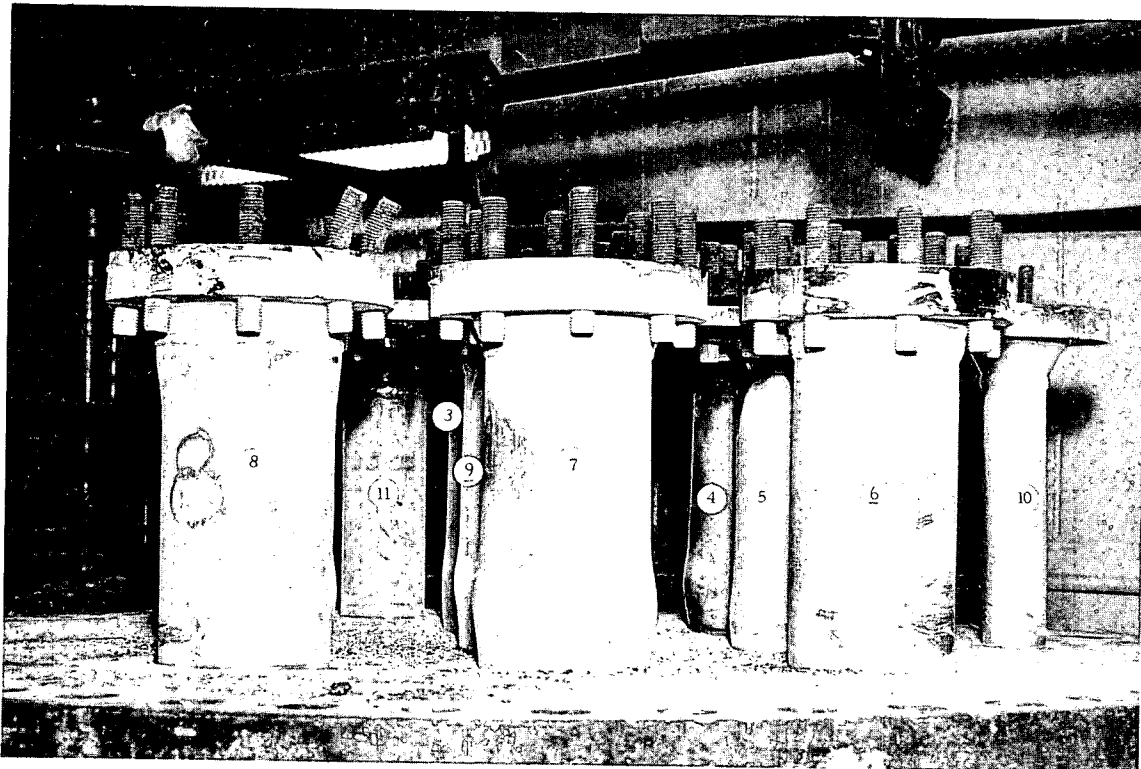


Figure III-37 Deformation of pressure vessel head nozzles

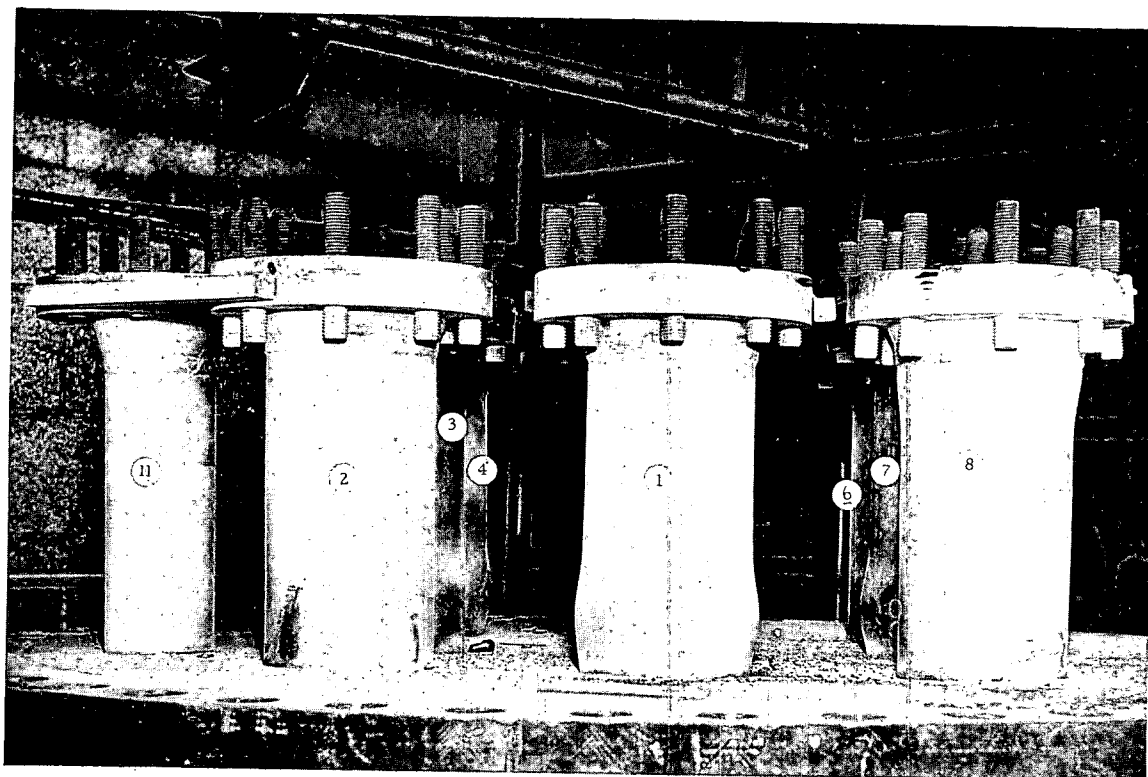


Figure III-38 Deformation of pressure vessel head nozzles

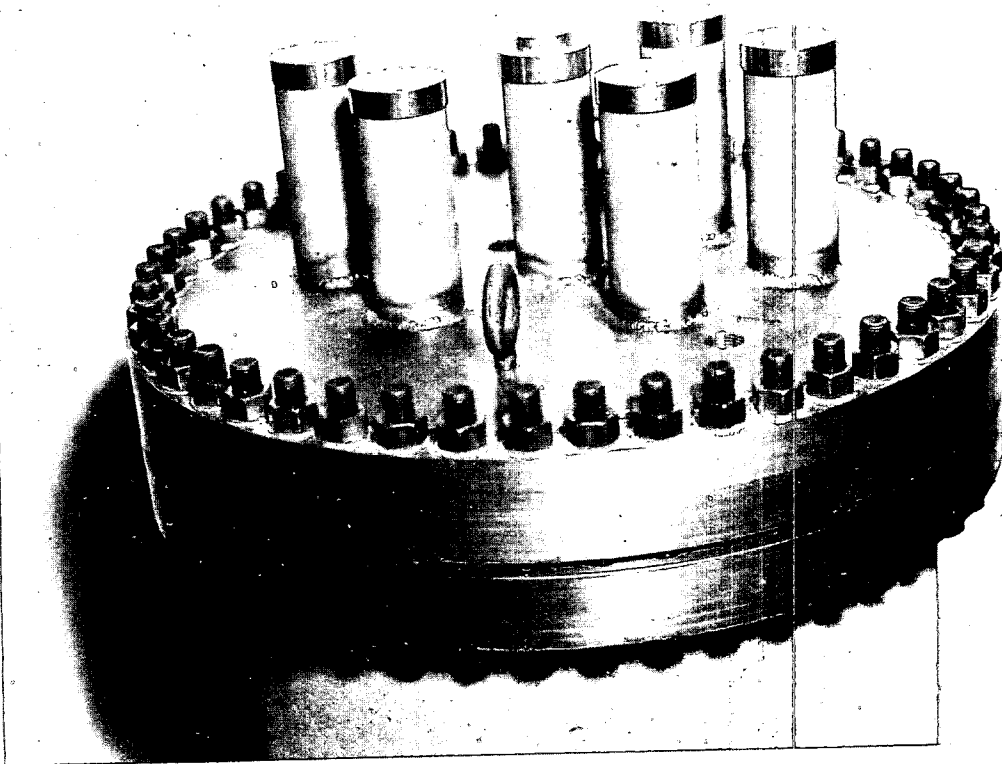


Figure III-39 1/4 scale model of pressure vessel head assembly

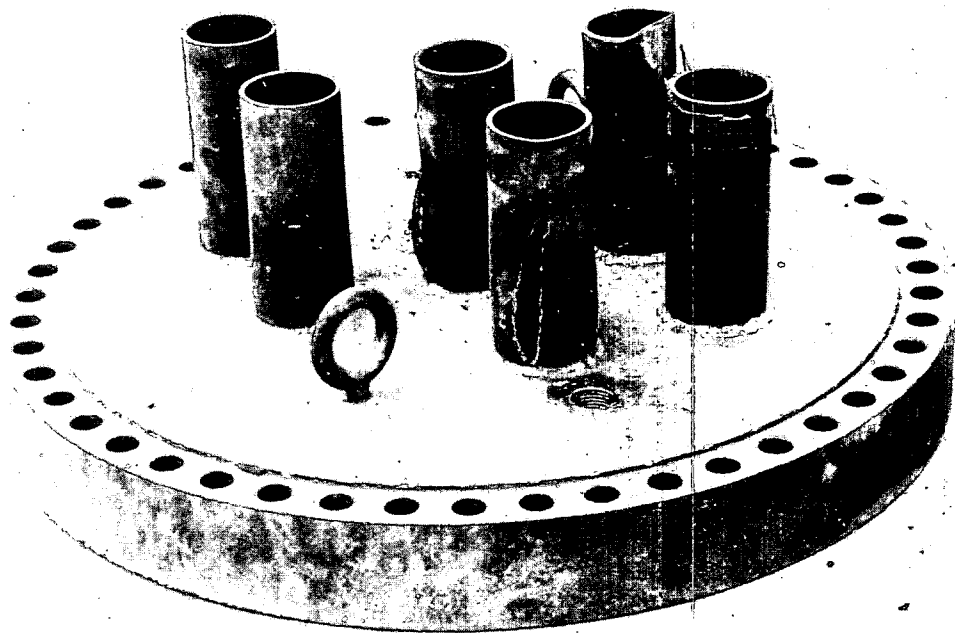


Figure III-40 1/4 scale model of pressure vessel head, showing damage to nozzles

was intended to take advantage of the well known pressure and impulse characteristics of the shock waves in air from high explosives, and thus serve as a guide to subsequent tests.

Five rounds were fired adjacent to the guide tube and extension rod combination using spherical charges of composition C-4 and Pentolite, as described on pages 186 through 204 of the Department of Army Technical Manual TM. 9-1910, "Military Explosives". When the required damage had not been obtained by firing the 8 pound charge, it was decided that the effect of a water environment was much greater than anticipated; therefore, no further testing in free air was attempted.

Phase II. This phase consisted of firing explosive charges inside the closed model. The pressure vessel wall was deliberately made thicker than 1/4 scale and lined with sponge rubber so that wall deformation would be reduced at the charge weight required to attain the guide tube seizure of the extension rod. Three sets of measurements were made. Those of pressure-time histories employed four piezo-electric pressure gages: two in the head and two in the vessel side located above the water level and 180° apart. The velocity of the water as it was expelled from the pressure vessel head was observed with a 35 mm camera and Fastex 16 mm camera. However, absence of distinguishable timing marks on the film made it impossible to get a precise measurement of the velocity. The water level was measured after the charge was detonated to determine the relative volume of water expelled.

The results of Phase II, in which four rounds of spherical charges of Pentolite were fired in the closed system, are as follows:

Round 1: A one ounce charge was used for the first firing. No film record is available since the high speed cameras did not function properly. A pressure record from one of the gages in the side of the vessel was obtained but the data were nebulous. The timing of the oscilloscope was such that the only data record was that of shock wave effects due to the detonation of the charge. As a result of the firing a crack developed at the bottom of the pressure vessel where the bottom head was welded to the cylinder allowing the water to run out. No guide tube collapse was obtained.

Round 2: A waterproof polyurethane sponge "cup" was placed in the bottom of the vessel to attenuate the shock wave and the charge weight was increased to two ounces. No pressure records were obtained on this round because of a delay in the charge firing. Seizing of the guide tube about the rod did not occur. Observation of the experiment through a telescope from a position 1000 feet away made it possible to view the plugs and water expelled from the model. The plugs lifted with the water following directly behind; however, the water eventually passed the plugs. The plugs shot straight up without any rotational or spinning motion to a height of approximately 16 feet. The double mass plug which simulated the weight of plug and man appeared to reach a height of 8 feet, which would be expected. The head was removed and the water level measured. The top of the thermal shield was in line with the new water level. This test indicated that all of the water above the core section was expelled.

Round 3: For this test the model was buried in the ground and the charge was increased to four ounces. As in the previous two firings, seizing of the guide tube about the rod did not occur. The pressure vessel raised out of the ground slightly when the charge was fired and it was noted that the vessel failed at the bottom head weld. The pressure vessel bulge and bottom head deformation resembled the contours which were present on the SL-1 pressure vessel after the excursion.

Round 4: The pressure vessel was rewelded and the charge weight increased to eight ounces. The model, which had been buried in the ground, lifted slightly during the firing but the actual height the model rose was not determined. There was sufficient collapse of the guide tube to indicate that conditions during this round were very nearly equivalent to the reactor incident. The extension rod no longer slid freely in the housing. The deformation in the lower section of the model was attributed to the repeated firings. However, the deformation just below the flange was due to the effect of the water hammer which was very nearly equivalent to that produced in the SL-1. The two side pressure gage holes were found to have been distorted elliptically, similar to the steam pipe hole in the original pressure vessel. The deformation of the bottom head was much more severe than it had been during round 3 and it resembled the deformation observed in the original vessel. The model pressure vessel failed at the bottom head weld and had a 1/4 inch wide split 15 inches long which started 6 inches from the bottom head. Figure III-40 shows three nozzles, #1, 7 and 9, split longitudinally. All nozzles were expanded adjacent to the head, the same effect observed in the original vessel. A pressure trace was obtained by a pressure gage mounted on the head. In Figure III-41 the oscilloscope sweep time was set for 500 milliseconds. The trace shows the pressure-time history of the accelerated water column hitting the bottom side of the head and the tremendous increase in pressure due to the compression of the water column. The discontinuity of the trace at approximately 10 milliseconds does not represent a pressure plateau but that the pressure produced exceeded the range of the pressure measuring equipment. It appears from the figure that the maximum pressure obtained was on the order of several thousand psi. After compression of the accelerated water column against the underside of the pressure vessel head, the pressure decreased to an average value of 550 psi and was maintained for nearly a second. This value corresponds to the estimated pressure required to accelerate the water column which created the water hammer in the SL-1 itself. It also indicates that the pressure under the water column remained essentially constant until all of the water was expelled. This constant pressure apparently did not allow the column of water to fall back into the core. The decrease in the pressure as the water escaped is roughly compensated by continued heat transfer to gas. Thus, the pressure remained essentially constant during the escape of the water*.

*Data from a second pressure sensing device substantiated the average decay pressure of 550 psi for those conditions.

Phase III. After the optimum charge size was obtained the firing was repeated with the head off to determine the water velocity and profile. The results of this phase were limited to the firing of a four ounce charge. The pressure vessel ruptured, so that further testing was impossible. The water velocity associated with this shot was 130 ft/sec.

Phase IV was not conducted. In this test the pressure vessel was to have been turned down to the scaled wall thickness and the optimum charge size fired in the closed system.

Conclusions: The results of the firing of the eight ounce charge in the closed vessel closely approximated the results of the incident. The velocity of the water column for this firing was estimated to be 25% greater than the 130 ft/sec. measured for the four ounce charge. The average pressure measured behind the water column and its estimated velocity at impact made calculations possible which supported the postulated maximum pressure of 7000 to 10,000 psi acting on the guide tube. This pressure and the period over which it acted are partially confirmed by the instrument trace. The experiment indicated that all of the water above the thermal shield was expelled through the nozzles. Damage to the model was similar to that produced by the SL-1 excursion. The desired measurements, although plagued by numerous troubles, substantiated the postulated behavior.

1.7 Core and Thermal Shield Deformation

1.7.1 Preliminary Observation Underneath Core

Prior to removing the vessel from its support cylinder at the SL-1 site, a 2 inch diameter hole was drilled through the support cylinder pressure vessel and thermal shield. The hole entered the vessel several inches below the main core support structure.

Photographs were taken by the use of a 1-3/4 inch diameter boroscope looking upward at the core. Visual observation was conducted as extensively as possible in trying to picture the appearance of the core.

Examination of the photographs and visual observation revealed the following information:

III-48

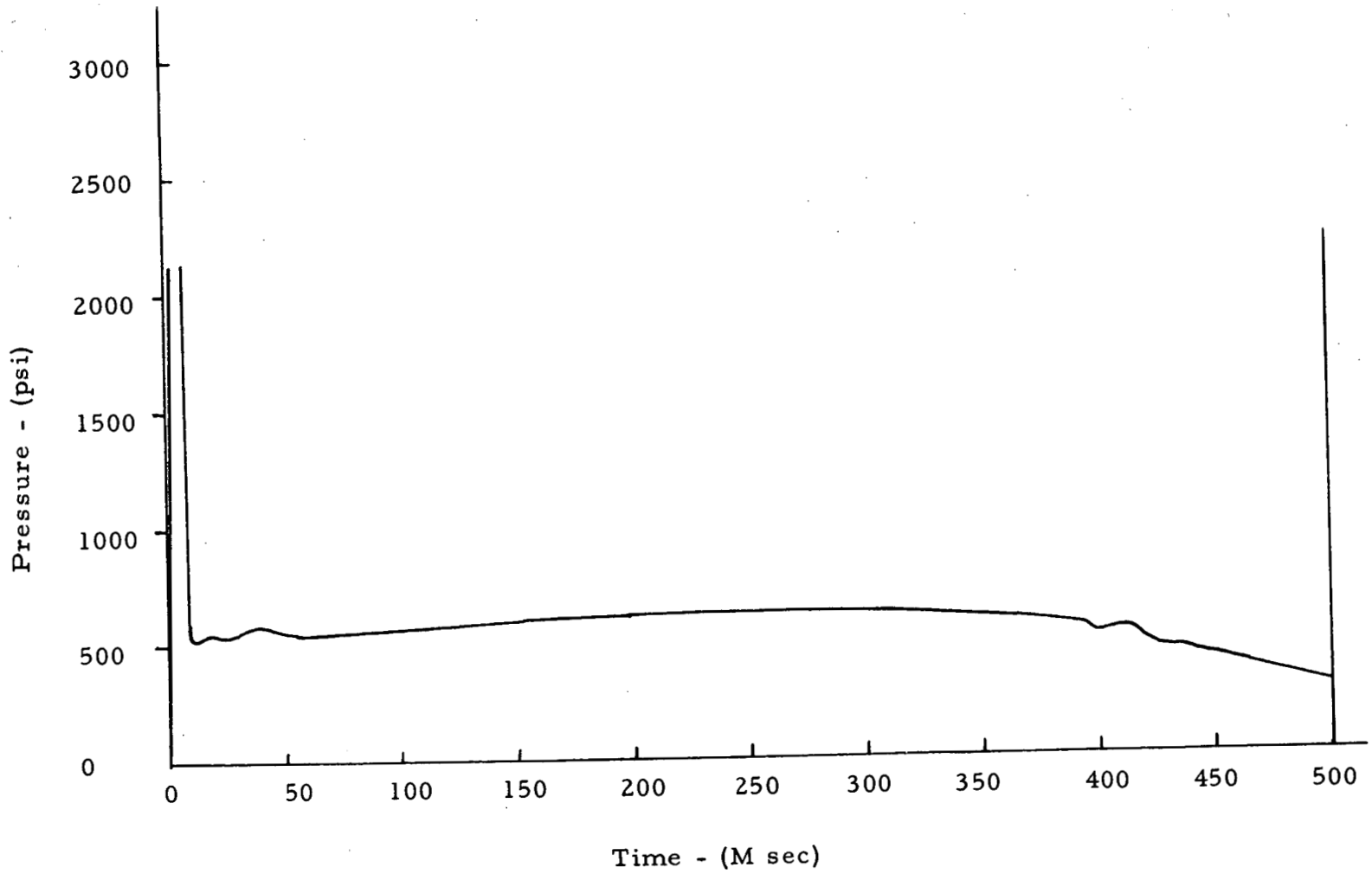


Fig. III-41

Pressure - Time History

- 1) The support structure had lifted up from the support bracket at two observable locations (Figure III-42).
- 2) Much of the support structure appeared to be out of its original position.
- 3) The outer fuel elements were partially collapsed and were thrust outward toward the thermal shield.
- 4) A large hole appeared to exist in the center of the core area.

1.7.2. Observations and Measurements of Core after Removal of the Reactor Head

After loose elements, plates and other debris were removed from the region above the active core and prior to the critical experiment, direct measurements were obtained remotely in the Hot Shop. These included the measurements of the vertical position of the significant parts of the top of the core from the top of the studs on the main pressure vessel flange. The tops of shrouds and control rods were measured and found to be between 3-1/2 inches to 4-1/2 inches above their as-built location in the core. The uncertainty in the displacement, which was believed to be $> \pm 1$ inch, is due to the uncertainty of the as-built dimensions, to the location and extent of elongation of the pressure vessel studs, and to the measurements themselves.

This measured displacement of the core helps to explain why the control rod extension of shield plug #5 was seized by its collapsed guide tube approximately 6 inches above normal scram position. (At the time of the accident this plug was completely installed, bolted down with seal housing attached.) Further confirmation of the upward rise of the core and thermal shield is indicated by the damage sustained to the guide pin support bracket of the auxiliary stillwell (nozzle #11). (Figure III-35).

Observation inside the core (Figure II-52) shows vividly the results of the radial forces collapsing all the cruciform shrouds and binding a major number of the peripheral fuel elements between the shrouds and the thermal shield. Shrouds Nos. 1, 2 and 9 were removed from the core structure and revealed the damage to the lattice support structure which included the shearing of the bolt stud threaded to the core support bracket. A cross shaped stanchion was bent outward and the shrouds disengaged from the stanchion by the rivets which were sheared. Figure III-43 shows three tee-shaped stanchions, two with the lattice support pads sheared off and one still in place. All rivets on all stanchions, as shown in the figure, have been sheared.

Observation of the thermal shield shows that three of the six hold-down bolts have been sheared while the other three are still intact with the lattice pads sheared from the tee-shaped stanchions. The two alignment pins and their support brackets were intact and undamaged.



Figure III-42 Bottom view of core. Note support bracket.

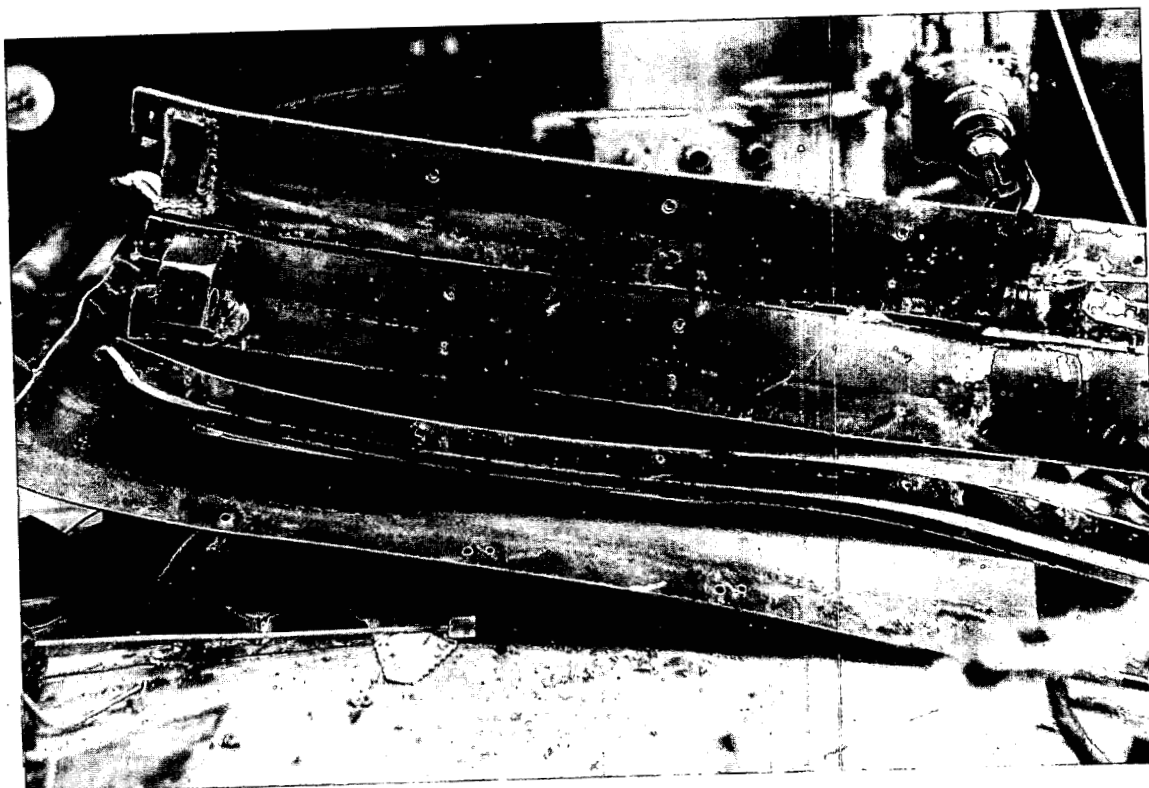


Figure III-43, Core, Tee-Stanchions

1. 8. Cadmium Blades and Shrouds

1. 8. 1. Shroud and Blade Recovery Examination

The control rod blades and their related shrouds were examined visually in the Radioactive Materials Laboratory (RML). Each assembly will be discussed independently except where they were recovered in pairs.

Shroud No. 1: One section of the shroud was torn away from the remainder, breaking along the weld seam (Figure III-44). Fuel element 17 was tightly bound in the collapsed shroud and element 44 had been captured in the shroud until the assembly was raised by the manipulator grip on the dummy cartridge which released element 44 (Figure III-45). The control blade was extended 4 inches below the bottom of the shroud and prominent rub marks can be plainly seen on the lower section of the exposed part of the blade as shown in Figure III-46. These marks are of pre-incident origin and also show some attack by corrosion.

Shroud No. 2: The assembly was received with the tee-section of the shroud and cadmium blades, as well as stanchions and support hardware attached (Figure III-47). A definite water level indication still remained visible above the upper row of relief holes. The three sections of cadmium blade appeared loose in the shroud. All edge rivets were missing from the shroud and the edge weld of the blades appeared to be partly fractured. Figure III-48 shows a weld seam separation on #2 control blade. The three blades were five inches* above the bottom of the shroud. The tee shroud was deformed but not collapsed. Subsequent to the visual examination this shroud assembly was sectioned and sampled for further analyses.

Shrouds No. 3 and No. 4: The shrouds and blades of control rods 3 and 4 arrived in the RML together. Element 54 was entrapped between the two shrouds as shown in Figure III-49. The lower part of plate E-255, element #10, was attached to shroud No. 3 by having been pressed into relief and rivet holes while heat softened. Both shrouds were collapsed radially outward with fuel plate material splattered inside the shroud. Seam welds were cracked and all rivets were sheared.

Shroud No. 5: This shroud had fuel plate E-674, element 50, very lightly attached to the face of the shroud by its being pressed into the relief holes (Figure III-50). The control blade extended 4-3/4 inches below the bottom of the shroud, but impact marks by relief holes indicate that the blade had moved downward 1-1/4 inches after impact. Rub marks are very pronounced along a major portion of the control blade and are of pre-incident origin (Figure III-51). Figure III-52 shows marks from the source cartridge and element 9 attached to shroud. The bottom section of the blade below the shroud also shows a considerable amount of sliding and abrasion marks. The shroud was collapsed radially outward and all rivets sheared. Seam welds were also partially fractured.

* Shrouds 2 and 6 each contained three cadmium strips which were not movable remotely, and therefore not control rods in the usual sense.

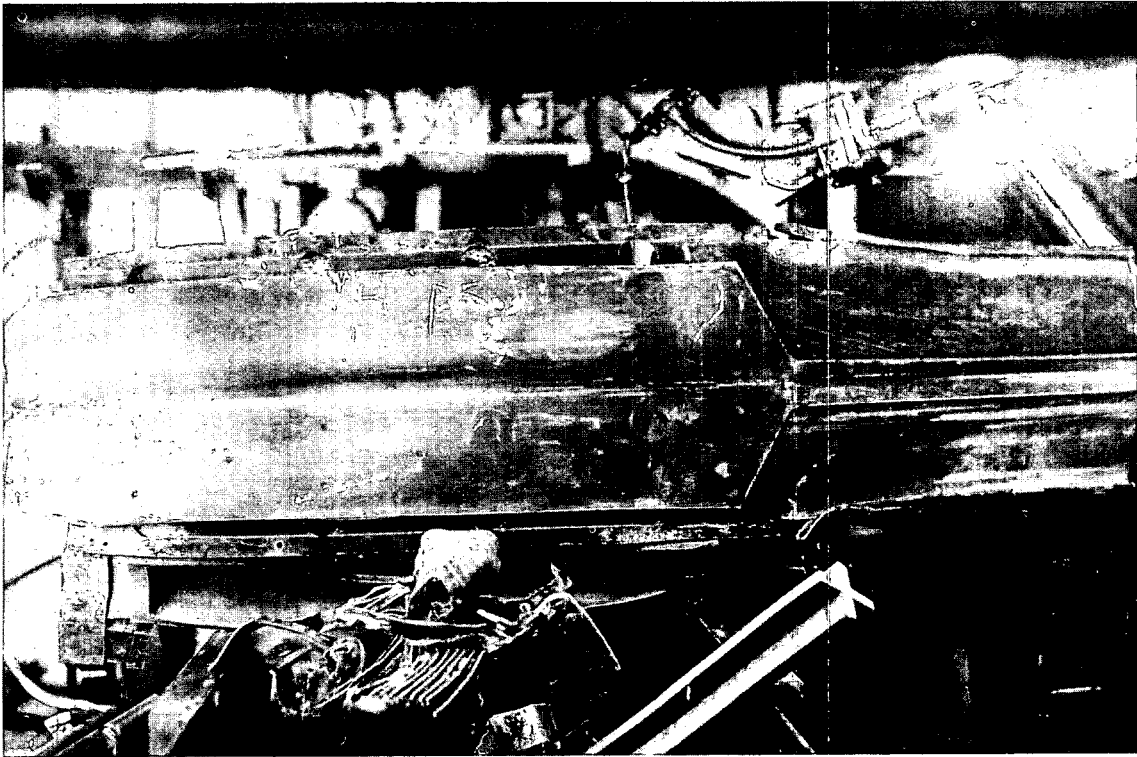


Figure III-44 Shroud and blade assembly #1. Blade exposed.

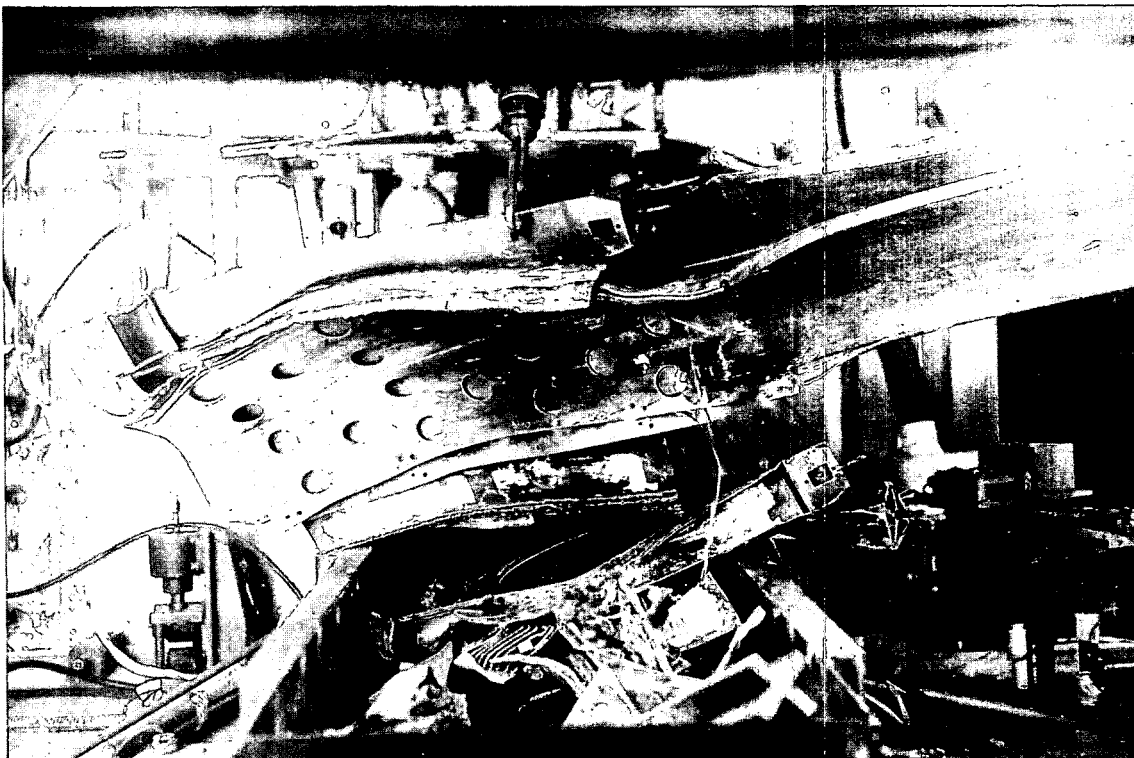


Figure III-45, Shroud and blade assembly #1.

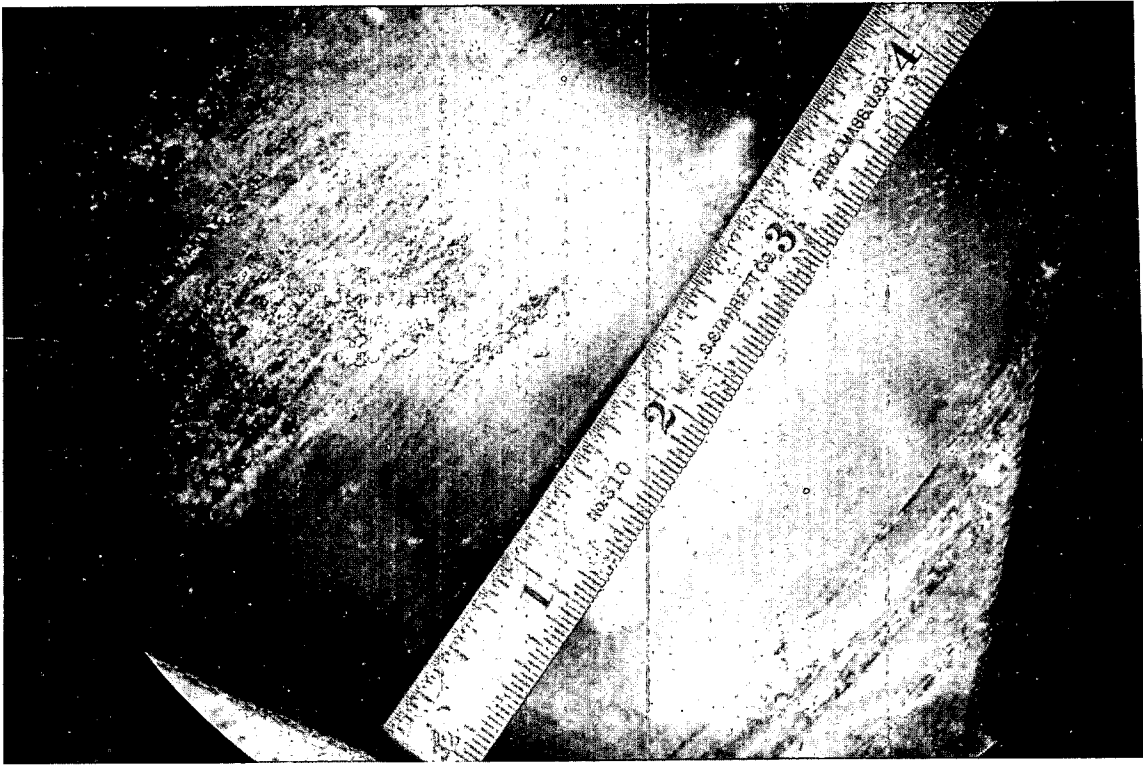


Figure III-46, Blade #1, note longitudinal marks.

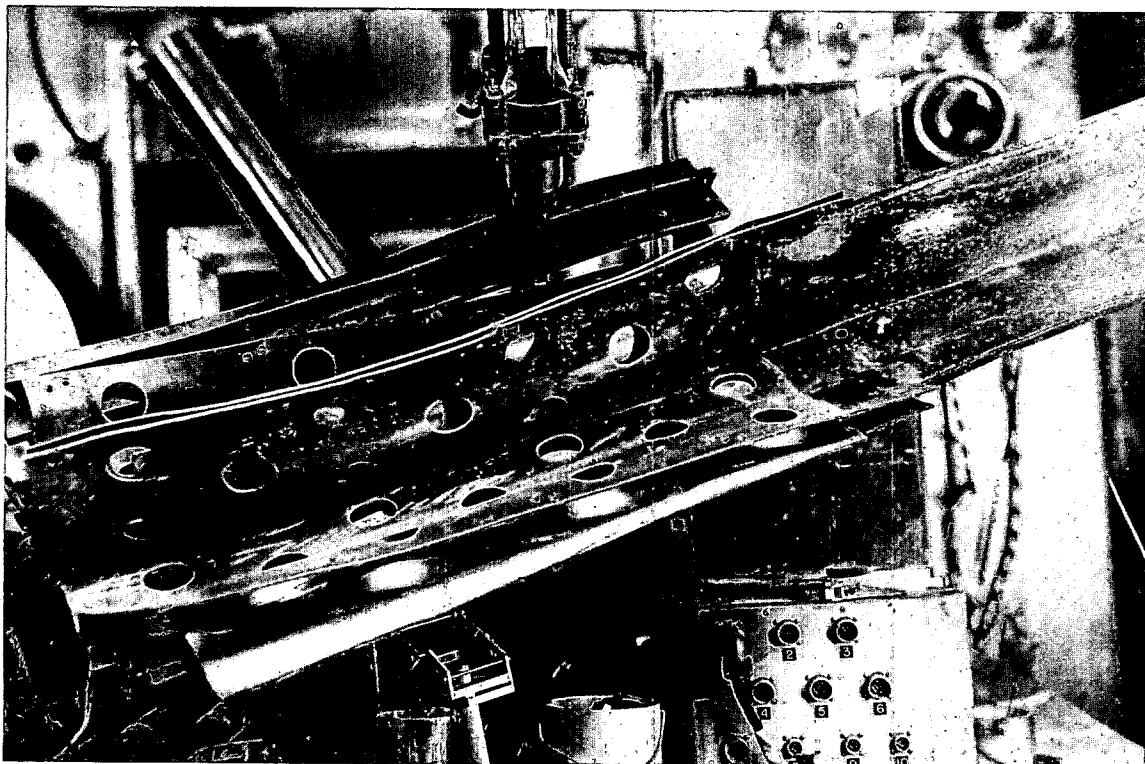


Figure III-47, Shroud and blade assembly #2.

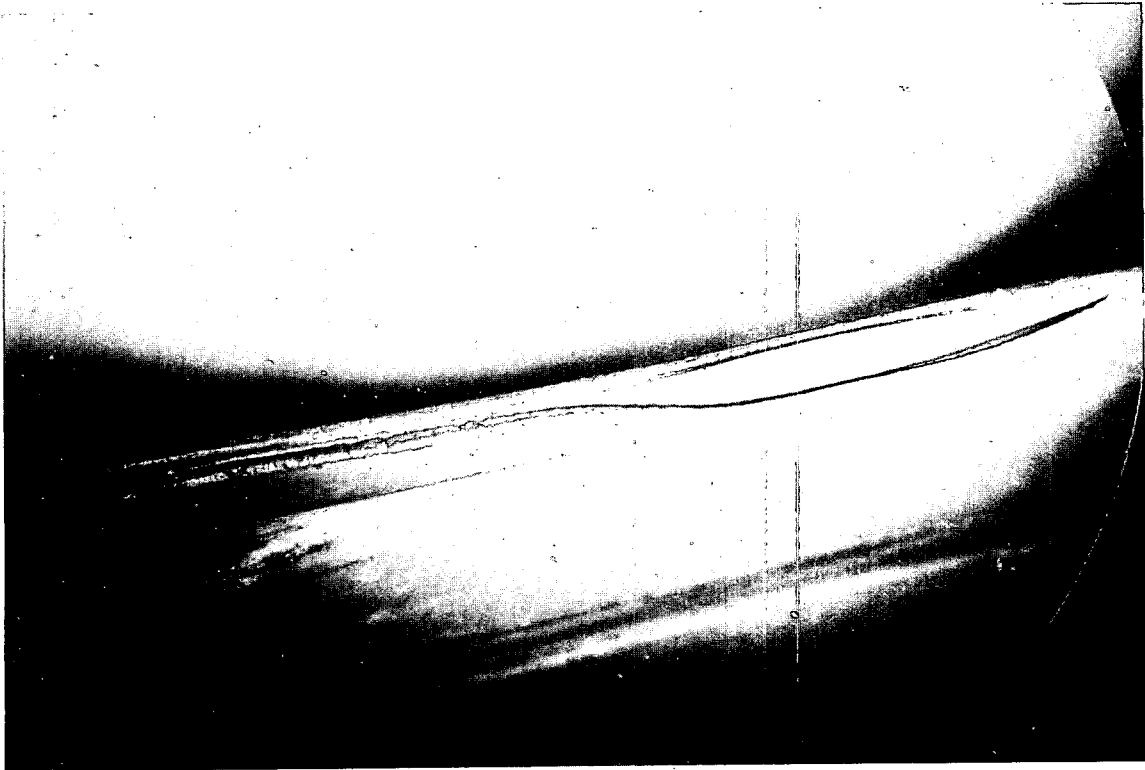


Figure III-48 Cadmium blade from assembly #2. Seam weld separation.

-329



Figure III-49, Shroud No. 3 and No. 4 assemblies.

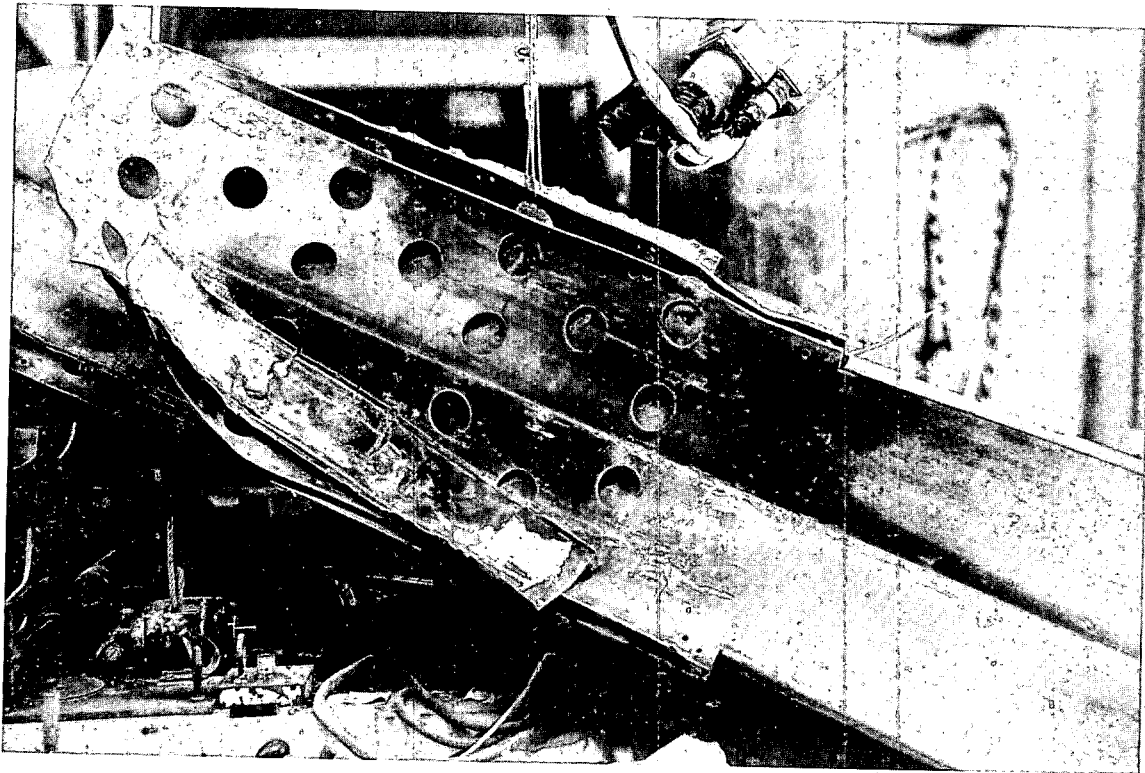


Figure III-50, Shroud Assembly #5.

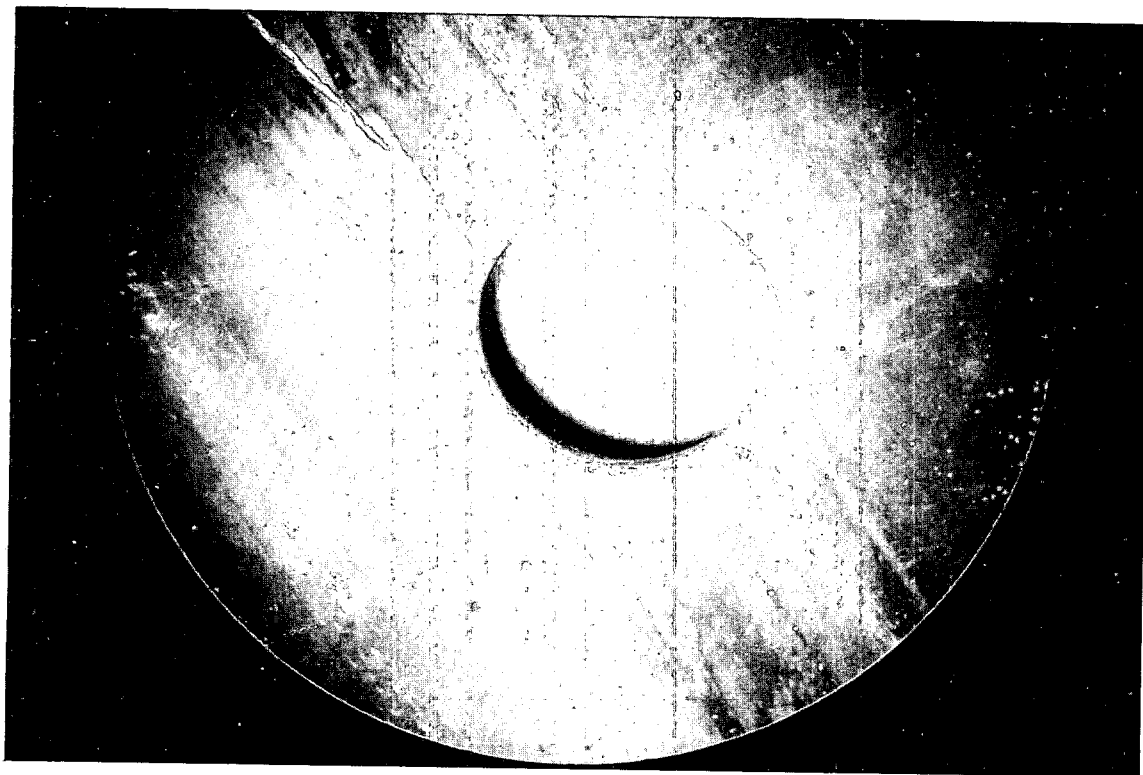


Figure III-51, Shroud Assembly #5.

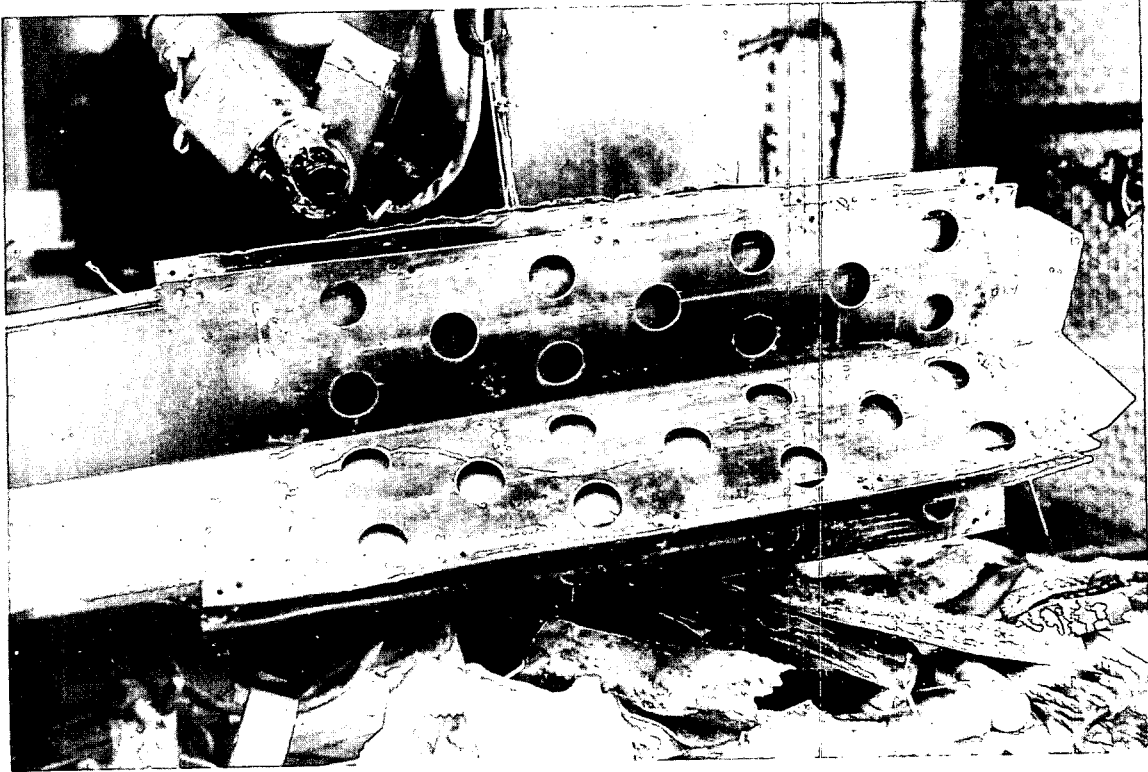


Figure III-52, Shroud Assembly #5.

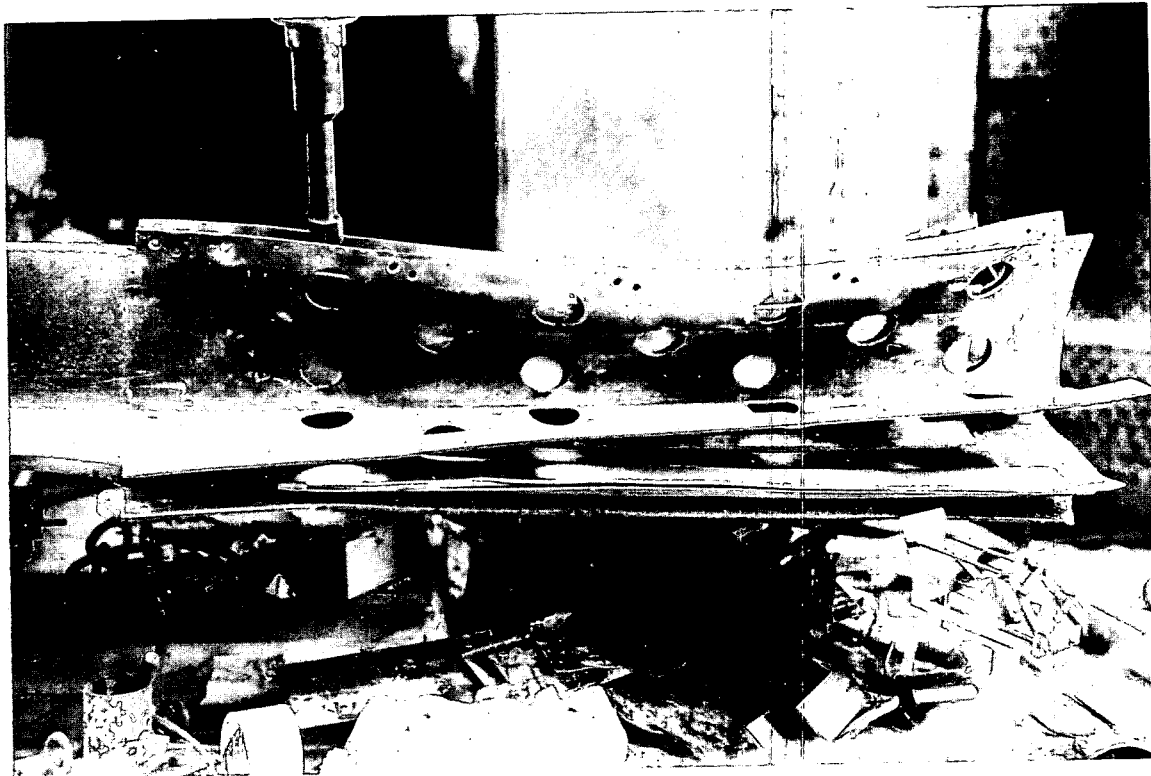


Figure III-53, Shroud Assembly #6.

Shroud No. 6: No fuel cartridges were attached to this shroud assembly. Figures III-53 and 54 show the separation of the cadmium blade edges. The welds at the upper end of the shroud appear to be partially fractured. One cadmium blade was 2-1/2 inches up from the bottom of the shroud, and the other two blades were 5 inches above the bottom of the shroud. One of the cadmium blades had the lifting fixture blown off. The tee-shroud was not collapsed but was deformed and all the rivets were sheared.

Shrouds No. 7 and No. 8: These two control-rod and shroud assemblies arrived together for examination and held elements 11, 43 and 61. (Figure III-55. A 14 inch section of an outer plate from element 3 was plastered on #7 shroud. The fuel plates were melted in the area of the relief holes. One relief hole was completely filled with molten metal. The #7 control blade extended 3-3/8 inches below the bottom of the shroud as shown in Figure III-56. Rub marks were very prominent on the lower end of the control blade and some pitting has resulted from corrosion.

Shroud #7 was collapsed outward, all rivets were sheared and seam welds were partially fractured.

Shroud #8 was not collapsed but was deformed; all rivets and seam welds were partially fractured.

No. 9 Control Blade and Shroud: The control rod cruciform blade, its shroud and the connector housing were lifted from the top of the core and removed from the pressure vessel intact and without difficulty. The following observations were made:

The gripper fingers, although sheared from the control rod connector, still held the connector housing to the control blade assembly. Only a small force with the manipulator was required to release the housing from the fingers.

The bottom of the extension (follower) of the cruciform control blade was bound in the shroud 4-1/2 inches* above the bottom end of the shroud (Figure III-58).

The control blade was firmly bound by the collapsed shroud and the blade had not moved after the shroud collapsed. This fact is verified by the imprint of the shroud relief holes on the surface of the control blade (Figure III-59).

Collapse of the shroud occurred before surface melting of the fuel (Figure III-59). The impression of the shroud relief hole on the control blade is vividly shown with fuel element splattered over the imprint.

Two series of rivet holes are along each edge of the shroud. The outer rivet holes were the ones used, as most of them indicated some extent of deformation. The inner holes show no observable deformation. No rivets have been recovered from or detected on the shroud.

* In the normal scram position, the bottom of the 17 inch follower would extend 15-1/2 inches below the shroud.

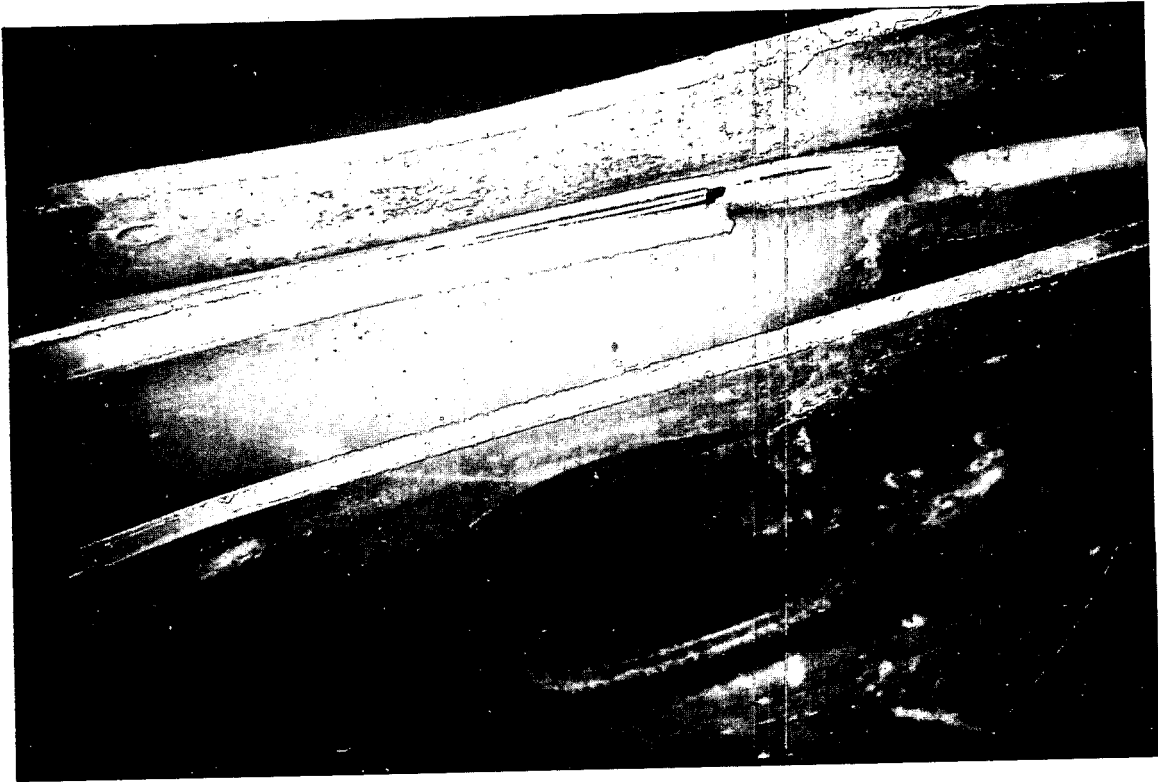


Figure III-54, Cadmium Blade, Assembly #6.

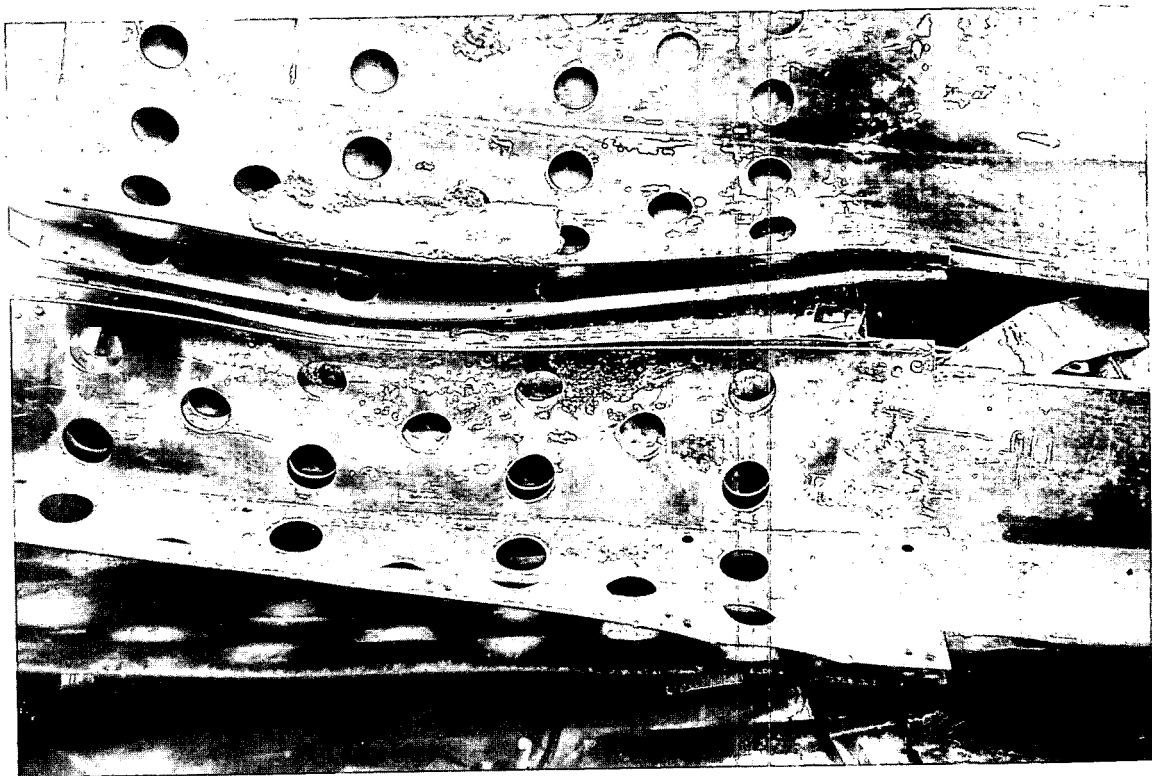


Figure III-55, Shroud Assemblies No. 7 and No. 8

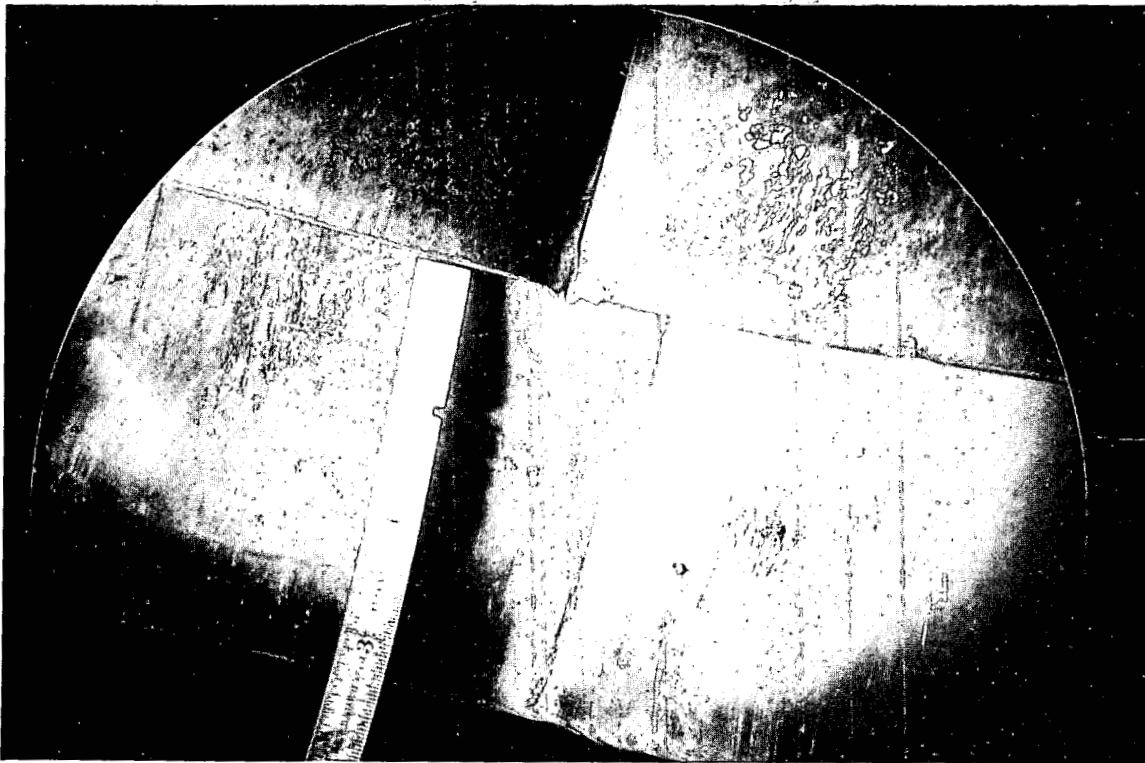


Figure III-56, Control Blade No. 7 extending 3-3/8 inches below bottom of its shroud.

U-5001-233

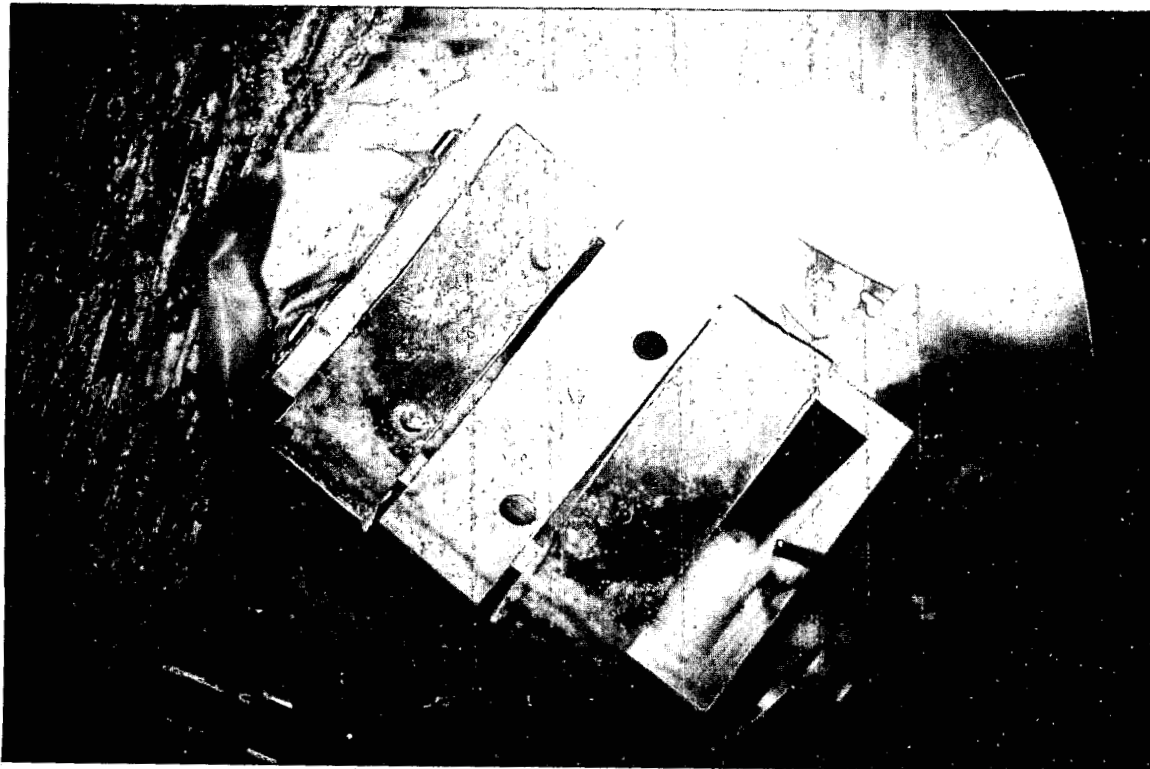


Figure III-57, Sample section from control blade #9.



Figure III-58, Control Blade #9 bound in its shroud.

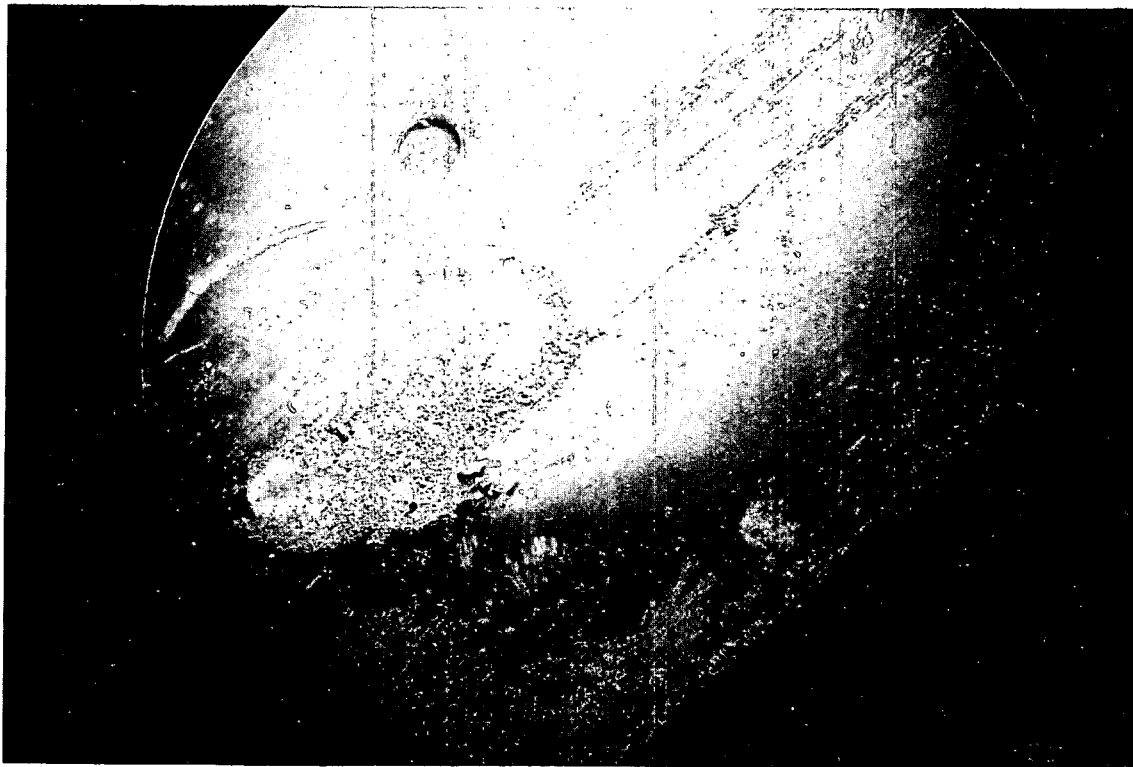


Figure III-59, Shroud relief hole imprint on control blade #9 and metal spatter

U-5001-176

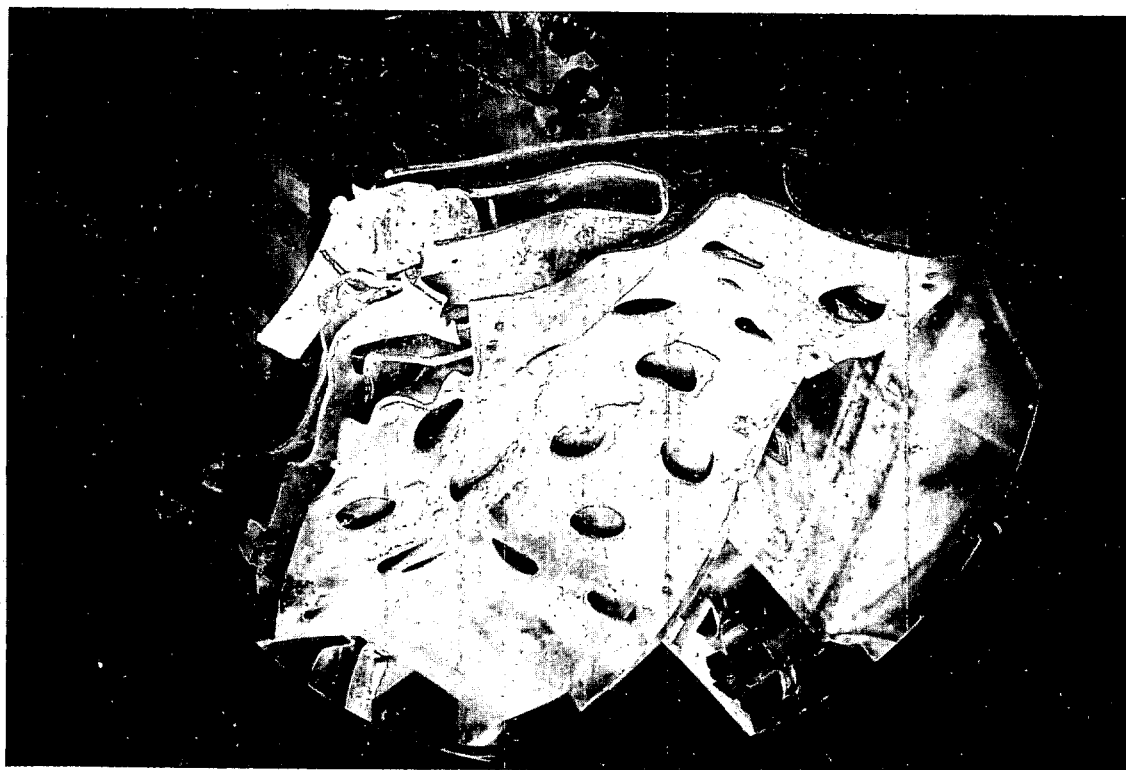


Figure III-60, Shroud and control blade #9.

Many scouring marks have been detected on the control blade. These marks appear to be of pre-incident origin since many of them are covered with splattered metal.

The control rod blade and shroud had undergone severe deformation (bending) and collapse principally in the region of the active core. Many areas of the shroud surface originally in the active core region were splattered with fuel plate material. Figure III-60 is a view showing distortion of the shroud and blade and metal spatter.

The overall length of the control blade was approximately 53" from the lower end of the tapered section. The length of the follower was measured to be $17\pm 1/4$ inches. The trailing edge of the cadmium plate sandwiched in the aluminum clad could be seen because of a weld fracture in the lower section of the blade (Figure III-61).

The control rod shroud was removed from the cruciform control rod blade. The cadmium and aluminum alloy cladding were separated along the blades edges on the lower half section of each of the four blades, as shown in Figure III-62. As the shroud was pulled away, it was noted that the aluminum clad seam welds tore apart easily by use of the manipulator grips. Previous attempts were made to section the shroud along the seam welds with an abrasive wheel. This procedure was slow and it was difficult to follow the shape of the deformed shroud. All sectioning or removal of the shroud from the control blade was subsequently accomplished by tearing the seam welds with the General Mills manipulator.

Sectioning and sampling for radiochemical and metallurgical analyses were completed on the control rod cruciform. Four 2 inch wide strips were sectioned from three of the blades. One was left intact. These four strips from each blade were sectioned corresponding to $1/4$, $1/2$, $3/4$ and maximum flux. Macroscopic observation indicated the cadmium metal and its alloy clad were in good condition (Fig. III-57).

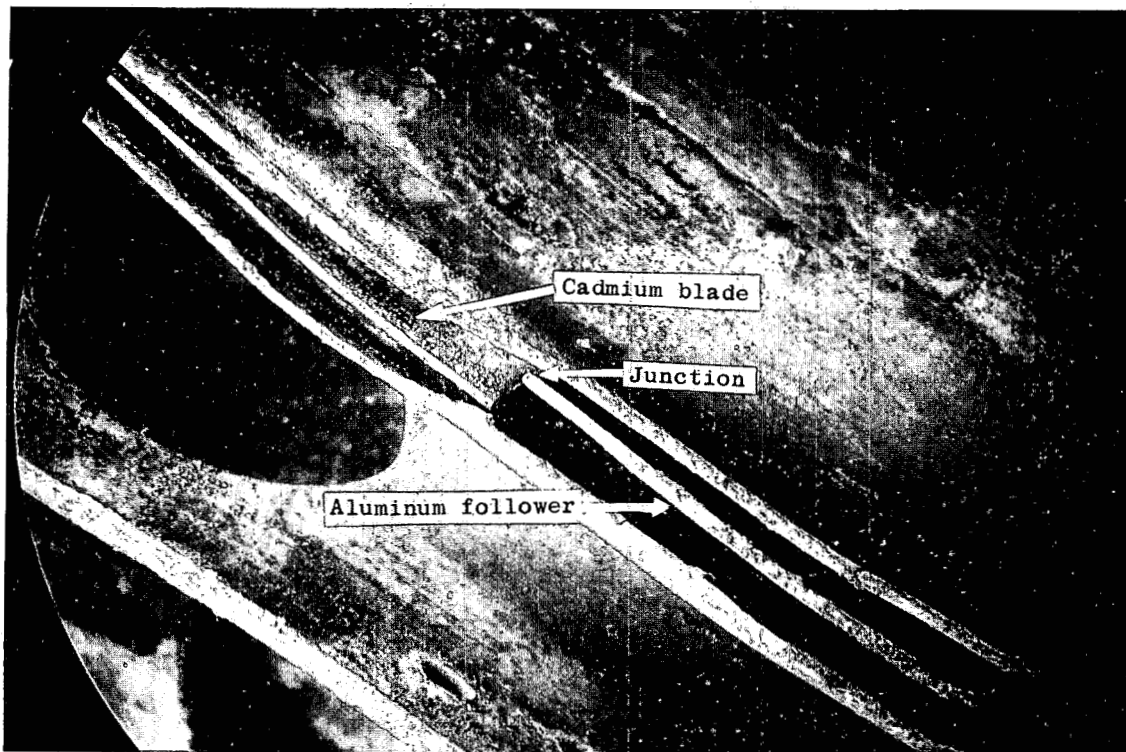


Figure III-61 Cadmium blade showing weld seam separation

U-5001-203

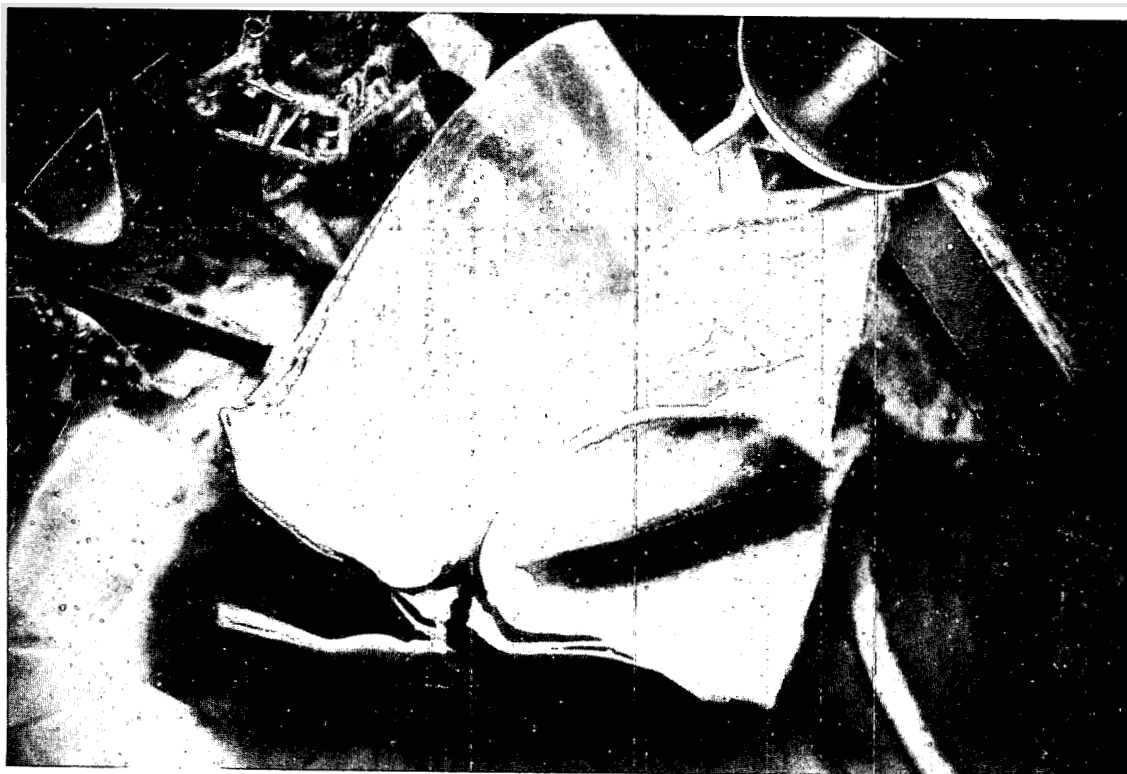


Figure III-62, Lower end of #9 control blade.

2. Chemical and Related Evidence

2.1 Identification of Deposits

Throughout the Phase 3 recovery a comprehensive program of chemical analysis was carried out. All foreign material and unexpected deposits and coatings were carefully identified, with particular emphasis on those inside the pressure vessel. It is believed that the major sources of such material were the shielding material from the head of the pressure vessel, and the thermal insulation around it. The plate which covered the shielding material was disrupted by the accident, and the gravel fines, boron oxide, and steel punchings were widely scattered. The insulation was similarly distributed. These conditions are shown in Figures II-1, 2, 3, and 4, Section II. The water expelled from the pressure vessel by the accident washed some of this material into the pressure vessel through the open nozzles, the gap formed between the vessel head and flange, and the sheared pipes. The leaching and oxidation of the steel punchings by this water represent a significant source for much of the iron oxide found. The gravel fines account for the silicon dioxide residue, while the boron oxide is judged to be the source of the white crystalline deposits which were identified to be mostly boric acid. Lead found in the debris came from the lead shot which was used during the recovery operation for shielding.

The type of deposits found within the pressure vessel can be seen in Section II, Figure II-33. Figures III-63 and 64 are photographs of the deposits on shield plug #5 and shield plug #4, respectively.

A tabulation of samples scraped from various areas of the pressure vessel and core is shown in Table III-2. Analysis of these samples was by optical emission spectroscopy and X-ray diffraction powder patterns.

An analysis was made of a block of the thermal insulation originally around the pressure vessel. Contrary to expectations, emission spectrography gave magnesium and calcium as major constituents with silicon, aluminum and iron present. The sample was then analyzed by X-ray diffraction means and showed calcium carbonate as the prime crystal structure with magnesium, iron, and aluminum silicate also present. The expected magnesium oxide was not present in the X-ray diffraction patterns. This is in contrast to the composition of 85% magnesia given in "Design of the Argonne Low Power Reactor", ANL 6076.

2.2 Burnable Poison Strips

The SL-1 core had been loaded with 39 full and 16 half strips of burnable boron-aluminum, as shown in Figure III-65. During the pre-incident

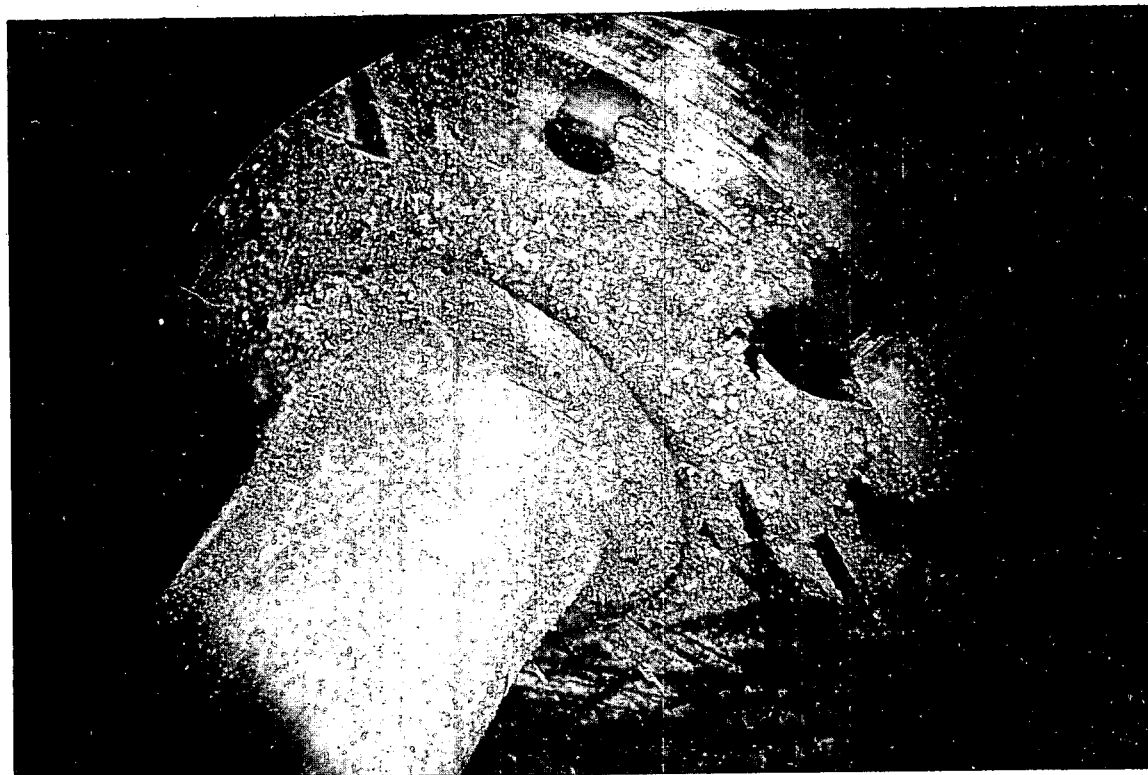


Figure III-63 Showing Vaporized Deposits on Shield Plug #5



Figure III-64, Deposits on Dummy Rod Assembly #4

TABLE III-2

Analysis of Samples from the Pressure Vessel & Core

Sample Description	Sample Origin	X-Ray Identification	Principal Constituents			Not Detected
			10%	1-10%	0.1-1.0%	
Scrapings of white deposit	Hold-down Box	--	Al	--	Fe, Si, Mg, B	U
Scrapings of white deposit	Under-side of pressure vessel head	H ₃ BO ₃ , B ₂ O ₃	--	--	--	--
Scrapings of white deposit	No. 4 control rod assembly (Figure III-	Al, H ₃ BO ₃ B ₂ O ₃ , γ -Al ₂ O ₃ α -Al ₂ O(OH) ₂ α Al ₂ O ₃ (?)	Al	--	Fe, B, Cu, Si, Mg	--
Scrapings of white deposit	No. 7 Shroud	H ₃ Bo ₃ , α -Al ₂ O(OH) ₂ , γ -Al ₂ O ₃	Al	--	Fe, Mg, B	--
Scrapings of white deposit	No. 6 T-Shroud	Mg(NO ₃) ₂ (?)	Mg, B	--	Al, Fe	--
Scrapings of white deposit	Pressure Vessel Wall (Figure II-33	B ₂ O ₃ , H ₃ BO ₃	--	--	--	--
H ₂ O leach of above samples	(See above)	--	Mg, B	--	--	U
H ₂ O leach residue from above	(See above)	--	(Same as above samples)			--
Metallic Slag	No. 9 Shroud	--	Al	--	B, U, Fe, Si, Cu, Ni, Mg, Mn	--
Corrosion Scale	Around each head-bolt hole	--	(Commercial Anti-Galling Compound)			
Cd control rod blade + Al Clad	No. 9 control rod	--	Al	Na, Mg, Si	B, Fe, Ni, Mn, Cr	--
Cd control rod blade + Al Clad	Oxide from Clad	Al, α -Al ₂ O(OH) ₂	--	--	--	--

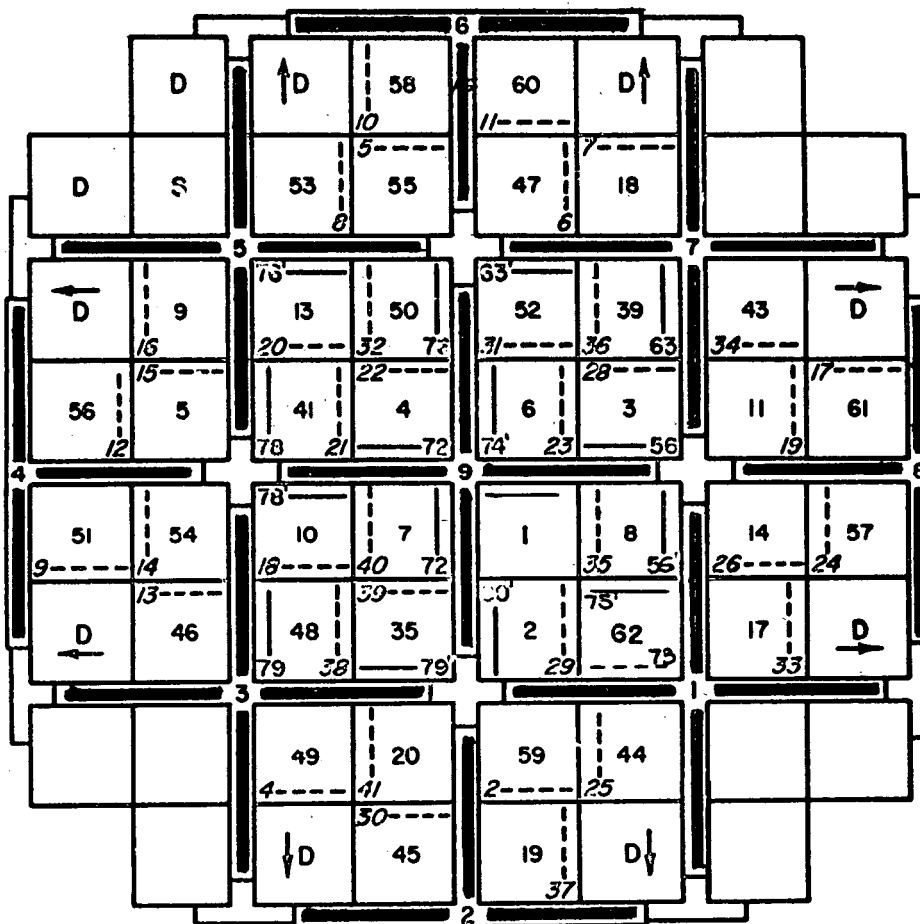
shutdown, fuel element 42 had been removed and replaced with element 62. The micro-examination of the boron-aluminum strips from element 42 showed the surfaces of both strips to be irregular and pitted with some boron particles having diameters of approximately 0.004 inches. Most of the boron particles, however, had diameters in the order of 0.0005 inches. Thicknesses of each of the two strips measured were in the 0.022 to 0.027 inch range.

The recovered boron strips were heavily corroded and embrittled. Figure III-66 indicates the severe corrosion of the full boron strip near the midpoint of element 45. Figure III-67 shows the deterioration of the boron strip from element 20 (strip at left in four pieces) and a more complete view of strip #30 from element 45. The corrosion was identified by X-ray diffraction and proved to be basic aluminum oxide (Boehmite) which has an orthorhombic crystal structure. A total of 29 boron strips (or portions thereof) were recovered and identified. These strips produced 2.88 kilograms for a recovery of 55.6%.

Table III-3 is a listing of the boron strips, the original weights, and related comments about their condition at recovery.

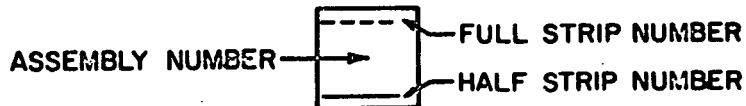
A considerable number of fragmented boron strips were recovered with the debris from the reactor pressure vessel. These pieces were not included in the inventory because of their lack of identification and difficulty in separation. Figure III-68 shows pieces of boron strips atop the cutter loaded with debris from the bottom of the core. An unanswered question is what percentage of flaking of the boron strips occurred during the incident and what took place during the preceding normal operation as reported in CEND-1005.

BORON STRIP LOADING



KEY:

- FULL STRIP OF BORON - DASH LINE
- HALF STRIP OF BORON - SOLID LINE
- D - DUMMY ELEMENT
- S - SOURCE



The position of the full and dotted lines indicate the orientation of the assembly and the position of the boron within a call of four assemblies. The direction of the side plates of the dummy elements are shown by an arrow.

SL-1 LOADING FOR 40 ELEMENT CORE

Figure III-65



Figure III-66, Corrosion and Deterioration of Boron Strip on Fuel Element #45 Side Plate

U-5001-336



Figure III-67, Portions of Corroded Boron Strips

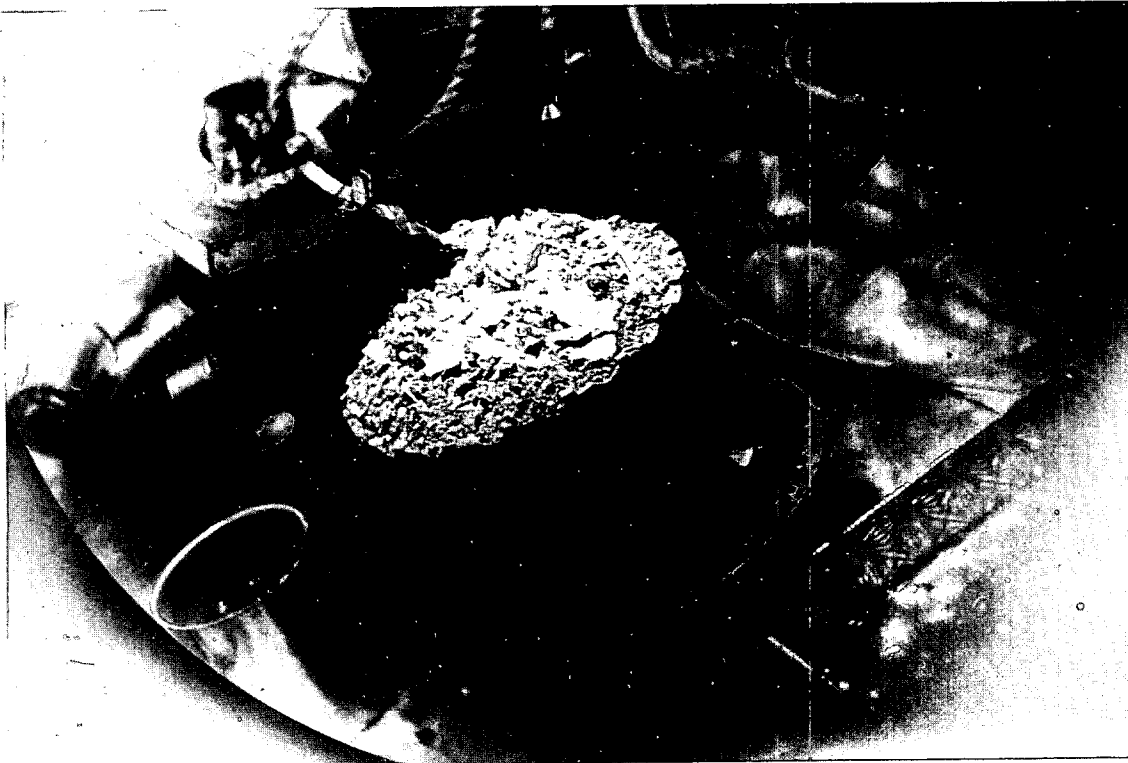


Figure III-68 Cutter Loaded with Debris from Bottom of Pressure Vessel

U-5103-3

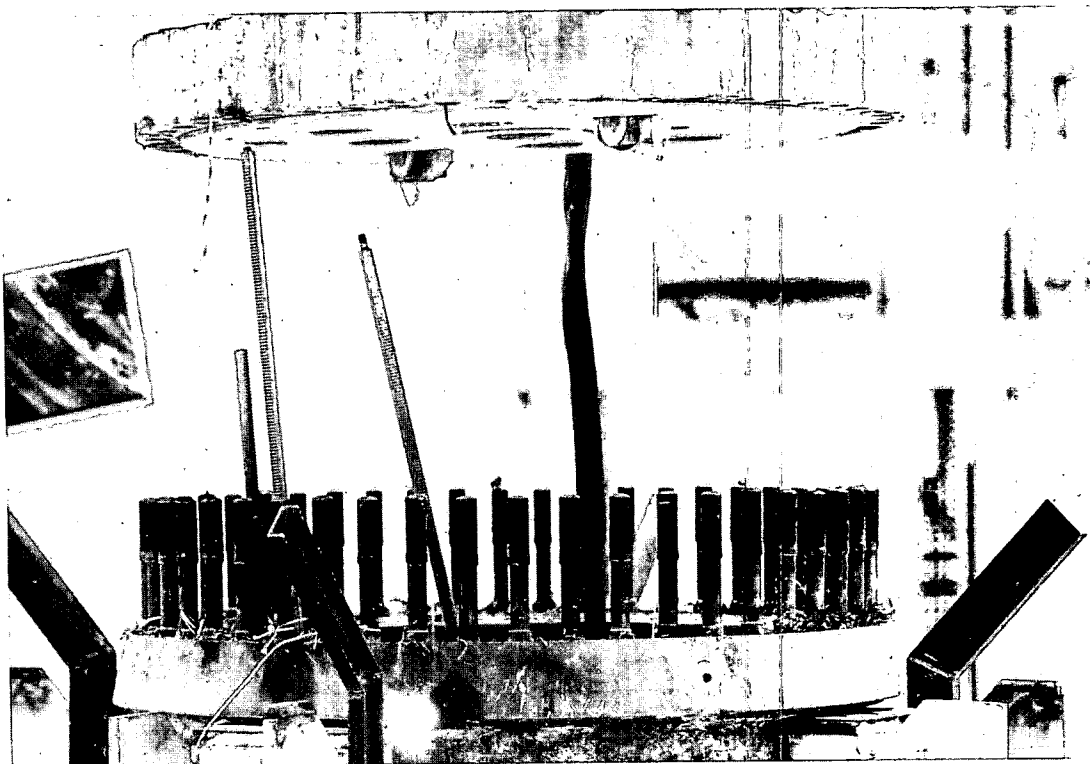


Figure III-69 Deposit Underneath Reactor Head Surface

TABLE III-3
Boron Strip Recovery Data

Element Number	Boron Strip Number	B-Al Strip Weight Grams	Remarks
1	1/2 strip	45.776	
2	29 80A	111.609 46.66	
3	28 56A	116.046 44.740	
4	22 72A	117.726 47.749	Recovered upper 10 inches
5	15	115.766	Recovered upper 15 inches Corrosion on left side
6	23 74	119.314 47.260	Recovered upper 4 inches Heavy corrosion
7	40 72B	116.031 47.750	Recovered upper 9 inches Twisted - crumpled
8	35 56B	116.887 47.740	Re covered upper 13 inches de- terioration on 3" of lower right
9	16	113.606	Recovered upper 15" break heavily corroded & embrittled
10	18 78A	117.580 44.756	
11	19	110.180	Recovered whole; deterioration on left edge
13	20 76B	116.769 39.655	
14	26	116.365	
17	33	112.468	Recovered upper and lower 8" center portion corroded away
18	7	111.433	
19	37	111.520	Recovered whole - Deterior- ation on right side and center
20	41	112.602	Recovered 6"
35	39 79B	117.893 46.248	
39	36 63	119.751 44.456	Recovered upper 5" - Deterior- ation on lower 2" of right side

TABLE III-3
Con't

Boron Strip Recovery Data

Element Number	Boron Strip Number	B-Al Strip Weight Grams	Remarks
41	21 78B	117.157 44.756	Recovered upper 16" - Deterioration on right side
43	34	113.960	Recovered 20" - lower end corroded away
44	25	114.176	
45	30	118.603	Recovered upper 12" - Badly corroded right edge 12"
46	13	112.384	Recovered completed - Deterioration on both sides
47	6	112.036	Recovered upper 18" - Last 6" deteriorated on left side
48	38 79A	120.775 46.248	
49	4	112.630	Recovered upper 8" - Lower end corroded away
50	32 76A	117.739 48.655	Recovered upper 12" - Deterioration of 2" lower right side
51	9	111.980	Recovered upper 12"-Last 3" left side deteriorated completely. Deteriorated along right side.
52	3 63	116.524 44.456	
53	8	111.530	Recovered upper 12" - Right edge deteriorated
54	14	112.926	Recovered complete - slight deterioration along left side
55	5	114.877	Recovered whole - slight deterioration along left side
56	12	109.242	
57	24	118.148	Deterioration on left edge
58	10	112.112	Center section missing - Deterioration along edge. Tied to 53
59	2	113.831	

TABLE III-3
Con't

Boron Strip Recovery Data

Element Number	Boron Strip Number	B-Al Strip Weight Grams	Remarks
60	11	112.551	Slight deterioration on left side
61	17	110.762	Recovered whole. Slight deterioration along one edge.
62	73	96.043	Grams of B-Al plate (half and full) prior to incident Grams of full B-Al plate prior to incident Grams recovered B-Al plate
	75A	45.507	
		5182.944	
		4453.532	
		2880.0	

2.3 Boric Acid Deposit Analyses

In Part 2.1 of this section it was pointed out that the white crystalline material found on the reactor components and the interior of the pressure vessel was identified as predominantly boric acid, H_3BO_3 . Before the Phase 3 investigation, it had been postulated that the boric acid injection system might have been operated, adding boric acid solution to the system by way of the upper spray ring. Investigation proved that this was not the case, however. The 120 gallon storage tank was expected to contain boric acid with a concentration of 100 grams H_3BO_3 per gallon of water or a 2.6% boric acid solution. Since an analysis of a liquid sample from the storage tank after the incident showed it to be a 2.9% boric acid solution and the total volume of solution was accounted for, it was concluded that the boric acid found within the pressure vessel came from another source.

A review of the design manual, "Design of The Argonne Low Power Reactor", ANL 6076, showed that directly above the reactor vessel head was a region 15 inches high through which the nozzles for the control rods passed. The remaining volume was packed with a shielding mixture containing 100 pounds of steel punchings, 30 pounds of boron oxide, and some gravel fines for each cubic foot of volume. The total of these shielding materials was approximately 26 ft³. This volume was enclosed by a ring of sheet metal capped with a plate. There was, therefore, approximately 780 pounds of boron oxide available to hydrolyze to boric acid.

A visual examination of the top of the pressure vessel, the inner walls and the fuel elements and shrouds produced evidence that the boric acid, leached from shielding atop the reactor, ran down these surfaces. Figure III-69 shows evidence of boric acid deposits on the top cap. This residue, deposited as boric acid, ran under the ring over the top cap and into the core through the opening between the top cap and the pressure vessel. Upon removal of the top cap it was noted that the complete under side area (approximately 23.5 square feet) was covered with the boric acid deposit. An analysis showed that 40 grams of boric acid had been deposited in this region.

Boron deposits were found on the shield plug surfaces which faced the reactor head prior to removal in the recovery operation. Scrapings from #4 dummy weight, which was believed to be a typical water deposit sample, were found to be 40% boron oxide compounds. Of this percent, 40% were water-soluble borates and 60% were water-insoluble. It was found that a 2% acetic acid solution dissolved these boric acid deposits considerably more rapidly than did pure water.

The definition of an apparent water level ring and its apparent changes are exhibited in Figure II-34, Section II. These deposits, identified as mostly boric acid, point to the fact that there was water in the core after the first expulsion. The deposits on the underside of the head and on the shield plugs indicate that there was sufficient afterheat to produce the volatilization action of the boric acid. ⁽¹⁾

2.4 Chemical Explosives

The possibility of a chemical explosive initiating or causing the SL-1 accident was investigated with the assistance of the Stanford Research Institute. ⁽²⁾ Their recommendations included analysis of the reactor debris for quantities of organic residues and remnants of inorganic explosives.

Representative samples of the reactor debris were extracted with carbon tetrachloride for organic residues, and with distilled water for residues from inorganic explosives. These extracts were subjected to infra-red spectrometry and qualitative chemical tests for the presence of organic material, nitro, and nitrate groups.

⁽¹⁾ Sedgwick, N. V., Vol. I. "Chemical Elements and Their Compounds".

⁽²⁾ See Appendix C

Standard colorimetric tests for nitro and nitrate groups were made on solvent blanks, known standards, and the debris extracts. These tests indicated no more than the expected traces of such groups in the extracted samples.

Infra-red analysis of extract samples and their residues indicated the following: "No organic materials were observed in the samples which were not present in the starting material (solvent)." (1)

In addition, visual examination of reactor components at all stages of disassembly gave no indication of any quantity of elemental carbon, which would have been expected to have been present.

2.5 Aluminum-Water Reaction

Considerable attention has been given the possibility that a metal-water reaction was associated with the SL-1 accident. Studies by L.F. Epstein^(2,3), R.C. Liimatainen, et.al.,⁽⁴⁾, F.J. Shipko⁽⁵⁾, and W.F. Zelezny⁽⁶⁾ indicate that a rapid, potentially dangerous chemical reaction between a metal and water in a nuclear reactor is possible. The conditions, however, for such a reaction are rather specific.

Violent chemical reaction between metals and water resulting from a temperature excursion in a nuclear reactor can occur only if the metal is molten. For a system such as the SL-1 reactor core (i.e., Al-U alloy and water) the important reaction must take place between liquid metal and water vapor. Below a certain critical temperature (about 1170-1225°C for Al), the rapid, violent reaction does not occur.⁽²⁾

It is also necessary that the metal to water ratio in the reacting region approach the stoichiometric ratio as given by: $2 \text{ Al} + 3 \text{ H}_2\text{O} \rightarrow \text{Al}_2\text{O}_3 + 3 \text{ H}_2$. An excess of either reactant would tend to subdue the reaction.⁽³⁾

1. R. Abernathey (Phillips Petroleum Company, NRTS) - private communication.
2. Epstein, L.F., Nuclear Science & Eng. 10, 247-253 (1961)
3. Epstein, L.F., Metal Water Reactions; VII, GEAP-3335 (1960)
4. Liimatainen, R.C., et.al., Studies of Metal-Water Reactions at High Temperatures, ANL-6250 (1962)
5. Shipko, F.J., & R.M. Haag, Thermal Stability of Hydrus Aluminum Oxides, KAPL-1740 (1957)
6. Zelezny, W.F., Metal Water Reactions, IDO-16629 (1960)

Experiments performed at atmospheric pressure have indicated that the reaction of molten Al-U alloys with water vapor is not an explosive (self-propagating) hazard at this pressure. (6)

No doubt some reaction occurred between metal and water during the SL-1 incident. Liimatainen, et.al., have observed as much as 25% complete reaction in their studies (private communication).

The fine screenings of the debris from the bottom of the pressure vessel, described in Section III-3.3, were analyzed for the presence and amount of alpha-alumina, α -Al₂O₃, the product of an aluminum-water reaction. The samples were prepared by acid dissolution and filtration, which facilitated extraction of the insoluble residue. The residue represented 68 weight percent or 23.7 kilograms of the total fines. A screening process was then performed on two samples of the residue which separated the samples into four grades of screenings. Table III-4 is a presentation of the screening data.

X-ray diffraction powder samples were prepared from the two finest grades and produced powder patterns of α -Al₂O₃ and α -Al₂O(OH)₂. The quantitative determinations were obtained with the use of standard samples and an X-ray diffractometer. The results showed that sample A (<200 mesh, Table III-4) contained 29% α -Al₂O₃ and the sample B (<60->200, Table III-4) was composed of 52% α -Al₂O₃. The screening process had produced 2.21 weight percent and 11.15 weight percent of A and B, respectively. The 34550 grams of original fines then included 1.49 kilograms of α -Al₂O₃.

TABLE III-4
Insoluble Residue Data

Sample	Total Weight	Sample Size (Screen Mesh)	Screened Sample Weight	wt. %	Visual Identification
56	25.9593	<12->18	17.2891	66.6	lead shot
		<18->60	4.8905	18.8	sand, insulation material
		<60->200	3.3234	12.8	fine grit
		<200	0.4563	1.8	fine powder
57	21.3805	<12->18	16.6910	78.1	lead shot
		<18->60	2.1455	10.0	sand, insulation material
		<60->200	1.9551	9.1	fine grit
		<200	0.5889	2.8	fine powder
56 + 57	47.3398	<12->18	33.9801	71.78	
		<18->60	7.0360	14.86	
		<60->200	5.2785	11.15	
		<200	1.0452	2.21	

3. Fuel Elements

Examination of the fuel elements was conducted to determine the extent and areas of damage to the assemblies, the extent of damage from thermal effects, the amount of fissionable material remaining and the uranium migration from the fuel matrix in areas of heat affected zones.

3.1 Extent of Melting

In order to determine the amount of fuel plate destroyed and where the loss occurred in the core, each fuel assembly, plate or section of plates was individually examined.

Appendix D is a tabulation of individual fuel plates and/or complete intact fuel assemblies listing percent of area destroyed and percent of area left unmelted.

Forty-seven percent of the fuel in the center 16 elements was destroyed. Relative to the total core, 20% of the fuel was destroyed.

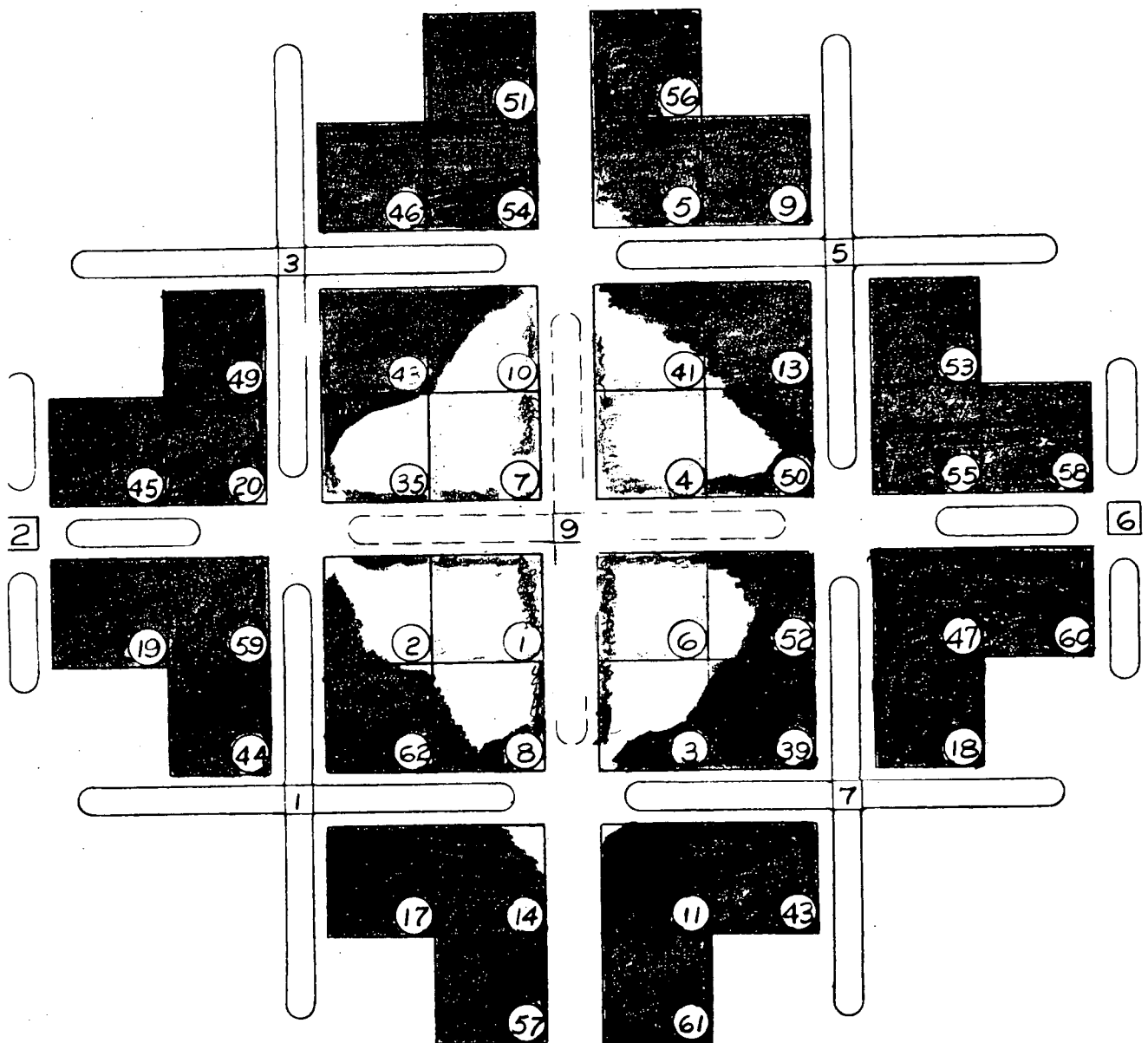
Figure III-70 is a schematic view showing approximately the damaged areas of the core (averaged throughout the vertical direction). The darkened areas represent intact or unaffected parts of fuel elements; the light areas represent the destroyed portions of the fuel assemblies. The four center-most elements were severely destroyed so that only the top 4 to 6 inches of fuel plate remained intact, with slightly less destruction adjacent to the central control blade.

By August of 1961, the only amount of significant fuel material recovered external to the reactor was four (4) small pieces on the fan room floor. See Figure III-71. Examination of these pieces showed that most of the fuel matrix melted and virtually exploded away from its clad, leaving behind a small amount of sponge-like fuel material. Most of the clad and side dead edge was relatively unaffected. The corrosion film still was evident on the pieces but for the most part it had spalled off. The trailing dead edge of one piece shown in the figure was unaffected and the corrosion film remains intact.

An upper portion of fuel plate from element #7, one of the center 16, was recovered from the debris in the bottom of the pressure vessel. See Figure III-72. Here again is seen the unaffected (leading) dead edge, though fuel matrix exploded away leaving portions of the aluminum clad. The dead-side edge was splattered with fuel material.

The corrosion film was intact on the leading dead edge and partly spalled off in the heat affected areas. Most of the corrosion film has been identified as an alumina hydrate and constitutes a small percentage of the insoluble material from the debris recovered from the pressure vessel. See Section III-2.5.

Examination showed the debris from the pressure vessel contained a large quantity of fuel material fragments. See Figure III-78. The small pieces, identifiable as fuel plate material, has a sponge-like appearance. Figure III-73 is a photograph showing fuel material which was ejected from fuel element #3, one of the center 16 elements, and has practically filled the relief hole of shroud #7.



Darkened areas - Unaffected plates

Light areas - Destroyed plates

Figure III-70 Schematic View of Core, Showing Areas of Destruction



Figure III-71 Sections of Fuel Plate Recovered from Fan Room Floor

U-5001-274



Figure III-72, Section of Fuel Plate from Element #7

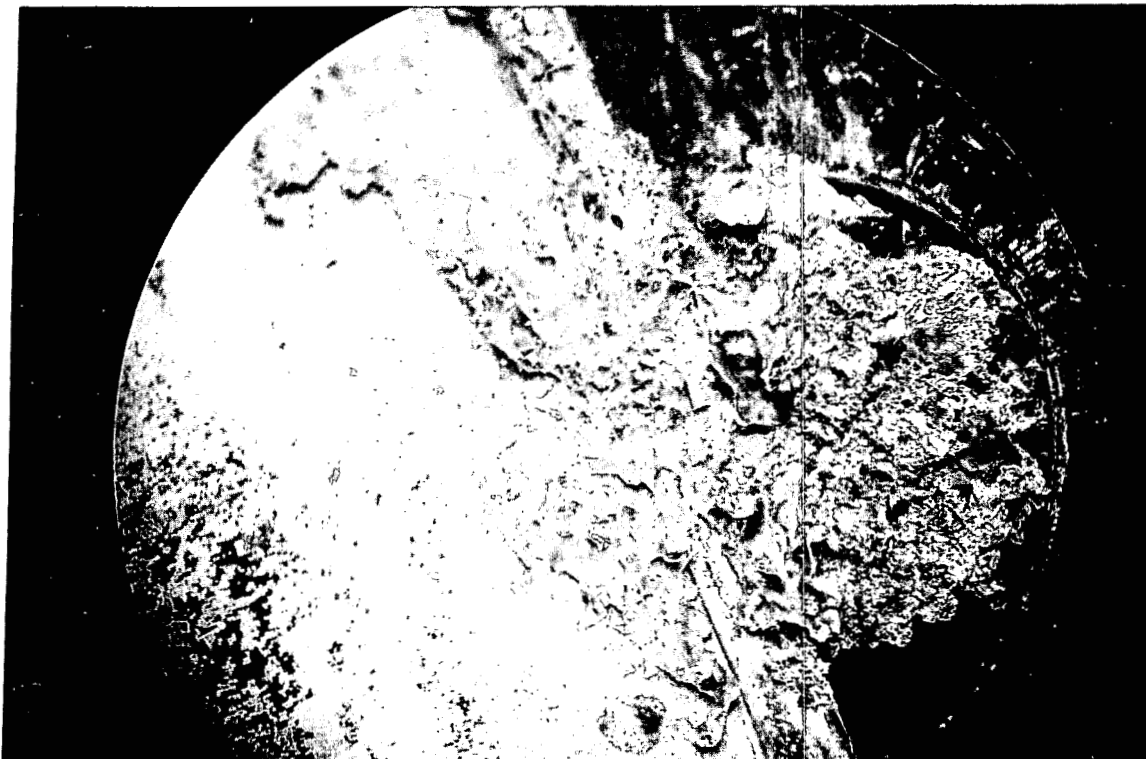


Figure III-73 Fuel Material Spatter from Element #3

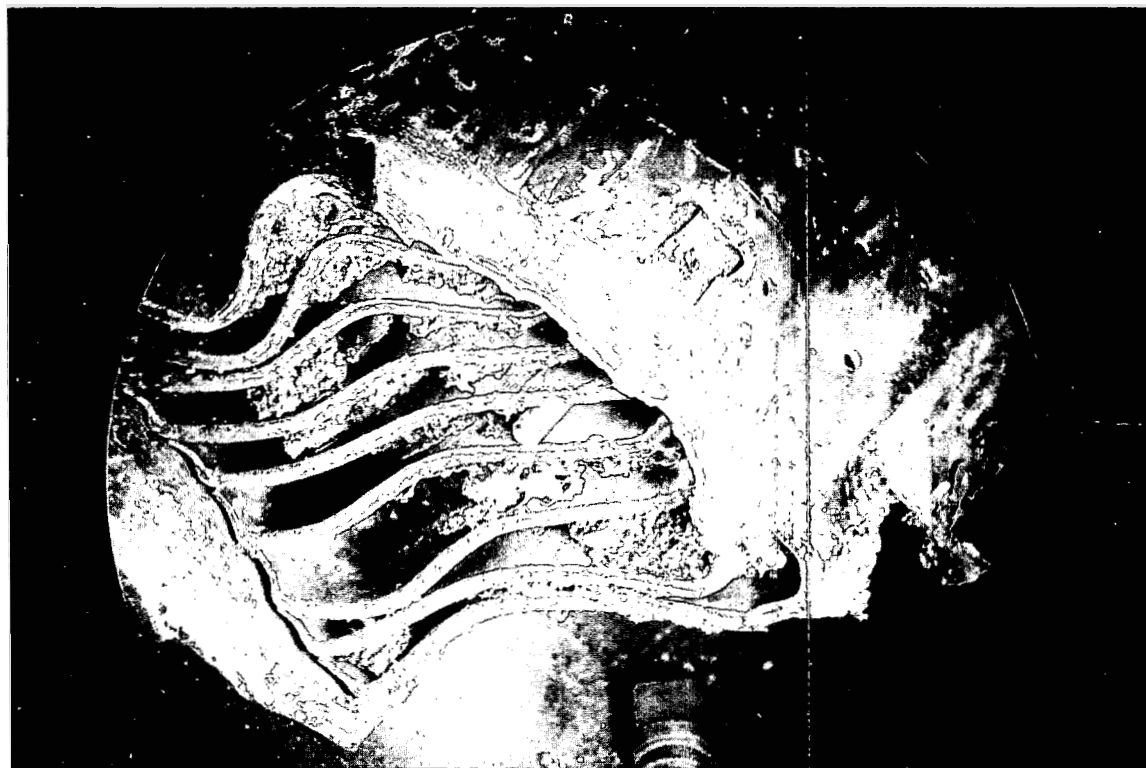


Figure III-74 Extraneous Material in Fuel Element #52

Figure III-74 shows the lower end of fuel element #52 with the spaces between plate filled with some molten material, sponge-like material and unmelted pieces.

The sponge-like appearance of fuel material results from a relatively fast cooling rate of a molten metal in contact with water or water vapor. The glazed appearance of a fuel material usually results from a slow cooling rate and may or may not be in contact with water or water vapor until such time that resolidification has begun. In only three instances has glazed appearance of melted fuel material been observed. See Figure III-75.

The preponderant amount of observed sponge-like material to the small amount of glazed material indicates that a relatively fast cooling rate was experienced during the excursion.

3.2. Temperature Ranges

Observation and examination (other than metallurgical) of recovered parts of fuel plates and fuel assemblies indicate a wide temperature range was experienced by the various core components.

A rather unusual aspect of the excursion is that no appreciable amount of glazed molten material was recovered or observed. During the examination of fuel assemblies for damage and fuel inventory, a small amount of unidentified molten material having the glazed appearance was found attached to a piece of burnable poison strip as shown in Figure III-75. Temperature of this melt was probably in the range between 1350°-1450°F.

A section of fuel plate recovered from a center section fuel assembly, shown in Figure III-76, is typical of damage sustained to many individual fuel plates that were blown off their assemblies. The darkened area, Figure III-76, indicates the leading dead edge with the corrosion coating relatively unaffected. It is estimated that it experienced only a moderate rise in temperature; probably in the range of 300°-450°F.

The light area, the corrosion coating having spalled off, shows undisturbed plate. This indicates a heat affected zone in the temperature range between 1000°-1150°F.

The disturbed area, characterized by the folds in the clad, probably reached a temperature between 1250°-1320°F. The fuel matrix in this region was above molten temperature, 1350°-1450°, and was ejected from the clad plate. There is no evidence of molten material having flowed out between the plates, although there is a small amount of sponge-like material along the edges of the plates.

Figure III-77 is a stereomicroscopic photograph at low power of a cross-section through a fuel plate. The clad is virtually unaffected. The fuel matrix has increased in thickness, due to swelling, while other portions have been ejected from the plate. The large voids seen in the figure indicates regions where the fuel matrix has vaporized and reached temperatures of at least 2060°C (3740°F).

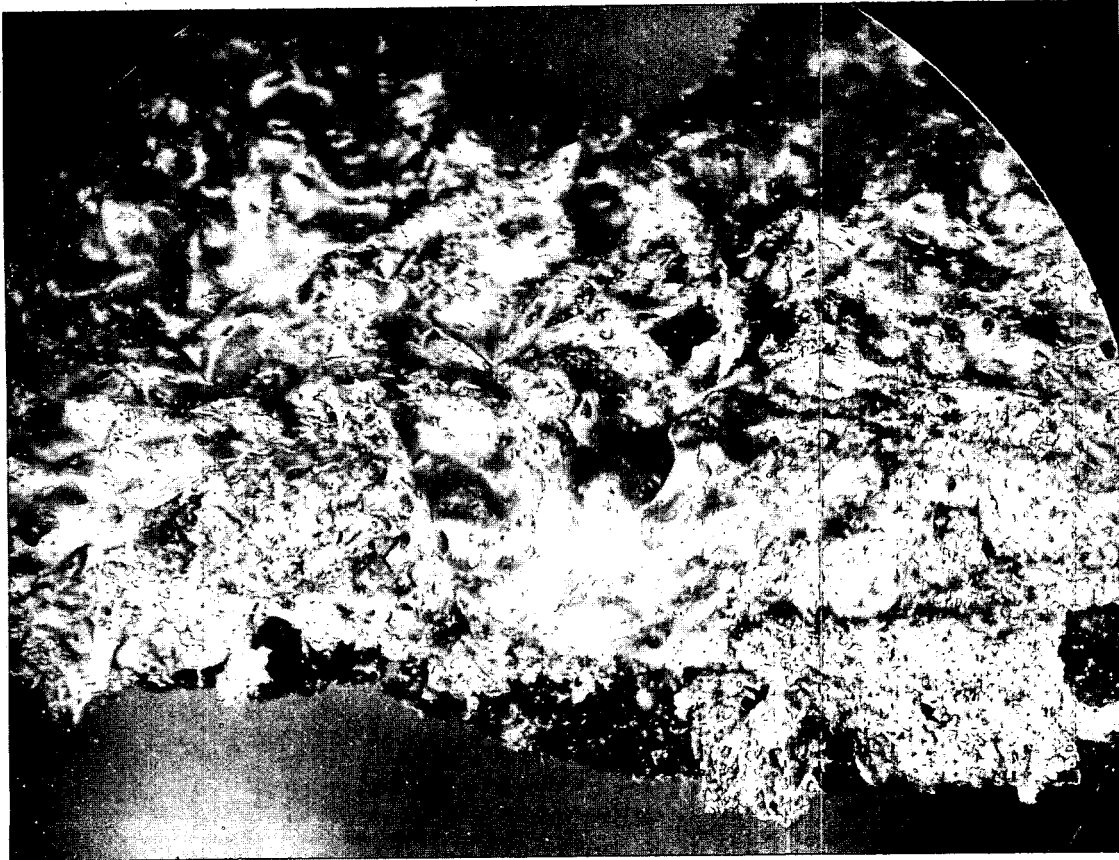


Figure III-75. Molten Metal on Boron Strip

U-5001-224

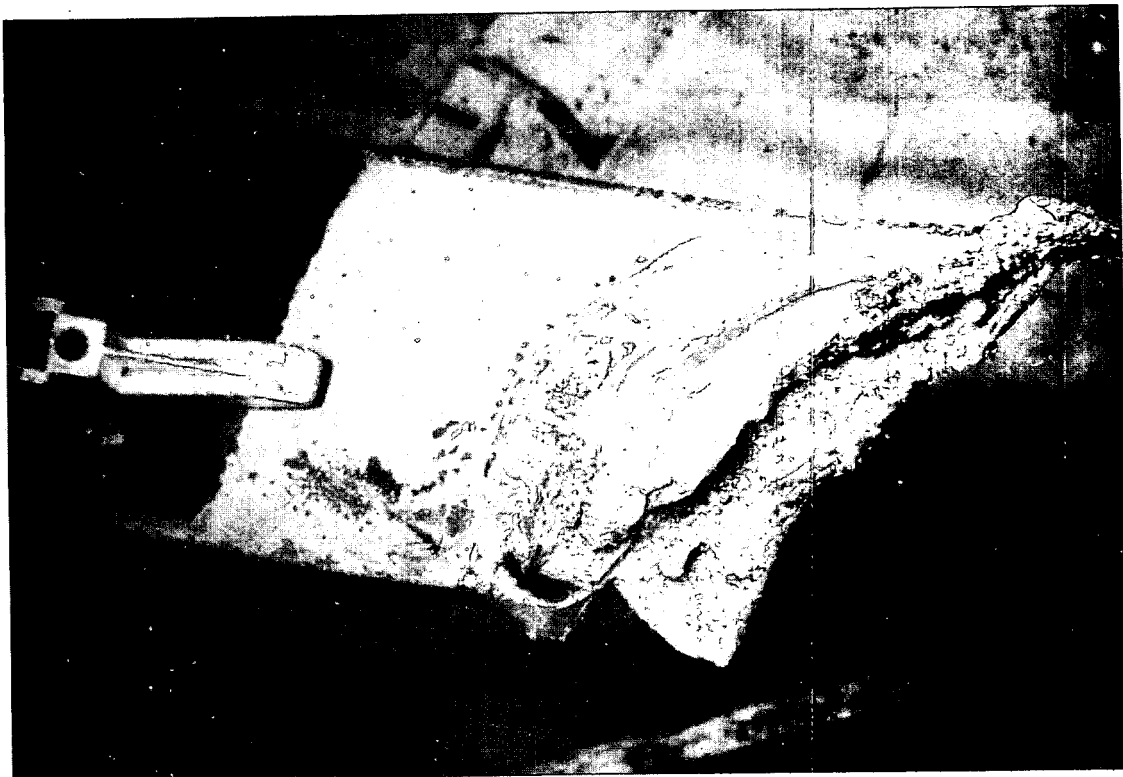


Figure III-76, Fuel Plate from Fuel Element #4
Showing Heat Affected Zones



Figure III-77 Cross-Section Through Fuel Plate Showing Swelling of Plate

U-5001-238

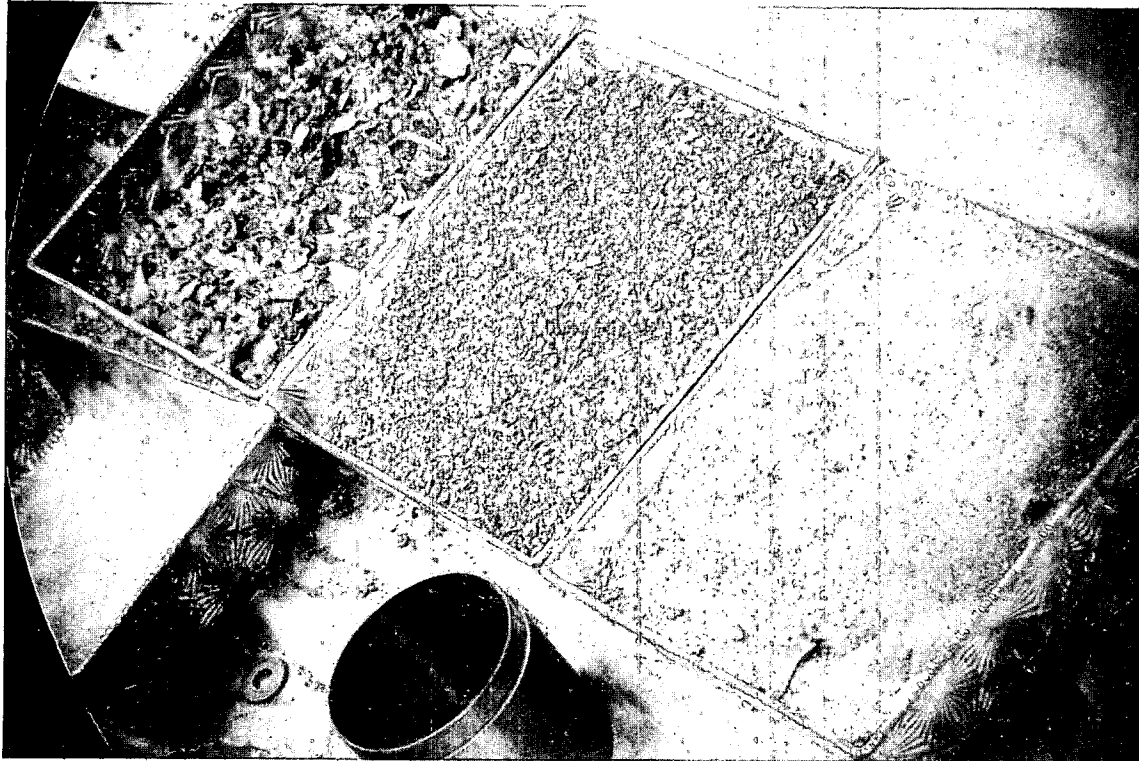


Figure III-78 Screened Debris Recovered from the Pressure Vessel

3.3 Uranium Inventory

The physical operations in making a fuel inventory of the SL-1 core and pressure vessel contents consisted of weighing each fuel element, fuel plate, or plate fragment remotely in the Radioactive Materials Laboratory. A Toledo scale of 20 Kg. capacity was used for weighing. Weights are considered accurate to $\pm 1\%$. To obtain the weight of active fuel material, the following allowances were made for non-fueled material:

Side plates = 241.0 grams each, 27.8 in. long; or 8.7 grams per inch
Dead-ends = 18.6 grams each
Dead-side edge, including weld area = 33.6 grams, or 1.2 grams per inch--except for the last plate which is 26 grams, or 0.94 grams per inch.

Using these relationships, the active weights of fragments and incomplete elements were determined. The uranium weights reported are those referenced to the original loading and do not account for burnup (i. e. 100% recovery would give a total U-235 weight of 14.1 Kg, the original inventory).

Debris from the reactor pressure vessel was collected and sized by screening into three (3) sizes. The coarse material was sized greater than 1/4 inch; the medium was less than 1/4 inch - greater than 12 mesh; and fines were less than 12 mesh. (See Figure III-78).

The following Table III-5 gives data for recovered fuel material from fuel elements, plates and fragments, and reactor vessel debris. The initial fuel element loading is included. It should be noted that in nine cases the recovery weight significantly exceeds the initial U²³⁵ loading. This discrepancy results from molten fuel material which was deposited between the plates or splattered onto other plates giving the additional weight. These elements are indicated with (*), and an example can be seen in Figure III-74.

Uranium in the reactor vessel debris is calculated on the basis of enriched U as in the initial material, allowing for $\sim 15\%$ operational depletion prior to the incident, since it is assumed this material originated from the high burnup regions.

A table listing recovered fuel plate condition with respect to melting, is shown in the Appendix D.

TABLE III-5

SL-1 Fuel Inventory

Fuel Element Number	Initial U ²³⁵ Loading	Active Plate Material Recovered	Final U ²³⁵ Recovered*
1	351.5	1121.2	83.39
2	353.0	3908.0	290.65
3	349.6	2506.0	186.38
4	350.3	1046.7	77.85
5	353.3	4480.4	333.23
6	351.9	1543.4	114.78
7	351.0	1206.8	89.75
8	351.7	1152.5	85.72
9	351.0	4700.0	349.56
10	352.9	2392.6	177.95
11	353.9	4707.0	350.08
13	350.4	4676.4	347.80
14	351.6	3975.4	295.77
17	348.1	4700.0	349.56
18	351.3	4700.0	349.56
19	350.1	4821.0	358.56*
20	349.8	4427.0	329.25
35	355.9	1718.0	127.78
39	354.0	4647.0	345.61
41	348.4	2206.4	164.10
43	353.9	4700.0	349.56
44	350.6	4768.0	354.62*
45	349.6	4867.0	361.98*
46	351.7	4700.0	349.56
47	352.8	4700.0	349.56
48	352.7	4657.0	346.36
49	348.9	4700.0	349.56
50	344.1	1912.9	142.27
51	346.0	4700.0	349.56*
52	346.6	3669.0	272.88
53	345.8	4700.0	349.56*
54	345.0	4717.0	350.82*
55	347.0	4700.0	349.56
56	351.8	4807.0	357.52*
57	348.6	4867.0	361.98*
58	349.7	4700.0	349.56
59	348.5	4803.0	357.22*

TABLE III-5

SL-1 Fuel Inventory
(Cont'd)

Fuel Element Number	Initial U ²³⁵ Loading	Active Plate Material Recovered	Final U ²³⁵ Recovered*
60	346.3	4700.0	349.56
61	349.3	4700.0	349.56
62	348.9	4387.0	326.27
		TOTAL	11,534.85
Miscellaneous Fuel Material not Identifiable as to Fuel Plate No.		4961.4	369.00
		TOTAL	11,903.85

Reactor Vessel Debris
Uranium Recovery

	Total Weight Recovered (grams)	Wt % U	Uranium Weight Recovered
Fine Screenings	34550	1.6 ± 0.9	552.8 ± 311.0
Medium Screenings	12970	3.2 ± 1.6	415.0 ± 207.5
Coarse Screenings	4480	1.0 ± 1.0	44.8 ± 44.8
Total U from Debris:			1,013.6 ± 453.0
Total U ²³⁵ (Allow ~16% ± 3% depletion of 93.20% enrichment)			1,124.6 ± 510.0
Total U ²³⁵ accounted for:			13,029.0 ± 548.0
Total Initial U ²³⁵ loading:			14,007.50 grams
% Total Accounted for:			93.0 ± 3.9

*Calculated at 7.44 w/o of Active Plate Weight

3.4 Fuel Element Thermal Effect

Much of the damage incurred in the core was the result of thermal effects associated with melting and vaporization of fuel plate material.

Figure III-79 shows two fuel element assemblies which have been subjected to some thermal effect as evidenced by the spalling off of dark oxide from the surfaces of the plates. Most of the fuel plates were separated from each other and the spot welded side plates partly blown away. Both upper and lower end boxes were either blown off or physically separated. No bonding of surfaces had occurred.

Figure III-80 shows a side plate from an element. All spot welds were broken due to impact shear and not as a result of heat effect.

Figure III-81 shows fuel element #4 which was destroyed principally from the effects of melted and vaporized fuel material. One of the side plates, however, remains intact and the dead edge of each plate is shown still spot welded to it. The heat transfer in this region must have been very poor even though contact was metal to metal. The fuel plates, although appearing to have fused together at the lower end, were actually without bond and plates were separated easily by use of slave manipulator hands.

Figures III-82 and 83 show one of the center 16 fuel elements, fuel element #3, which was over 50% destroyed. The center of greatest destruction is approximately 3 to 4 inches below the midpoint of element. However, both side plates remain relatively intact, the two flux wire assemblies were unaffected, and residue of fragmented and melted material was blown both upward and downward into the spaces between the fuel plates. Figure III-83 shows that a portion of the outer fuel plate is missing. The missing portion of plate was found attached, but unbonded, to the neighboring shroud. The portion of plate was intact, distorted and partly splattered with metal.

Even for those fuel elements or plates which had undergone some degree of destruction from melting or vaporization of the fuel, parts adjacent to them remained relatively intact, principally due to the water acting as an insulation blanket and thereby effectively reducing heat conduction.

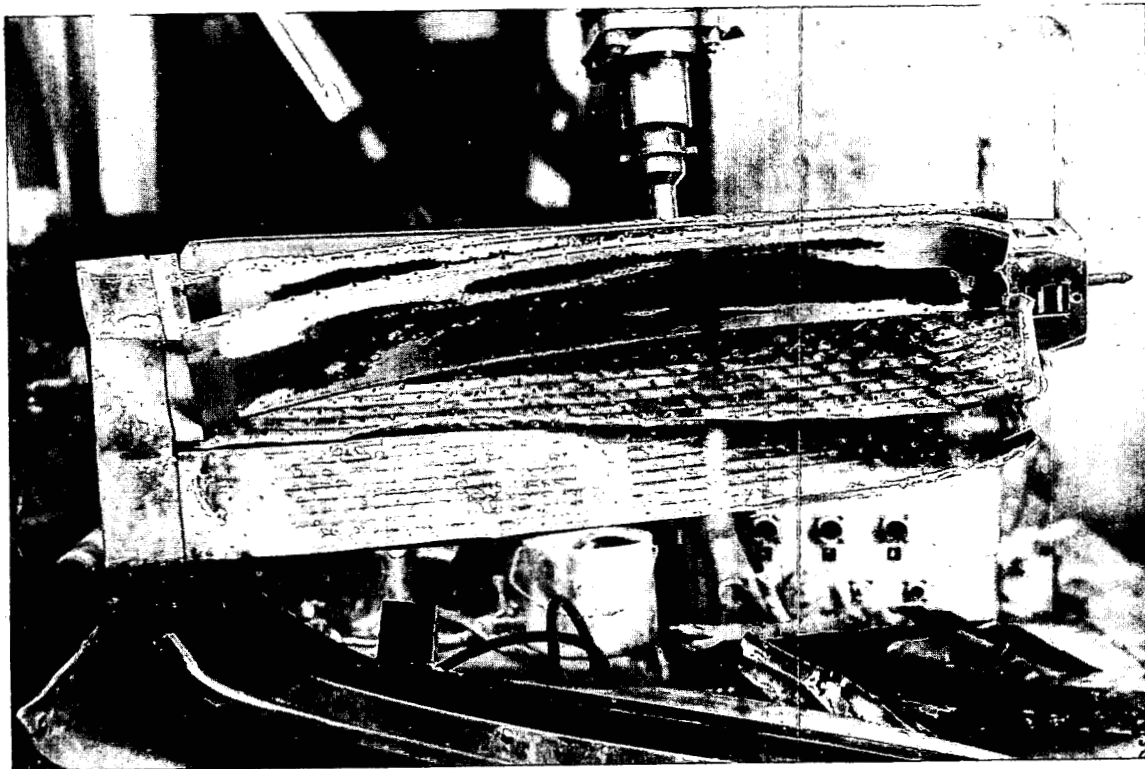


Figure III-79 Fuel Elements #60 and 18, Showing Heat Affected Areas

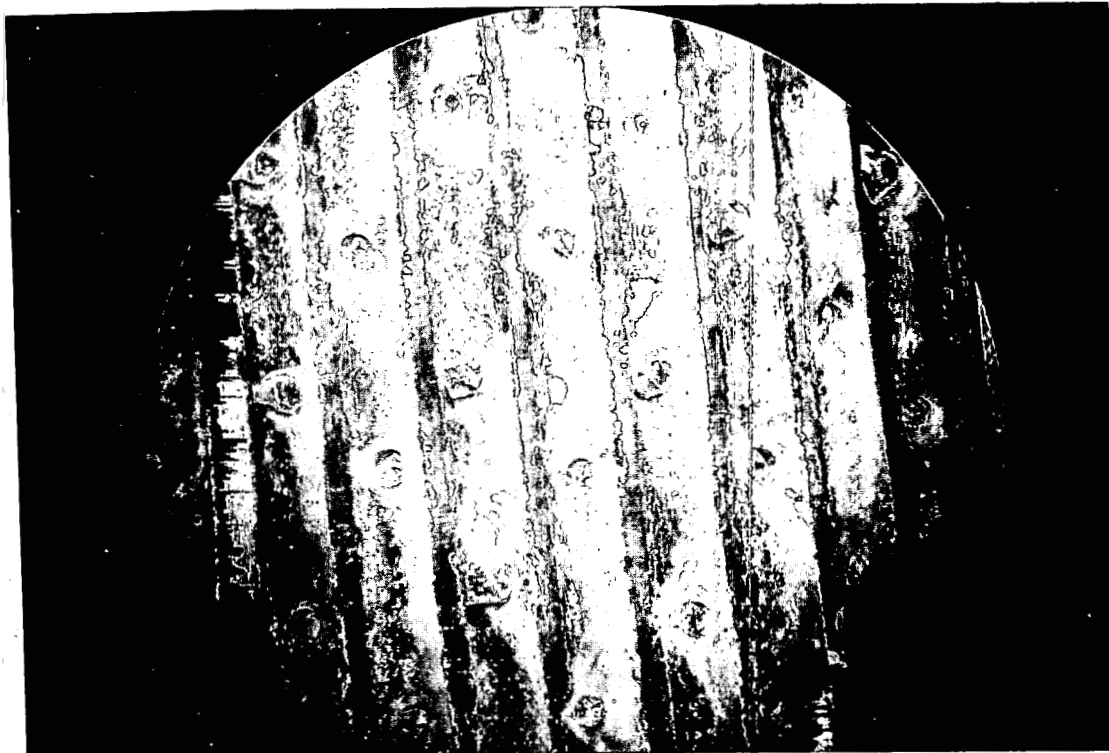


Figure III-80 Fuel Element Side Plate Showing Fracture of Spot Welds

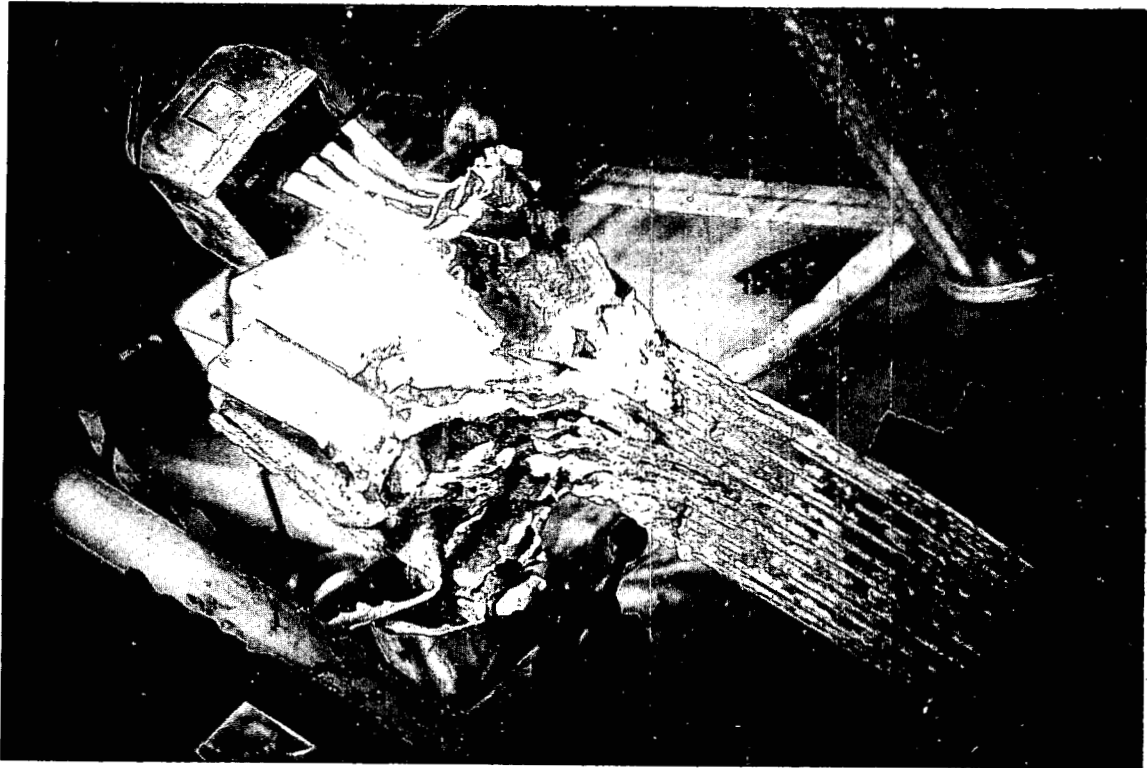


Figure III-81, Upper Section of Fuel Element #4

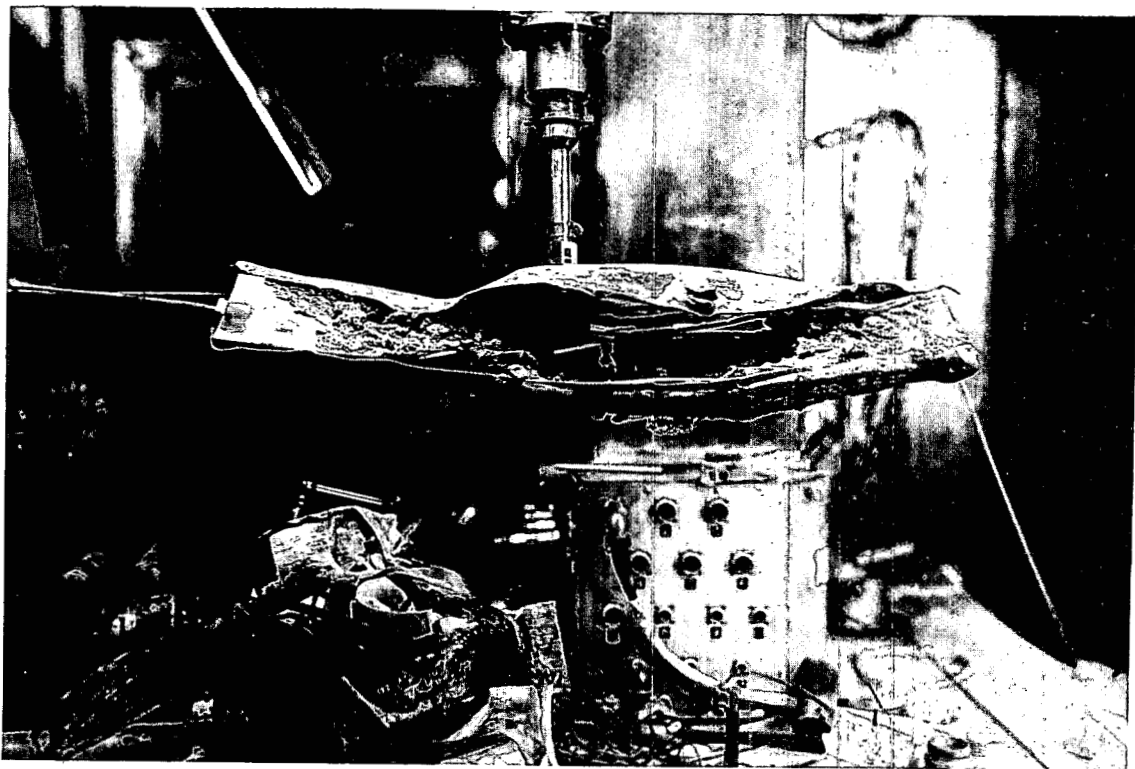


Figure III-82, Fuel Element #3

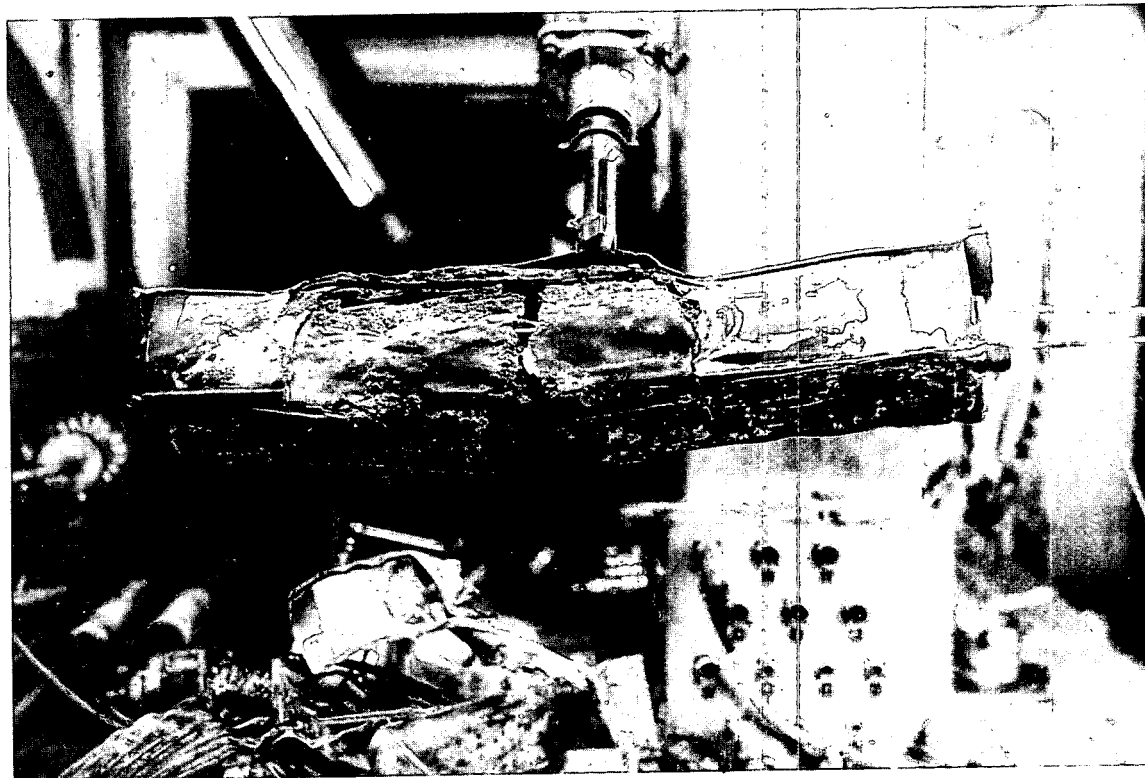


Figure III-83, Fuel Element #3

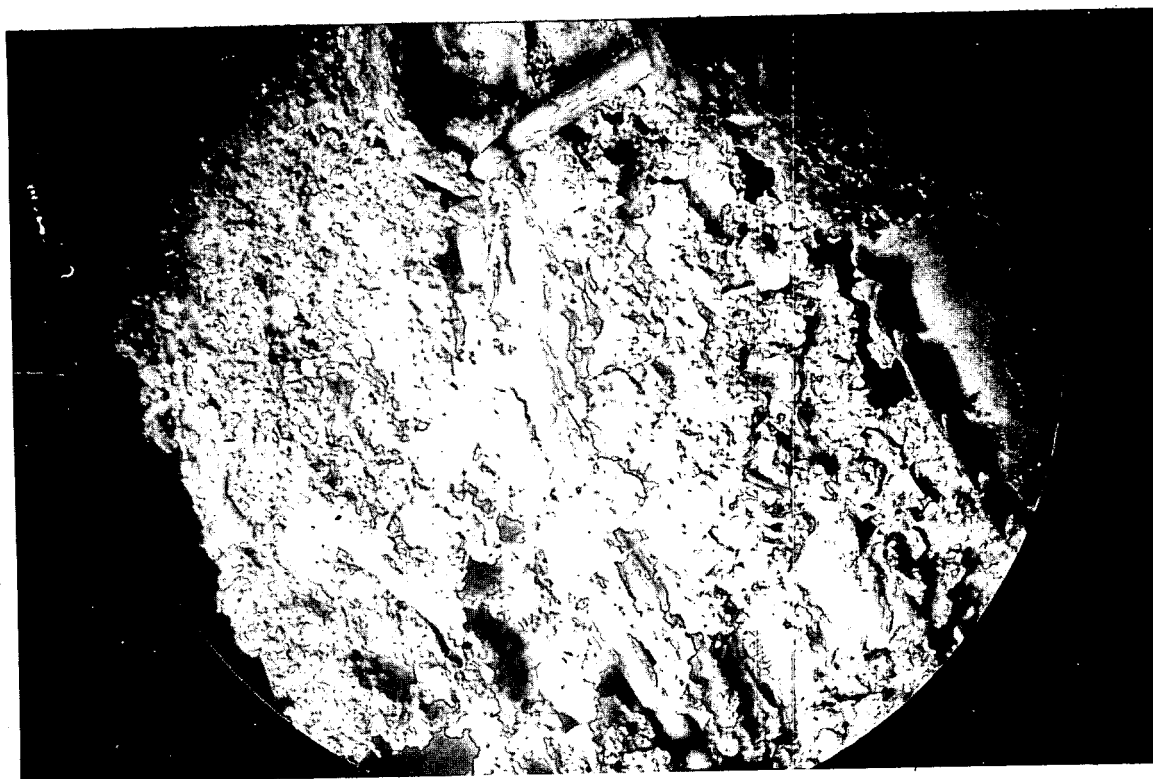


Figure III-84, Fuel Element #52, Showing Melted Region and Flux Wire Undamaged

Flux Wire Thermal Effects

Aluminum flux wires, containing alloy pellets, had been placed between the plates of some elements prior to the incident. Attempts were made to extract and identify each of these wires from the damaged elements without breaking apart the elements. The wires were generally restricted by the mechanical deformation of the elements; and in the majority of cases the plates had to be separated to extract the wires.

Despite the high temperatures attained by the plates, none of the flux wires appeared to have been damaged by the heat. Figure III-84 is a view of a severely melted region of element #52, showing intertwined flux wire to be undamaged except for mechanical bending. Deposits of spattered fuel have been found on the wires, and some wires were fractured. Most fractures appeared to have been entirely mechanical, although some of the breaks may have been induced by the action of a hot piece of fuel element coming in contact with the wire.

The wires, 0.188 inches in outside diameter, were in 0.310 inch wide water channels. Quite likely contact of the wires with the fuel plates occurred at relatively few points along the length of the wire. Heat transfer from the plates to the wires thus had to occur primarily through the water, which effectively provided an insulating blanket for the flux wires.

Aluminum-Uranium Ratio

In an effort to determine the fuel loss from areas of melting, the ratio of aluminum to uranium in selected areas of fuel plates was determined. 1/4" diameter punchings were taken from plate E-8 of fuel element #5 (Figure III-85) and from plate E-83 of fuel element #6 (Figure III-86). The punchings from plate E-8 were taken from upper, center, and lower regions shown in the photograph (Figure III-85). Punchings from plate E-83 were from the threshold of melt area. Photos in Figure III-87 shows the molten area and the swelling of plate E-83. Table III-6(a) shows the existing data from the above areas.

TABLE III-6 (a)

Aluminum/Uranium Ratios

Plate No.	Sample Region	Wt % Al	Wt % U	Al/U Ratio
E-8	Upper end	84.8	8.87	9.6
E-8	Center	95.7	0.69	138.7
E-8	Lower End	90.7	5.68	15.9
E-83	Threshold of Melt	80.9	7.23	11.2
E-83	Threshold of Melt	79.4	8.20	9.7
E-83	Threshold of Melt	87.7	7.99	10.9
E-316	New Fuel	90.56	7.98	11.35

Ratios of Al to U less than control samples of non-irradiated fuel plate can be explained by swollen regions forcing fuel between the cladding to enlarged thicknesses. Greater ratios indicate uranium loss from fission or possible volatilization.

Another set of punchings from plate E-550 of fuel element #39 was analyzed for Al and U. The punchings were selected to give an axial profile of uranium loss from element #39. The punching locations are shown by reference number in Figure III-88. The analytical results are given in Table III- 6 (b)

TABLE III-6 (b)
Aluminum-Uranium Ratios
Plate E-550/Fuel Element 39

Punching No.	wt/% Al	wt/% U	Al/U Ratio
41	95.67	1.42	67.4
42	89.49	8.06	11.1
43	88.67	7.07	12.5
44	83.86	5.54	15.1
45	92.85	3.42	27.2
46	90.79	4.39	20.7
47	93.63	2.64	35.5
48	89.18	5.84	15.3
49	90.02	5.85	15.4
50	88.35	7.71	11.5
316 New Fuel	90.56	7.98	11.35

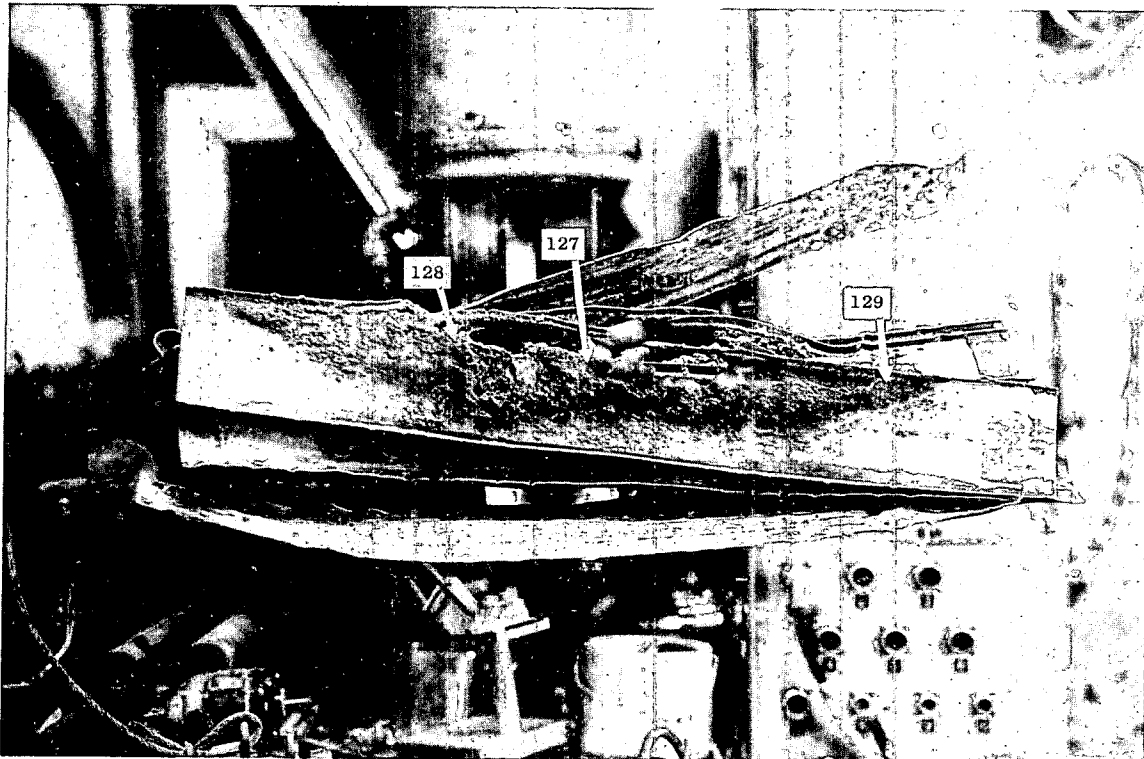


Figure III-85, Sample Locations on Fuel Element #5

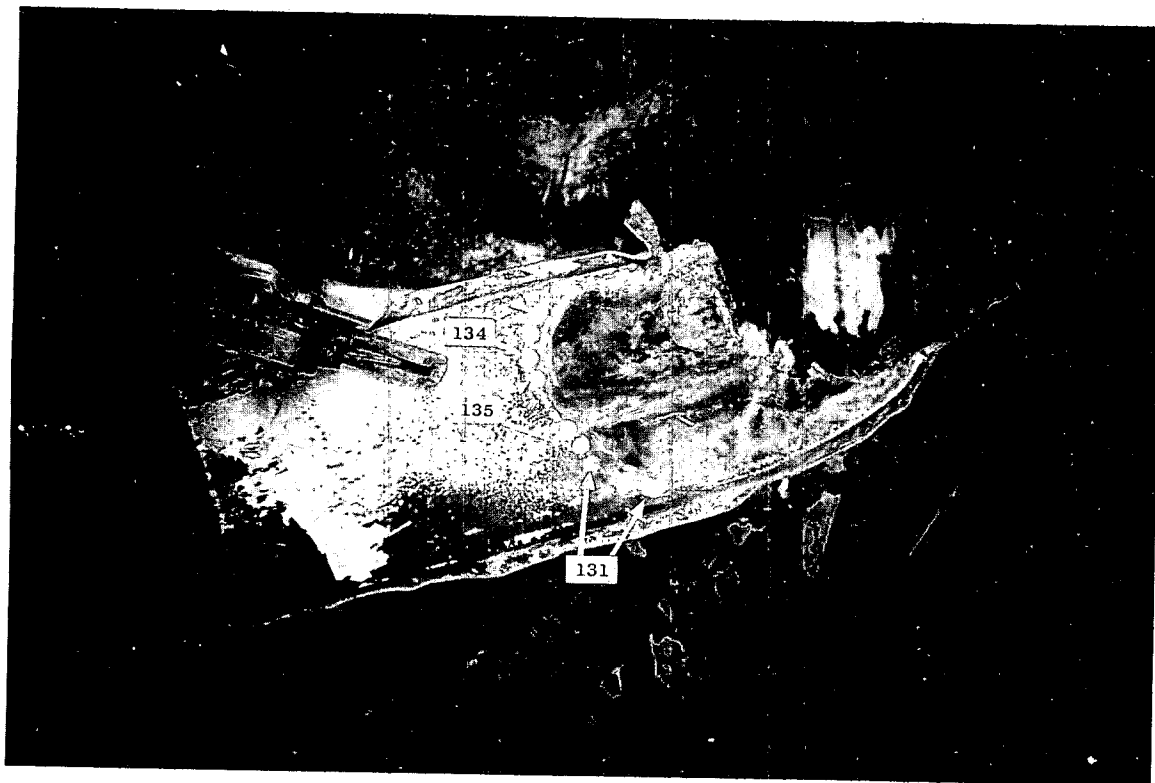


Figure III-86, Sample Locations on Fuel Element #6



Figure III-87, Cross-Sectional View of Fuel Plate Swelling from Fuel Element #6

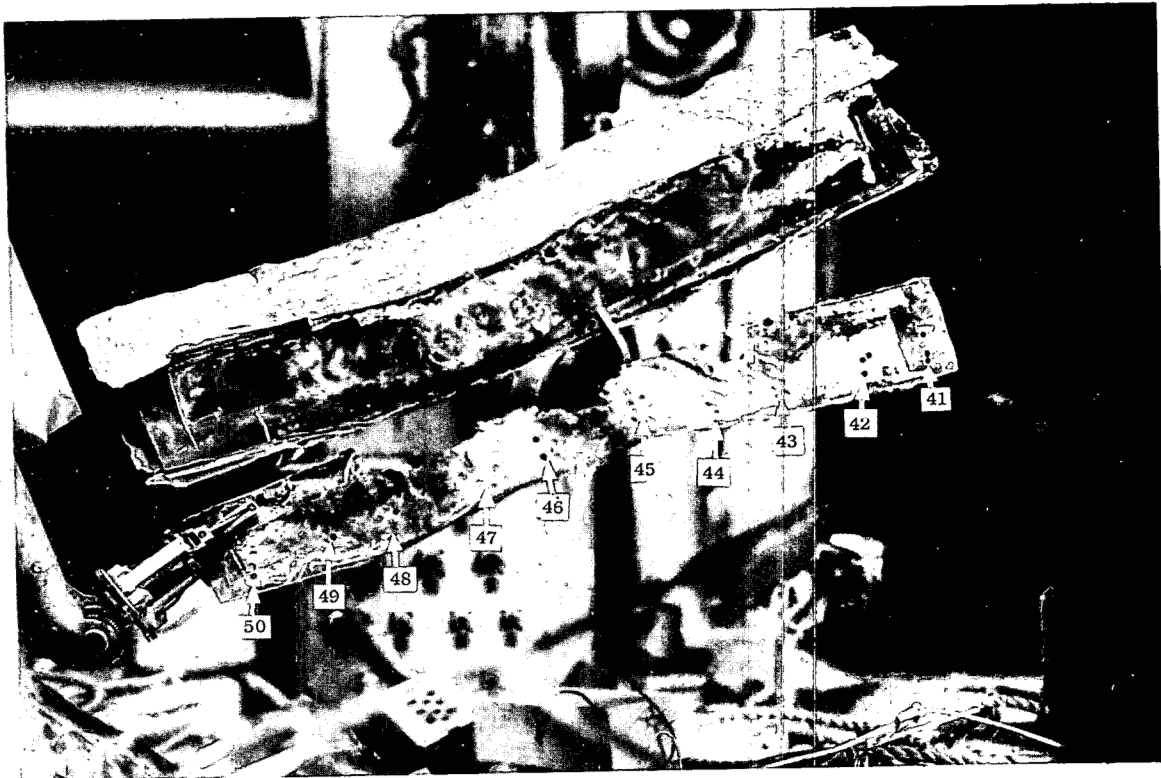


Figure III-88, Sample Locations on Fuel Element #39

4. Nuclear Evidence

4.1 Flux Wires

Just prior to the SL-1 incident, 45 flux wires had been placed between fuel plates at various regions throughout the core. Each wire contained either 10 or 13 small cobalt - aluminum pellets, spaced three inches apart (476 pellets total). Each pellet was 3/32-inch long by 40 mils in diameter, weighed approximately 5 milligrams, and contained cobalt in the concentration of 0.5% by weight, for a net of 25 micrograms of cobalt per pellet. It was intended that these wires would receive approximately a 35 megawatt-day exposure during normal reactor operation. The pellets had received no exposure prior to the incident, and therefore provided a direct measurement of flux and energy densities for the incident.

The wires containing the pellets were enclosed in protective aluminum sheaths with an identifying number printed on the plate attached to the top of the sheath. All of the wires have been recovered in whole or in part. In some cases the identifying tags were broken off or the wire was broken in several pieces making it impossible to identify wires or sections thereof. However, approximately 352 pellets have been recovered, identified, and analyzed. Figure III-89 shows the locations of the wires in the core.

Since the exposure received by the pellets was about 10^{-4} of that for which they were designed, the activity was quite low. The surface of the pellets was badly contaminated with the usual fission products which normally masked the cobalt activity. (Typical wires read about 25 R per hour gamma at one foot) Some attempts were made at chemically separating the small amount of cobalt from the fission products, but this method generally proved unreliable. Most of the pellets were counted whole after being cleaned ultrasonically. Cobalt activity, accurate to about $\pm 10\%$, was obtained from the pellets in the high flux regions using nominally two hour count times on a 3×3 NaI (Tl) crystal at a distance of three centimeters from the source (256 channel gamma analyzer). Pellets from the lowest flux regions had cobalt activity barely discernible from the fission product background following 10 hour counting times.

It can be shown that the measured cobalt activity (A) in $\frac{\text{dis}}{\text{min}}/\text{gm}$ of cobalt, corrected back to the time of the incident, when multiplied by 1.06×10^7 gives the equivalent 2200 m/sec flux in n/cm^2 for short exposure times and a Co^{60} half life of 5.3 years.

A more useful quantity pertaining to the effect of the flux on the fuel plates is the nuclear energy generated per unit mass of fissile material. Using a flux disadvantage factor of 0.91 for the fuel and a value of 3.2×10^{10} fissions to produce one watt-sec (joule) of total nuclear energy (of which only 86% is immediately deposited in the plates), the following conversion factor is obtained:

$$\frac{\text{MW sec}}{\text{Kg U235}} = 4.1 \times 10^{-14} (\phi t) \frac{\text{n}}{\text{cm}^2}$$

Knowing the original fuel loading per element (350 gm of U^{235}) and the approximate burnup (8% average over core, 20% peak), the energy generated per element or per cm^3 of a portion of the fuel meat can be easily calculated. In determining the total energy generated, the average over the longitudinal flux distribution was obtained for the active fuel. Corrections for the radial variation of the flux were made for cases in which a single wire from an element was located significantly off the center-line of the element (C. W. Luke, Combustion Engineering, Incorporated-private communication). This radial correction in no case was taken to be greater than 20%.

The energy generated per element for those elements containing flux wires is shown in Figure III-90. The tabulated results of flux recorded on each pellet is given in Appendix . The longitudinal flux distribution was peaked downward in the center section of the core because of the partially inserted central control rod, while near the outer portion of the core, the flux distribution was a flattened and chopped cosine. Typical longitudinal flux distributions are shown in Figures III-91 and 92. A summary of the most significant data obtained from the flux wires is given Figure III-93.

Using this data, the total power generated in each typical section is summed:

<u>Center Section</u>	<u>Totals</u>
4 at 6.3 ± 1.0	25.2 Mw-sec
8 at 4.7 ± 0.5	37.6 Mw-sec
4 at 3.7 ± 0.8	14.8 Mw-sec
Center Total	78 ± 7 Mw-sec

<u>Outside Section (No Cd strips)</u>	
4 at 3.3 ± 0.4	13.2 Mw-sec
4 at 2.1 ± 0.4	8.4 Mw-sec
4 at 1.9 ± 0.3	7.6 Mw-sec

<u>Outside Section (with Cd strips)</u>	
4 at 2.0 ± 0.5	8.0
4 at 1.9 ± 0.5	7.6
4 at 1.3 ± 0.4	5.2
Outside Total	50 ± 4 Mw-sec

Total Energy of Excursion: 130 ± 10 Mw-sec

Positive flux wire data for the very center of the core, the highest flux region, were not obtained. All of the pellets from this region were either lost during the excursion or unidentifiable. One wire, found intact, but without an identification tag, was interpreted as having been in one of the four center elements. From its activation, a peak energy

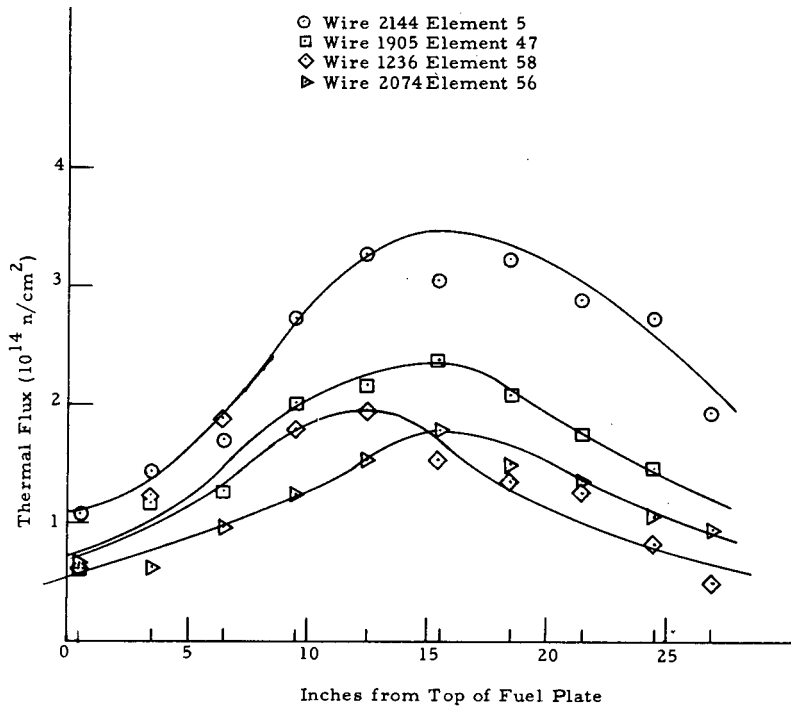


Figure III-91 Longitudinal flux distributions in outer 24 elements (in water)

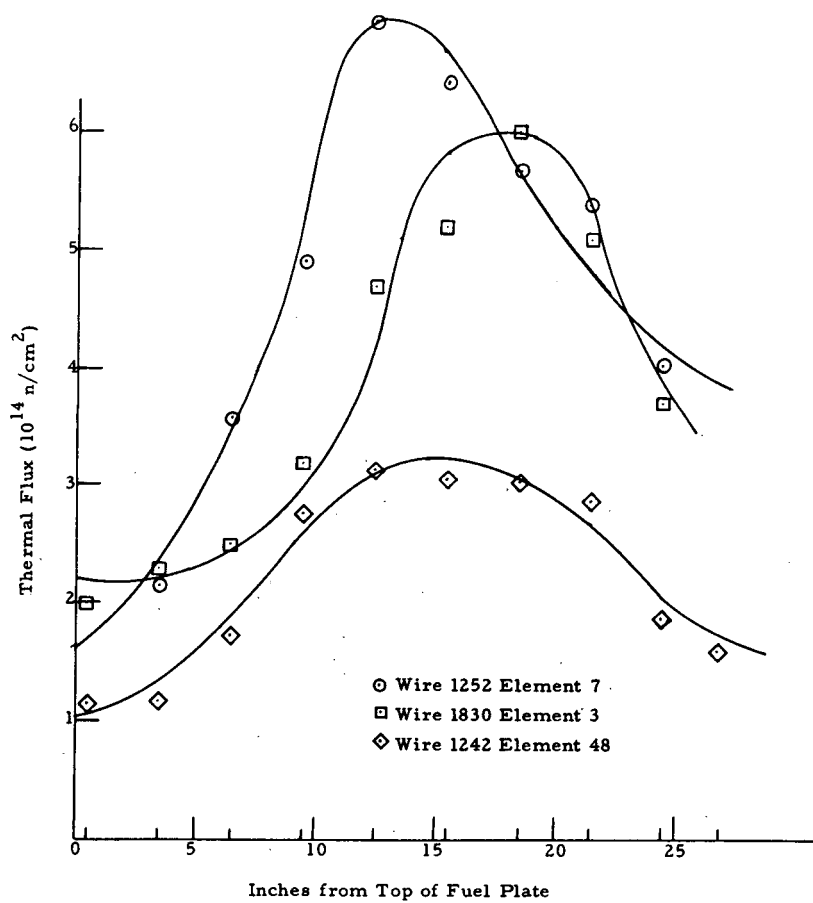


Figure III-92 Longitudinal flux distributions in center 16 elements (in water)

Quadrant of Core - energy generated per element in Mw-sec and estimated inventory of U-235

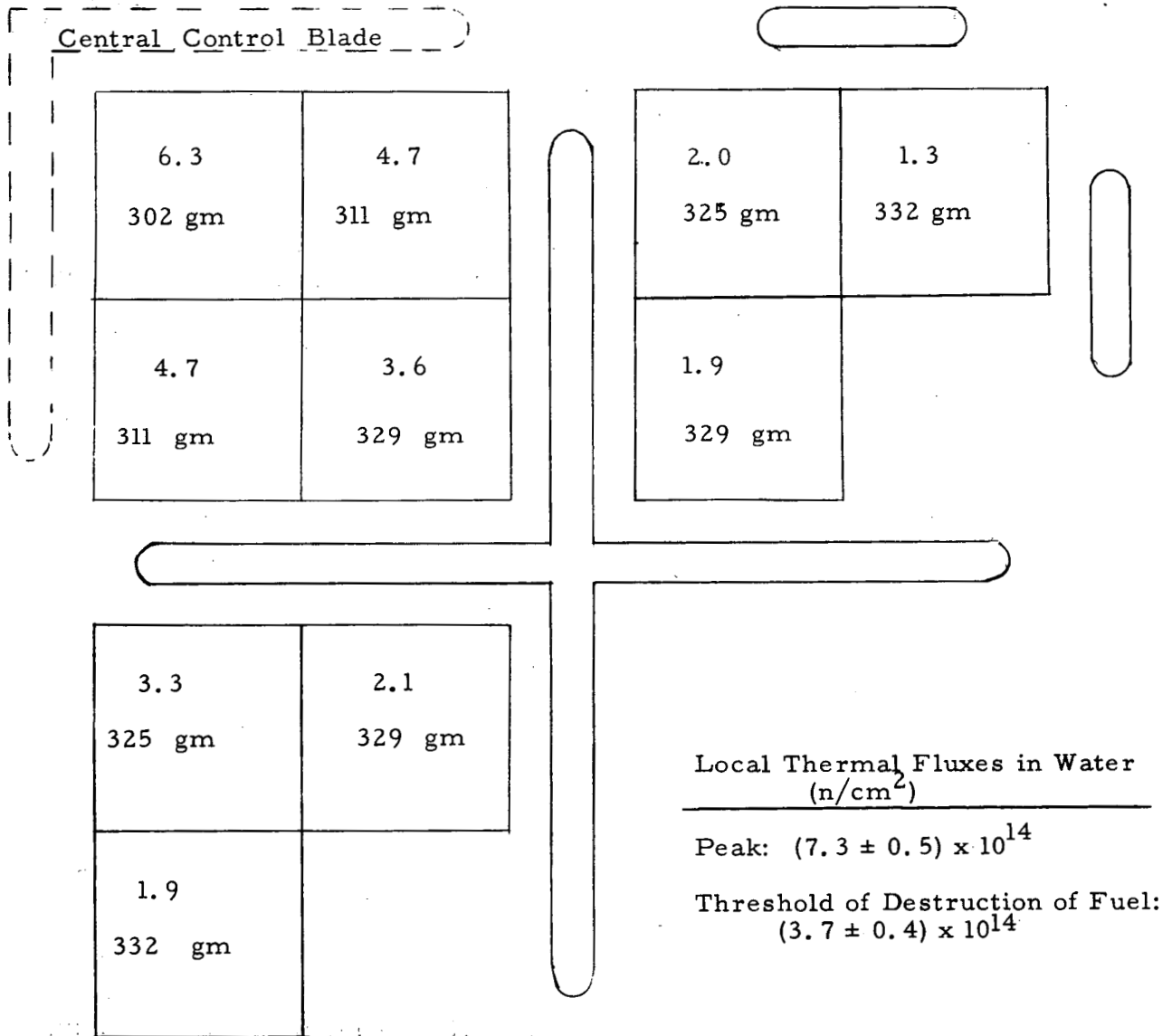


Figure III-93

Energy distribution during SL-1 excursion

density of between 30 and 35 Mw-sec/Kg of U-235 has been deduced. The accuracy of most of the other data has a standard deviation of approximately 15%. The peak to average energy density ratio was approximately 3/1.

4.2 Other Activation Data

Initial Data

Soon after the incident, some thermal and fast neutron activation data were obtained from materials on or near the three victims. The reported fluxes are given in Table III-7, below Samples for which previous exposure history was uncertain have not been included.

TABLE III-7

<u>Sample</u>	<u>Activation Product</u>	<u>Neutron Flux (n/cm²)</u>
1. Cigarette lighter (1) screw from first victim	Cu-64	9×10^9 (thermal)
2. Watch band buckle (1) from second victim	Cu-64	2×10^{10} (thermal)
3. Ring from third (1) victim	Au-198	9×10^9 (thermal)
4. Scalp hair (2) first victim	P-32	2×10^{12} (fast)
5. Pubic hair (2) first victim	P-32	8×10^9 (fast)
6. Scalp hair (2) second victim	P-32	2×10^{13} (fast)
7. Pubic hair (2) second victim	P-32	5×10^{11} (fast)
8. Scalp hair (2) third victim	P-32	9×10^{12} (fast)
9. Nuclear accident dosimeter (1) at top of stairway Stellite Bearing from #4 Shield Plug	Au-198	6×10^7 (thermal)

The #4 shield plug had seen no previous service in the reactor (except during the initial critical experiment). Normally, the Stellite bearing was located one foot below the pressure vessel head, surrounded by 0.2 inch thick stainless steel guide tube wall with the extension rod through its center. The bearing was found in its guide tube in the fan room.

The Stellite was 55% cobalt, and showed barely measurable activity when recovered in July, 1961. The surface of the bearing was machined

1. SL-1 Reactor Accident Report, Combustion Engineering, Inc. May 15, 1961, IDO-19300
2. SL-1 Reactor Accident Autopsy Procedures and Results, LAMS-2550

away to remove contamination. An activity of approximately $20 \frac{\text{dis}}{\text{min-gm}}$ was measured over most of the bearing. This corresponds to 4×10^8 n/cm² thermal flux. The stainless steel guide tube would provide about 10% attenuation, while the self-shielding effect of the bearing is about 40%. The flux which impinged on the bearing was probably not isotropic, and was apparently no greater than 10^9 n/cm². A direct upward streaming beam of neutrons would have been ineffective in activating the bearing.

Shield Plug Flanges and Caskets

Samples of the shield plug flanges were analyzed for Co-60 activity as were the "Flexitallic" gaskets. The previous history of the latter was uncertain. This fact and the shielded location of the gaskets made it impractical to attempt to derive useful information from them.

The flange material from the shield plugs known to have been in the reactor head for all previous operation indicated total thermal fluxes of about 3×10^{12} n/cm². This value, which reflects activation during normal operation and not during the incident is consistent with flux measurements taken four feet above the reactor head during normal operation (IDO 19005, Vol. II, 4×10^3 n/cm² - sec at 1.3 MW).

Instrument Support Pipe

Approximately five months before the incident, a stainless steel pipe was attached to instrumented element #1 so as to provide support for the thermocouple wiring. Though the activation on this pipe from the incident was negligible, the pipe was useful in obtaining a flux profile during normal reactor operation between the top of the core and the top of the #8 nozzle. The pipe was analysed for Co-60 activity and the results are shown in Figure III-94.

These data show that a factor of 1.5×10^4 existed between the flux at the top of the core and the flux at the top of the nozzle during normal operation. This condition existed with four feet, four inches of water containing approximately 15% steam voids above the core. During the initial excursion, seven feet of water containing no voids was above the core. Thus, an attenuation factor of considerably greater than 1.5×10^4 existed between the top of the core and the top of the nozzle during the initial SL-1 excursion.

PL-II Sample

A sample of structural material for the newly designed PL-II core had been placed on top of one of the dummy elements during the pre-incident shutdown period. A portion of this sample was blown out of the pressure vessel and recovered early in the cleanup operation. The indication of excursion energy derived from the activation of the cobalt (0.1%) in this sample gave one of the earliest estimates of the total energy of the excursion, though this result has been superseded by the more accurate flux wire data. The 250 ± 80 Mw-sec obtained by various methods of extrapolating the measured 2.5×10^{13} n/cm² flux from the PL-II sample to the core was higher than the flux wire results by 1-1/2 standard deviations.

SL-1 Instrumentation Support Pipe

Co⁶⁰ Activity

vs.

Longitudinal Position

Elemental Cobalt = .0162% ± .0035

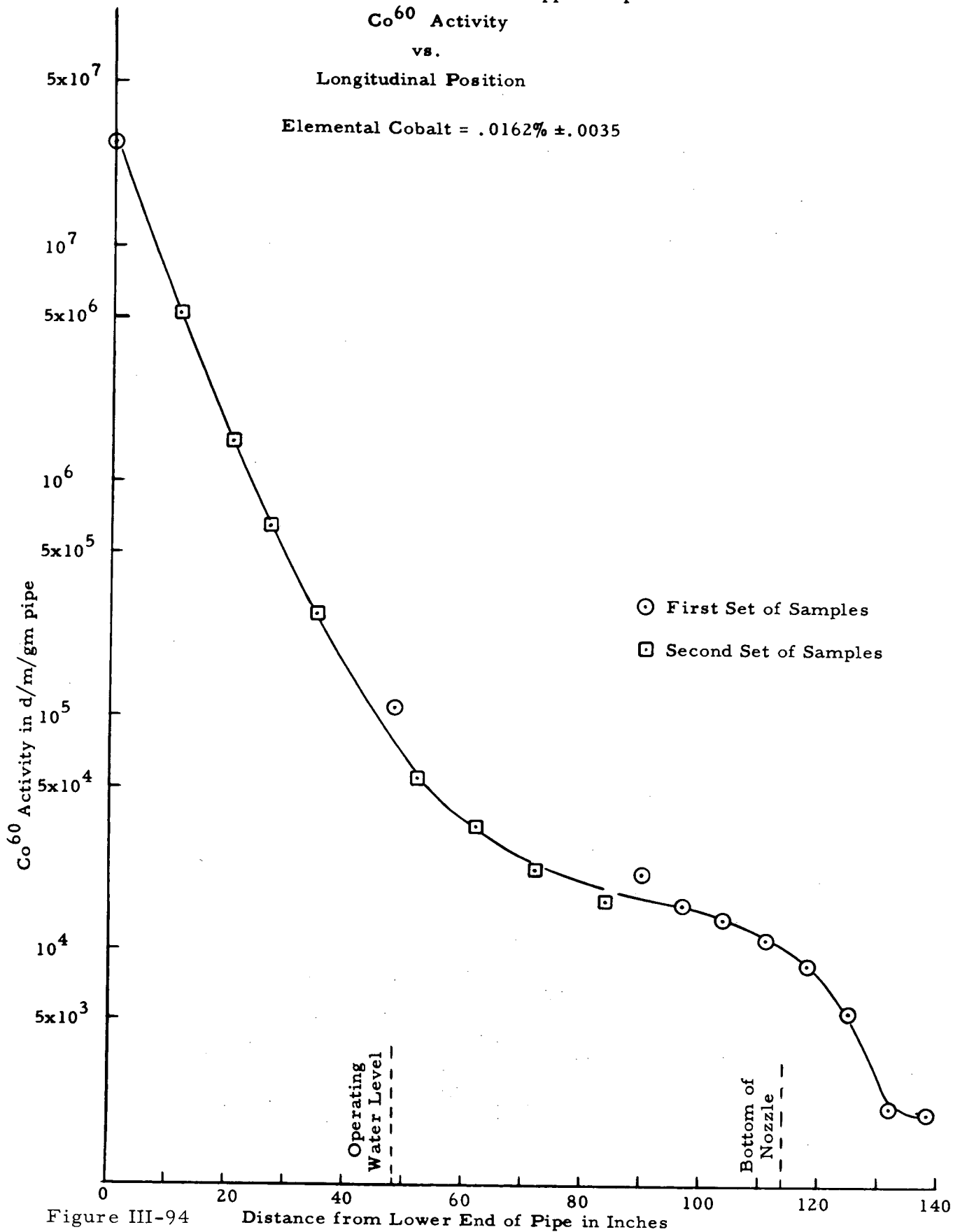


Figure III-94

Distance from Lower End of Pipe in Inches

However, the flux of 2.5×10^{13} n/cm² is useful in estimating what the fluxes might have been further away from the core.

Film Badge Activation

The film badges of the victims were not recovered until nearly seven months after the incident. The nuclear accident dosimeters in the badge packets had no measurable activity because of the long decay time. The most promising material in the badge was silver, with its resultant 250 day Ag-110 activation product, resulting from a 2.8 b thermal cross section. Each badge contained about 1/6 gram of silver, which was thoroughly decontaminated. A disintegration rate of 20 dis/minute, about 1/2 of normal background, could have been detected. This value corresponds to a thermal flux of 1.5×10^{10} n/cm², which is therefore an upper limit to the thermal fluxes experienced by the badges.

4.3 Fission Product Release

At the time of the incident, the SL-1 had been shut down 11 days since its last power operation, with most of its operation having been spread out over a three year period. The main gaseous fission products remaining at this time were I-131, I-132, and Xe-133. These represented a small fraction of the total inventory of gamma emitting fission products, the I-131 being only 6% of this inventory at the time of the incident.

The gross gamma-emitting fission product inventory, calculated by the Way-Wigner formula (1), is listed in the table below at various significant times during the SL-1 post-incident history.

<u>Time</u>	<u>Gross Gamma Fission Product Inventory</u>
Incident, January 3, 1961	500 x 10 ³ curies
March 1, 1961	200 x 10 ³ curies
June 1, 1961, cleanup began	120 x 10 ³ curies
August 1, 1961, cleanup of fan room	90 x 10 ³ curies
December 1, 1961, reactor in Hot Shop	65 x 10 ³ curies
April 10, 1962, critical experiment	50 x 10 ³ curies

On June 1, 1961, the average gamma radiation level throughout the operating room (exclusive of local hot spots and the area immediately over the reactor) was approximately 60 R/hr. four feet above the floor. This field could be produced by about 1800 curies scattered over the floor (uniformly) and 300 curies in the ceiling above the reactor. Since significant shielding of the radiation by various equipment, shield blocks, etc. occurred, and with due consideration for the local hot spots, particularly the top of the reactor, it is believed that the curie release represented by a 60 R/hr. field would be twice as great as calculated, or about 4000 curies, representing 3% of the fission products.

(1) Glasstone, Principles of Nuclear Reactor Engineering, P. 118-120.

As an independent check, the activity of the truckloads of debris removed from the operating room and fan room was measured with a survey meter from a distance so as to simulate a point source. Each load of debris was approximately corrected for self absorption (factor of 1.5 to 2.0). The total gamma activity of all the debris, including the building walls and equipment, was measured to be about 2400 curies, corrected to June 1, 1961. This represents about 2.1% of the total gamma fission product inventory, and is probably an underestimate.

Very little of the particulate fission products that left the vessel actually escaped outside of the building, and the gaseous fission products emitted at the time of the incident were only a small fraction of the total. Thus, it appears that about 5% of the core inventory can be accounted for outside of the pressure vessel.*

A film badge from one of the victims was recovered from the operating floor seven months after the incident. The polyethylene picture was badly darkened from radiation damage. Tests on a similar polyethylene sheet showed that at least three million rad of ionizing radiation was received by the badge in question. This total far exceeds the general gamma levels in the region of the badge, and therefore, was probably produced primarily by beta contamination of the badge. Note that many of the personnel involved in the early cleanup operations received large beta to gamma dose ratios, some as large as 15 to 1.

Attempts to account for the amount of uranium on the operating floor were unsuccessful. Shoe covers of personnel entering the building, for instance, picked up trace amounts of uranium. The only specific identifiable quantity of fuel recovered was in the form of several small pieces of spongy metal containing only two grams of uranium, these being found in the fan room. All the evidence indicates that fuel and fission products were rather finely divided and scattered throughout the operating room.

4.4 Excess Reactivity

The central control rod was bound in its shroud at a position corresponding to $20 \pm 1/2$ inches withdrawn from normal scram. The other four control blades were found bound essentially in their scram positions. Details of the collapsed central shroud and imprisoned rod are given in Section III-1.1. The rod was grasped by the shroud at the time of the first high pressure surge, which developed at or very near to the time of peak power during the burst, and no motion of the rod relative to the blade occurred thereafter. The 20 inch withdrawn position does not necessarily represent the exact maximum reactivity of the excursion. However, the time during which most of the energy was released was quite short, so that during this time the rod would have been able to move less than $1/2$ inch as a result of any plausible forces applied external to the core (see the following section, III-4.5). Therefore the 20 inch position of withdrawal corresponds to the approximate upper limit of the reactivity of the excursion, taking into consideration that it is unlikely that the control blade was being inserted when seized.

*Note added in proof: Both these measurements are obviously crude, and are prone to underestimate the fission product release. The apparent inconsistency with the uranium inventory is the subject of continued work.

The SL-1 core was normally operated with all five control rods banked (equally withdrawn), and there is very little data from which to estimate the excess reactivity of the central rod withdrawn by itself in a cold clean reactor. A summary of existing pertinent critical position data taken within several months of the incident is given in Table III - 8 . These values had been obtained during reactor physics measurements. Cadmium strips had been added to two of the outer T- shrouds in November to enhance the reactor shutdown margin.

Table III- 8

Summary of Critical Positions and Rod Worths (ambient temperature, no xenon)

September, 1960 - before adding Cd strips:	
5-rod bank critical at	10.5 inches
central rod alone critical at	14.3 inches
After adding Cd strip - November, 1960	
5-rod bank critical at	12.0 inches
central rod alone critical at	not measured

Thus, the addition of the cadmium strips in two of the outer T-shrouds raised the clean, cold critical position of the banked rods from 10.5 to 12.0 inches.

The effect of this change in rod position on reactivity has been obtained by reference to the differential rod-worth curves of zero power experiment loadings (1) #19 and #45, which were identical loadings, each with one full boron strip on each of the forty elements. The incident core had uranium burnup, high boron burnup on the 1/2-strips and on the lower part of the full strips, with lesser boron burnup near the top of the full strips. By calculating the variation of thermal neutron leakage in the boxes defined by the control blades, it was concluded that the central rod's differential worth would have been approximately 20% higher in the highest burnup region of the incident core compared to loadings #19 and #45. Assuming approximately the same increase would apply to the banked rod-worth, the effect of moving the bank from 10.5 to 12.0 inches, near the region of maximum burnup, is calculated to be 3.2 dollars (ref. cited, Figure 26, P. 56 showing 1.8 dollars/inch in this region for loading #45). Thus, the cadmium strips added about 3.2 dollars to the shutdown margin.

The differential rod-worth curve for the central rod operating with the other rods fully inserted is shown in Figure III- 95 . The solid curve is the general shape of a differential worth curve for loading #45 (ref. cited, Figure 24 and Figure 25) normalized to two data points for the central rod with the others fully inserted (ibid, P. 44). The dashed curve is the approximate correction made for the half-strips and the burnup between the incident core and loading #45. Note that the peak of the curve has been shifted to a lower position in the core. From this curve, it is

(1) ALPR Zero Power Experiments On the Argonne Low Power, D.H. Shaftman, ANL 6078

found that the 14.3 inch critical position, before adding cadmium to the T-shrouds, is raised to 16.7 inches with the cadmium. Prompt critical is at 17.6 inches. The 20 inch position is worth 3.4 dollars or 2.4% $\Delta k/k$ above delayed critical. Some representative reactor periods in this range of K-excess are listed in Table III-9, using calculated lifetime of 6.1×10^{-5} seconds for the SL-1.

Table III- 9

Reactivity (% $\Delta k/k$)	Period (milliseconds)
1.7	6.0
1.9	5.0
2.0	4.5
2.2	4.0
2.4	3.5
2.7	3.0
3.6	2.0

Estimated reactivity at 20 inches - 2.4% $\Delta k/k$

The results given above for the critical position and worth of the 20-inch position for the central control rod are derived from very limited applicable data. In particular, the differential rod worth curve indicates a very large total worth for the central rod, though it is probably not completely valid to interpret the integral of this complete curve, covering such a large variation in reactivity, as being a true total rod worth. The curve does imply a high shutdown margin existed. The small correction for burnup (and the 1/2 boron strips), amounting to less than 20%, is not precise, but is not likely to be far enough in error to effect the results significantly. No correction was applied for the effect of the added cadmium in the T-shrouds on the worth of the central rod, an effect which would probably be positive. It is estimated that the effect of all the uncertainties is to make the reactivity corresponding to 20 inch withdrawal certain by about $\pm 0.3\%$ ΔK standard deviation. Since the rod may not quite have been at 20 inches, and since some plate expansion effects would have occurred at the time the major shutdown mechanism of steam formation began (see Section IV-1.2), the representative period was between about 3.3 and five milliseconds, with a best value of four milliseconds.

Between the time that the Cd strips were added and the time of the incident, it is assumed that the critical position of the banked rods did not change significantly, at least in reference to the position uncertainty of a banked rod measurement (within 0.3 inch). The change due to normal burnup of the uranium and boron would have been small during this six week period. There is no evidence to indicate that any significant amount of boron strip material had been physically lost from the reactor during this period,⁽²⁾ as can be shown by a careful study of the rod positions corrected for variations in xenon poison and steam void effect.

(2) H. Cahn, Combustion Engineering, Inc., - SL-1 Control Rod Positions, November - December, 1960 ; September 18, 1961.

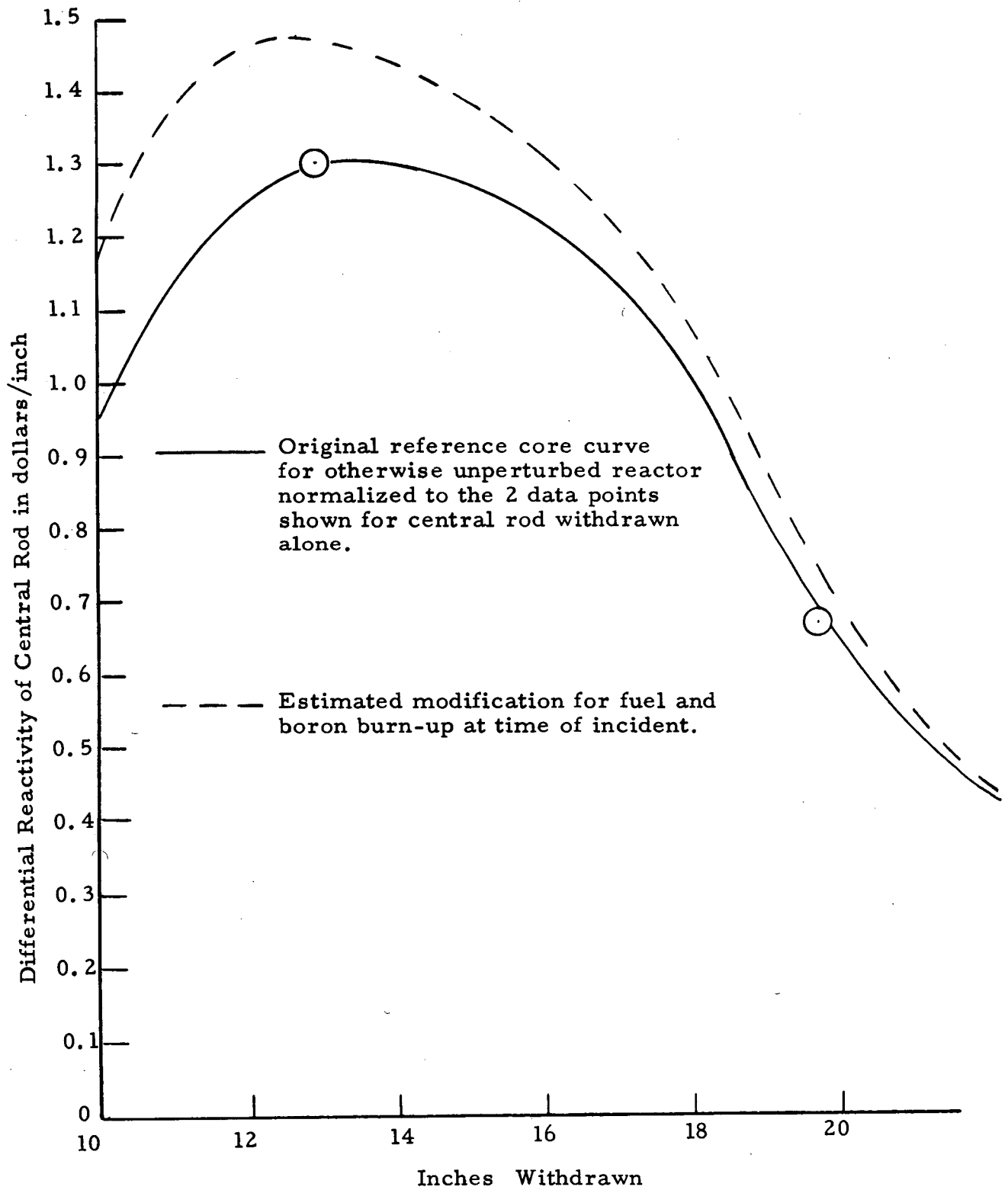


Figure III-95 Differential worth curve for central control blade with four blades completely inserted.

4.5 Central Control Rod Withdrawal

Motion of the central control blade from its inserted position, past the 16.7 inch critical position, and to the 20-inch withdrawn position must have been sufficiently rapid to permit the blade to reach the 20-inch position before significant steam was formed, about 1/10 second after delayed critical. As stated in Section III-2.3, the evidence will not support the hypothesis that the central control blade was ejected by a chemical explosion. The only known mechanism for getting the control blade to the 20-inch withdrawn position consistent with the physical evidence is manual withdrawal.

To evaluate the possibility of manual withdrawal of the rod, a mockup was made using a spare central control blade attached to the end of a control-rod and shield-plug mechanism, with the blade in a pool of water so as to simulate conditions of the incident (the blade was not enclosed in a shroud for the simulation). Using the actual "incident" handling tool, several different subjects withdraw the blade, under various conditions. The motion always commenced from the scram position or with the rod held up by a C-clamp, approximately three inches above the scram position.

A summary of the various conditions for which the subjects were told to expend maximum effort and the relative results obtained is shown in Table III-10

Table III-10

Manual Withdrawal of the Central Control Rod
With Maximum Effort

<u>Conditions*</u>	<u>Average time from critical (16.7inches) to 20 inches</u>	
1) C-clamp in place	49 m sec	
2) No C-clamp, rod resting on spring	46 m sec	375 m sec from fully inserted to 20 inches
3) No C-clamp, two men withdrawing rod	45 m sec	
4) Stuck rod, quickly released	56 m sec	
5) With C-clamp, Handling tool grasped at middle	77 m sec	Subject was unable to pull rod past 27 inches
6) With C-clamp, handling tool grasped at top	94 m sec	Subject was unable to pull rod past 22 inches

*Only one subject at a time pulled the rod. The handling tool was gripped near the bottom, unless otherwise noted.

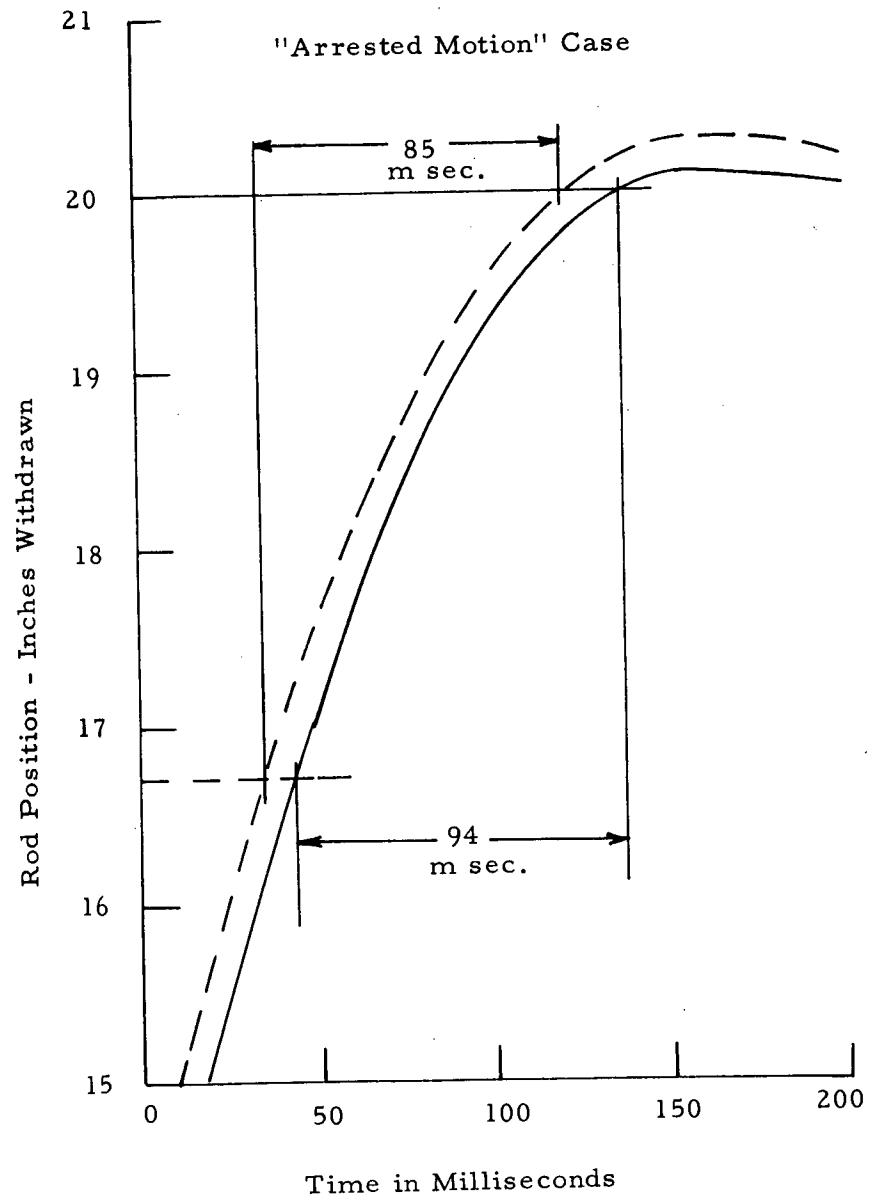
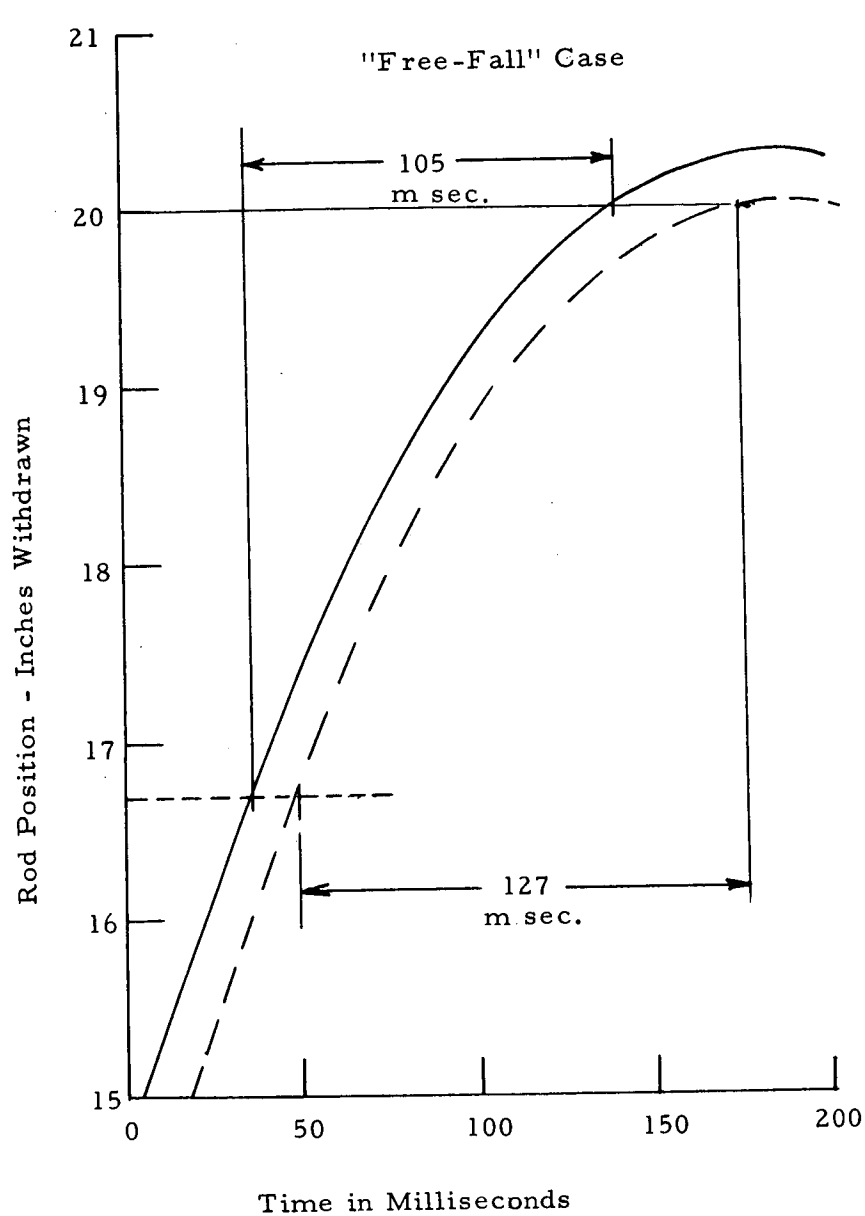


Figure III-96 Two experimental rod-withdrawal situations in which the rod was not pulled completely with maximum effort. Solid and dashed curves are results of two different tests.

As will be shown in the subsequent section, the control rod withdrawal times from critical to 20 inches of the order of 50 m sec are more than adequate to assure that the rod reaches the 20-inch position before steam is formed. The time differences between any of the first four cases, in which the handling tool was gripped near the bottom, are not significant. The less proficient gripping positions higher up on the handling tool resulted in significantly slower times of withdrawal.

Other motivations besides the expenditure of maximum effort to withdraw the rod as fast as possible were simulated. A "casual" but complete withdrawal of the rod averaged 75 m sec from the critical position to the 20-inch withdrawn position, about 60% longer than the time for maximum effort withdrawal.

A rapid pull, not followed through for complete rod withdrawal, might have caused the blade to rise to the vicinity of 20 inches, followed by a free fall trajectory. The data obtained for the simulation of such an event are presented in the left-hand graph in Figure III-96 . The blade would have been moving slowly near the 20 inch position, and the elapsed time from the critical position could have varied from the minimum possible 50 milliseconds to more than a hundred milliseconds, depending on the particular free fall trajectory. A curve within this range will certainly satisfy the excursion conditions rather accurately.

A rapid pull followed immediately by an attempt to stop the rod is shown in the right-hand graph of Figure III- 96 . The subject would not have had time to respond to the occurrence of the nuclear excursion, but only to his realization that he should not have pulled the rod. This operation also provides considerable latitude in the possible time for the rod to move from the critical position to the 20-inch position, depending on the time at which the attempt was made to arrest the rod motion.

4.6 Reactivity Insertion Rate

To determine the ability of the various methods of manual withdrawal to produce the excursion, an analog simulation was set up on a G. E. D. A. Analog Computer. The computer circuitry for the problem and a more detailed discussion of the system is given in Appendix F . For the purpose of studying reactivity insertion rates, ramp rod-withdrawals of various speeds from critical (16.7 inches) to the 20 inch position were used, for which the reactivity insertion rate became a modified inverted parabolic section because of the decreasing worth of the rod near the higher withdrawn positions. The rod withdrawal was limited to 20 inches. The three shortest lived groups of delayed neutrons were used. The reactor power level at critical was generally set at about 300 to 400 watts. The power was integrated and a portion fed back for reactivity compensation due to plate expansion. The excursion was shut off rather abruptly by a large feedback reactivity proportional to the generated energy, at such a time that the total accumulated energy would be 130 Mw-sec.

Typical results of the simulation are shown in Figures III-97, 98, and 99. Each figure contains the analog computer plot of: 1) reactivity inserted, 2) log of power, and 3) inverse period. Figure III-97 contains the results of the 75 millisecond ramp (16.7 inches to 20 inches withdrawal) which approximates the casual rod withdrawal rate. The rod reached the 20-inch position (actually set for 2.5% $\Delta K/K$ in the computer) approximately 30 milliseconds before the peak of the excursion, at which point the computer amplifier maintained the 2.5% $\Delta K/K$ inserted reactivity until the end of the excursion. Had the rod withdrawal not been terminated at 20 inches but continued on the same ramp, it would have reached 21.2 inches (including consideration for the faster period) corresponding to 2.9% $\Delta K/K$ by the time of peak power. This result is outside of the standard deviation of the reactivity estimates.

Figure III-98 shows the results of the 100 millisecond ramp, which brought the rod to the 20-inch position 13 milliseconds before peak power. This result is not unreasonable to within the error of the 20-inch reactivity estimate. Figure III-99, showing the 125 millisecond ramp, found the rod just reaching the 20-inch position at peak power, and therefore is the best fit. The results indicate that the steady ramp rod withdrawal rate that best fits the conditions of the excursion is much slower than even the "casual" rod withdrawal rate. Note that a lower starting power at critical (below the nominal 400 watts used) makes the casual rod withdrawal rate an even worse fit for the excursion. The "maximum effort" rate is obviously much too fast. Had it been employed, the rod would have gone far past the 20-inch position.

Based on the reactivity estimates for the 20-inch position, which in themselves are subject to the uncertainty previously discussed, the analog simulation indicates there is little doubt that the central control rod could be withdrawn rapidly enough to produce the excursion. In fact, the results indicate that even a casual (average) effort to completely withdraw the rod exceeds that rate consistent with the known and estimated conditions of the excursion. Comparison of these rates is shown in Figure III-100.

However, the rod withdrawal curves corresponding to either the "free fall" case or the "arrested motion" case (Figure III-96 Sec. III-4.5) can, if properly selected, produce the excursion and permit the rod to be at or very near to the 20-inch position at the time of peak power. The reactivity insertions which these create insert the major portion of the total reactivity well in advance of peak power, and thus amount to essentially step insertions of reactivity.

In fact, a variety of ways (such as gripping the handling tool near the top, pulling of a stuck rod, etc.) exist in which the rod could be withdrawn manually to the observed 20-inch position in the time interval indicated by the analysis of the reactor kinetics. There seems to be no way of choosing between these various ways, since all of them can result in the same final reactor period.

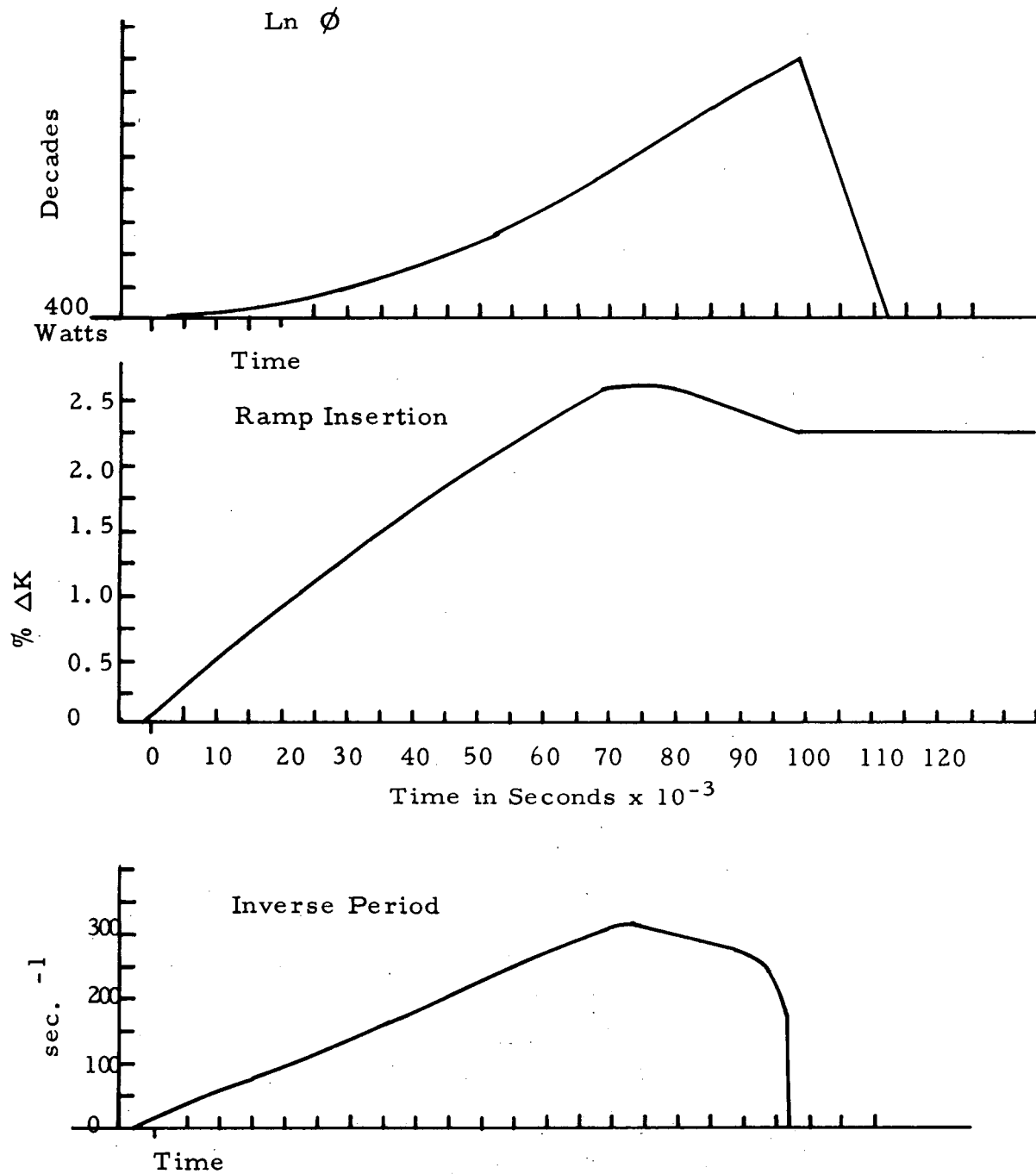


Figure III-97 Analog computer traces of 75 millisecond rod-withdrawal ramp (from critical to 20 inches)

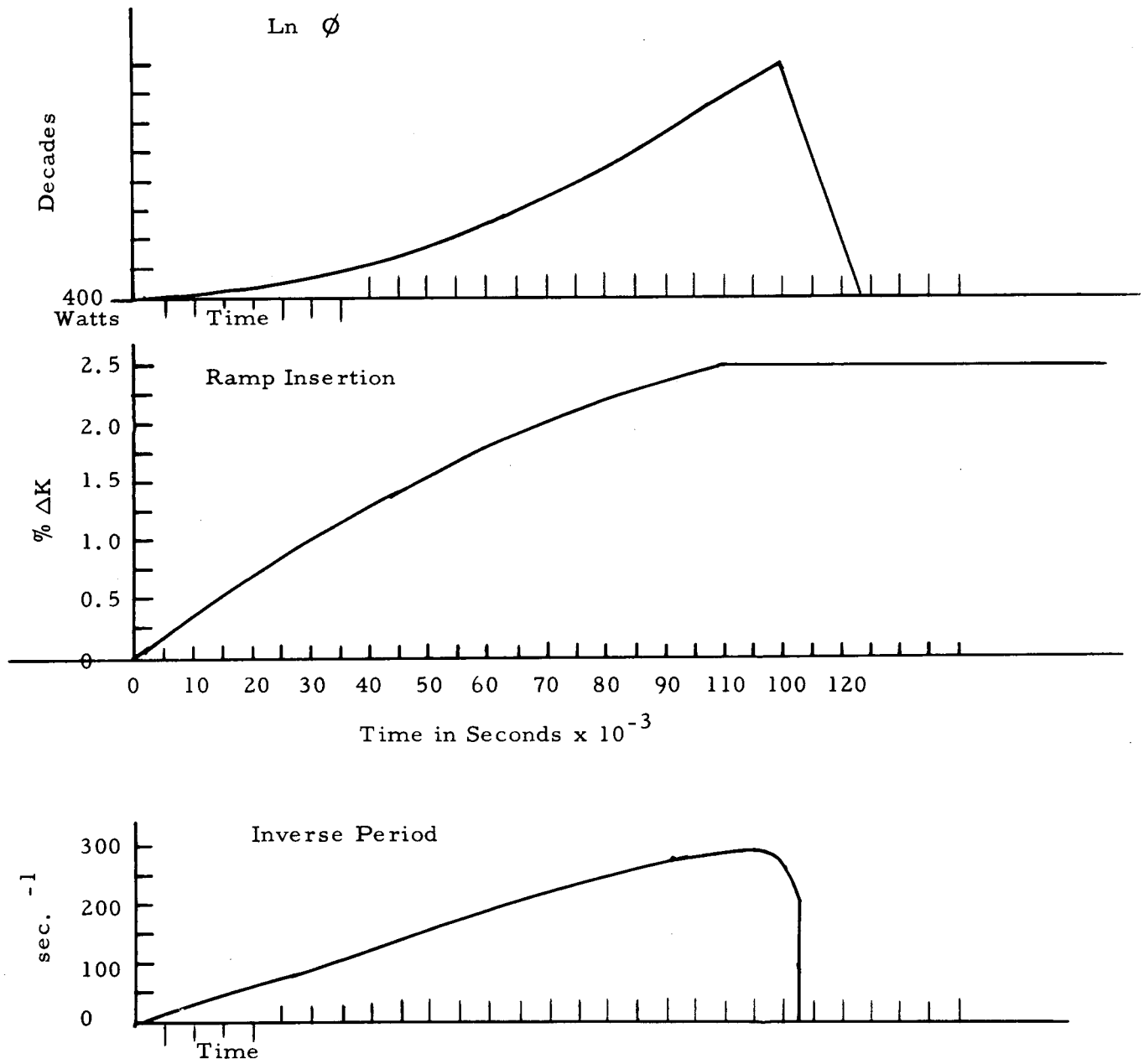


Figure III-98 Analog computer traces of 100 millisecond rod-withdrawal ramp (from critical to 20 inches)

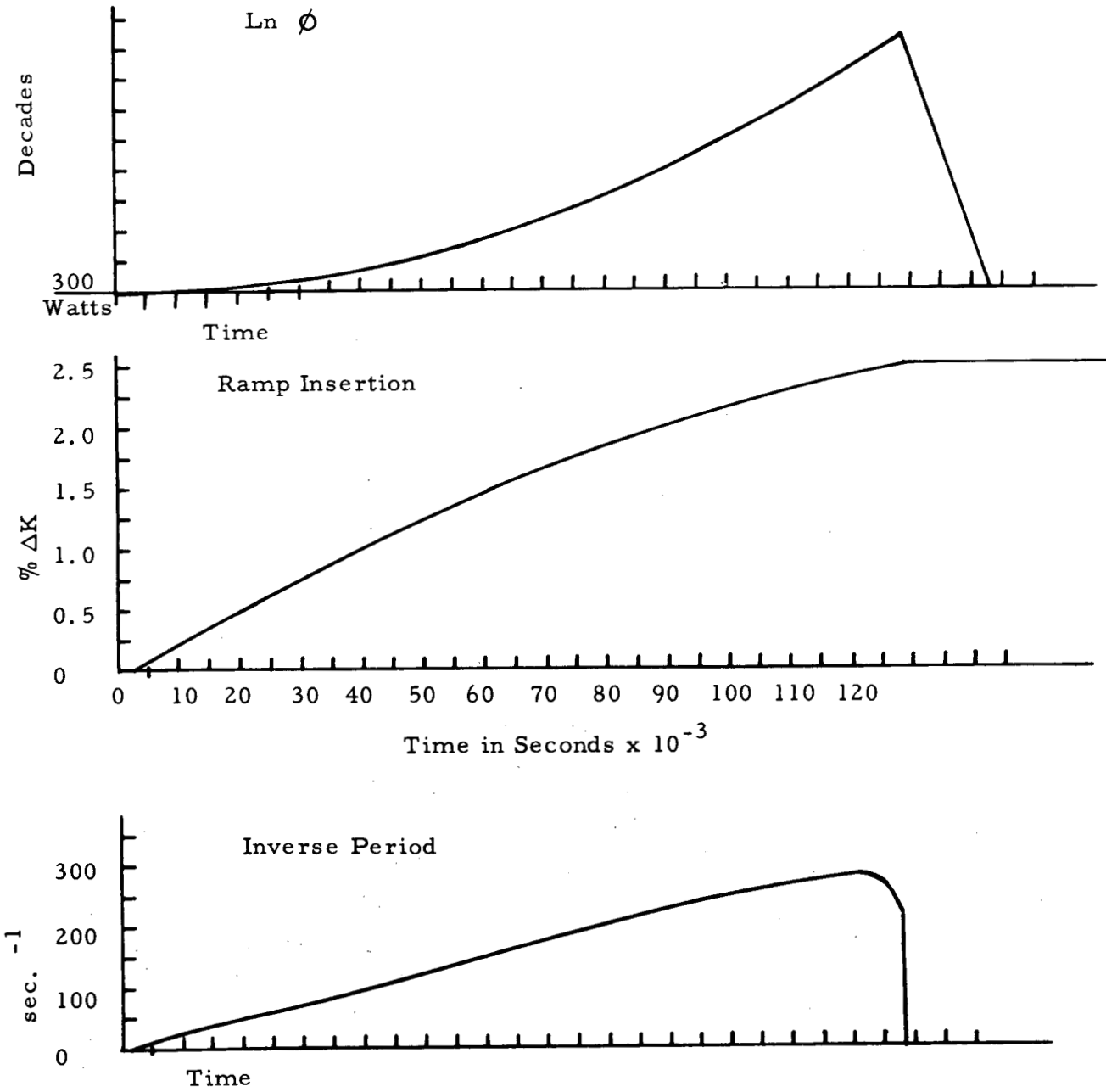


Figure III-99 Analog computer traces of 125 millisecond rod-withdrawal ramp (critical to 20 inches)

III-116

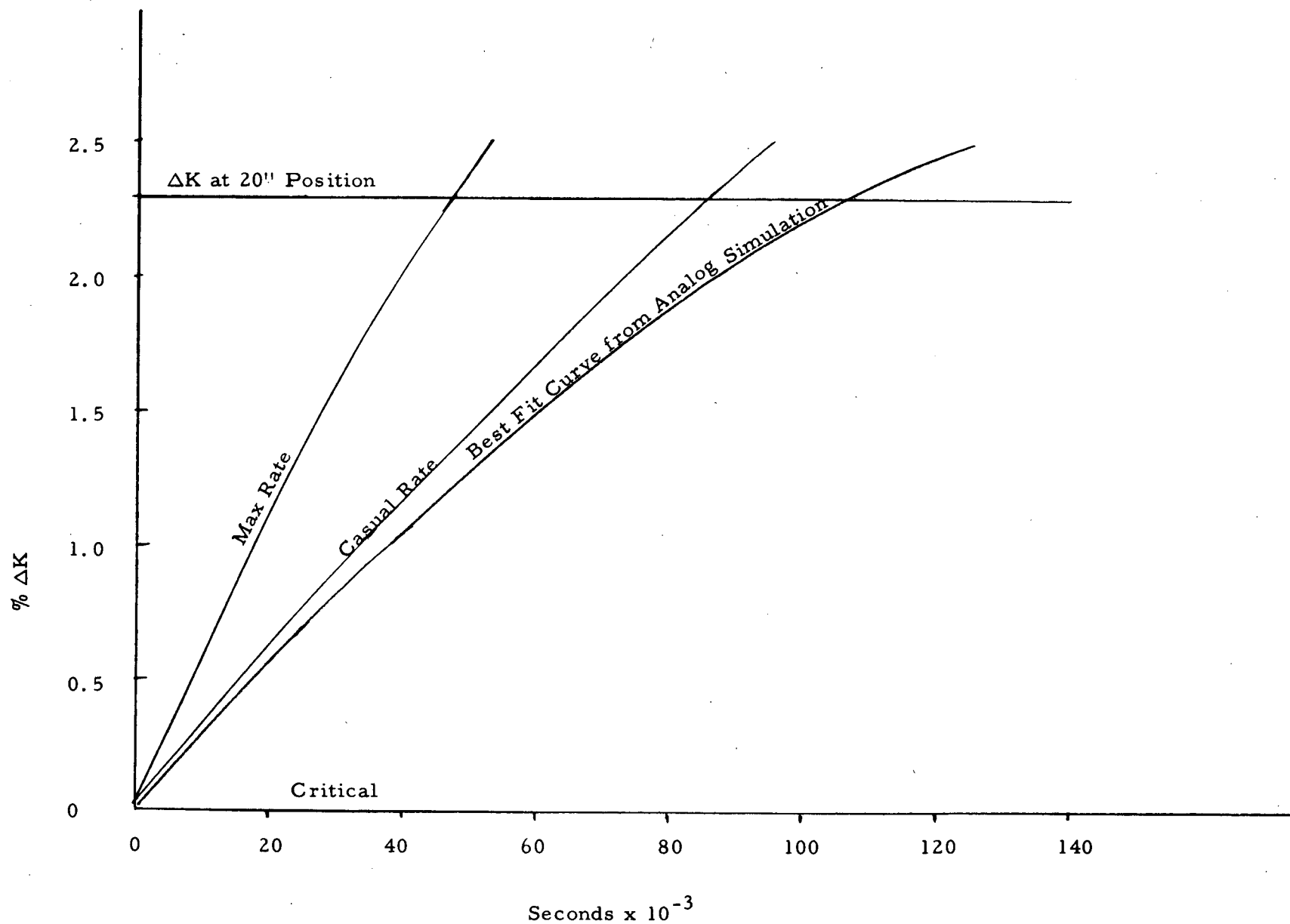


Figure III-100 Comparison on maximum and "casual" rod-withdrawal rates with the best fit obtained on the analog computer.

4.7 Critical Experiment Results

The experimental arrangement for the critical experiment on the post-incident core in the Hot Shop is described in Section II-2.6. The experiment was intended to determine if the destroyed core was capable of sustaining a chain reaction, or if not, how close to criticality it was. The possibility of a subsequent excursion following the initial excursion would have explained the high activation on the reactor operating floor. Since boron oxide from the reactor head had found its way into the vessel, it may have contributed ultimately to ending the sustained reaction, as could have either the loss of water moderator, loss of fuel, or the geometrical deformation of the core. Therefore, it was decided to attempt to wash out any boron compound deposits during the course of the critical experiment, without, however, disturbing metallic boron present in the poison strips.

During the first and last fillings with water and the three intermediate fillings with dilute acetic acid, no total multiplication effect was observed on any of the three scintillation chambers.

In each case the counters did show the normal increase in count rate due to moderation of source neutrons as the water moved between the source and the counter. Each filling removed some boron compound from the core and pressure vessel, for a total boron content removal of about 150 grams for the five fillings. The multiplication curves for successive fillings showed no significant difference which could be attributed to the removal of boron. When the reactor was disassembled, very little boron was found on the active fuel plates, apparently less than one gram on the total plate surface area.

The multiplication curves for the counter located furthest below the core are shown in Figure III-101. The major cause of the decreasing count rate with increasing water height is merely the attenuation of the water between the counter and source, and subsequently the shielding of the scattered source neutrons by the water above the source. It was completely impractical to remove just the fuel from the core and determine the overall attenuation created by filling the tank, pressure vessel, and core structure with water. The cadmium in the control blades certainly had a pronounced effect on the attenuation observed by the counters. However, the empty critical experiment tank was filled with water with source and counters in place in an effort to estimate the attenuating effect of the rising water height in the critical experiment configuration.

In the region from water level of 45 inches above the bottom of the critical experiment tank (where some fuel could have been lying on top of the bottom support structure) to the 58 or 60 inch level, the slope of the actual critical experiment multiplication curves was decidedly less than the slope of the "empty tank" multiplication curve. Above and below these levels, the two types of curves have similar slopes. This general appearance of the curves was observed with all the counters. However, since the #2 counter

was 21 inches below the bottom of the fuel in the intact outer elements, and about 18 inches below the cadmium, this counter was least influenced by the presence of the cadmium control blades. It was also least influenced by scattered neutrons from the source. Therefore, the difference between the slopes of the curves with the reactor in place and of the "empty tank" curve for this counter is due, in part, to a multiplication effect of the fuel in the core's central region, which was largely concentrated below the 60 inch level. From this data, a crude estimate of the multiplication factor of the reactor was obtained. The core, when full, had a k-effective of about 0.6. This is not to be construed as an accurate number, but only as an indication of how far from criticality the core was. Some cobalt foils had been dropped into the core and were allowed to remain there throughout the critical experiment. When removed, the foils showed a total thermal flux of 5×10^{10} n/cm². This result is an order of magnitude above what was expected from the source in a non-multiplying medium during the time it was surrounded by water moderator, as well as for the time it was unmoderated. Therefore, it appears that these foils may have been located near a concentration of fuel where significant local multiplication was occurring.

The post-incident critical experiment showed that the reactor was grossly subcritical and that this condition was apparently independent of the presence or absence of boron in the core region.

In view of the other facts discussed in previous sections, it appears that the subcritical condition was due in part to the radial displacement of the core and the resulting increase in water volume fraction, resulting in over moderation, i. e. poisoning. It was also subsequently found that nearly 50% of the fuel from the center section of the reactor was missing, resulting in a very low thermal utilization for this region. Furthermore, the intimate proximity of the collapsed cadmium control blades with the outer 24 elements made these elements very ineffective contributors to the overall multiplication of the core. In general, overall conditions in the core were not conducive to creating neutron multiplication.

Counter 2
(Normalized at 50")

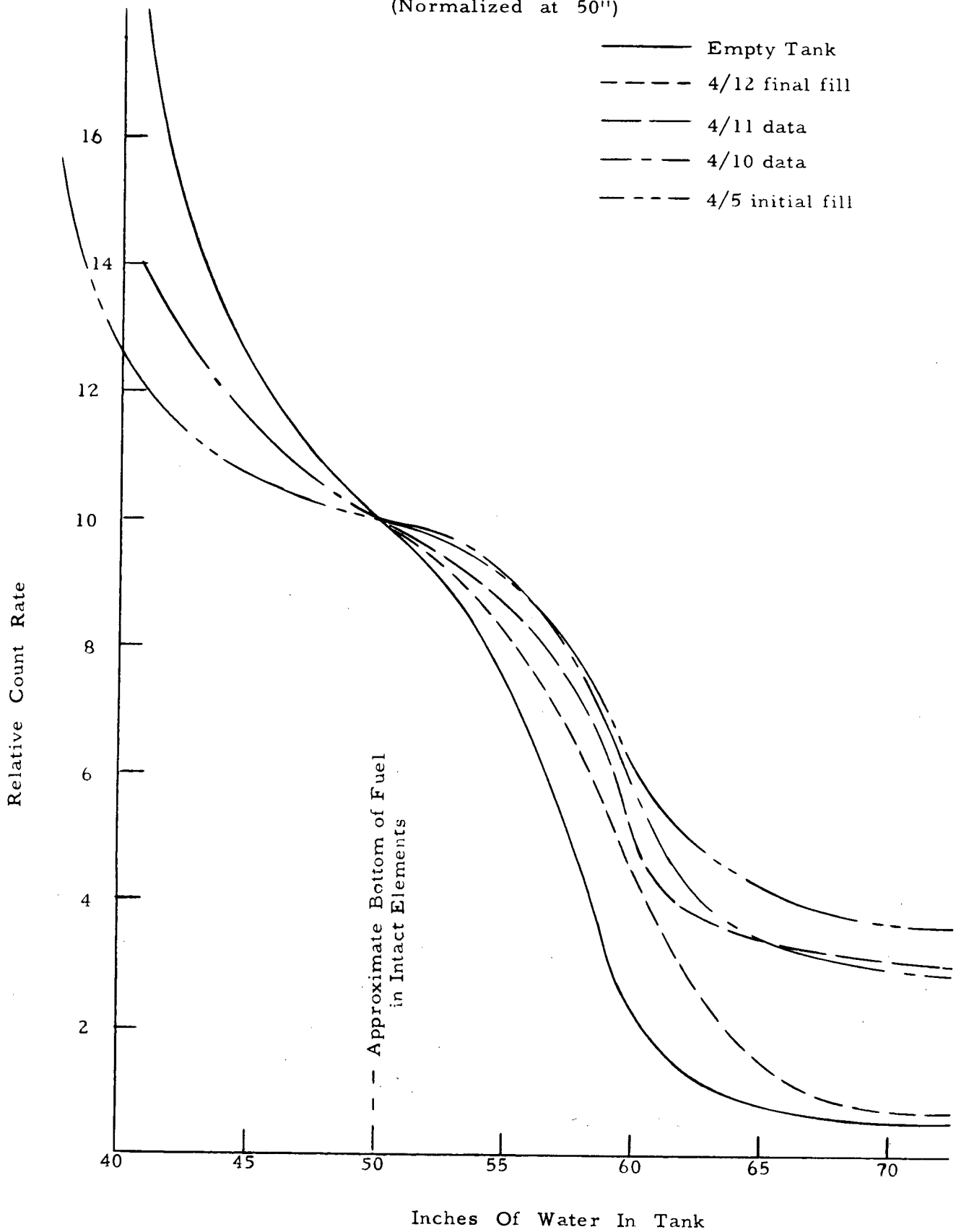


Figure III-101 Multiplication curves obtained during post-incident critical experiment.

IV- ANALYSIS AND CONCLUSIONS

1. Nuclear Excursion

1.1 Initiating Mechanism

The key fact determined in the investigation was that the central control rod was found bound in its shroud at the 20 inch withdrawn position, as described in Section III-1.1 and 1.8. The reactivity associated with this position, while not known precisely for the conditions existing, has been estimated in Section III-4.4 to be 2.4% $\Delta K/K$. This is enough reactivity to account for the observed damage to the core. It is not necessary to postulate any additional mechanism to add reactivity, for example by loss of boron strips, although the condition of the core after the accident precludes direct determination of the location of the strips from the center of the reactor. To explain the accident it is, therefore, necessary and sufficient to explain how the central rod got to the 20-inch position.

One mechanism has been discussed in Sections III, 4.5 and 4.6, namely, manual withdrawal of the rod. It was shown in that section that the rod could be withdrawn manually in a variety of ways to produce the observed effects. In addition, the position of the bodies indicates that two men were standing on the reactor head at the time of the accident. Furthermore, the presence of the nut, washer, and handling tool on the central control rack at the time of the accident, and the probable presence of the C-clamp on the rack, make it appear that the operation being carried out at the instant of the accident was to raise the central rod manually a sufficient amount to remove the C-clamp. No attempt has been made to suggest possible motivations for pulling the rod 20 inches instead of 2.

One alternative mechanism which has been proposed is the use of chemical explosives in or under the core. Explosives experts from the Stanford Research Institute examined the core. Their report, given in full in Appendix C, makes it clear that chemical explosives were not the agent responsible for the withdrawal of the central rod.

A second possibility, sometimes mentioned, is concerned with the explosion of hydrogen formed by the radiolytic decomposition of water. Experimental information quoted in the literature indicates that it would be credible for sufficient hydrogen gas to produce an explosion to have been formed in several hours time by the fission product activity present in the core. The explosion of a hydrogen-air mixture between the pressure vessel head and the top of the water above the core would have created a uniformly high pressure in this region. The five loose shield plugs would have then been ejected. It is known that nuts and washers were in place on the racks of all five of these control rod mechanisms at the time of the incident. Ejection of a shield plug would then result in the lifting of the control blade. It is inconceivable that only the central control blade, the heaviest of the five, would have been lifted by the hydrogen explosion. Since the other blades were found in their normal scram positions after the incident, it

is immediately apparent that the initiating mechanism was not a hydrogen explosion or any other explosion in the space between the water and the vessel head. (Note, the black coating on the extension rods, originally attributed to a high temperature reaction, was identified as chromous acid which accrues during long operation in a steam atmosphere. The product of a high temperature reaction produced in a laboratory test was a green coating of chromium oxide.)

In conclusion, the various proposed methods for initiating the mechanism without requiring manual withdrawal of the central control rod, are definitely inconsistent with the facts. The motivation for withdrawing the rod is not known, but the analysis indicates that the action was not a maximum effort attempt to withdraw the rod completely (reference Section III-4.6.).

1.2 Power Behavior

Since there was no direct record of the reactor power behavior during the excursion, a correlative method has been used to obtain an estimated power behavior using the results of SPERT experiments and analysis (the appropriate references cited in the text refer to SPERT documents).

The burst approximation equation for a reactor transient given in SPERT Quarterly Report (July-September, 1958, IDO 16512) assumes the power burst can be represented by a two term exponential expression. It has been decided to adopt this model for the SL-1 to facilitate the calculation of temperature distributions.

The two-term power burst equation is:

$$I \quad \phi(t) = \phi(0) \left[r \exp(\alpha t) - (r-1) \exp\left(\frac{r}{r-1} \alpha t\right) \right]$$

where:

$$\begin{aligned} \phi(0) &= \text{measured peak power} \\ \alpha &= [\text{reactor period}]^{-1} \\ \phi_x(0) &= \text{extrapolated peak power} \\ r &= \frac{\phi_x(0)}{\phi(0)} \end{aligned}$$

Peak power occurs at $t = 0$

Using equation I, the total energy, $E(T)$, energy in the water, $E(W)$, and energy in the plate, $E(P)$, becomes:

$$\text{II} \quad E(T) = \frac{\phi(0)}{\alpha} \left[r \exp(\alpha t) - \frac{(r-1)^2}{r} \exp\left(\frac{r}{r-1} \alpha t\right) \right]$$

$$\text{III} \quad E_w(T) = \frac{AC \rho \sqrt{d}}{H \alpha^{1.5}} \phi(0) \left[r \exp(\alpha t) - \frac{(r-1)^{2.5}}{r^{1.5}} \cdot \exp\left(\frac{r}{r-1} \alpha t\right) \right]$$

$$\text{IV} \quad E_p = E(T) - \frac{AC d}{H \alpha^{1.5}} \phi(0) \left[r \exp(\alpha t) - \frac{(r-1)^{2.5}}{r^{1.5}} \cdot \exp\left(\frac{r}{r-1} \alpha t\right) \right]$$

where:

A = heat transfer area

C = specific heat of water

ρ = density of water

H = average effective heat capacity of core

$d = \frac{K}{\rho C}$ = the diffusivity of water

K = the conductivity of water

The two term approximation is limited in its application to sharp power bursts (short periods) (IDO-16636, by R. W. Garner). The value of r which best seems to fit the SPERT power burst shapes is $r = 1.5$ ($r = 1$ is a sawtooth; $r = \infty$ is a symmetrical burst). The resulting two-term exponential usually has a more rapid drop from peak back to zero power than was generally observed with the SPERT and BORAX non-destructive tests. However, this difference is actually believed to exist between these tests and the SL-1 excursion (see Section V-3.1).

The remaining terms in equation I through IV are self explanatory, except the value of \bar{H} . This was calculated using the following: (Ref. IDO-16489, page 75);

$$\bar{H} = F_w H_w + F_s H_s + F_p H_p;$$

where:

H_w = total heat capacity of water

H_s = total heat capacity of aluminum

H_p = total heat capacity of fuel plates

$F_w = \frac{l_w}{d_w}$ = fraction of moderator heated

$F_s = \frac{l_s}{d_s}$ = fraction of structure heated

F_p = ratio of actual heat content of fuel plate to that indicated by surface temperature

d_w = half thickness of water channel

d_s = half thickness of structural aluminum fuel plate

The above equations and assumptions were used along with the data available from the reactor designers to shed some further light on the incident.

From the design information and the position of the central control rod after the incident, the reactivity insertion was obtained. From this the associated period could be determined. The flux wires gave the total integrated power and the energy distribution. Using this information and the above stated assumptions, the values shown in Table IV-1 were calculated from equations I through IV. Of particular significance is the high peak power (19,000 Mw) and the small amount of energy transferred from the plates to the water up to the peak of the excursion (0.92 Mw sec). In contrast, approximately eight times as much energy is deposited uniformly in the water by nuclear heating.

TABLE IV-1

SL-1 Excursion Values Calculated from SPERT Model

sec ⁻¹	t_1^* sec.	$\phi(0)$ Mw	E (0) Mw-sec	\bar{H} cal/°C	EW (0) Mw-sec	EP (0) Mw-sec	EM ⁽¹⁾ Mw-sec	Eg ⁽²⁾ Mw-sec
250	2.2×10^{-3}	19000	100 Mw-sec	5.39×10^4	0.92	99	45	78

* t_1 = time at end of excursion. $t = 0$ is time of peak power

(1) EM = energy required to bring center 16 elements to 640°C (melting temperature)

(2) Eg = energy generated by center 16 elements.

The energy generated in the center 16 elements was 60% of the total energy generated in the core.

1.3 Shutdown Mechanisms

The primary shutdown mechanism in the SL-1 (short of fuel loss or geometrical deformation) is moderator displacement, which can occur in four ways.

1. Expansion of fuel plates due to temperature increase - Reported void coefficients for the SL-1 are:
 - a. $-1 \times 10^{-4}\% \Delta K/cm^3$ for average steam void⁽¹⁾
 - b. $-6 \times 10^{-4}\% \Delta K/cm^3$ for void throughout central region of a center element⁽²⁾

The fuel plate expansion effect, at peak power, would be a maximum of about $-0.5\% \Delta K$, but would more likely be around the $-0.1\% \Delta K$ given by the average steam void coefficient, since plate expansion is a similar "average" effect.

2. Moderator expansion due to both nuclear heating of the water and transfer of heat from the plates to the water - Both create "average" void effects. At the peak of the burst, approximately 6 Mw-sec. of energy will be in the water, creating a $-0.7\% \Delta K$ effect.

(1) IDO 19300 - May 15, 1961 - SL-1 Report

(2) D.H. Shaftman, ANL, - private communication

3. Bubble Dilation - Recently Zivi⁽³⁾ has demonstrated that dilation of adsorbed bubbles on the surface of fuel plates will precede boiling and insert a small amount of negative reactivity into the system. The total effect of bubble dilation is about $-0.1\% \Delta K$.
4. Steam Production - This process, under transient conditions from a non-boiling state, is little understood. However, some of the work at the University of California on void volume development in transient boiling of water⁽⁴⁾ presents some helpful points.

The void growth due to steam formation occurs at a time when sufficient heat has been transferred to the water to bring it to the saturation temperature. However, the temperature measurement that is made in most systems is not the water temperature but the plate surface temperature. This problem, along with the predicted temperature distribution in the water under transient conditions shown in Section IV-1.4, Figure IV-2, creates some difficulty in defining a water volume, and an average temperature from which to compute steam formation. Complicating the problem further is the heat transfer coefficient after steam formation has begun. The curves of temperature and void formation given in reference (4) are produced by an exponential power source. The data taken from the above was used to predict a delay time. The delay time from plate saturation temperature until the beginning of void volume formation appeared to become asymptotic for short periods; approaching a value of approximately 3 milliseconds.

SPERT data⁽⁵⁾ for very short periods (ω greater than 150 seconds^{-1}) was examined for SPERT I aluminum cores "A" and "B" and the stainless steel core in order to obtain further information on the delay in void formation. From the data, it has been concluded that there will be a temperature overshoot, the amount depending upon the period, and that the delay time between plate-surface saturation temperature and the beginning of boiling is, for very short periods, approximately three milliseconds.

This temperature overshoot could cause two effects. The first is superheated water. The amount of superheat would, of course, depend on the period, and may allow an initial surge in the void volume formation. This is indicated in the curves contained in reference (4). However, of more significance is the effect of fuel plate temperature overshoot. If the period is sufficiently short, the amount of energy generated in the three millisecond delay may be sufficient to produce internal plate melt. This is indicated by the temperature distributions in Section IV-1.4. Since the center temperature is approximately 4.5 times the surface temperature, a 100°C overshoot would produce melt in the center region before steam would be formed on the surface of the plates.

- (3) S.M. Zivi - Trans. of Amer. Nuc. Socl, Vol. 5, No. 1, p. 161.
- (4) V.E. Schrock, et al, Series 163, Issue #2, January, 1961.
- (5) Private communication - courtesy of R.W. Miller, G.F. Brockett, E. Feinauer, - Phillips Petroleum Company.

In summary, it appears as though there is a fixed time delay between saturation temperature and the beginning of void formation. This delay has been interpreted to be approximately 3×10^{-3} seconds for reactor periods less than 10 milliseconds. The delay produces problems in two areas. It delays the formation of void to produce shutdown, and it allows internal plate temperatures to rise to very high values.

1.4 Temperature Distribution (Fuel Plate)

Fuel plate temperature distribution as a function of time plays an important role in the shutdown mechanism postulated for the SL-1 incident. Since the exact transient power behavior is not known, it is not possible to accurately determine the plate temperature distributions. However, the two term burst discussed in Section IV-1.2 approximates the actual burst. Using this two term approximation the following equations were derived to approximate the temperature distribution.

$$\begin{aligned}
 \text{I} \quad \Theta_1 \text{ (meat temp.)} &= \frac{Q_0}{\alpha \rho c} \left[1 - \frac{D \cosh \mu_1 x}{D \cosh \mu_1 a + \frac{K_1 \mu_1}{K_2 \mu_2} \sinh \mu_1 a} \right] e^{\alpha t} \\
 &- \frac{1}{9} \frac{Q_0}{\alpha \rho c} \left[1 - \frac{D' \cosh \mu_1' x}{D' \cosh \mu_1' a + \frac{K_1 \mu_1'}{K_2 \mu_2'} \sinh \mu_1' a} \right] e^{3\alpha t} \\
 \text{II} \quad \Theta_2 \text{ (clad temp.)} &= \frac{Q_0}{\alpha \rho c} \frac{K_1 \mu_1}{K_2 \mu_2} \sinh \mu_1 a \\
 &x \left[\frac{\cosh \mu_2 (x-a) - D \sinh \mu_2 (x-a)}{D \cosh \mu_1 a + \frac{K_1 \mu_1}{K_2 \mu_2} \sinh \mu_1 a} \right] e^{\alpha t} \\
 &- \frac{1}{9} \frac{Q_0}{\alpha \rho c} \frac{K_1 \mu_1'}{K_2 \mu_2'} \sinh \mu_1' a \\
 &x \left[\frac{\cosh \mu_2' (x-a) - D' \sinh \mu_2' (x-a)}{D' \cosh \mu_1' a + \frac{K_1 \mu_1'}{K_2 \mu_2'} \sinh \mu_1' a} \right] e^{3\alpha t}
 \end{aligned}$$

where:

$$D = \frac{\frac{K_2 \mu_2}{K_3 \mu_3} \sinh \mu_2 (b-a) + \cosh \mu_2 (b-a)}{\frac{K_2 \mu_2}{K_3 \mu_3} \cosh \mu_2 (b-a) + \sinh \mu_2 (b-a)}$$

$$D' = \frac{\frac{K_2 \mu_2'}{K_3 \mu_3'} \sinh \mu_2' (b-a) + \cosh \mu_2' (b-a)}{\frac{K_2 \mu_2'}{K_3 \mu_3'} \cosh \mu_2' (b-a) + \sinh \mu_2' (b-a)}$$

a = half thickness of meat

b-a = thickness of clad

K₁ = conductivity of meat

K₂ = conductivity of clad

K₃ = conductivity of water

$$\mu = \sqrt{\frac{\alpha \rho c}{K}}, \text{ and } \mu' = \sqrt{\frac{3\alpha \rho c}{K}} \text{ for the particular medium in question,}$$

where:

ρ = density

c = specific heat

From the above equations and the energy density given by the flux wire analysis, the temperature distributions shown in Figures IV-1, 2, and 3 were calculated for a four millisecond reactor period ($\alpha = 250$). Each figure shows the comparison between the maximum flux region and the "threshold of destruction" region. Figure IV-1 shows the temperature distribution four milliseconds (one period) before peak power, Figure IV-2 at the peak, and Figure IV-3 at the end of the excursion. The results are not exact, for there was no provision in the calculations to account for the constant temperature during the melting process (640°C).

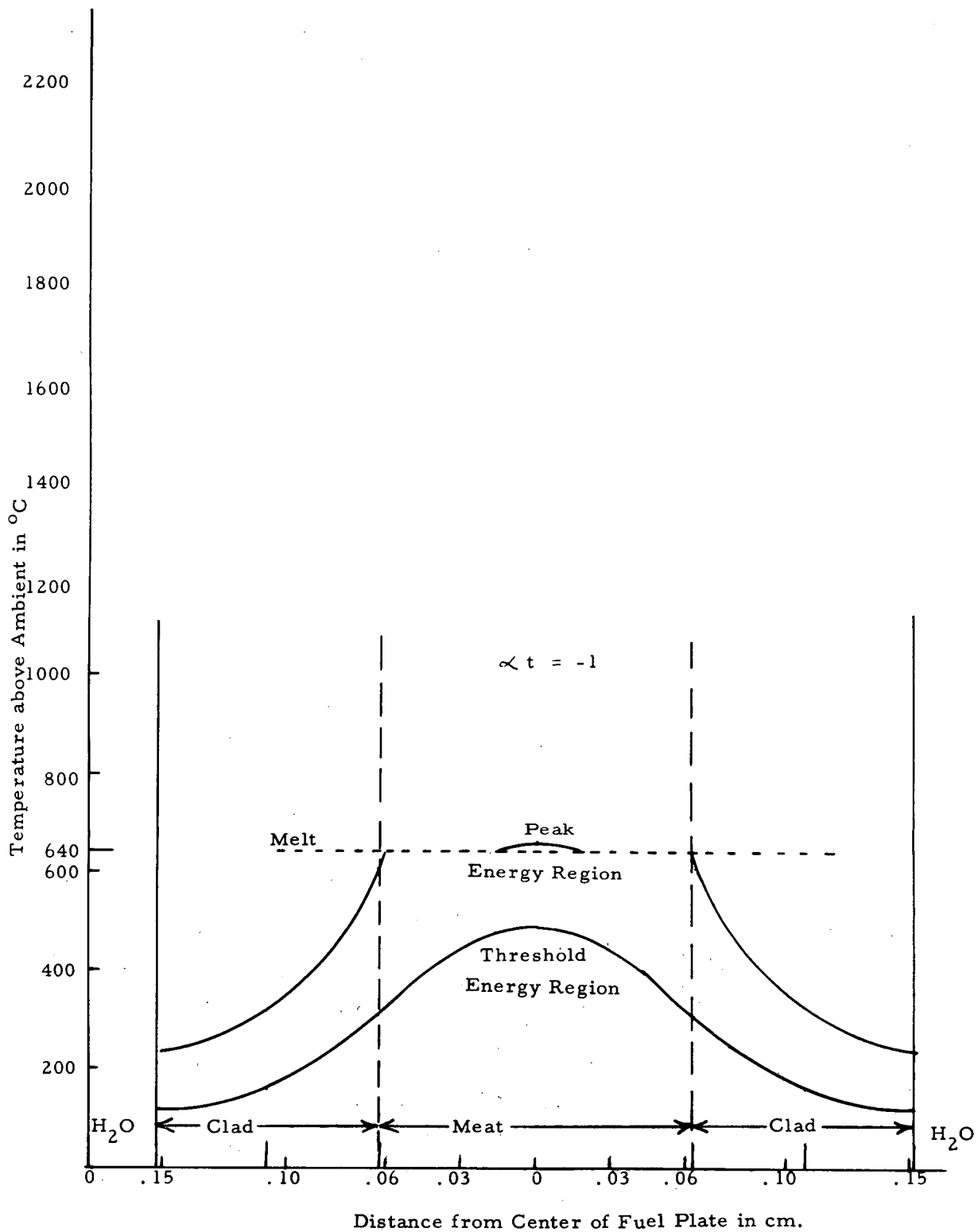


Figure IV-1 Temperature distribution in fuel plate, for 4 m sec transient, 4 m sec before peak power, for both peak energy density region and "threshold of destruction" region.

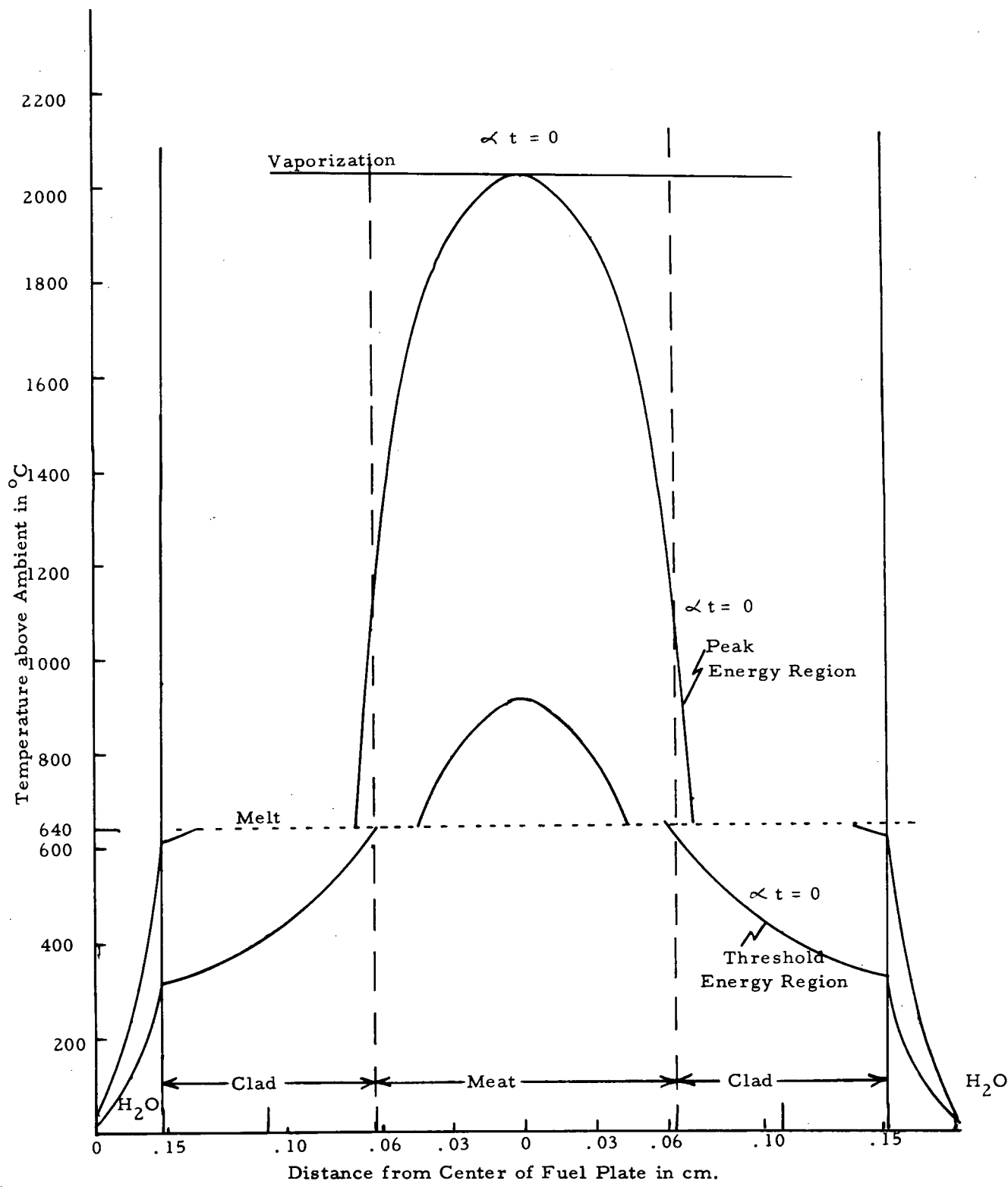


Figure IV-2 Temperature distribution in fuel plate, for 4 m sec transient, at time of peak power, for both peak energy density region and "threshold of destruction" region.

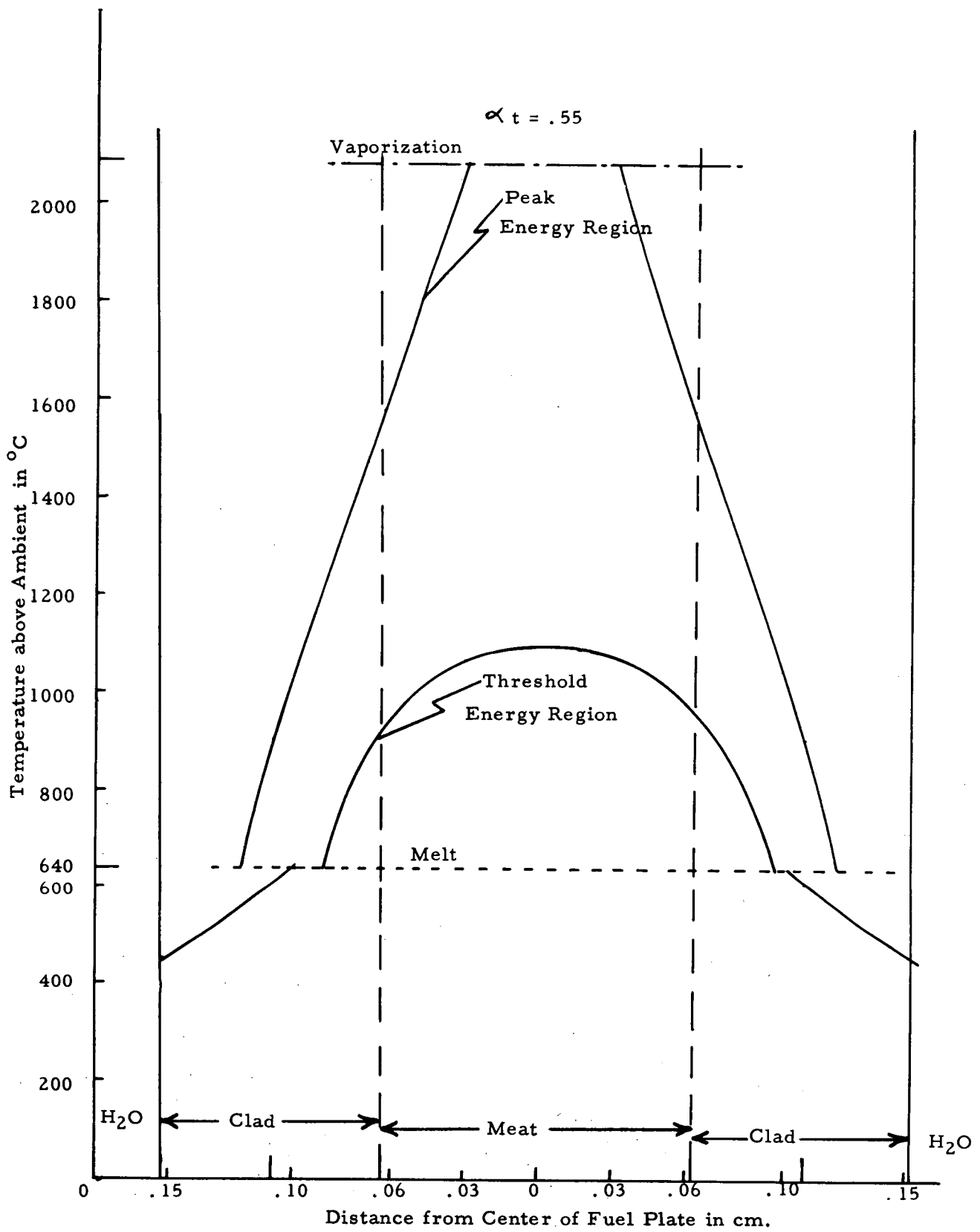


Figure IV-3 Temperature distribution in fuel plate, for 4 m sec transient, at end of excursion, for both peak energy density region and "threshold of destruction" region.

The highest energy density region just reached vaporization in the meat center at peak power. Thus a considerable potential existed to cause the explosive void formation and the resultant self-destruction.

The cladding surface in the "threshold of destruction" region was well below melting at peak power and only 490°C at the end of the excursion. The energy density in this region is just sufficient to melt the entire plate thickness. Since temperature equalization will occur quite rapidly (in a few milliseconds) after the end of heat generation, the cladding surface temperature must be significantly below melting at this time so that while the temperature is being equalized, sufficient heat can be removed to avoid destruction of the entire plate. Though a positive quantitative statement is not possible without more heat transfer information for transient conditions, it seems that the temperature distributions for a four millisecond transient are consistent with the observed core damage.

The temperatures at both the surface of the clad and the center of the meat are given at both peak power and the end of the excursion for three different transients in Table IV-2 below. These temperature distributions show that the five-millisecond period is too slow, permitting the cladding surface temperature to reach melting in the "threshold of destruction" region by the end of the prompt nuclear energy release. There is no latitude to allow for "drift" of this temperature up to melting during the temperature equalization process, while some heat is being removed from the plates. Thus, the five-millisecond "threshold of destruction" should have extended into a lower energy density region than was observed. The three-millisecond period resulted in temperature distributions that brought the center-of-meat temperature to vaporization (2060°C) by the end of the excursion in nearly 20% of the center section of the core. It is believed that such a large region of vaporization would have created much more metal-water reaction than seems to have occurred (see Section III-2.5 and IV-3.2).

Thus, it appears that there is sufficient evidence to conclude that the five-millisecond temperature distributions are such that this period is too slow to account for the observed damage to the core. The three-millisecond period seems to be so fast that it would have vaporized more of the meat than one would assume occurred, on the basis of presently available information. The four-millisecond transient, however, creates temperature distributions which apparently account for the observed core damage. This period also is consistent with the estimates of the excess reactivity with the central control rod at the 20-inch position (Section III-4.4), with due consideration for the minor effects of plate expansion, moderator heating, and other reactivity compensating effects occurring before steam formation.

TABLE IV-2

Temperatures in SL-1 Fuel Plate in °C (above ambient) for Different
Reactor Transient Periods

	<u>3m sec</u> <u>Period</u>	<u>4m sec</u> <u>Period</u>	<u>5m sec</u> <u>Period</u>
A) Region of Threshold of Destruction			
1. At peak of burst			
a) center of meat	945	853	792
b) surface of clad	254	310	440
2. At end of burst			
a) center of meat	1193	1147	973
b) surface of clad	393	491	melting ⁺
B) Region of Peak Energy Density			
1. At peak of burst			
a) center of meat	2200*	2015	1895
b) surface of clad	508	619	melting ⁺
2. At end of burst			
a) center of meat	2695*	2605*	2255*
b) surface of clad	melting ⁺	671	1095

* Vaporization at one atmosphere occurs at 2060°C.

+ Melting occurs at 640°C.

2. Effects Following Excursion

2.1 Acceleration of Water Slug

The steam resulting from the nuclear excursion displaced water from the core and eventually from the region above the core. At the time of the incident, seven feet of water were above the fuel plates, leaving an air void of 40 cubic feet between the top of the water and the pressure vessel head. The water displaced from the core region pushed this water upwards against the head of the pressure vessel. The collision of the water column with the head resulted in the rapid conversion of the column's kinetic energy to potential energy of compression. †

An estimate of the pressure attained in the compressed water has been obtained from the damage sustained by the control-rod guide tubes extending from the end of the shield plugs. These 304-stainless steel tubes, 0.2 inches thick with 1.9 inches OD, yielded under the pressure. The static yield-pressure is 7000 psi. Because of the higher pressure required to yield material under transient conditions, an estimated 10,000 psi existed in the compressed water column surrounding the guide tubes.

If 10,000 psi was the peak pressure in the slug of water at the bottom of the head, the energy of compression in the entire slug was:

$$E_{\text{comp.}} = \frac{1}{3} V \beta (P_{\text{max}})^2$$

if a linear distribution of pressure between the head and the bottom of the slug is assumed. The kinetic energy of the column of water (in the center of mass system) is $1/2 \rho V v^2$, where

V = volume

ρ = density

v = velocity

β = compressibility = $5 \times 10^{-5} \text{ atm}^{-1}$

Equating the kinetic energy and energy of compression gives a velocity of 130 ft/sec in the center of mass.* In the laboratory system,

$$v = 159 \text{ ft/sec.}$$

† The air between the water and the head will have little effect on the analysis, since it will initially be forced into the space in the nozzles below the plugs. Also, the system was not tightly sealed.

* If a uniform pressure exists in the slug, the energy of compression will be $1/2 V \beta P^2$, giving a variation of less than 20% in the final result of velocity.

The time history of the steam pressure, in and above the core, that accelerated the column of water is not known. Had the pressure been uniform in time, it would have been 450 psi and the accelerating process would have lasted 34 milliseconds (for the 2.75 feet distance). This pressure represents only an average pressure that would accelerate the column of water to the required velocity. The peak steam pressure might have initially been several thousand psi for a short duration until pressure relief was obtained by propagation of the wave through the column of water and the resulting motion of the water occurred. Such exceedingly high pressures might occur because steam was probably formed, near the end of the excursion, quite rapidly and violently by contact of water with metal heated to beyond the critical temperature of water (374°C, with corresponding critical pressure of 3200 psi), in fact heated to the vapor temperature of aluminum (2060°C at atmospheric pressure).⁽¹⁾ Steam pressures of several thousand psi existed for no more than a few milliseconds, if at all, not long enough to actually rupture the thermal shield or pressure vessel.

The estimates of velocity of the water column and average steam pressure are not much different from the empirically measured values during the model - explosive tests (Section III-1.6). These tests indicate that a water velocity of about 165 feet/sec and an average sustained pressure of about 550 psi create effects similar to those produced by the incident.

2.2 Effects of Water Slug

2.2.1 Pressure Damage

The compression of the water column upon impact against the vessel head caused not only the collapse of the rod guide tubes but produced high pressure damage to other metal parts.

The nozzles in the vessel head were bulged, an effect requiring 3,500 psi to yield and 11,000 psi to break under static conditions.

The vessel wall was bulged outward about two inches on the radius in the region of highest pressure (near the head). The vessel should yield (under static conditions) at about 1000 psi and break at about 3000 psi. However, the high pressure compression-pulse had a width at half-maximum of about the propagation time of sound through the column of water, or about 1.4 milliseconds. The average excess pressure above that necessary to yield the vessel was about 4000 psi for that time, during which the wall would have been accelerated through a distance of five inches. Since the transient yield stress is generally higher than the static yield, it is quite conceivable how such a high pressure (peak of 10,000 psi) for such a short duration expanded the vessel wall only about two inches but failed to rupture it. The head nozzles and the rod guide tubes were much thinner, offering less mass to be transported by the pressure pulse,

(1) Kinetic Studies of Heterogeneous Water Reactors, Quarterly Report September 30, 1961, Space Technology Laboratories, Inc.

in contrast to their higher yielding pressures. Note also that the steam baffle plate was bent against the vessel by the same high pressure pulse.

2.2.2 Motion of Vessel

The impact of the fast moving column of water (mass about 200 slugs, velocity = 159 feet/sec) against the vessel head produced a transfer of momentum to the vessel. The model-explosive tests (Section III-1.6) have shown that essentially all of the water above the "core" was accelerated and left the vessel through the nozzles, indicating that the upward moving column of water was a complete piston, that it did not rebound into the core allowing the pressure to escape from the nozzles, and that the collision was, therefore, mostly inelastic. Transfer of the 32,000 slug feet/sec momentum of the water column to the 900 slug vessel (including water below the top of core) by means of an inelastic collision would impart a 29 feet/sec velocity to the combined 1100 slug mass.

The pressure vessel, however, was not free to move, being constrained by the outlet four-inch steam line and four smaller connecting pipes. It is estimated that these pipes could be sheared with about 60,000 ft-lb of energy, leaving the vessel with about 400,000 ft-lb of energy and an initial velocity of 27 feet/sec, with which it could rise 11.4 feet. The connecting piping was not ultimately the only constraining item, for the 1/4 inch steel insulation liner was constrained by the sheared piping so that the vessel was required to break the welds which connected the liner to the vessel flange. This action cost the vessel perhaps a foot of free rise, leaving about a 10 foot rise potential. The vessel's #5 seal housing apparently hit the bridge-crane drive shaft after a 9 feet-1 inch rise, limiting the height of the vessel travel, damaging the contacting components, but leaving no noticeable impact marks because of the very small relative velocity at the time of impact.

When the vessel rose nine feet out of its support cylinder, the thermal insulation (three-inch magnesia) from around the wall of the vessel generally rose with it. When the vessel struck the crane drive shaft, it may have become cocked toward the side that struck. As the vessel fell back into its support cylinder, the insulation on this side probably was stripped off and perhaps blown by the draft created as the vessel displaced air, thus accounting for the scattered insulation primarily in the region below the bridge crane. The steel punchings from the lid shielding were generally scattered toward the opposite side of the room. These were probably jarred loose and ejected by the initial impact of the water against the vessel head.

2.2.3 Shield Plug Ejection

Another effect of the water hammer was to eject the unbolted shield plugs from the vessel. If momentum transfer to the plugs vs. the vessel is assigned on an area basis, the shield plugs would receive twice the initial velocity of the vessel (each plug has 1/167 the mass of the vessel and 1/80

the area). It is estimated that the plugs would each lose 2000 ft-lb of energy in fracturing the rack and connecting rod fingers, leaving the plug with about 7000 ft-lb of energy. During the travel of the plugs out of their nozzles, they were further accelerated by the approximate 500 psi in the steam void below the water column. It is estimated that most of the plugs had 20,000 ft-lb of kinetic energy when they finally left the vessel nozzles. The #7 plug carried the third victim, who had been standing on the vessel. His mass was approximately equal to the mass of a shield plug. Had the victim not been partially accelerated by the rising vessel before meeting with the plug, the velocity of the combination man and plug would not have been sufficient for the plug with victim to leave the vessel, due to the impact of the water column alone. However, the water attempting to escape from the vessel promoted the separation of plug and vessel. A combination of these two effects was adequate for the #7 plug to become free of the vessel well in advance of the vessel hitting the ceiling, but such that this plug still trailed the others in flight.

2.3 Subsequent Excursions

Whether the reactor was rendered permanently subcritical by the initial excursion rests on the basis of pertinent evidence previously discussed and summarized below.

1. Critical Experiment

The core (as received in the Hot Shop) was grossly subcritical (k_{eff} about 0.6), a condition independent of the presence of boron poison.

2. Geometry

The core was radially expanded and the center of the core was blown apart and upward (most of it eventually falling back), leaving the reactor larger, but well over-moderated.

3. Missing Fuel

Approximately 2 Kg of U-235 was missing from the active core region, most of this from the center 16 elements, leaving this section with about 60% of its original fuel content and a resultant low thermal utilization.

4. Reactivity Insertion

The rate at which the central rod could be manually withdrawn exceeds that necessary to get the rod to the 20-inch position well in advance of the peak of the power burst. The reactivity change can, therefore, be considered equivalent to a step insertion of reactivity.

5. Neutron Activation in Operating Room

The activation, both thermal and fast, at the position of the victims was many orders of magnitude above what can be accounted for by direct radiation from under the 7 ft. water head.

There seems little doubt, from the first three items above, that the core was rendered grossly subcritical by a very violent excursion. The withdrawal of the central control rod, regardless of the trajectory it followed, was such that motion near the 20 inch position was small over the time that the major portion of energy was developed during the excursion. Therefore, the shutdown mechanism developed while essentially the entire excess reactivity was inserted, and the resulting excursion was the most violent that could occur with this amount of reactivity (i. e. - a step insertion gives the worst excursion). Therefore, any subsequent excursions could have been no worse than the initial one provided they involved the same amount of excess reactivity.

With the control rods bound in their shrouds, the only means of enhancing reactivity was to remove the boron strips. The strips on the outer 24 elements were found in place, though generally unattached, during core disassembly. Therefore, it is unlikely that the small amount of boron remaining in the center of the core at the time of the incident would have been quickly removed by any action short of displacing the fuel elements from each other, such as was done in the final burst. Note that further evidence to support this contention is the fact that during normal operation, the fuel elements vibrated in the core structure, and yet this vibration apparently created no sudden detectable losses in boron. It is concluded that an insignificant amount of boron would have been quickly knocked out of the core by a mild excursion, and that such a mild excursion, therefore, did not precede the final violent one.

The high neutron activation on the operating floor is the one item that does not substantiate a single burst hypothesis. The fact that most of the water above the core would be blown out by even a mild excursion (model explosive tests, Section III-1.6) provides a reasonable mechanism for obtaining high floor-level activation on the subsequent burst. However, the fact that a dual excursion could conveniently explain the activation levels does not a priori eliminate other explanations which would still be compatible with a single burst. Such explanations are contained in Section IV-3.3.

The evidence for a single violent burst with no subsequent nuclear chain reaction seems overwhelming. The analysis of the predicted reactor behavior following the apparent reactivity insertion rate is completely self-consistent with the current data on reactor and fuel element transient behavior. It is quite certain that the final burst was a very severe and violent one, and it seems rather unlikely that this was preceded by a non-destructive, mild burst which precipitated the final one.

3. Core Damage

3.1 Temperatures, Destruction, Melt, and Vaporization

The fluxes recorded by the flux wires in the center 16 elements of the core were sufficiently high over approximately 50% of the plate area to heat the entire thickness of the fuel plate to the molten state. During the nuclear energy release, most of which occurred in about 10 milliseconds, a negligible amount of heat was transferred through the cladding to the water. At most, only 2% of the total heat deposited in the plates could have been removed under the most efficient nucleate boiling heat transfer conditions. Thus, the fuel plates initially retained essentially all of the prompt nuclear energy deposited in them except for those plates whose cladding surface did not remain intact.

As Figures IV-1, 2, and 3 show, if the energy is developed by an approximate four milliseconds excursion, the center of the meat can reach vaporization (at atmospheric pressure) while the surface of the clad is still below the melting temperature. Such apparent vaporization had occurred only over a small region of the reactor, less than 1% of the center 16 elements, by the time of the approximate peak of the power burst. By the end of the excursion, however, the center of the meat is about 5% of the central core region had reached vaporization temperature, based on the two term exponential model. The meaning of fuel "vaporization" at the high pressures which existed adjacent to the plates is somewhat nebulous. Nevertheless, once the meat region had reached 2060°C, conditions in the plate must have been extremely adverse to the plate maintaining its integrity, despite the existence of high pressures on the outer, still unmelted surface of the clad.

The disintegration of most of the destroyed plate area probably did not occur until the melting proceeded to the outer surface of the clad and therefore came after the peak of the power burst and did not contribute significantly to limiting the power rise, which may have been accomplished largely by normal steam formation from intact plates. However, before the nuclear excursion had been terminated by this latter mechanism, it is quite probable that very violent disintegration of a small fraction (approximately 5%) of the center section of the core had occurred, producing extremely fast steam formation, and terminating the excursion abruptly. It is this back side of the excursion power curve which probably differed most from the normal SPERT non-destructive power traces.

The two term exponential model, $\text{Power} = e^{\alpha t} - 1/3 e^{3\alpha t}$, generally provided a sharper drop to the back side of the power curve than was observed in most SPERT and BORAX non-destructive tests. The more abrupt drop deduced for the SL-1 incident would, therefore, make this two-term model even more suitable for the SL-1. The model gives 77% of the total energy release before the peak power.

Most of the destroyed regions of the center 16 elements (47% destroyed 5% reached vaporization) resulted from normal melting which eventually spread to the outer clad surface and destroyed the integrity of the plate. Normal internal melting, resulting in a volume expansion of the order of 5%, would not be expected to destroy the plate. This melt spread relatively

slowly to the surface of the clad (for the unvaporized regions) so that even by the end of the excursion, the surface of the clad throughout most of the destroyed region had not yet become molten. Thus, it is believed that the destruction of the unvaporized portion of the plates occurred generally after the end of the nuclear excursion, and that this non-violent destruction did not contribute to the shutdown mechanism.

3.2 Energy Distribution and Metal-Water Reaction

3.2.1 Nuclear Energy Distribution

Of the total 130 Mw-sec released by the nuclear excursion, 50 Mw-sec was produced in the outer 24 elements. These elements easily absorbed this energy with little resulting damage. Therefore, transfer of heat from these outer 24 elements to the water occurred over a relatively long time by the slow process of nucleate or film boiling from smooth surfaces. This process would require a minimum of about two seconds, a time exceedingly long compared to the time scale of the incident.

Of the 80 Mw-sec produced by the center 16 elements 86 percent (69 Mw-sec) was promptly deposited in the plates and was distributed such that 12 of these elements suffered severe damage due to melting and possibly vaporization. Heating of the entire fuel plate material in these 16 elements to the melting temperature would require 45 Mw-sec. However, the energy was distributed so that half of the plate area was heated to melting or above while half of it was heated to less than the threshold of destruction. The portion of the plates that quickly disintegrated transferred heat very rapidly to the water. Approximately 44 Mw-sec of energy was deposited in the destroyed areas of the core, and most of this energy was transferred to the water when the disintegration of these regions occurred.

The amount of energy that could have been quickly deposited in the water and thus have contributed to the acceleration of the water column against the vessel head is listed in Table IV-3.

TABLE IV-3

Energy Rapidly Deposited in Water (within 30 milliseconds following peak power)

Prompt nuclear energy during the excursion (neutron heating of water)	7 Mw-sec
Normal heat transfer from smooth plates (approx. maximum)	4
From disintegration of plates (44 Mw-sec max.)	<u>39</u>
	50 Mw-sec

This is the energy which contributed to the mechanisms creating the mechanical damage of the incident. The explosive-model test (Section III-1.6) produced equivalent damage with a 1/2 pound charge of "Pentolite" in a 1/4 scale model. This would be equivalent to a 32 pound charge in a full scale model, depositing approximately 74 Mw-sec of energy in the water. However, the explosion of "Pentolite" conceivably produced more violent disturbance of the water, mixing it more thoroughly and permitting unvaporized water to absorb more heat than probably occurred in the SL-1 excursion.

An additional consideration requires that enough water be vaporized to produce the 500 psi approximate average pressure needed to accelerate the water column. This pressure endured for about 1/2 second until the water was ejected from the vessel. Using the 40 ft³ of void into which the water vapor could expand with the water column against the lid, an energy of 52 Mw-sec is needed to vaporize sufficient water to produce a 500 psi pressure in this volume. Certainly, additional heat would be absorbed by unvaporized water. It appears, therefore, that of the total 130 Mw-sec of nuclear energy produced, 50 to 60 Mw-sec was rapidly inserted into the water, primarily by the portions of the fuel plates which disintegrated. It was this energy which created the steam that accelerated the column of water.

3.2.2 Metal-Water Reaction

In the peak energy density region of the SL-1 core, the energy deposited in the fuel plates was approximately 500 cal/gm (meat and clad). This is a little more than twice the energy density required to melt the plates (220 cal/gm). Experiments on fuel pins of aluminum and uranium oxide at TREAT⁽¹⁾ have shown that energy densities of 500 cal/gm produce an aluminum-water reaction in approximately 10% of the metal, while essentially no reaction occurs below energy densities of 220 cal/gm. However, not only did the fuel in the TREAT experiments differ from SL-1 fuel, but the reactor period was an order of magnitude longer than the SL-1 excursion period. At an energy density of 500 cal/gm, some of the SL-1 meat vaporized, while it is not certain that any vaporization of aluminum occurred in the TREAT experiments.

To obtain an estimate of the extent of an aluminum-water reaction in the SL-1 excursion, very liberal estimates were made using the TREAT experimental results as a guide. The reaction of aluminum with water, $2 \text{ Al} + 3 \text{ H}_2\text{O} \rightarrow \text{Al}_2\text{O}_3 + 3 \text{ H}_2$, releases 231×10^3 calories per mole of Al_2O_3 formed, or 18 Mw-sec per kilogram of aluminum metal reacting. It has been assumed that, in the portion of the plates which reached vaporization, 25% of the aluminum in the meat reacted with water; and for the remainder of the destroyed plate area, 5% of the aluminum has been assumed to have reacted with water. This amount of aluminum reacting with water would release 35 Mw-sec of chemical energy and produce 3.6 Kg of α - aluminum oxide.

(1) Liimatainen et al, ANL 6250

The aluminum oxide formed should be very finely divided. Presumably, it was distributed throughout the pressure vessel, and the major portion of it which did not leave the vessel would have settled to the bottom and would be found in the 53 Kg of material removed from that region. Diffractometer analysis of the fine material in the bottom of the vessel has indicated 1.5 kilograms of aluminum oxide (α -phase) existed in the fine material alone (see Section III-2.5).

The amount that was in the coarser material would be expected to be small because it is unlikely that particles of Al_2O_3 coalesced with each other. Since only one-half of the uranium particles not still in or on fuel plates was found in the bottom of the vessel (see Section III-3.3), it is conceivable that not much more than half of the total aluminum oxide formed would be found in the bottom of the vessel. If one kilogram escaped from the vessel, a total of 2.5 kilograms of α -aluminum oxide was produced.

Thus, the amount of metal-water reaction indicated from chemical analysis of the debris is about 2/3 of the value estimated, rather liberally, using the results of the TREAT experiments. The amount of energy released by this chemical reaction was (24 ± 10) Mw-sec, which is about one-fifth of the nuclear energy release. Table IV-4 lists the products of the apparent aluminum-water reaction.

TABLE IV-4

Aluminum-Water Reaction Estimated Effects
($\pm 40\%$ uncertainty)

Energy generated	24 Mw-sec
Total aluminum oxidized	1.3 Kg
Al_2O_3 (α -phase) produced	2.5 Kg
Hydrogen gas produced	74 moles

The chemical energy generated is only a small fraction of the nuclear energy, despite the fact that some of the aluminum had reached vaporization temperature. The hydrogen gas formed would not have significantly boosted the average pressure under the column of water during its acceleration toward the vessel head, but might have inserted an initial high pressure surge compared to the rate at which steam was formed.

3.3 Activation

Since the 130 Mw-sec generated by the SL-1 excursion probably occurred in a single burst from under a seven foot, undisturbed column of water, it is difficult to account for the high neutron activation reported for various samples taken from the bodies of the victims. Through seven feet of water, the thermal and fast neutron fluxes from a 130 Mw-sec excursion would be between 10^3 and 10^4 n/cm², in sharp contrast to the

10^9 to 10^{13} n/cm² reported in the analysis of Phase I and II Operations and listed in Section III - 4.2 of this report.

With a much smaller column of water above the reactor, higher activation levels would occur, with each foot of water being worth about 1-1/3 decades of attenuation. However, the height of water above the core just prior to the incident is well known. Witnesses from the day shift of January 3, 1961, are certain that the water was within six inches of the head before the level was reduced to bring the level-instrumentation on scale. The water pumped from the vessel was in the contaminated waste tank (previously emptied) and was measured after the incident to be about 250 gallons, sufficient to reduce the water level in the pressure vessel 2-1/4 feet, leaving about seven feet of water above the core.

Since the critical experiment and certain other considerations strongly indicate that there was but one excursion (see Section IV-2.3), other explanations have been sought to explain the occurrence of such high neutron activation from under so much water. One consideration is the scattering of neutrons up the three inch insulation gap around the vessel after they have traveled through about ten inches of water and two inches of steel from the face of the reactor. However, from the top of the insulation gap the neutrons either must travel through sixteen inches of steel or undergo multiple scatterings to get to the operating floor. The resulting flux would be less than 10^8 (a liberal estimate), still much too low to account for the measured activations.

Other considerations are that the activation on the operating floor may have been produced predominantly by the delayed neutrons originating after the excursion, either (1) from fuel ejected from the reactor pressure vessel, or (2) from the core and its remnants inside the vessel while the vessel was above its rest position. These two hypotheses are considered below.

1. If delayed neutrons were emitted from 1% of the fuel at a distance of one foot from a detector, a fast flux of 6×10^{10} n/cm² would result. The same flux would result from 10% of the fuel inventory at a three foot distance. Lumps of fuel were not found in great quantity outside the pressure vessel (only a few identifiable lumps containing two grams of uranium were recovered). Therefore, most of the ejected fuel was probably in fine-particle form, easily and widely dispersed throughout the building. The uniform dispersing of fuel can explain why all the thermal receptors from the victims received similar doses. From the fission product and fuel escape estimates (see Section III-3.3 and 4.3), it is difficult to account for much more than 10% of the delayed neutrons being emitted outside of the pressure vessel, giving rise to fast fluxes certainly less than 10^{11} n/cm² and thermal fluxes (moderation by the bodies) which should be considerably less than 10^{10} n/cm² (assuming 10% moderation). The ejected fuel hypothesis is, therefore, somewhat insufficient to account for all the observed activation.

2. While the vessel was traveling upwards and falling back, the core was for a time close to the operating floor. In fact, most of the center section of the reactor was ejected upwards by steam and water and may have been well above the operating floor for part of the vessel's flight. Approximately 50% of the delayed neutrons are emitted within four seconds of fission. Though a freely falling body would go through a 10 foot high trajectory in 1.5 seconds, it is conceivable that the pressure vessel became cocked and remained out of the support cylinder for several seconds near the top of its trajectory. If such was the case, it can be shown that 50% of the delayed neutrons from the center section of the core (60% of total energy) would give a thermal dose of 5×10^9 n/cm², five feet from the core center, through the vessel wall, but not through the head. (Based on six inches of water and two inches of steel from reactor face.) The fast neutron dose would be less than the thermal dose.

It appears that a combination of hypotheses (1) and (2), above, probably explain thermal neutron activations of the order of 10^{10} n/cm², and fast neutron activations of less than 10^{11} n/cm².

The thermal flux near the #4 shield plug's Stellite bearing was an order of magnitude lower (10^9 n/cm² maximum). The plug and bearing were in the fan room at the time most of the delayed neutron irradiation occurred. Neutrons from inside the vessel would have had to penetrate the vessel head (except for the 8% open area) to reach the bearing; and of the ejected fuel and fission products, only a small fraction reached the fan room. Thus either hypothesis (1) or (2) correctly infers a lower activation for the #4 Stellite bearing than for the receptors on the victims.

The fast neutron activation of the hair samples from the victims (except the pubes of the first victim) is one to two orders of magnitude higher than can reasonably be accounted for by any combination of the above hypotheses. Furthermore, it is somewhat of an anomaly that for the two victims for which data exists, activation at the head level was approximately 100 times the activation of the pubes. It is suspected that contamination of the samples by the ejected reactor water, a problem alluded to in reference 2 of Section III-4.2, was the cause of the exceedingly high apparent activation of the exposed head areas and the much lower apparent activation (but still unusually high for the second victim) of the clothed pubic areas.

In general, the thermal neutron activation data from outside the pressure vessel, levels of about 10^{10} n/cm² on the victims and 6×10^7 n/cm² from the Nuclear Accident Dosimeter at the doorway at the side of the operating room seem to have been caused by delayed neutrons. Whether these neutrons originated mostly from fuel ejected from the pressure vessel or from fuel inside the vessel during the time this fuel was above or near floor level is uncertain. Quite likely each source of neutrons made a significant contribution.

4. Summary of Excursion

The SL-1 excursion and its effects are summarized in graphical form in Figure IV-4. Despite the unfortunate nature of the incident, it has provided a valuable insight into the overall understanding of reactor excursions and the problems of reactor safety. The most significant items of information obtained from the analysis of the incident are listed below, with reference being made, when appropriate, of their relation to the BORAX destructive test. (1)

- 1) Reactivity Insertion - The withdrawal of the central control blade to the 20-inch position could have been performed manually with more speed than was actually necessary to create the excursion. Though the condition of the boron poison strips in the reactor at the time of the incident is not known, it appears unnecessary to postulate that any significant change in boron inventory occurred since the cadmium strips were added in the T-shrouds. The estimated reactivity of the 20-inch position was equivalent to the reactivity of a four millisecond transient.
- 2) Reactivity and Energy - The total energy generated by the SL-1 and BORAX-1 were about the same, yet considerably less reactivity was needed for the SL-1 excursion. (2.4% ΔK compared to 3.3% ΔK) Basic design differences between these two water-moderated, plate-type reactors created two opposite effects: one in which the SL-1 shutdown mechanism was less effective than that of the BORAX, followed by a potentially more rapid shutdown mechanism whereby the SL-1 excursion was terminated quite abruptly.
- 3) Shutdown Mechanism vs Energy - The SL-1 average void coefficient was small compared to BORAX and similar cores, thus reducing the effects of all non-destructive shutdown methods. The plate area, from which steam formation occurs, was also much smaller for the SL-1. Of more significance was the larger thickness of the plates and the cladding of the SL-1, permitting a larger amount of energy to be internally stored in the plates before significant heat transfer took place between the plate surfaces and the water.
- 4) Reactor period and temperature distributions - The large plate thickness of the SL-1 permitted a high ratio of center to surface temperature. The estimated four millisecond transient caused the fuel-meat in portions of the reactor to reach vaporization temperature before the surfaces of the plates had melted or had an opportunity to transfer much heat to the water. Due to these high center temperatures, the shutdown mechanism of steam formation suddenly became very rapid as portions of the plates exploded (presumably), resulting in an abrupt termination of the excursion.

(1) AECD-3668, BORAX-1 Experiments, 1954 - J. R. Dietrich

- 5) Fission product release - The empirical information, obtained during deliberate melt tests, of fission product release cannot, in general, be applied to the SL-1. For in this excursion, the primary method of fission product release occurred as a result of the bursting of internally vaporized plates, a condition that has not successfully been reproduced in controlled, out-of-pile tests. Furthermore, the partial containment provided first by the pressure vessel and secondly by the building shell obscured the correct interpretation of the amount of fission product release in an excursion of this magnitude.
- 6) External Effects - The damage outside of the pressure vessel was somewhat extraordinary, having been created primarily by the effects of a fast moving column of water slamming against the pressure vessel lid. This event had unusual consequences, strikingly destructive in view of the fact that the pressure vessel itself did not rupture but did jump nine feet into the air.

Thus the energy relationships between the nuclear, thermal, and mechanical phenomena can be cross-linked by the calculational methods of engineering physics. Moreover, the kinetics of the energy transformations are compatible with the behavior of other reactor systems in which destruction was deliberately produced by a similar rapid insertion of reactivity through control rod motion. As can be seen from the foregoing analysis, even differences that do exist between SPERT, BORAX and SL-1 behavior can be qualitatively explained in terms of physical differences in reactor structure.

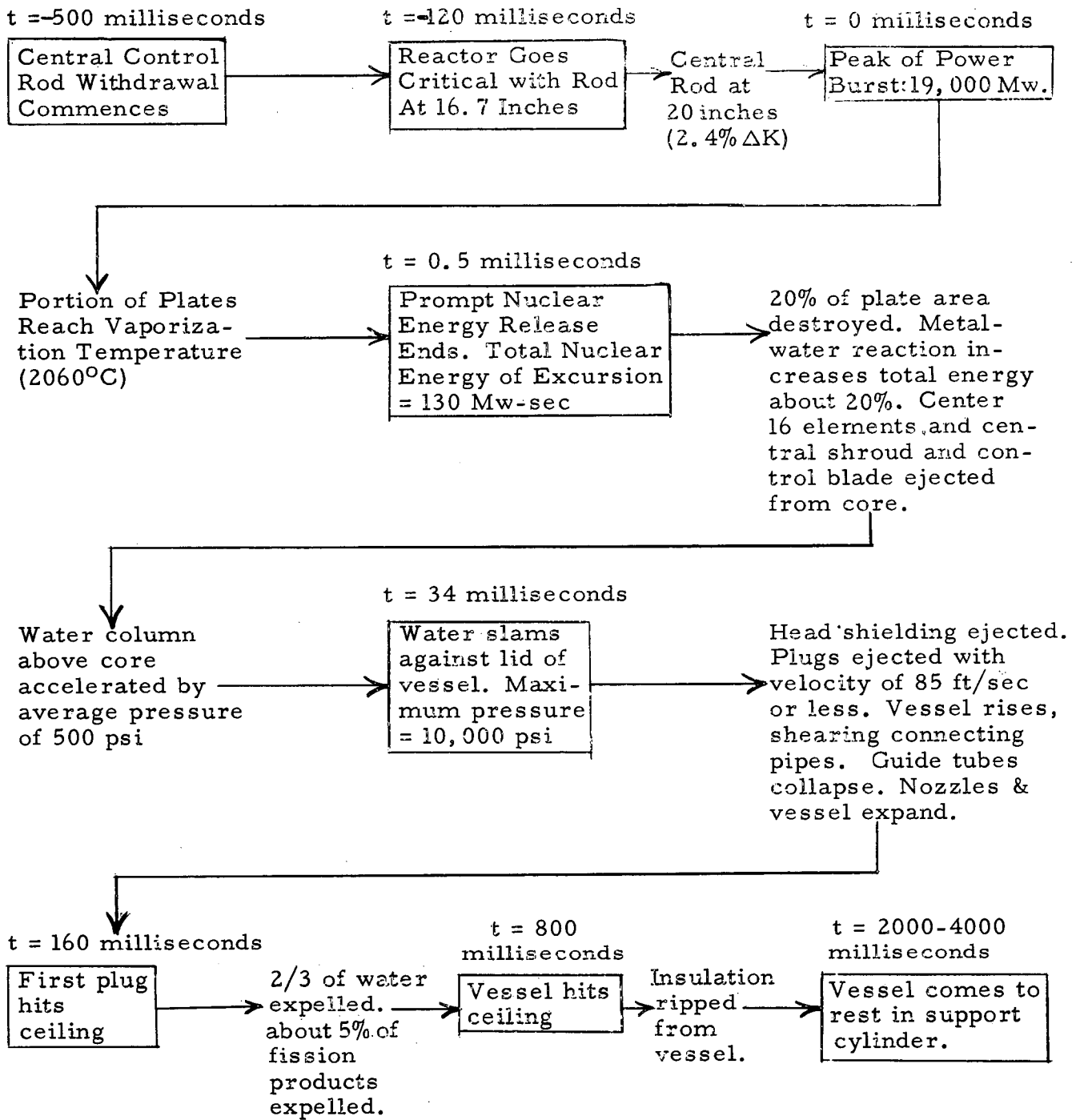


Figure IV-4 SL-1 Excursion Summary. Values are approximate (see text for estimated uncertainties). Time is in milliseconds.

APPENDIX A

Description of the SL-1

The SL-1, a small, natural circulation, direct cycle, boiling water reactor, was designed by Argonne National Laboratory and put into operation at the National Reactor Testing Station near Idaho Falls, Idaho. The first operation at significant power was on October 23, 1958. On February 5, 1959, operating responsibility of the reactor was transferred from ANL to Combustion Engineering, Inc. Figure A-1 shows the entire power plant. The large tank in back houses the reactor, power generating equipment, blower fans, etc. The concrete building in the foreground is the administration building, and the building between the reactor and administration building is the support facilities building. The remaining buildings shown in Figure A-1 are support and training buildings.

Figure A-2 shows a cutaway view of the reactor building and the north corner of the support facilities building. This cutaway shows the lower portion of the cylindrical building which contains the reactor pressure vessel surrounded by gravel shielding. The turbine generator and plant support equipment are located in the center portion of the building above the reactor pressure vessel proper. The upper portion of the building contains the air cooled condenser and its circulation fan.

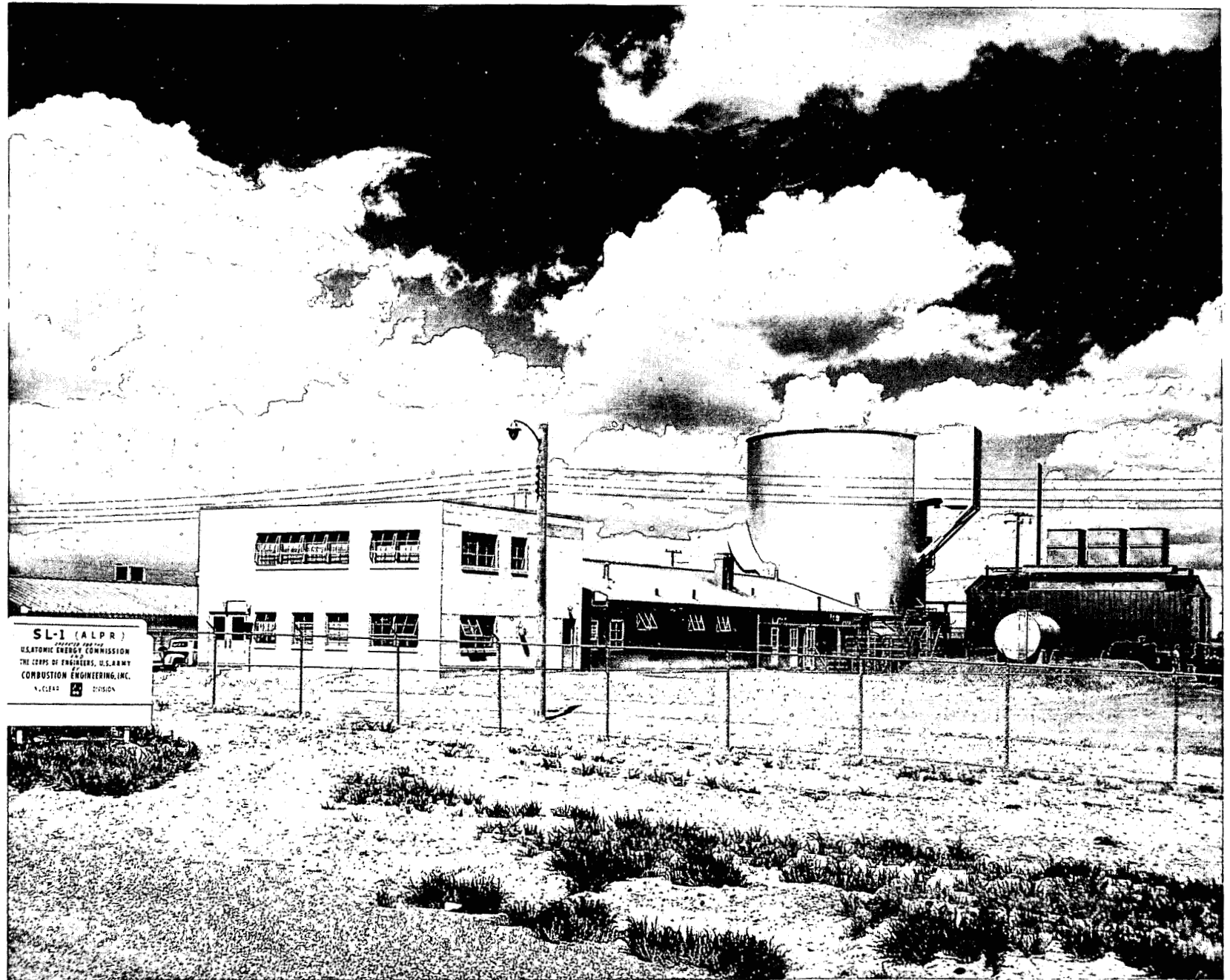
At the time of the incident, the shield blocks were moved back. Except for this, the reactor floor was as shown in Figure 2.

The perspective cutaway shown in Figure A-3, depicts the pressure vessel, core, biological shield, and the control rod drive mechanisms. The lower portion of the cutaway shows the core support, support lugs, support grid, thermal shield, and thermal shield support. In the center cutaway of the core, the control rod shrouds, X-stanchions and fuel element positions can be seen. The upper left portion of the pressure vessel just below the head shows the steam and water lines. Above the head are the biological shield, still wells, cover assembly and the control rod drive mechanism. The biological shield contains steel punchings, sand, and 30 pounds per cubic foot of boric oxide. At the time of the incident, the #5 control rod drive mechanism, blind plugs #2 and #6, blind flange cover #8, and the still wells were secured as shown. The remainder of the rod drives had not been secured.

Figure A-4 is a top view of the core taken through the head showing the control rod coupling, shrouds, and the top fuel element hold down boxes.

The above gives the condition of the reactor at the time of the incident on January 3, 1961.

A-2

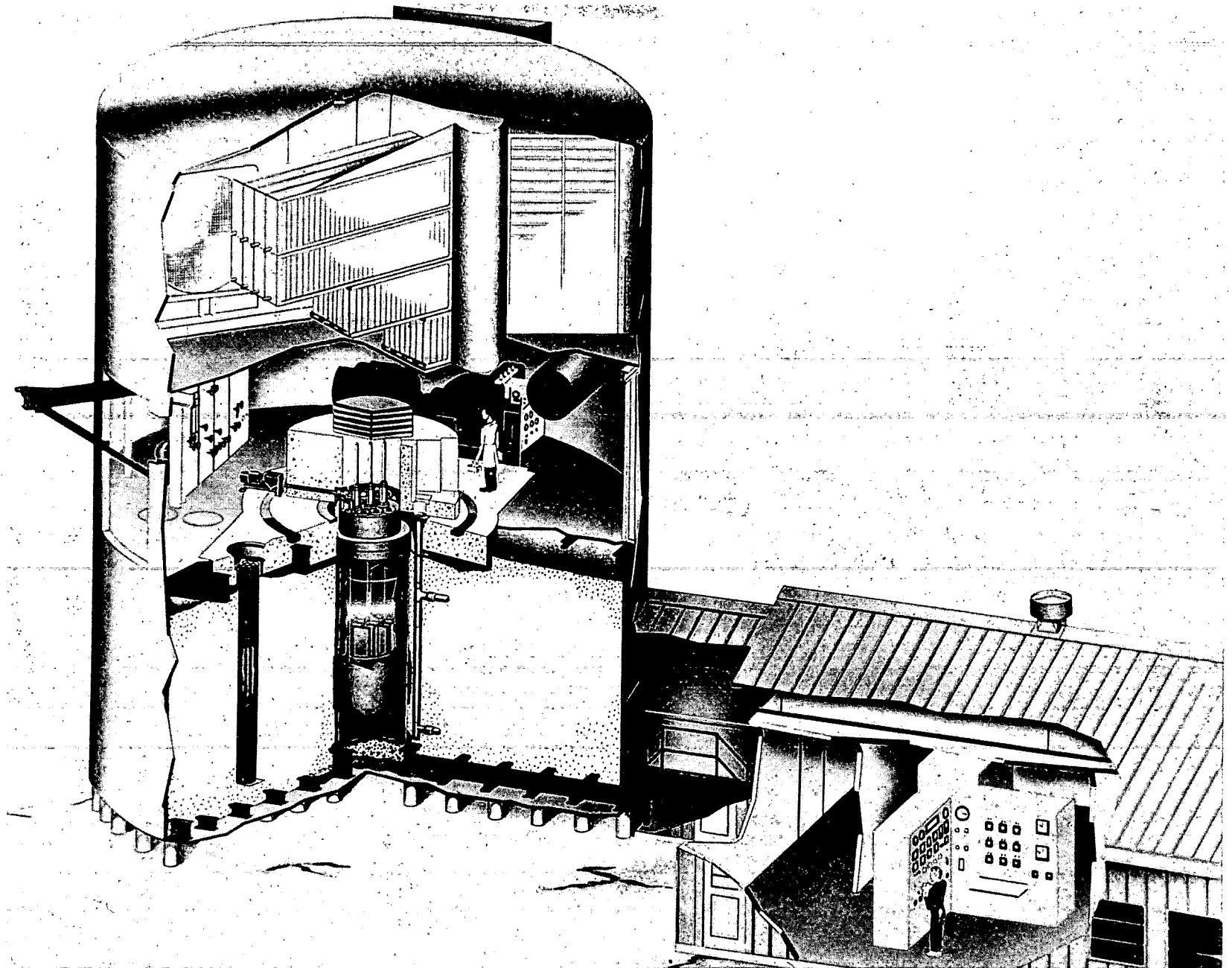


NRTS-60 4749

Figure A-1

SL-1 Plant Area

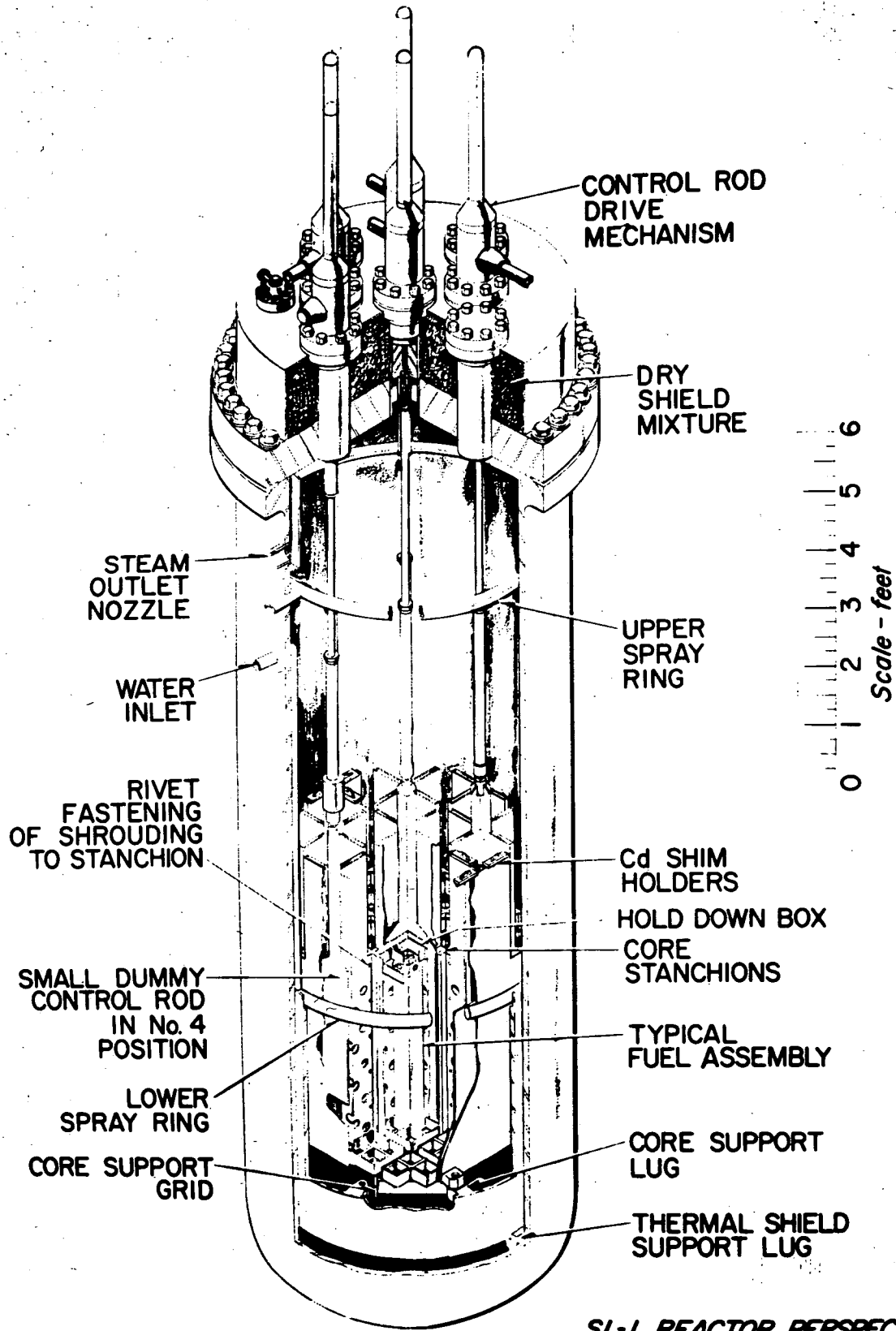
A-3



NRTS-60 3227

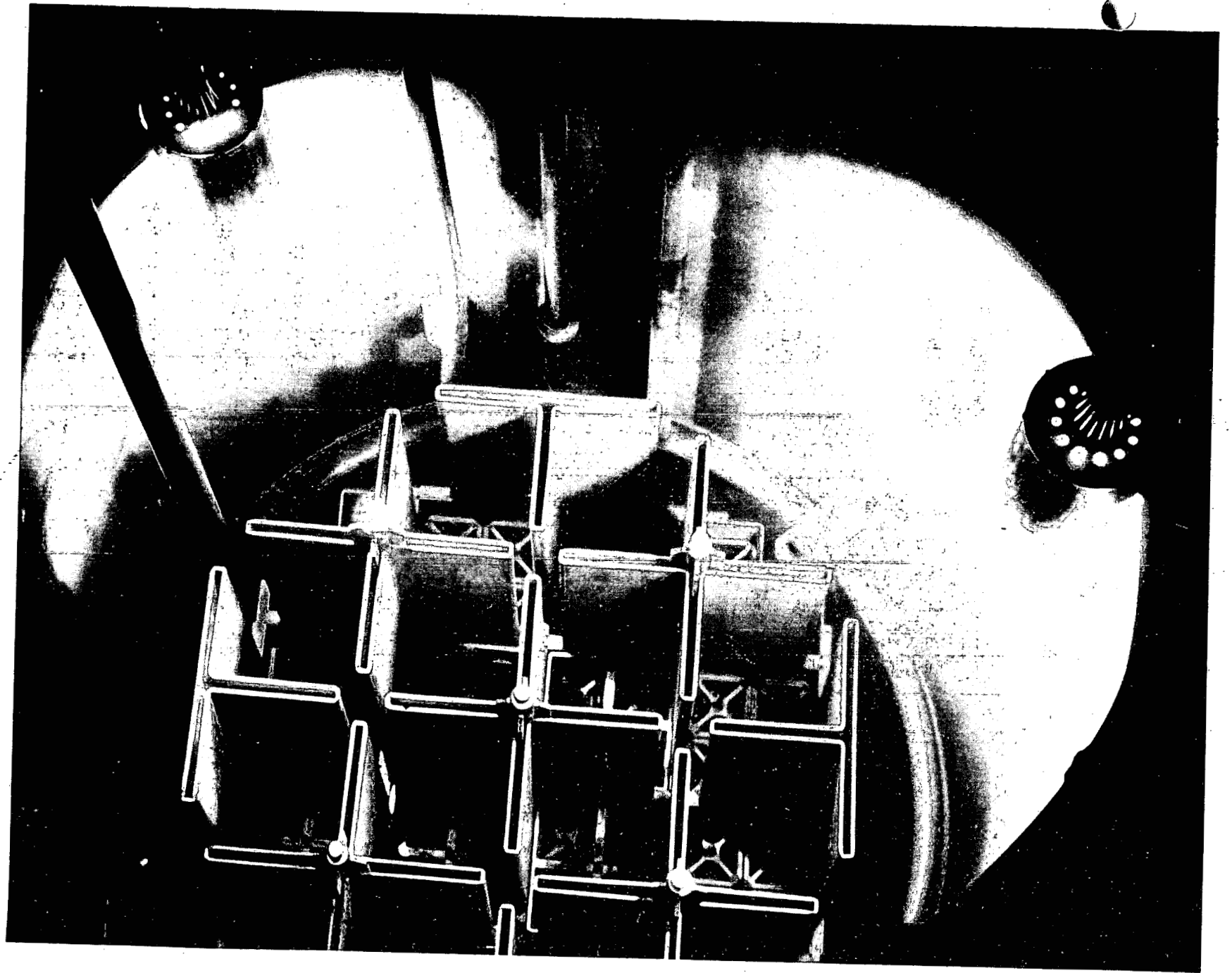
Figure A-2

SL-1 Plant Perspective



SL-1 REACTOR PERSPECTIVE

Figure A-3



A-5

U-5116

Figure A-4

SL-1 Core Plan

APPENDIX B

List of SL-1 Photographs by Series Numbers

Site and in Transit

U-5003	Pictures of SL-1 and reactor floor
U-5004	Enlargement of movies frames
U-5005	Checkout on pin-hole camera
U-5006	Operating room photographs
U-5009	Photostat of flow diagram
U-5011	Operating room photographs (6-29-61)
U-5013	Operating room photographs (7-3-61)
U-5016	Operating room photographs (7-13-61)
U-5018	Operating room photographs (7-21-61)
U-5019	Fan room photographs
U-5020	Fan room photographs
U-5021	Fan room photographs
U-5027	Fan room photographs
U-5032	Fan room photographs
U-5035	Operating room photographs
U-5040	Fan room photographs
U-5041	Operating floor photographs
U-5042	Operating floor photographs
U-5043	Operating floor photographs
U-5047	Fan room photographs
U-5049	Pinhole camera pictures

Site and Transit (Continued)

U-5050	Pictures of Core
U-5051	SL-1 Building and Reactor
U-5053	Pressure Vessel
U-5054	Fan Room and Reactor Floor Ceiling
U-5055	Operating Floor
U-5056	Pressure Vessel
U-5057	Boroscope
U-5058	Boroscope
U-5059	Boroscope
U-5060	Pressure Vessel
U-5061	Mockup in 607
U-5062-3	Exterior of Core-Lift on Pressure Vessel
U-5068	Reactor Building
U-5071	Cask and Truck enroute to SL-1
U-5073	Reactor Building
U-5075	Removal of Core from Vessel
U-5076	Inside Pressure Vessel, Cocoon, Crane, Shield, Fan Room, Gravel Fill, etc.
U-5077	Moving Core to ANP
U-5078	Mockup - SL-1 Core
U-5101	Austin-Western Crane
U-5114	Facilities and Gravel Removal from Building
U-5145	SL-1 Area and Containment Vessel
U-5163	Final Area Inspection

Hot Shop

U-5008 Material from SL-1 Floor

U-5010 Component and Shield Plug

U-5017 Parts removed from SL-1 Floor

U-5079 Top of Core

U-5081 Control Rod #9

U-5083 Top of Vessel - Shield can removed

U-5084 Top of Vessel - Shield can partially lifted

U-5085 Core through binoculars

U-5086 Core through boroscope

U-5087 Bulged Control Nozzles

U-5089 Sand, boron, steel punchings shielding material on top of pressure vessel head

U-5090 Criticality test stand

U-5092 Inside pressure vessel (boroscope)

U-5094 Core removed from cask

U-5095 Inside pressure vessel (boroscope)

U-5096 Insulation in bottom cap

U-5097 Dished head

U-5098 Bulged nozzles

U-5099 Light leaks around head

U-5100 Control Rod #5

U-5103 Removing head from pressure vessel

U-5104 Inside pressure vessel - head removed

Hot Shop (Continued)

U-5105 Inside pressure vessel after removal of various parts
U-5109 Color photos - inside pressure vessel
U-5112 Inside pressure vessel
U-5117 Inside pressure vessel No Sun-Gun
U-5118 Inside pressure vessel No Sun-Gun
U-5119 Pressure Vessel head - elongated holes
U-5122 Before and after boric acid neutralization test
U-5123 Inside pressure vessel
U-5124 Boroscope - bottom of pressure vessel
U-5130 Bottom of pressure vessel (boroscope)
U-5131 Light coming through core from mirror
U-5132 Inside pressure vessel
U-5134 Criticality stand and cutting stand set up
U-5138 TV-Monitor views inside pressure vessel
U-5144 Critical control panels
U-5147 Core during cutting operation of pressure vessel
U-5148 Core disassembly
U-5150 Thermal shield and other reactor parts
U-5161 Pressure vessel in Warm Shop
U-5167 Hot Shop - final wash down
U-5170 Head nozzle deformation

Laboratories

U-5001 RML Photos of SL-1 Components
U-5002 Components HL-1 to 14
U-5007 Material in HCA
U-5010 Component and Shield Plug
U-5012 Hot Lab
U-5014 Film Badge (Legg)
U-5022 Shield Plug A
U-5023 Shield Plug B
U-5024 Misc. part, (Legg film badge)
U-5025 Seal control unit in disassembly position
U-5029 HL-64 to HL-79
U-5031 Shield Plug assemblies 3 and 4 and component parts
U-5034 Front and back views of boron poison strips
U-5038 Shield Plug #1
U-5039 Microscope photos (components)
U-5044 Rack assemblies
U-5045 Seal assembly
U-5046 Connectors
U-5048 Shield Plug A
U-5052 Shield Plug #7 and #9
U-5066 Boron metallograph

Laboratories (Continued)

U-5080 Mockup in 607 of SL-1 ceiling
U-5102 Control rod parts
U-5125 Baffle plates
U-5137 #9 Control Rod Sketch
U-5157 Shield Plug Projectories
U-5162 Weld on pressure vessel

Miscellaneous

U-5135 Memory scope #9 rod pulling
U-5140 #9 Rod set-up in 607 pool
U-5143 Turbine - generator from SL-1
U-5146 Fan Room Floor section above Reactor
U-5149 Scale model pressure vessel
U-5160 Memory scope #9 rod pulling
U-5164 Mock-up and Fan Floor Section
U-5165 Aberdeen Model Test

APPENDIX C

Report from Stanford Research Institute

STANFORD RESEARCH INSTITUTE

MENLO PARK, CALIFORNIA

June 26, 1962

Dr. C. L. Storrs
P. O. Box 2147
Idaho Falls, Idaho

Reference: Project PLD-3959

Dear Dr. Storrs:

Stanford Research Institute has been asked to make an investigation into the possibility that the reactor runaway which destroyed the S1-1 reactor could have been a result of sabotage in the form of some type of explosive.

Three visits - one by Poulter and two by Poulter and Davenport, have been made to the Idaho Falls facility to inspect the various elements of the reactor as it has been dismantled. These first-hand inspections of the damaged reactor and a study of the extensive photographs that have been taken, have made it possible to establish a number of basic facts from which very definite conclusions can be drawn.

Absence of Explosive or Explosive Decomposition Products

- (1) The entire interior of the reactor assembly was comparatively free of elemental carbon such as would most certainly have been present if most types of high explosives or propellants had been exploded within the reactor.
- (2) A chemical analysis of both water and carbon tetrachloride extracts of the residue showed the absence of more than traces of nitro or nitrate groups which further shows that neither a high explosive nor a propellant type charge had been exploded inside of the reactor even though it be one of a carbon-deficient type.

- (3) From an examination of control rod No. 9 after it was removed from the shroud, it can be stated definitely that it was not raised by means of a high detonating rate-type explosive charge located under it in the space below the reactor proper; otherwise it would definitely show characteristic high explosive damage marks on the lower end.
- (4) Likewise, control rod No. 9 could not have been blown upward by means of any reasonable quantity of a low order detonating explosive or propellant-type explosive, because of the relatively large annular space between the reactor elements and the shell of the pressure chamber.
 - (a) The comparatively large volume of open space in the lower portion of the pressure chamber below the reactor elements would have allowed such a free radial distribution of pressure that a pressure gradient sufficiently high at the center to lift control rod No. 9, and yet low enough so as not to lift the surrounding and lighter control rods, is physically impossible.
- (5) The possibility of control rod No. 9 being raised by a very rapid pulse or steady state flow of water upward through and around the reactor elements can be eliminated on the following bases:
 - (a) The annular space around the reactor elements is too large and so much water would flow up through that route that pressure sufficient to raise element No. 9 could not develop.
 - (b) The four similar elements surrounding No. 9 would raise first because they all have the same cross-sectional area and are lighter in weight so would have moved first, and none of them did move.
 - (c) There is no inlet pipe opening in the bottom portion of the pressure chamber sufficiently large to admit a sufficient quantity to do this by many fold.

- (6) An examination of control rod No. 9 after it had been removed from its shroud or control rod No. 9 plus its shroud, shows no evidence whatever of any explosive or propellant having been detonated or burned within the reactor proper in such a manner that could have caused rod No. 9 to have been raised the 20 inches, as is evident from the seizure marks.
- (a) Any such explosive would have collapsed the shroud on the rod before it moved, rather than forcing it up 20 inches first.
- (b) Neither the shroud encased control rod No. 9 nor any of the surrounding fuel elements exhibit the type of damage that could have been caused by any such explosion.
- (7) An examination of the character of the failure of the fuel elements which were adjacent to control rod No. 9, plus the radially outward displacement of all reactor components surrounding control rod No. 9 and the adjacent fuel elements shows conclusively that the major destruction occurred in those fuel elements adjacent to control rod No. 9 and at a distance of from three to six inches below the center of the fuel elements.
- (8) The fact that in almost all cases the surfaces of the fuel elements which were in contact with the control rod were the least damaged shows that the major reaction during the excursion took place in that portion of those fuel elements which would be affected if the excursion were caused by the central control rod No. 9 having been raised 20 inches, at which point the shroud was collapsed on the control rod. This would have been true if control rod No. 9 had been raised by any amount exceeding 16 inches.
- (9) Not only does a physical examination of all fragments from the control rod system and the contents of the reactor pressure chamber show no evidence of any chemical explosive or propellant having been exploded in or adjacent to the reactor, but a chemical analysis of residues from within this chamber plus the absence of any black deposits or residues of free carbon show not only that no such chemical explosives were detonated but that they were not even present.

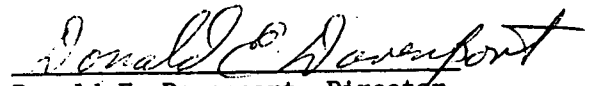
Not only do we not find any evidence of any chemical-type explosive or propellant having been exploded within this reactor, but there is very strong evidence that no such materials had been present, and there is certainly no evidence of any portion of the reactor having been within the immediate proximity of exploding propellant or high explosive.

We are therefore convinced from these facts that there was no sabotage involved in this event of the nature which could have been caused by a chemical type of explosion.

Sincerely,



Thos. C. Poulter
Senior Scientific Advisor



Donald E. Davenport, Director
Poulter Laboratories

APPENDIX D

TABULATION OF % AREA DESTROYED & % AREA UNMELTED ON
OUTSIDE OF CLAD

<u>Fuel Element No.</u>	<u>Plate No.</u>	<u>% Area Destroyed</u>	<u>% Area Unmelted</u>
1.	E- 9	84.7	15.3
	E-82	78.0	5.0
	E-52	78.0	13.0
	E-69	76.0	14.0
	E-80	78.0	15.0
	E-11	78.0	14.0
	E-48	78.0	11.5
	E-25	76.0	13.0
	E-24	<u>72.0</u>	<u>11.5</u>
		Avg. 77.6	Avg. 12.5
2.	E-72	57.0	1.0
	E-26	63.0	13.0
	E-59	83.0	11.0
	E-81	76.0	12.0
	E- 6	87.0	7.6
	E-46	85.0	10.0
	E-79	85.0	10.0
	E-13	87.0	7.6
	E- 4	<u>88.0</u>	<u>7.6</u>
		Avg. 79.0	Avg. 8.9
3.	E-45	7.0	38.0
	E-34	5.0	35.0
	E-18	64.0	27.0
	E-74	68.0	20.0
	E-30	65.0	20.0
	E-66	66.0	20.0
	E-56	69.0	20.0
	E-47	70.0	20.0
	E-68	<u>69.0</u>	<u>20.0</u>
		Avg. 53.7	Avg. 24.4
4.	E-78	74.0	23.0
	E-33	74.0	19.0
	E-75	77.0	12.0
	E-85	81.0	12.0
	E-35	81.0	12.0
	E-62	85.0	11.0
	F-44	85.0	11.0
	E-73	85.0	11.0
	E-39	<u>85.0</u>	<u>11.0</u>
		Avg. 80.7	Avg. 13.6

APPENDIX D (Cont'd)

TABULATION OF % AREA DESTROYED AND % AREA UNMELTED ON
OUTSIDE OF CLAD

<u>Fuel Element No.</u>	<u>Plate No.</u>	<u>% Area Destroyed</u>	<u>% Area Unmelted</u>
5.	E- 8	30.0	70.0
	E- 88	0.0	100.0
	T-253	2.0	98.0
	E- 21	12.0	88.0
	E-280	12.0	88.0
	E- 31	12.0	88.0
	E- 16	0.0	100.0
	E- 7	0.0	100.0
	E- 57	0.0	100.0
		Avg.	7.6
	E- 22	69.0	19.0
	E-163	69.0	11.2
	E- 28	69.0	15.0
	E-160	69.0	11.2
	E- 32	69.0	15.0
	E-165	69.0	15.0
	E- 83	69.0	15.0
	E-155	69.0	15.0
	E-166	69.0	17.0
	Avg.	69.0	Avg. 14.8
	E-164	70.0	27.0
	E-140	68.0	19.0
	E-162	72.0	10.0
	E-158	73.0	15.0
	E-141	73.0	14.0
	E-273	69.0	17.0
	E-139	70.0	16.0
	E-157	81.0	15.0
	E-137	78.0	6.0
	Avg.	72.7	Avg. 15.4
	E-250	0.0	100.0
	E-252	75.0	6.0
	E-256	80.0	4.0
	E-260	74.0	7.0
	E-264	70.0	8.0
	E-265	69.0	10.0
	E-269	69.0	9.0
	E-270	73.0	8.0
	E-274	72.0	8.0
	Avg.	64.7	Avg. 28.9

APPENDIX D (Cont'd)

TABULATION OF % AREA DESTROYED AND % AREA UNMELTED ON
OUTSIDE OF CLAD

<u>Fuel Element No.</u>	<u>Plate No.</u>	<u>% Area Destroyed</u>	<u>% Area Unmelted</u>
9.	All plates Complete - No melting		
			<u>100</u>
10.	E-255	3.0	24.0
	E-278	55.0	39.0
	E-279	66.0	21.0
	E-272	62.0	11.0
	E-261	62.0	6.0
	E-257	58.0	8.0
	E-244	58.0	7.0
	E-277	66.0	11.0
	E-281	<u>65.0</u>	<u>8.0</u>
		Avg. 55.0	Avg. 15.0
11.0	E-195	19.0	19.0
All Others	--	--	<u>100.0</u>
			Avg. 91.0
13	E-147	8.0	30.0
	E-153	3.0	20.0
	E-145	0.0	20.0
	E-146	0.0	20.0
	E-143	0.0	23.0
	E-121	0.0	48.0
	E-123	0.0	46.0
	E-245	0.0	45.0
	E-167	<u>0.0</u>	<u>34.0</u>
		Avg. 1.2	Avg. 31.8
14	E- 99	24.0	40.0
	E- 96	24.0	50.0
	E-110	12.0	75.0
	E-119	12.0	75.0
	E-130	8.0	84.0
	E-134	0.0	100.0
	E-171	0.0	100.0
	E-131	0.0	100.0
	E-129	<u>0.0</u>	<u>100.0</u>
		Avg. 8.9	Avg. 80.4

APPENDIX D (Cont'd)

TABULATION OF % AREA DESTROYED AND % AREA UNMELTED ON

OUTSIDE OF CLAD

<u>Fuel Element No.</u>	<u>Plate No.</u>	<u>% Area Destroyed</u>	<u>% Area Unmelted</u>
17.	All Plates Complete	<u>0.0</u>	<u>100.0</u>
		0.0	100
18.	All Plates Complete	<u>0.0</u>	<u>100.0</u>
		0.0	100
19.	All Plates Complete	<u>0.0</u>	<u>100.0</u>
		0.0	100
20.	E-297	12.0	48.0
	E-290	5.0	57.0
	E-287	2.0	98.0
	E-304	0.0	100.0
	E-303	0.0	100.0
	E-307	0.0	100.0
	E-302	0.0	100.0
	E-299	0.0	100.0
	E-298	<u>0.0</u>	<u>100.0</u>
		Avg. 2.1	Avg. 89.2
35.	E- 15	85.0	4.0
	E-458	85.0	5.0
	E-472	84.0	7.0
	E-439	83.0	4.0
	E-442	80.0	4.0
	E-441	73.0	5.0
	E-445	65.0	7.0
	E- 27	65.0	8.0
	E-464	<u>43.0</u>	<u>15.0</u>
		Avg. 73.7	Avg. 6.6
39.	E-550	0.0	17.0
	E-516	0.0	100.0
	E-551	0.0	100.0
	E-525	0.0	100.0
	E-553	0.0	100.0
	E-546	0.0	100.0
	E-555	0.0	100.0
	E-527	0.0	100.0
	E-528	<u>6.0</u>	<u>97.0</u>
	Avg. 1.3	Avg. 90.4	

APPENDIX D (Cont'd)

TABULATION OF % AREA DESTROYED AND % AREA UNMELTED ON
OUTSIDE OF CLAD

<u>Fuel Element No.</u>	<u>Plate No.</u>	<u>% Area Destroyed</u>	<u>% Area Unmelted</u>
41.	E-519	51.0	17.0
	E-466	40.0	19.0
	E-455	51.0	19.0
	E-463	57.0	16.0
	E-465	65.0	13.0
	E-473	68.0	12.0
	E-470	73.0	11.0
	E-474	75.0	10.0
	E-540	<u>80.0</u>	<u>4.0</u>
	Avg. 62.2	Avg. 13.4	
43.	All Plates Complete	Very Slight Melting	<u>100.0</u> 100
44.	All Plates Complete	<u>0.0</u> 0	<u>100.0</u> 100
45.	All Plates Complete	<u>0.0</u> 0	<u>100.0</u> 100
46.	All Plates Complete	<u>0.0</u> 0	<u>100.0</u> 100
47.	All Plates Complete	<u>0.0</u> 0	<u>100.0</u> 100
48.	E-573	0.0	23.0
	All Other Plates Complete	0.0	<u>100.0</u>
			Avg. 91.4
49.	All Plates Complete	<u>0.0</u> 0	<u>100.0</u> 100

APPENDIX D (Cont'd)

TABULATION OF % AREA DESTROYED AND % AREA UNMELTED ON
OUTSIDE OF CLAD

<u>Fuel Element No.</u>	<u>Plate No.</u>	<u>% Area Destroyed</u>	<u>% Area Unmelted</u>
50.	E-618	70.0	24.0
	E-625	70.0	21.0
	E-631	63.0	23.0
	E-628	61.0	25.0
	E-676	54.0	19.0
	E-672	53.0	15.0
	E-619	40.0	15.0
	E-677	15.0	68.0
	E-674	16.0	19.0
		Avg. 49.1	Avg. 25.0
51.	All Plates Complete	<u>0.0</u> 0	<u>100.0</u> 100
52.	E-673	9.0	16.0
	E-634	10.0	22.0
	E-669	11.0	23.0
	E-627	10.0	19.0
	E-624	15.0	20.0
	E-718	24.0	19.0
	E-663	20.0	18.0
	E-626	27.0	21.0
	E-689	28.0	12.0
		Avg. 17.1	Avg. 18.9
53.	All Plates Complete	<u>0.0</u> 0	<u>100.0</u> 100
54.	All Plates Complete	<u>0.0</u> 0	<u>100.0</u> 100
55.	All Plates Complete	<u>0.0</u> 0	<u>100.0</u> 100.
56.	E-723	0.0	75.0
	All other Plates Complete	0.0	<u> </u>
			Avg. 97.2

APPENDIX D (Cont'd)

TABULATION OF % AREA DESTROYED AND % AREA UNMELTED ON
OUTSIDE OF CLAD

<u>Fuel Element No.</u>	<u>Plate No.</u>	<u>% Area Destroyed</u>	<u>% Area Unmelted</u>
57	All Plates Complete	<u>0.0</u> 0	<u>100.0</u> 100
58.	All Plates Complete	<u>0.0</u> 0	<u>100.0</u> 100
59.	E-777	0.0	40.0
	E-695	0.0	40.0
	E-811	0.0	40.0
	E-815	0.0	30.0
	E-788	0.0	30.0
	E-790	0.0	30.0
	E-813	0.0	30.0
	E-809	0.0	30.0
	E-749	0.0	<u>40.0</u>
			Avg. 34.4
60.	All Plates Complete	<u>0.0</u> 0	<u>100.0</u> 100
61.	All Plates Complete	<u>0.0</u> 0	<u>100.0</u> 100
62.	E-704	0.0	30.0
	E-765	0.0	30.0
	E-699	0.0	30.0
	E-728	0.0	30.0
	E-709	0.0	30.0
	E-702	0.0	30.0
	E-661	0.0	30.0
	E-732	10.0	2.0
	E-774	<u>10.0</u>	<u>2.0</u>
		Avg. 2.2	Avg. 24.9

Total Core: 19.8% Destroyed; 68.0% "ostensibly" unmelted
 Core Center (16 elements): 47.4% Destroyed
 Core Center 4 corner elements: 1.2% Destroyed

APPENDIX E

Tabulation of Flux Measured by Each Cobalt - Aluminum Pellet
(Pellets not reported were either unrecovered or unidentified)

Element	Wire Number	Position Between Fuel Plates	Position from top of fuel plate Inches	Thermal Flux n/cm ² x (10 ⁻¹⁴)
1	2157	G	-8.5	3.05
			-5.5	1.84
			-2.5	1.54
2	1368	B		
	1403	G		
3	1251	B	0.5	1.7
			3.5	1.9
			6.5	
			9.5	3.8
			12.5	
			15.5	5.2
			18.5	5.1
			21.5	4.7
			24.5	4.0
			27.0	3.9
	1563	G	0.5	1.54
			3.5	1.66
			6.5	2.17
			9.5	3.17
			12.5	4.19
			15.5	4.06
			18.5	4.01
			21.5	3.93
			24.5	2.70
27.0	2.55			
1830	E	0.5	2.0	
		3.5	2.3	
		6.5	2.5	
		9.5	3.2	
		12.5	4.7	
		15.5	5.2	
		18.5	6.0	
		21.5	5.1	
		24.5	3.7	
		27.0		
4	2027	B	0.5	1.95
			3.5	1.74
	1533	D	0.5	1.42
			3.5	1.78
			6.5	4.85
			9.5	4.13

Element	Wire Number	Position between Fuel Plates	Position from top of fuel plate Inches	Thermal Flux $n/cm^2 \times (10^{-14})$	
5	2144	G	0.5	1.07	
			3.5	1.42	
			6.5	1.70	
			9.5	2.73	
			12.5	3.28	
			15.5	3.03	
			18.5	3.21	
			21.5	2.88	
			24.5	1.72	
	27.0	1.91			
	2054	B	0.5		
			3.5	.84	
			6.5	1.90	
			9.5	2.47	
			12.5	2.52	
			15.5	3.16	
			18.5	2.79	
			21.5	2.83	
			24.5	2.11	
27.0	1.92				
6	1339	B	-8.5	.68	
			-5.5	.94	
			-2.5	1.56	
			0.5	3.00	
			3.5	3.83	
			6.5	5.40	
			9.5		
			12.5		
			6	1685	G
-5.5	.38				
-2.5	1.06				
0.5	1.19				
3.5	1.21				
6.5	3.75				
9.5	6.18				
12.5					
1349	E	3.5		1.70	
		6.5		2.21	
		9.5		4.70	
		12.5		6.50	
7	1799	B		0.5	1.46
				3.5	2.03
				6.5	2.80

Element	Wire Number	Position between Fuel Plates	Position from top of fuel plate Inches	Thermal Flux $n/cm^2 \times (10^{-14})$
	1252	G	3.5	2.15
			6.5	3.58
			9.5	4.90
			12.5	6.91
			15.5	6.41
			18.5	5.67
			21.5	5.39
			24.5	4.03
8	1409	G	0.5	3.1
			3.5	2.9
			6.5	
			9.5	5.6
	1435	B		
9	1258	G	0.5	
			3.5	.89
			6.5	1.17
			9.5	1.54
			12.5	2.31
			15.5	2.50
			18.5	2.78
			21.5	1.98
			24.5	1.84
			27.0	1.01
10	1243	E	0.5	1.67
			3.5	1.54
			6.5	2.67
			9.5	3.95
			12.5	5.37
			15.5	5.78
			18.5	6.17
			21.5	4.94
			24.5	4.00
11	1274	B	0.5	1.38
			3.5	1.17
			6.5	1.69
			9.5	1.96
			12.5	2.68
			15.5	3.45
			18.5	2.84
			21.5	2.88
			24.5	1.89
			27.0	1.88

Element	Wire Number	Position between Fuel Plates	Position from top of fuel plate Inches	Thermal Flux $n/cm^2 \times (10^{-14})$
	1872	D	0.5	1.16
			3.5	1.75
			6.5	3.32
			9.5	3.20
			12.5	3.55
			15.5	2.88
			18.5	1.92
			21.5	1.87
			24.5	1.30
			27.0	
	1972	G	All pellets missing from wire	
13	2162	E	0.5	
			3.5	.91
			6.5	1.82
			9.5	+
			12.5	+
			15.5	+
			18.5	+
			21.5	+
			24.5	+
			27.0	1.25
18	1605	E	0.5	.64
			3.5	.84
			6.5	.90
			9.5	1.58
			12.5	1.63
			15.5	2.18
			18.5	2.33
			21.5	1.97
			24.5	.89
			27.0	.96
19	2010	B	0.5	*
			3.5	.84
			6.5	.82
			9.5	+
			12.5	3.39
			15.5	2.23
			18.5	1.70
			21.5	1.27
			24.5	.95
	1247	G	0.5	*
			3.5	*
			6.5	*
			9.5	.64

+ Contaminated during chemical separation

* Below threshold of detection

Element	Wire Number	Position between Fuel Plates	Position from top of fuel plate Inches	Thermal Flux $n/cm^2 \times (10^{-14})$
			12.5	.32
			15.5	1.06
			18.5	1.06
			21.5	.74
			24.5	.64
			27.0	.53
39	1257	G	0.5	1.28
			3.5	1.52
			6.5	
			9.5	2.30
			12.5	3.03
			15.5	3.31
			18.5	2.74
			21.5	
			24.5	2.28
			27.0	2.33
	2013	B		
41	1249	G		
	1433	B		
43	1278	E	0.5	.59
			3.5	.80
			6.5	.97
			9.5	1.08
			12.5	2.18
			15.5	1.94
			18.5	1.79
			21.5	1.24
			24.5	1.03
			27.0	1.02
47	1388	D	0.5	.25
			3.5	.50
			6.5	.63
			9.5	.70
			12.5	.76
			15.5	1.02
			18.5	.94
			21.5	.76
			24.5	.56
			27.0	.68

Element	Wire Number	Position between Fuel Plates	Position from top of fuel plate Inches	Thermal Flux n/cm ² x(10 ⁻¹⁴)	
47	1526	G			
			1905	B	
				5.5	.08
				2.5	.48
				0.5	.64
				3.5	1.17
				6.5	1.27
				9.5	2.01
				12.5	2.17
				18.5	2.37
			21.5	2.09	
			24.5	1.74	
				1.46	
48	1242	G	0.5	1.16	
			3.5	1.18	
			6.5	1.72	
			9.5	2.76	
			12.5	3.12	
			15.5	3.04	
			18.5	3.01	
			21.5	2.86	
			24.5	1.88	
			27.0	1.60	
51	1272	B			
52	2187	E	-8.5	.65	
			-5.5	.39	
			-2.5	4.2	
			0.5	4.5	
			3.5	3.6	
53	1784	B	0.5	.82	
			3.5	.84	
			6.5	1.04	
			9.5	1.15	
			12.5	1.35	
			15.5	1.64	
			18.5	1.72	
			21.5	1.35	
			24.5	.74	
			27.0	.37	
55	1201	E			

Element	Wire Number	Position between Fuel Plates	Position from top of fuel plate Inches	Thermal Flux $n/cm^2 \times (10^{-14})$
56	2074	D	0.5	.64
			3.5	.61
			6.5	.97
			9.5	1.23
			12.5	1.53
			15.5	1.78
			18.5	1.50
			21.5	1.33
			24.5	1.06
58	1245	G	0.5	.71
			3.5	.53
			6.5	.50
			9.5	.49
			12.5	.65
			15.5	.99
			18.5	.90
			21.5	.65
			24.5	.54
58	1236	B	0.5	.62
			3.5	1.22
			6.5	1.87
			9.5	1.79
			12.5	1.94
			15.5	1.51
			18.5	1.34
			21.5	1.26
			24.5	.81
59	1426	D	0.5	.44
			3.5	.58
			6.5	1.0
			9.5	1.44
			12.5	1.60
			15.5	2.68
			18.5	3.0
			21.5	2.27
			24.5	2.06
27.0	2.05			
60	1766	D		
62	1546	E		

APPENDIX F

ANALOG COMPUTER STUDY OF REACTOR INCIDENT

The analog study, conducted using the setup shown in Figure F-1, allows a 10 decade power excursion without re-scaling. Since the calculated values from the SPERT model predicted a peak power of less than 40,000 megawatt seconds, the critical level could be as low as 4 watts and still be within the 10 decade range of the computer.

The nuclear portion of the simulation was contained in amplifiers 1, 3, 9, 13, 25, and integrating amplifiers 5 and 23. Amplifiers 1 and 3, coupled with their multipliers, comprise the three shortest-lived delayed groups. The other delayed groups were eliminated by a series of trial runs which showed that they contributed no noticeable effect to the results. The system gain was established such that potentiometers P1, P2, and P3 could be set to the λ_i values (delayed neutron group decay constants) directly. In like manner potentiometers P11, P12, and P13 were set to the β_i values (delayed neutron group fraction) directly. Integrating amplifier 5 along with P8 was used to generate the various ramps of reactivity (ΔK) used in the simulation. This circuit was modified to produce the non-linear ramp functions which are shown on the traces in Figures III-97, 98, and 99 of Section III, 4.6. The potentiometer P10 was used to set the value of $\sum \beta_i$ directly. Summing the above variables produces ℓ/τ at amplifier 13. Amplifier 14 permitted varying the generation time (ℓ). The output of 14 is $1/\tau$. The negative value of $1/\tau$ is integrated by amplifier 23, producing $\ln \phi$. (ϕ = reactor flux or power.)

The remainder of the setup is used to simulate the temperature in a fuel plate, converting $\ln \phi$ to ϕ , integrating ϕ , then inserting a feed back of ΔK proportional to energy, both linear and delayed. Only the top four decades of linear power are employed. Amplifier 12 covers two decades, and then amplifier 6 switches in producing the top two decades of linear power. This approximation of the total power trace is very good since the first 6 decades do not contribute an appreciable amount of energy (approximately 1/100% of total.) The output of integrating amplifier 17 is the total energy. This unit is used to supply the linear energy feed back through the 2 megohm summing resistor plus the delayed energy feed back through the multiplier.

The temperature simulation represents the following equations:

$$\text{I} \quad \frac{dT_0}{dt} = 3.18 Q_0 - 630 (T_0 - T_1),$$

$$\text{II} \quad \frac{dT_1}{dt} = 3.18 Q_1 + 630 (T_0 + T_2) - 1260 T_1,$$

$$\text{III} \quad \frac{dT_2}{dt} = 605 (T_1 + T_3) - 1210 T_2,$$

$$\text{IV} \quad \frac{dT_3}{dt} = 300 (T_2 - T_3)$$

where:

T_0 = centerline of meat temperature,

T_1 = temperature at meat clad interface,

T_2 = temperature at 0.030 cm from surface,

T_3 = surface temperature.

The output of amplifier 24 represents surface temperature. This temperature is used to drive the switch and delay circuit consisting of amplifiers 15, 16, 18 and 31.

The system described allows simulation of the incident based on a gross reactor behavior. The overall system calibration is performed by the ratio of peak meat source energy and energy required to bring the peak section to 100°C (85°C above assumed ambient temperature of 15°C). This value was calculated by simulating the energy deposited in a unit volume of meat. The source energy in the maximum flux region is known from the flux wire analysis; and the energy required to bring the surface to 100°C can be calculated, using the average plate temperature as shown in Section IV-1.4. The ratio of these two energies is approximately 10.

Using the system as described, a number of runs were made, each recording the total energy for several different ramp rod-withdrawal rates and different delay times. These results can be seen in Figure III-97, 98, and 99 of Section III-4.6. As shown in these figures the critical power level was determined to be approximately 400 watts. This value produces a conservative estimate for the time from critical to the occurrence of the peak power. The temperature output of the peak energy density region was used to calibrate the total energy output, which in turn was used to calibrate the power trace and establish the value of the initial power. The calibration between energy and log of power could be changed by varying the gain of amplifier 17, thus, in essence, changing the initial power.

Figure F-2 is a typical run, showing outputs of energy, log of power, and reactivity, which consisted of the ramp input plus the two feed back terms. A reactivity feed back becomes apparent approximately 10 milliseconds before the peak of the burst. This is, of course, the plate expansion term. With the assumed void coefficient of 0.0039% ΔK /megawatt second, the total effect of the plate expansion, based on a linear coefficient of expansion, would be less than 0.55%. This linear energy feed back term is small in comparison to the total reactivity to be overcome by the shutdown mechanism.

The major remaining portion of the shutdown must come from steam void formation. As discussed earlier, this mechanism is quite complicated, but is evidently delayed by approximately 3 milliseconds, for short period excursions, from the time the

plate surface temperature reaches 100°C until the appearance of any steam voids. The 130 Mw-sec total energy generated in the excursion was used as a constraint on the shutdown mechanism. It was found that without a delay between saturation temperature on the plate surface and the beginning of void formation, it was impossible to achieve a reasonable power trace in which the feedback was proportional to energy and the total accumulated energy was about 130 Mw-sec. For the tests of simulated rod-withdrawals, discussed in Section III-4.6, the excursion was made to approach a chopped exponential, a condition approximating the bursting of plates due to vaporization. Such an approximation will have little influence on the conclusions derived concerning the rate of reactivity insertion and the position of the central control rod at the peak of the excursion.

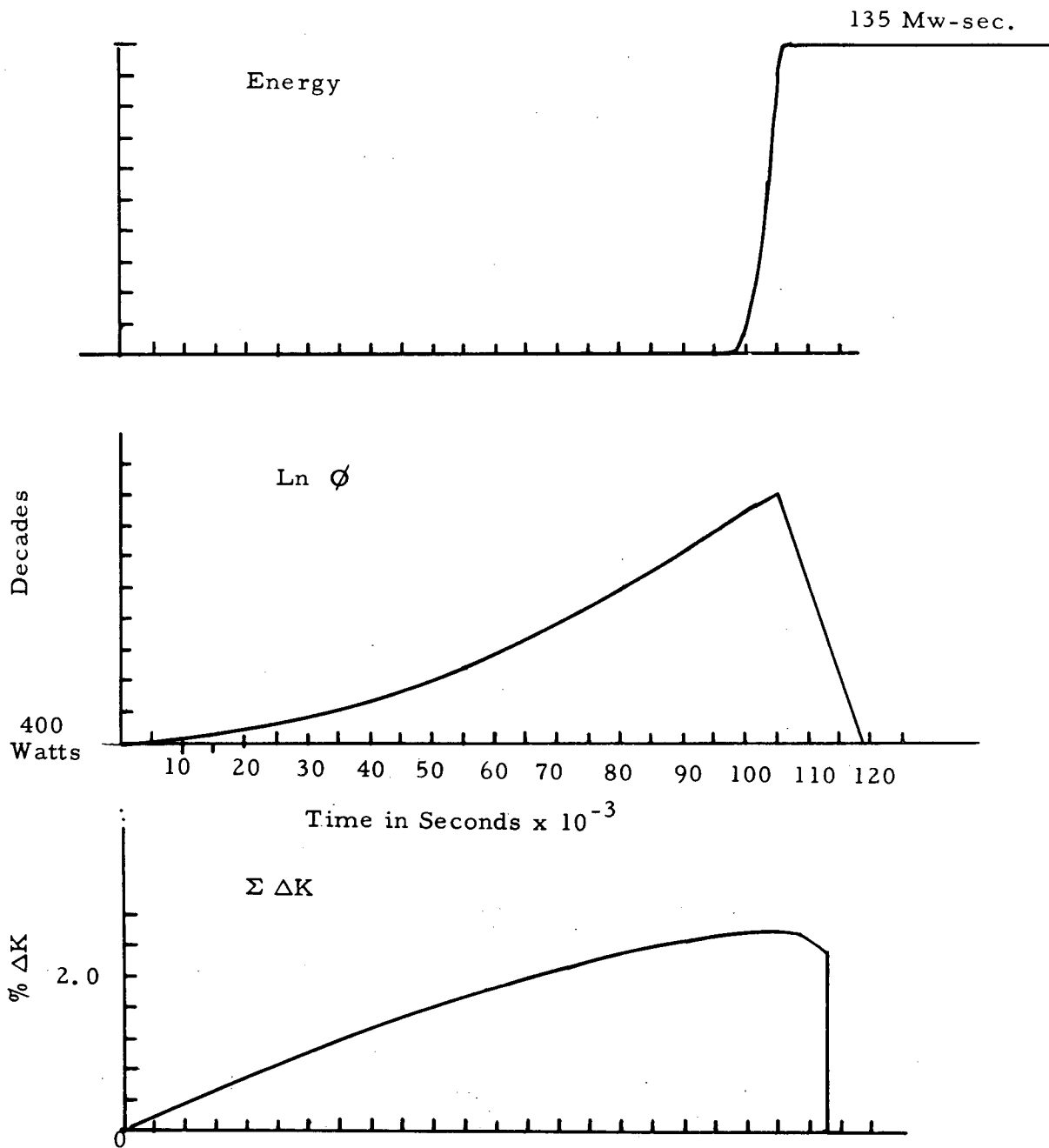


Figure F-2 Typical Transient Power Run